TCR signalling in response to affinity stimulation

Annika Målin Bruger

Lincoln College

University of Oxford

A thesis submitted for the degree of Doctor of Philosophy
October 2013

"So steht es denn da, unser Werk, so steinern und fremd, so eigenmächtig, so ein für allemal. Es sieht dich an, ohne zu nicken, ohne zu lächeln, so, als hätte man sich nie gekannt; ohne zu danken und ohne zu verzeihen. Nachdem man es lange betrachtet und auch die ersten Schrecken überwunden hat, sagt man sogar: Es ist nicht schlecht, man kann nicht sagen, es ist schlecht! Es erinnert an dieses und jenes, was uns im Entwerfen, da es noch ein Einfall war, erfreut und beglückt hat."

Max Frisch, Swiss playright, 1911-1991

"Wat mutt, dat mutt"
Low German proverb

Abstract

T cells are an essential part of the adaptive immune system and protect the body from intracellular infections. The specificity with which αβTCR-bearing T cells recognise cognate antigen presented on MHC molecules is paramount to maintaining the balance between mounting effector functions against pathogens and establishing peripheral tolerance to self. The mechanism by which T cells translate qualitative differences in TCR:pMHC binding to sensitive proximal signalling events which ultimately result in specific T cell effector responses to infected cells but not to self is mostly unknown.

To address how T cell signalling responds to qualitative differences in TCR triggering by pMHC, I established a system of stimulating T cells bearing the 1G4 TCR specifically *in vitro* with a panel of four NY-ESO-$1_{156-165}$ peptide variant MHC tetramers. Single amino acid substitutions to the NY-ESO-$1_{156-165}$ peptide conferred a maximum 35-fold difference in the monomeric affinity for the 1G4 TCR. The system allows the highly controlled investigation of very rapid TCR proximal signalling events simultaneously and quantitatively using flow cytometry. Stimulations with pMHC tetramers showed rapid sensitive sequential signalling responses which were able to confer ligand discrimination. Very early signalling events such as CD3ζ phosphorylation showed analogue responses to the different affinity pMHC tetramers. Later signalling events including phospho-ERK showed a distinct on/off switch-like response. The amplitude of the very early analogue signalling responses determined the extent of later digital ERK signals. This indicates that a certain analogue signalling threshold must be passed to result in T cell activation.

The thymocyte protein Themis has been shown proximal TCR signalling to modulate thymocyte selection thresholds. Its deletion results in profound defects in positive thymocyte selection. Themis locates to the LAT signalosome of the TCR signalling cascade via Grb2, yet its molecular function is unknown. Employing the system I established, I demonstrate that Themis-k/d cells show increased levels of CD3ζ-chain phosphorylation, phospho-ERK signalling and signal-induced apoptosis which was independent of the ERK signal. This shows that Themis is a global attenuator of proximal TCR signalling. We are currently investigating possible associations of Themis to proteins phosphastases such as SHP-1 which could attenuate TCR proximal protein tyrosine signalling events.

Acknowledgements

At this point I would like to pause for a bit and thank but a few of the many people who have enriched my life by travelling along this exciting path through Oxford with me for a little while.

First and foremost, I would like to thank my supervisor Prof Oreste Acuto for the opportunity and great privilege to work in his laboratory and to learn from him personally. His generous support and guidance throughout my studies were invaluable to the progression and success of this project. I would also like to thank my co-supervisor Dr Simon Hunt, my college advisor Dr Pietro Roversi and my graduate advisor Prof Anton van der Merwe for their inspiring advice and kind encouragement. My thanks also extend to Dr Alison Maloney from UCB Celltech for her supervision and the opportunities granted to me by UCB Celltech during my studies.

I am grateful to all the members of the Acuto lab, past and present. It is a pleasure to work with all of them and I wish them only the best for all their future adventures. Special thanks go to Wolfgang Paster whose support, advice and generous help are tremendous. Thank you for all your patience and for reading so many chapters of my thesis. I would like to thank Konstantina Nika especially for her helping me to find my feet in the lab and my project. My thanks also extend to Kristin Katsch for her help on the Themis project. I would further like to thank Andre Cohnen, especially for the coffee and the liquorice, and my fellow student Vincent Geoghegan. Last but not least, I would like to thank the good soul of the lab, Kelly Molder, who is probably unaware of how much her hard work is valued and appreciated.

I would furthermore like to thank our collaborators. Prof Vincenzo Cerundolo and his laboratory, especially Dr Ji-Li Chen and Dawn Shepard, for their generous sharing of expertise and reagents which form the basis to my work. I am grateful to Prof Anton van der Merwe and Dr Omer Dushek for their support and excellent advice on my project in particular and for their collaboration on the kinetic aspects presented. The Sir William Dunn School of Pathology and Lincoln College have been excellent and diverse environments to support and develop my research.

Friends, it is said, represent a family away from home. And even though you should not pick favourites within families, I would like to express my special gratitude to Bokani Tshidzu and Zsofia Novak who simply are like sisters to me. I am very fortunate to have such sterling friends as Varun Ramraj

and Matthew Stott who know how to make the most of the moment in great style. The longest nights and darkest days were ever sweetened with cakes and scones and copious amounts of tea and sympathy thanks to the forever adopted Marlena Whiting and Lauriane Angué. New and always exciting challenges were presented to me not only during the course of my academic studies but also by the Oxford University Women's Boat Club. To the club and its members past and present, but especially the Blue Boat of 2012 and Mike Genchi, I am grateful. Your excellence inspires me and has installed in me persistence, patience and the passion to pursue my dreams.

My most heartfelt and profound thanks I would like to extent towards my family. My mother, Gabriele, who is always supporting me in all my adventures with love and patience and whose giant parcels filled with chocolate always arrive at exactly the right time, Thank you!, and I would also like to thank my sisters, Hana Katalin and Maëla Natalie who are both wise beyond their years. Thank you for being the rocks and foundations to my life. Finally, I would like to thank my father, Joachim, for everything. I will love you always.

Abbreviations

Abbreviation	Definition
%	percent
°C	degree Celsius
aa	amino acid
ADAP	adhesion and degranulation promoting adapter protein
ADP	adenosine diphosphate
AMP	ampicillin
AP-1	activator protein 1
APC	antigen presenting cell
APS	ammonium persulfate
ATP	adenosine triphosphate
B2M or β2M	B or β2 microglobulin
BcL-X_L	B-cell lymphoma-extra large
BCR	B cell receptor
BSA	bovine serum albumin
C	cysteine
CABIT	cysteine-containing all-β in Themis
$CaCl_2$	calcium chloride
CaMK	calcium-calmodulin-dependent kinase
Cbl	CasitasB-lineagelymphoma
CD	cluster of differentiation
CDR	complementarity determining region
CEA	carcinoembryonic antigen
CLP	common lymphoid progenitor
CRAC	calcium release activated channels
CREB	cyclic-AMP-responsive element binding protein
Csk	C-Src tyrosine kinase
CTL	cytotoxic T lymphocyte
CXCL	C-X-C motif chemokine
CXCR	C-X-C chemokine receptor
dH_2O	deionised water
D	aspartic acid
DAG	diacylglycerol
DAMPs	damage-associated molecular patterns
DC	dendritic cell
DMSO	dimethyl sulfoxide

DN	double negative
DNA	deoxyribonucleic acid
DP	double positive
EDTA	ethylenediaminetetraacetic acid
ELISA	enzyme-linked immunosorbent assay
ENU	ethylnitrosourea
ER	endoplasmic reticulum
ERK	extracellular signal-regulated kinase
F	phenylalanine
FasL	Fas ligand
FCS	foetal calf serum
FLICA	fluorescent labelled inhibitor of caspases
FoxP3	forkheadbox P3
FPLC	fast protein liquid chromatography
Fyn	feline yes-related protein
Gads2	Grb2-related adapter protein 2
GATA-3	trans-acting T-cell-specific transcription factor GATA-3
GDP	guanosine diphosphate
GEF	guanine nucleotide exchange factor
GEM	glycolipid-enriched microdomain
Grb2	growth factor receptor-bound protein 2
GTP	guanosine triphosphate
H_2O_2	hydrogen peroxidase
HBS	HEPES buffered saline
HLA	human leukocyte antigen
HPK1	hematopoietic progenitor kinase 1
HSC	hematopoietic stem cell
I	isoleucine
ICAM-1	intercellular adhesion molecule1
ICOS	inducible T-cell costimulator
IFN	interferon
Ig	immunoglobulin
IKKβ	IκB kinase β
IL	interleukin
IP_3	inositol trisphosphate
IPEX	immunodysregulation polyendocrinopathy enteropathy X-linked syndrome
IPTG	β-D-1-thiogalactopyranoside

IS	immunologial synapse
ITAM	immunoreceptor tyrosine-based activation motif
ITK	IL-2-inducible T-cell kinase
K	lysine
k_{off}	off-rate or dissociation-rate
K_D	affinity
k_{on}	on-rate or association-rate
k/d	knock-down
KCl	potassium chloride
kDa	kilo Dalton
KH_2PO_4	monopotassium phosphate
L	leucine
LAT	linker for activation of T cells
LCK	lymphocyte-specific protein tyrosine kinase
LFA-1	lymphocyte function-associated antigen 1
M	methionine
M	molar
m	meter
MAPK	mitogen-activated protein kinase
MEF2	myocyte enhancer factor 2
MEK	mitogen-activated protein kinase kinase
$MgCl_2$	magnesium chloride
MHC	major histocompability complex
min	minute
MLP	myeloid-lymphoid progenitor
MPEC	memory precursor effector cells
MTOC	microtubule organizing center
Na_2HPO_4	disodium phosphate
Na_3VO_4	pervanadate
NaCl	sodium chloride
NaN_3	sodium azide
NCK	non-catalytic region of tyrosine kinase
NFAT	nuclear factor of activated T-cells
NK cell	natural killer cell
NK-$\varkappa$B	nuclear factor kappa-light-chain-enhancer of activated B cells)
NLS	nuclear localisation signal

NMR	nuclear magnetic resonance
ns	not significant
p	phosphorylated or protein (context-dependent)
P	proline
PAGE	polyacrylamide gel electrophoresis
PAMPs	pathogen-associated patterns
PBS	phosphate-buffered saline
PDK-1	3-phosphoinositide-dependent protein kinase
pen-strep	penicillin-streptomycin
PH	Pleckstrin homology
PI3K	phosphatidylinositide 3-kinase
PIP_2 or $PtdIns_{4,5}P_2$	phosphatidylinositol 4,5-bisphosphate
PIP_3 or $PtdIns_{3,4,5}P_3$	phosphatidylinositol (3,4,5)-triphosphate
PKC	protein kinase C
PLC-γ1	phospho-lipase C-γ1
PMA	phorbol 12-myristate 13-acetate
PMSF	phenylmethanesulfonylfluoride
PP2	protein phosphatase 2
PRRs	pattern recognition receptors
PTK	protein tyrosine kinase
PTP	protein tyrosine phosphatase
Q	glutamine
R	arginine
Rac1	Ras-related C3 botulinum toxin substrate 1
Raf-1	rapidly accelerated fibrosarcoma-1
RasGRP1	Ras guanyl-releasing protein 1
RBC	red blood cell
RhoH	Ras homolog gene family, member H
RNA	ribonucleic acid
RT	room temperature
RTE	recent thymic emigrant
S	serine
s	second
SDS	sodium dodecyl sulfate
SEM	standard error of mean
sh	short-hairpin
SH2	Srchomology 2

SH3	Srchomology 3
SHP-1	Src homology region 2 domain-containing phosphatase-1
SLEC	short-lived effector cells
SLP-76	SH2 domain containing leukocyte protein of 76 kDa
SMAC	supramolecular activation cluster
SOS	son of sevenless
SP	single positive
SPR	surface plasmon resonance
STAT3	signal transducer and activator of transcription 3
STIM1	stromal interaction molecule 1
T	threonine
TBS	Tris-buffered saline
T_C	cytotoxic T cell
T_{FH}	follicular helper T cell
T_H	helper T cell
T_H17	IL-17 helper T cell
T_{mem}	memory T cells
T_{Reg}	regulatory T cell
TAP	transporter associated with antigen processing
TCM	T central memory
TCR	T cell receptor
TEM	T effector memory
TEMED	tetramethylethylenediamine
TGF-β	transforming growth factor-β
Themis	thymus-expressed molecule involved in selection
Th-POK	T-helper-inducing POZ/Krueppel-like factor
TMB	3,3,5,5-tetramethylbenzidine
TNF-α	tumour necrosis factor-α
TNFRSF	tumour necrosis factor receptor superfamily
V	valine
VAV	guanine nucleotide exchange factor Vav
W	tryptophan
Y	tyrosine
ZAP-70	zeta-chain-associated protein kinase 70

Contents

List of Figures

List of Tables

Chapter 1

Introduction

1.1 T cell immunobiology

1.1.1 General immunology

The immune system protects the individual from effectively and lastingly from disease by microbial infections or pathologic cell tranformations by carrying out four precise functions: Firstly it recognises pathogenic material and secondly eradicates it through initiating strong effector functions. Thirdly, immune responses occur in a highly regulated manner which does not attack or damage healthy self tissue. Finally, the generation of immunological memory provides protection from re-occurring infections [Murphy et al., 2008].
In vertebrates, the immune system is divided into innate and adaptive immunity [Kasamatsu, 2013]. The first line of immunological defence is formed by the innate immune system. Macrophages, dendritic cells (DCs) and natural killer (NK) cells are but a few of the cell types which comprise the innate immune system. Commonly, they recognise invading microbial pathogens within hours of infections through conserved pattern recognition receptors

(PRRs) which bind to microbial structures called pathogen-associated patterns (PAMPs) and molecules released from damaged cells (called damage-associated molecular patterns - DAMPs) [Takeuchi and Akira, 2010]. Innate immune cells respond in a nonclonal fashion to infection. This means that each cell has the potential to mount an immune response to a particular environmental cue [Murphy et al., 2008]. Upon activation, the cells of the innate immune system induce inflammation via the release of cytokines and chemokines. Inflammation recruits further cells of the immune system to the site of the infection including cells of the adaptive arm of the immune system. However, these cells require the activation by innate immune cells to initiate highly specific immune responses. Professional antigen presenting cells (APCs) include macrophages and DCs. Macrophages in particular are phagocytic cells which fulfil the important role of removing bacteria or cell debris by ingestion [Takeuchi and Akira, 2010] [Murphy et al., 2008]. Pathogenic proteins taken up in this way are processed intracellularly to antigenic peptides which are presented alongside self-derived peptide fragments on major histocompability complex (MHC) class I or II molecules. T cells of the adaptive immune system recognise foreign particles through their clonotypic antigen receptors [Kindt et al., 2007].

In humans and most other vertebrates, the adaptive immune system consists of two types of lymphocytes which express unique antigen receptors: B and T cells [Murphy et al., 2008]. B cells originate and mature in the bone marrow and respond to extracellular pathogens by secreting the B cell receptor (BCR) as antibodies [Murphy et al., 2008]. The antigen which activates the B cells becomes the epitope of the secreted antibodies. T cell

precursors also originate in the bone marrow but emigrate to the thymus to mature [Murphy et al., 2008]. T cells recognise specific antigen through the membrane-bound T cell receptor and upon activation eliminate intracellular infections and cell tranformations or mediate tolerance to self tissues and activate B cells [Murphy et al., 2008]. In both cell types the antigen receptors' high diversity is achieved through the rearrangement of V(D)J gene segments which is thought to have evolved in jawed fish about 500 million years ago [Kasamatsu, 2013]. Activation through the antigen receptors crucially results in the clonal expansion of these particular cells and thus in a highly specific immune response [Flajnik and Kasahara, 2010] [Kasamatsu, 2013]. Usually between 0.0003 to 0.001% of the entire T cell population display the specificity for a particular TCR [Blattman et al., 2002] [Obar et al., 2008]. After clonal expansion this percentage can rise to 10% of the T cell pool [Blattman et al., 2002] [Obar et al., 2008] [Amsen et al., 2013]. The requirement of APC priming of T cells and the dramatic clonal expansion process means that, unlike the immediate responses of the innate immune system, the adaptive immune response reaches peak efficiency a few days after infection [Obar et al., 2008].

1.1.2 T cell development

Unlike all other cells of the immune system, T cells develop in the thymus. T cell-competent precursors such as myeloid-lymphoid progenitors (MLPs) and common lymphoid progenitors (CLPs) arise in the bone marrow from hematopoietic stem cells (HSCs) [Bhandoola and Sambandam, 2006]

[Schwarz and Bhandoola, 2006]. MLPs and CLPs travel to the thymus via the blood stream. The earliest thymic T cell precursor stage is called double-negative 1 (DN1) because the thymocytes express neither co-receptor CD4 nor CD8 (Figure 1.1).

However, DN1 thymocytes are still very diverse in their phenotype and retain multi-lineage developmental potential. The genes encoding both TCR chains remain in their germline state at this stage [Bhandoola and Sambandam, 2006] [Murphy et al., 2008]. During the next developmental stage, double-negative 2 (DN2), the thymocytes lose the B cell-lineage potential but retain the ability to develop into DCs and NK cells [Bhandoola and Sambandam, 2006]. DN2 thymocytes express the interleukin-2 (IL-2) receptor α-chain CD25 for the first time on their surface [Murphy et al., 2008]. The thymocytes are only fully committed to the T cell lineage in the DN3 stage [Bhandoola and Sambandam, 2006]. DN3 thymocytes are characterised by the expression of the pre-αTCR chain and the somatic rearrangement of the βTCR-chain [Germain, 2002] [Murphy et al., 2008]. Similarly to the B cell receptor and its secreted form called antibodies, TCR diversity and specificity is generated through the rearrangement of V(D)J (variable, diversity and joining) gene segments at the TCR α and β loci that proceeds in a RAG-recombinase-dependent fashion [Schatz and Ji, 2011]. During the DN3 thymocyte stage, the rearranged βTCR-chain associates to the pre-αTCR and CD3-chains to form the pre-TCR (Figure 1.1). Active signalling through the pre-TCR is required for further thymocyte development. Unsuccessful βTCR-rearrangement and failure to signal through the pre-TCR results in cell death. DN4 is the last DN stage. Successful pre-TCR signalling results

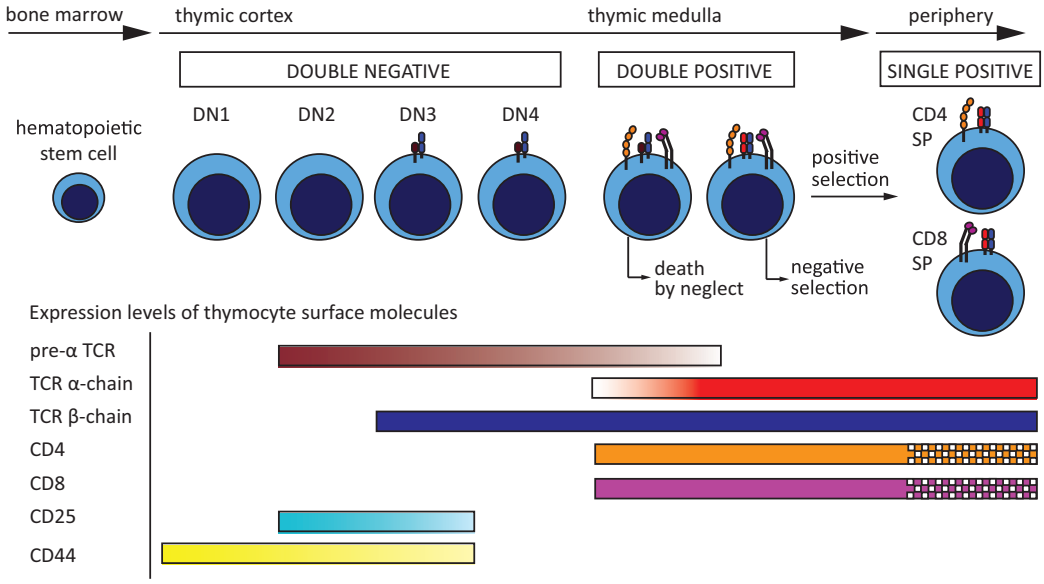

Figure 1.1: Thymic T cell development. T cell maturation occurs in the thymus. Thymic progenitors derive from hematopoietic stem cells which egress the bone marrow and migrate to the thymus via the blood. The major population of αβTCR-expressing T cells pass through a sequence of developmental stages. The stages are characterised by the expression of a variety of surface molecules as indicated by the coloured bars. The first four stages of thymic development are characterised by the lack of CD4 and CD8 co-receptor expression and are thus called double-negative (DN). The TCR β-chain is rearranged during the DN3 stage and expressed together with a pre-αTCR chain. The failure to produce TCR signalling through the pre-TCR results in death by neglect. Surviving thymocytes proliferate through the DN4 stage and progress into the double-positive stage during which both co-receptors are expressed. At this stage the pre-α-chain is lost and the mature TCR α-chain is rearranged and expressed together with the mature β-chain. Thymocytes with unresponsive or self-reactive TCRs die either by neglect or are eliminated in a process called negative selection. Positively selected thymocytes progress to the single-positive stage during which either CD4 or CD8 is expressed and migrate into the periphery.

in substantial thymocyte proliferation, the re-arrangement of the αTCR and the replacement of the pre-TCR by the mature αβTCR [Germain, 2002]. This step completes the DN thymocyte development in the outer thymic cortex. During the next stage, the thymocytes migrate towards the inner cortex and express the re-arranged TCR as well as both CD4 and CD8 co-receptors [Germain, 2002]. This stage is thus called the double-positive (DP) stage. The expression of Aire causes the expression of a wide variety of non-thymic self-peptides on MHC class I and II molecules on medullary thymic epithelial cells [Starr et al., 2003] [Rybakin and Gascoigne, 2012]. A failure to induce thymocyte signalling responses leads to cell death. DP thymocytes which respond too strongly to self-antigens and are hence likely to cause autoimmune disease in the periphery are eliminated by activation-induced cell death (ACID) in a process called negative selection [Hogquist et al., 2005] [Rybakin and Gascoigne, 2012]. Weak thymocyte responses lead to positive selection and the further development of the thymocyte [Starr et al., 2003]. The threshold of TCR:pMHC interaction affinities which induce positive or negative selection is finely tuned [Hogquist et al., 2005] [Daniels et al., 2006] [von Boehmer and Kisielow, 2006]. Positively selected thymocytes lose the expression of one co-receptor to become either CD4- or CD8-single positive (SP) T cells and egress from the thymus into the periphery as recent thymic emigrants (RTE) [Germain, 2002] [Boursalian et al., 2004]. Over the course of three weeks, the RTE mature in secondary lymphoid tissues into naive peripheral T cells. Maturation of RTE is independent of TCR signalling, exposure to IL-7 or homeostatic chemokines CCL19 and CCL21 [Houston et al., 2012]. Instead, interactions with DCs drive the phenotypic and functional

progression to naive T cells. RTEs initially home to secondary lymphoid tissues in the gut which suggests a role in developing tolerance to peripheral and environmental antigens [Houston et al., 2012] [Fink and Hendricks, 2011].

Mature naive T cells circulate continually through the blood and the lymph system. It is estimated that each naive T cell migrates through the lymphatic system in a 12 to 24 hours cycle during which the cells first reside within a lymph node, then exit the node through the efferent lymphatic system and enter the blood stream at the thoracic duct [Kindt et al., 2007].

The precise mechanisms regulating the thresholds which determine thymocyte development are yet unclear [Morris and Allen, 2012]. However, key processes of thymocyte development including positive and negative selection and the CD4-CD8 lineage decision are driven by the strength of TCR:pMHC interactions and the amplitude of the resulting intracellular signalling responses [Daniels et al., 2006] [Jang et al., 2010] [Stritesky et al., 2012].

Negative selection is associated to strong signals induced by high affinity binding of self-pMHC molecules [Hwang et al., 2012]. The strong signals are characterised by strong and transient activation of the MAP-kinase ERK at the plasma membrane [Daniels et al., 2006]. Ca^{2+} entry through CRAC channels results in a prelonged influx of ions and thus a strong Ca^{2+} signal of high amplitude [Lo et al., 2012]. Positive selection on the other hand is characterised by both weaker localised ERK responses which are focussed around the Golgi apparatus, and lower, more transient and persistent Ca^{2+} signals [Lo et al., 2012] [Daniels et al., 2006]. Recently, T cell-lineage-specific proteins which are most highly expressed in thymocytes have been described.

These proteins include Themis, Tespa1 and RhoH and have been shown to modulate thymocyte signalling [Gascoigne and Palmer, 2011] [Wang et al., 2011] [Wang et al., 2012]. Since the binding affinity threshold which defines between positively and negatively selecting ligands is very slight, small modulations of intracellular signalling strengths can impact thymocyte cell fate decisions significantly. Themis, which has been shown to regulate ERK activity, will be discussed in further detail in later chapters.

Signal amplitude and temporal cues have been implicated in determining CD4- or CD8-lineage fate. The rapid emergence of CD4-SP T cells has been linked to stronger TCR-dependent signals defined by a high abundance of ZAP-70 [Saini et al., 2010] [Gascoigne and Palmer, 2011]. Signal duration was shown to influence gene expression patterns that are exclusive of each other and could influence the activity of master transcription factors that determine fate decisions between the CD4 and CD8 lineages [Yasutomo et al., 2000]. CD4-lineage-specific transcription factors include Th-POK and GATA-3 [Park et al., 2010]. Runx-3 activity on the other hand is essential for the CD8-SP lineage decision. It is induced by IL-7 stimulation which implicates not only TCR-dependent but also cytokine-induced signalling in determining the T cell lineage in the thymus [Yasutomo et al., 2000] [Park et al., 2010].

1.1.3 T cell subsets

Mature naive peripheral T cells bearing the αβ-TCR are defined into several subsets. The function of T helper (T_H) and T cytotoxic (T_C) cells corre-

lates with the expression of CD4 and CD8 co-receptor molecules respectively [Kindt et al., 2007]. Regulatory T (T_{reg}) cells express the high levels of the Foxp3 transcription factor and CD4 and CD25 co-receptors [Sakaguchi, 2003]. While T_H and T_C cells promote immune effector functions, T_{regs} regulate peripheral tolerance to self and environmental antigens [Kindt et al., 2007] [Gottschalk et al., 2010].

CD4 and CD8 co-receptors CD4 and CD8 co-receptors are the main subset-defining surface molecules of peripheral T cells. Despite sharing no overall homology, CD4 and CD8 carry out similar functions. Both molecules are transmembrane glycoproteins of the immunoglobulin gene superfamily [Janeway, 1992]. The extracellular domains of CD4 and CD8 bind to both the pMHC complex classes II and I respectively (Figure 1.2) [Janeway, 1992]. Whether these interactions promote TCR signalling by stabilising TCR:pMHC interactions by lowering the off-rate is controversial since the binding affinity of CD4 and CD8 to the TCR and pMHC molecules is very low as further discussed later [Artyomov et al., 2010] [Hutchinson et al., 2003]. The intracellular domains of both molecules bind through the conserved CxCP motif to the Src-kinase LCK via its CxxC sequence and mediate the delivery of LCK to the TCR:CD3 complex (Figure 1.2) [Shaw et al., 1990] [Turner et al., 1990]. Phosphorylation of CD3-ITAM tyrosines by LCK is essential to the induction of TCR signalling events. However, while the expression of CD4 and CD8 augments T cell responses to weak ligands, their presence is not essential to produce positive TCR signalling. TCR:pMHC interactions with an affinity greater than 10 μM result in strong T cell activation regardless of

CD4 or CD8 expression [Stone et al., 2009] [Artyomov et al., 2010].

CD4 is a transmembrane monomer whose extracellular tail contains four immunoglobulin-like domains (Figure 1.2) [Kindt et al., 2007]. The first two membrane-distal domains (D1 and D2) are closely associated to each other and linked through a flexible joint to the second two membrane-proximal domains (D3 and D4) [Kindt et al., 2007] [Li et al., 2013]. CD4 interacts through its D1 domain with the membrane-proximal invariable α2 and β2 chains of pMHC class II [Li et al., 2013]. The binding of CD4 to pMHC class II is very weak at 150 to 200 μM [Krummel et al., 2000] [Li et al., 2013]. Both the TCR and CD4 are able to bind to a pMHC class II molecule simultaneously yet independently because CD4 does not directly interact with the TCR (Figure 1.2). Instead a rigid CD4 arch is formed which poses constraints for the organisation of CD3 and LCK around the TCR. LCK is recruited to the TCR by binding via its N-terminal unique domain to the flexible intracellular C-terminal tail of CD4 [Li et al., 2013] [Boggon and Eck, 2004].

In contrast, CD8 exists as a αα homo- or αβ heterodimer which are both recruited to the immunological synapse (Figure 1.2) [Sun and Kavathas, 1997] [Rybakin et al., 2011]. While CD8αα is expressed by γδ T cells and NK cells, CD8 αβ dimers are present in αβTCR thymocytes and peripheral T cells [Sun and Kavathas, 1997] [Li et al., 2013]. The extracellular N-terminal domain of both CD8 subunits is characterised by a long stalk and a membrane-distal globular domain [Boursier et al., 1993]. During T cell recognition of antigenic ligands, the TCR binds first to the pMHC class I complex. Binding of the CD8α domain to a protruding loop on the α3 subunit of MHC class

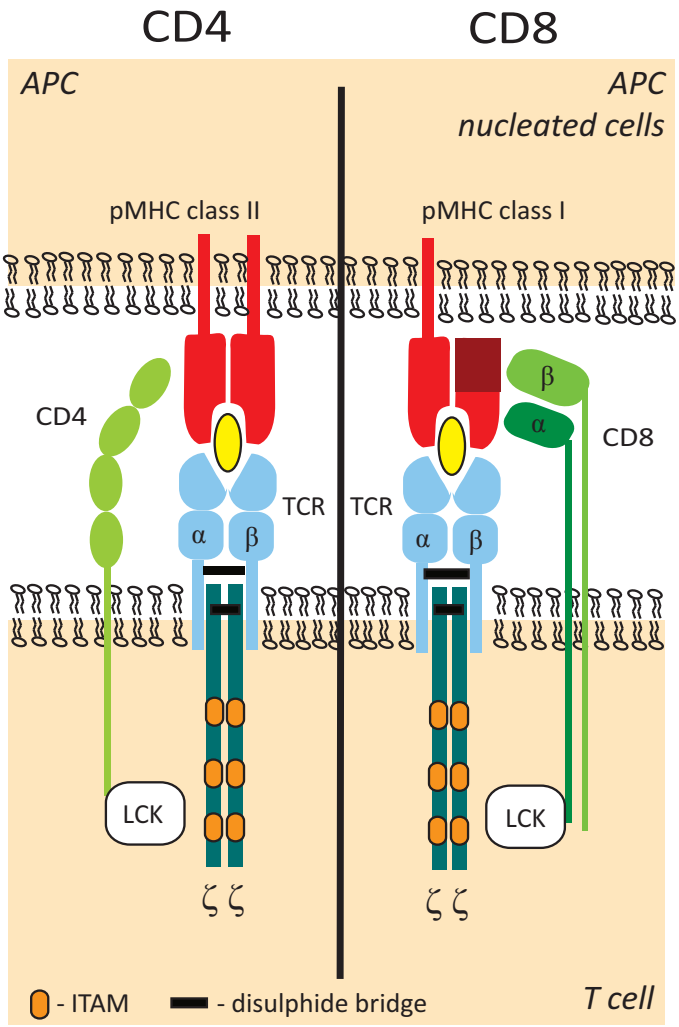

Figure 1.2: The CD4 and CD8 co-receptors. T cell lineage is defined by the expression of either CD4 or CD8 co-receptor. Both receptors interact with MHC molecules through their extracellular domains and with LCK through their intracelluar domains. CD4 is a monomer which contains four globular domains. The most membrane-distal domain interacts with pMHC class II which is expressed on professional APC and presents longer peptides derived from endocytosed extracellular proteins. CD8 exists as either $\alpha\alpha$ or $\alpha\beta$ dimers. The subunits each contain a long extracellular stalk region with a single globular domain at the end. This domain binds to MHC class I which is expressed on all nucleated cells and presents short peptide fragments of intracellular proteins.

I follows suit. This sequence of events ensures that TCR specificity and binding kinetics determine T cell responses [Li et al., 2013]. The affinity of CD8α for MHC class I is low between 65 and 200 μM and the interactions display fast off-rates of 18 sec^{-1} [Kern et al., 1999] [Wyer et al., 1999]. The intracellular C-terminal domain of CD8α binds to LCK and recruits it to the TCR signalling interface [Purbhoo et al., 2001] [Li et al., 2013]. Rather than structurally stabilising TCR:pMHC interactions, the recruitment of LCK to the TCR is the primary function of CD8 [Purbhoo et al., 2001] [Hutchinson et al., 2003]. Unlike CD8α, CD8β is palmitoylated at the cytoplasmic tail [Arcaro et al., 2000] [Arcaro et al., 2001]. This locates the CD8αβ dimer to the same lipid raft as CD4 or the TCR and is thought to underline the increased efficiency of CD8αβ in augmenting TCR signalling [Arcaro et al., 2000] [Arcaro et al., 2001].

$CD4^+$ effector T cells CD4-positive T_H cells reside preferentially in the T cell zones of the secondary lymphoid tissues [Kindt et al., 2007]. Here, the APC and B cell density is particularly high and T_H cells are able to interact very frequently with either cell type [Kindt et al., 2007]. The major function of T_H cells is to provide help to other lymphoid cells in the form of co-stimulation and cytokine release [Magombedze et al., 2013]. Three signals are necessary to activate T_H cells: The first signal is represented by the binding of the cell's TCR to pMHC class II on APC. Secondly, the co-stimulatory molecule CD28 binds to CD80 or CD86 on APC. Lastly, the exposure to cytokines released by APC or already present at the site of T cell activation determines the development of T_H cells into particular effector

cell subsets [Magombedze et al., 2013]. Exposure to IL-12 provided by DCs initiates the differentiation of naive T_H into T_H1 effector cells. T_H1 cells express the transcription factor T-bet and secrete IFN-γ and TNF-α. This subset is important to activate macrophages to kill intracellular pathogens and provide help to B cell activation and antibody production [Magombedze et al., 2013] [Murphy et al., 2008]. T_H2 cells emerge following the exposure to IL-4. These $CD4^+$ T cells express the transcription factors GATA-3 and orchestrate the immune responses to extracellular bacterial infections and parasites [Magombedze et al., 2013]. Another $CD4^+$ effector T cell class is termed T_H17 cells due to their secretion of IL-17 and IL-22 that IL-17 and IL-22 stimulates epithelial and mucosal barrier cells to produce anti-microbial molecules and protect the body from opportunistic infection. Differentiation to the T_H17 phenotype requires exposure to the cytokines IL-6 and TGF-β [Magombedze et al., 2013]. Follicular T helper cells (T_{FH}) are specialised to provide help to B cells within germinal centres to promote B cell antibody affinity maturation, class switch recombination, plasma cell and B memory cell differentiation [Crotty, 2011]. The formation of follicles by B cells mediated by the secretion of chemokine CXCL13 by T_{FH} and its recognition by the correspondent B cell receptor CXCR5 [Crotty, 2011]. Their phenotype depends on the expression of the transcription factor Bcl-6 [Crotty, 2011].

CD4-$^+$ regulatory T cells Regulatory T (T_{reg}) cells are a further remarkable CD4-positive T cell subset. This subset is defined by the expression of the transcription factor Foxp3 and the high levels of the surface IL-2-receptor CD25 [Gratz et al., 2013] [Tang and Bluestone, 2008]. Heredi-

tary fatal multiorgan autoimmunity conditions such as immunodysregulation polyendocrinopathy enteropathy X-linked syndrome (IPEX) in humans and mice are linked to mutations of the *foxp3* gene locus and a resultant absence of T_{regs} [Sakaguchi, 2003]. T_{regs} develop primarily from thymocytes which recognise self-antigen with relatively high affinity (called agonist selection) but are not negatively selected as a consequence of the strong agonist [Stritesky et al., 2012] [Gratz et al., 2013]. The TCR repertoire of T_{regs} is diverse and their maturation life-cycle closely resembles that of effector T cells [Hsieh et al., 2006] [Gratz et al., 2013]. Furthermore, the regulatory phenotype is inducible in the periphery following persistent exposure to high affinity self antigen or common harmless environmental antigens. Epithelial cells of the respiratory and gastric tracts are sensitive sites which are gateways for infection. But these organs are also exposed to many inert environmental agents such as pollen, food antigens or commensal bacteria towards which the immune system remains inactive [Sakaguchi, 2003].

T_{regs} maintain tolerance by exerting suppression on the proliferation, survival, maturation, cytotoxicity and cytokine and chemokine release of other lymphocytes [Tang and Bluestone, 2008] [Huang et al., 2012]. The activation of regulatory functions depends on TCR:pMHC interactions and exposure to TGF-β. Yet the suppressive activity of T_{regs} itself is antigen-nonspecific and APC-independent [Tang and Bluestone, 2008]. Upon activation, T_{regs} release IL-10 and TGFβ suppressive cytokines which inactivate the responses of other immune cells within the vicinity [Magombedze et al., 2013]. Additionally, IL-2 plays a vital role in the function of T_{regs}. The high expression of CD25 is thought to deplete the T_{reg} environment of effector-function-

promoting IL-2 [Gratz et al., 2013]. In fact, IL-2 seems to be involved in a negative feedback loop regulating T_{reg} function [Gratz et al., 2013]. IL-2 is secreted by activated effector lymphocytes but not T_{regs}. Yet T_{regs} require IL-2 to maintain the suppressive phenotype [Gratz et al., 2013].

CD8-$^+$ effector T cells CD8-positive T cells are also known as cytotoxic T lymphocytes (CTL). They recognise virus-derived antigenic peptides or cancer-specific self-peptides presented on pMHC class I molecules on most nucleated cells of the body [Murphy et al., 2008]. Their primary function is to eliminate infected or transformed cells specifically without damaging surrounding healthy tissues [Murphy et al., 2008]. Similarly to CD4-positive lymphocytes, naive CD8-positive lymphocytes reside primarily in the secondary lymphoid tissues and require priming by antigen-bearing professional APC for full activation [Zhang et al., 2011]. During the priming process the APCs also provide crucial co-stimulation for effective activation. Upon recognition of cognate antigen, the CD8-positive T cells exit the lymph nodes, enter the peripheral tissues through the blood stream and proliferate extensively such that CD8 T cell numbers are able to increase by 10^4-fold [Zhang et al., 2011] [Amsen et al., 2013]. CD8-positive T cells require proinflammatory cytokines such as IL-12 and IL-2 for inducing terminal T effector cell differentiation and effector functions [Zhang et al., 2011]. Upon recognition of the cognate antigen at the site of infection, primed CD8-positive T cells enhance adhesion to the target cell by upregulating LFA-1 and CD2. They proceed to kill the infected cell through the directed release of cytotoxic granules. Finally, they recruit further cells of the immune system by the release of

pro-inflammatory cytokines IFN-γ and TNF-α. Macrophages are among the cells that are recruited to remove the debris of killed target cells [Northrop and Shen, 2004] [Zhang et al., 2011] [Murphy et al., 2008].

Two modes of cytotoxicity have been described: The Ca^{2+}-dependent killing by perforin and granzymes and the Ca^{2+}-independent interactions of Fas-ligand (FasL) and Fas on the surface of the target cells. The two pathways are closely linked to each other [Dustin and Long, 2010]. Perforin-mediated killing is based on injury to the membranes of the target cell and on endosomal lysis which causes the release of granzymes into the target cell's cytosol [Dustin and Long, 2010]. Killing through FasL interactions requires cell-cell contact and is often located to the cytotoxic granules which carry perforin and granzymes [Dustin and Long, 2010]. The cytotoxic granules are transported to the immunological synapse upon TCR triggering in a Ca^{2+}-dependent manner analogous to the release of neurotransmitter granules into neurological synapses [Murphy et al., 2008]. Sequestering Fas in cytotoxic granules in resting T cells ensures that the T cells remain innocuous against uninfected cells [Dustin and Long, 2010]. The release of the cytotoxic granules into the immunological synapse is highly directed to furthermore ensure the specific killing of the target cell and the preservation of surrounding tissues [Dustin, 2008]. T cell activation causes the re-orientation of the centrosome (called microtubule-organizing center (MTOC) in T cells) into a membrane- and IS-proximal position [Huppa and Davis, 2003]. This causes the re-arrangement of the cytoskeleton towards the IS. The cytotoxic granules travel towards the IS along the re-directed microtubules [Dustin, 2008] [Dustin and Long, 2010].

During the later stages of the immune response, CD8-positive T cells exert self-regulatory functions. The increased release of the anti-inflammatory cytokine IL-10 dampens their cytotoxic immune response and prevents excessive tissue damage [Zhang et al., 2011]. The T cell response is ablated by the programmed contraction by cell death of up to 90 to 95% of the activated T effector cell population [Remakus and Sigal, 2013].

Memory T cells The establishment of an immunological memory is a fundamental property of the adaptive immune system. CD8 T cell numbers expand up to 10^4-fold during an active immune response [Gourley et al., 2004]. Following the successful eradication of the infection, 90 to 95% of effector T cells die [Remakus and Sigal, 2013]. The surviving cells form a pool of memory T (T_{mem}) cells which constitute 5 to 10% of the total peripheral T cell population [Amsen et al., 2013]. T_{mems} are activated by low levels of antigenic pMHC and require little or no co-stimulation for activity [Gourley et al., 2004]. The rapid mobilisation of T_{mem} effector function enables the efficient eradication of recurrent infection and assists any new naive T cell responses [Gourley et al., 2004] [Remakus and Sigal, 2013]. Two subpopulations of T_{mem} are recognised based on their residence in either the secondary lymphoid tissues of the spleen and the lymph nodes (T central memory, TCM) or non-lymphoid tissues (T effector memory, TEM) [Amsen et al., 2013].

The T_{mem} pool is build alongside the immune response. Activation of CD8-positive T cells generates two types of effector cells: short-lived effector cells (SLEC) and memory precursor effector cells (MPEC) [Northrop and Shen,

2004] [Joshi et al., 2007] [Chang et al., 2011]. SLECs provide immediate immune protection. MPECs form the memory T cell pool. These cells are longer lived and depend on IL-15 for survival. Commitment to the memory T cell line is thought to be determined by asymmetric division of TCR-engaged CD8-positive T cells [King et al., 2012]. Daughter cells of the cSMAC proximal half of the T cell develop into SLEC, while the distal half produces MPECs [Joshi et al., 2007] [Chang et al., 2011] [Amsen et al., 2013]. Besides IL-15, T_{mem} require stimulation by IL-12 and through the TNF-receptors CD27 and OX40 [Chang et al., 2011] [King et al., 2012] [Amsen et al., 2013]. In contrast to $CD8^+$ memory T cells the nature and function of $CD4^+$ is more elusive and less well understood [MacLeod et al., 2010] [Pepper and Jenkins, 2011]. The development of $CD4^+$ T_{mem} is thought to be induced by strong TCR signals and exposure to IL-7 [MacLeod et al., 2010] [Pepper and Jenkins, 2011]. $CD4^+$ T_{mem} reside in the secondary lymphoid tissues [Pepper and Jenkins, 2011]. Upon re-stimulation, they show less proliferative capabilities than $CD8^+$ T_{mem} [MacLeod et al., 2010]. Instead, their primary function might lie in emigrating to the sites of re-infection and produce pro-inflammatory cytokines to help induce fast and effective immune responses *in situ*. This could represent a very important contribution of $CD4^+$ T_{mem} to the efficacy of modern vaccines [MacLeod et al., 2010].

1.2 The T cell receptor

The recognition of agonist pMHC by TCR and the following signalling events determine the specificity and extent of T cell effector functions [Morris and

Allen, 2012]. Since its discovery in 1983, the TCR has been studied extensively [Haskins et al., 1983] [Meuer et al., 1983b]. However, the TCR is an unconventional and complex receptor and many aspects of its mechanism of function still remain elusive.

1.2.1 Structure and arrangement

The TCR is a type I transmembrane heterodimer of disulphide-bond-linked α and β subunits (Figure 1.3). Both the TCR α- and β-chains present with extracellular membrane-distal Ig-variable and membrane-proximal Ig-constant domains which together resemble the structure of antibodies [Acuto et al., 1983] [Gascoigne et al., 1984] [Acuto and Reinherz, 1985] [Garcia et al., 1996]. The TCR ligands are MHC molecules. The class I complex is expressed on the surface APC and the class II complex on APC and all nucleated cells. MHC molecules present linear peptide fragments of processed intracellular proteins. Details about the structure and function MHC molecules specifically are discussed later. The TCR contacts the pMHC complexes through the highly variable CDR3 loops of the variable TCR domains [Jorgensen et al., 1992]. The TCR is thought to recognise antigenic pMHC via a two-step process. First, the relatively rigid CDR1 and CDR2 loops of the α and β variable domains dock to the pMHC complex. This process is comparable to a 'lock and key' process and involves minimal interactions with the peptide in the MHC groove [Jorgensen et al., 1992]. Secondly, the CDR3 loop displays the structural flexibility to 'fold' into the peptide groove [Jorgensen et al., 1992]. This induced fit model confers the specificity of TCR

recognition. A poor fit results in fast TCR:pMHC dissociation and does not bind long enough to support the establishment of a signal [Wu et al., 2002] [Krogsgaard et al., 2003] [Krogsgaard and Davis, 2005].

The cytoplasmic tails of the αβ-TCR are short and without signal propagating function [Berkhout et al., 1988] [Weissman et al., 1988]. Instead, the TCR intricately but non-covalently associates with three CD3 dimers: CD3γε, CD3δε and CD3ζζ (Figure 1.3) [Berkhout et al., 1988] [Weissman et al., 1988] [Kuhns et al., 2006]. The subunits of the CD3γε and δε dimers associate extracellularly through paired single Ig folds [Kuhns et al., 2006]. The extracellular domain of CD3ζζ is only nine amino acids long and of unknown structure [Kuhns et al., 2006]. CD3ζζ dimers associate covalently through cysteine residues within the transmembrane region of the protein. The cysteine residues form disulphide bridges to link the two CD3ζ monomers [Call et al., 2002]. The TCR α and β-chains associate non-covalently to the CD3 subunits through basic transmembrane residues to acidic transmembrane residues of the CD3 chains [Meuer et al., 1983a] [Manolios et al., 1994] [Call et al., 2006].

All CD3 cytoplasmic chains contain at least one, and in the case of CD3ζ three, immunoreceptor tyrosine-based activation motifs (ITAMs). The total number of ITAMs within the CD3 compex is ten [Zarnitsyna and Zhu, 2012]. The motif contains two tyrosine residues each separated from an isoleucin or leucin residue by two further amino acids ($YxxL/Ix_{(6-8)}YxxL/I$ - x denominates any amino acid) [Kuhns et al., 2006] [Murphy et al., 2008] [Zarnitsyna and Zhu, 2012]. The simultaneous binding of co-receptors CD4 and CD8 to pMHC class II or I during TCR:pMHC binding recruits the Src-kinase LCK

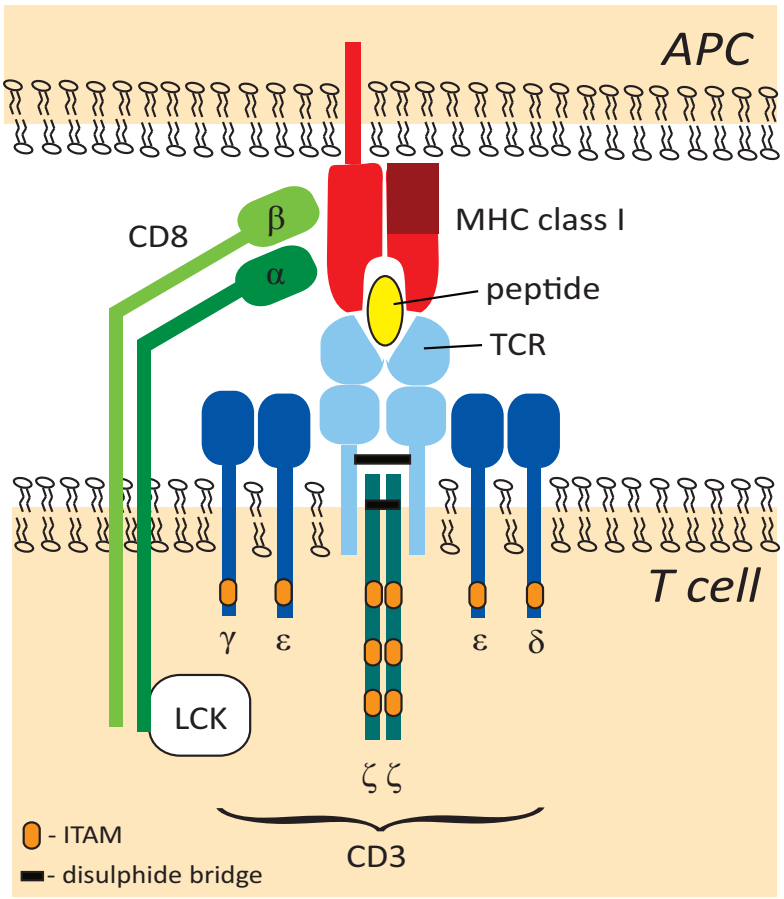

Figure 1.3: Structure of the T cell receptor. The TCR contains the clonotypic α and β chains which are linked to each other by disulphide bridges. Each chain is comprised of a membrane-proximal constant and a membrane-distal variable region. pMHC binding proceeds through the CDR chains of the variable regions. The TCR chains associate non-covalently with three CD3 dimers: γε, δε and ζζ. Unlike the TCR the CD3 chains contain signal transducing immunoreceptor tyrosine-based activation motifs (ITAMs).

to the TCR:CD3 complex. Upon TCR triggering, recruited active LCK phosphorylates the ITAM tyrosines of the CD3 cytoplasmic chains [Nika et al., 2010]. This is the initial step of the TCR signalling cascade which is discussed in more detail at a later point. It is unknown how the CD3-ITAMs remain unphosphorylated or poorly phosphorylated during quiescence. The cytoplasmic tails of all CD3 molecules are intrinsically disordered and highly flexible [Sigalov, 2010]. Basic residues of CD3ε and ζ preceeding the ITAMs have been shown to associate to acidic phospholipids on the inner leaflet of the plasma membrane thus embedding the ITAM-tyrosines into the plasma membrane and may be rendering them inaccessible for LCK-phosphorylation [Risueño et al., 2008] [Xu et al., 2008] [Gagnon et al., 2012]. Slight conformational changes during TCR triggering are thought to be transmitted to the cytoplasmic tails of CD3ε and ζ which then adopt random coil conformation instead of a helical one [Risueño et al., 2008] [Sigalov, 2010]. This may cause the dissociation from the plasma membrane and the induction of the signal by phosphorylation of the ITAMs by LCK.

From the crytallographic structural data, the TCR undergoes no major conformational changes upon pMHC binding, which might explain how TCR:pMHC binding is converted into CD3-ITAM phosphorylation and signal transduction [Krogsgaard and Davis, 2005]. However, until dynamic structural data for example from NMR (nuclear magnetic resonance) will be available, it is difficult to determine with confidence whether conformational changes do not take place. Four scenarios focus on extracellular domain conformational changes which link the TCR and CD3 chains [San Jose et al., 2000] [Kuhns et al., 2006]. The first scenario proposes a conformational change of the TCR

which causes the re-orientation of loosely associated CD3 dimers rendering the ITAMs accessible for phosphorylation. In the second scenario, the CD3 extracellular domains are strongly associated to the TCR. When the TCR is engaged it undergoes a conformational change which causes the CD3 heterodimers to move. Yet, no major conformational changes in the TCR:CD3 complex has been observed experimentally [Kjer-Nielsen et al., 2003]. In contrast to the first two, the third scenario suggests that CDR3 conformational changes during pMHC binding are subtly transmitted through the TCR. This causes a subtle reorientation of the TCR and the loosely associated CD3 heterodimers [Krogsgaard et al., 2003] [Kuhns et al., 2006]. The fourth scenario suggests that the TCR works as a mechanoreceptor which converts the mechanical energy generated by the torque of molecular movements between the cell membranes of the T cell and the APC into a biochemical signal [Kim et al., 2009] [Kim et al., 2012]. Experiments with tweezers have shown that the TCR responds to mechanical stress [Kim et al., 2009]. The torque generated when the TCR and pMHC bind to each other within moving molecular environments could cause structural rearrangements to the TCR and CD3 chains which induce CD3-ITAM phosphorylation [Kim et al., 2012]

As yet, any consensus structural mechanism for how TCR triggering translates into signal propagation through the CD3 chains remains elusive and controversial.

1.2.2 Major histocompability complex molecules

T cells only recognise antigens which are presented to them via major histocompability complex (MHC) molecules [Murphy et al., 2008]. There are two classes of MHC molecules - classes I and II - which possess different structures and tissue-specific expression patterns. .

Both classes are highly polymorphic and present peptides to the TCR [Bouvier, 2003]. The peptide fragments derive from intracellularly processed proteins. The two complexes present peptides of proteins from different sources [Murphy et al., 2008]. This is also reflected in the cell types which express the respective pMHC complexes. The MHC class I molecules are expressed on virtually all nucleated cells of the body [Murphy et al., 2008]. The molecule consists of an α-chain which spans the plasma membrane and a smaller β_2-microglobulin-chain (Figure 1.2) [Bouvier, 2003]. The α-chain is furthermore divided into three subdomains of which the membrane-distal $\alpha 1$ and $\alpha 2$ domains form the peptide-binding groove [Bouvier, 2003]. MHC class I molecules present short peptides of 8 to 10 amino acids in length [Rock et al., 2002]. These peptides are produced through proteosomal degradation of cytosolic proteins and loaded onto the MHC molecule in the endoplasmic reticulum [Rock et al., 2002]. Both peptides derived from self or intracellular pathogens can be displayed by MHC class I molecules which is recognised by CD8-positive cytotoxic T cells.

MHC class II molecules are displayed on cells of the immune system including DCs, macrophages and B cells [Murphy et al., 2008]. CD4-positive T helper cells interact with pMHC class II-positive antigen presenting cells. The pep-

tides presented by MHC class II at least 13 amino acid residues long and derive from extracellular proteins which have been endocytosed and degraded and loaded on MHC class II molecules within acidified endosomes [Kobayashi and van den Elsen, 2012]. Structurally, MHC class II molecules also contain an α- and β-chain. Each chain contains a membrane-distal peptide-binding domain and a transmembrane region (Figure 1.2) [Fremont et al., 1996].

1.2.3 TCR co-receptors and co-stimulatory molecules

While TCR engagement represents the determining signal for the induction of T cell effector functions, TCR signalling on its own is not sufficient to cause full physiologic T cell activation [Morris and Allen, 2012] [Chen and Flies, 2013]. Almost all cells, but especially professional APCs, display a large array of co-signalling receptors. The engagement of co-signalling receptors is able to positively or negatively modulate T cell signalling [Chen and Flies, 2013]. Co-signalling signals are constant and invariable in the strength of the stimulation they provide: Co-stimulatory molecules lower the TCR signal threshold and augment the commitment of the T cells towards effector functions, proliferation and differentiation [Kalland et al., 2011]. Co-inhibitory signals in turn dampen T cell responses [Chen and Flies, 2013]. Most co-stimulatory or -inhibitory molecules belong to either the immunoglobulin (Ig) superfamily or the tumour necrosis factor receptor superfamily (TNFRSF) [Chen and Flies, 2013]. In the following section I will briefly summarise some important co-stimulatory molecules and their contribution to T cell activation.

The CD4 and CD8 lineage-defining co-receptors were already discussed in

detail in previous chapters (Figure 1.2). Briefly, both molecules are transmembrane glycoproteins which alongside the TCR interact with pMHC via their extracellular domain. CD4 recognises the pMHC class II and CD8 the pMHC class I molecule [Janeway, 1992]. The cytoplasmic tails of CD4 and CD8 interact with the Src-kinase LCK. The co-receptors fulfil two functions: the stabilisation of weak TCR:pMHC interactions and, more importantly, the recruitment of LCK to the signal transducing ITAMs of the cytoplasmic chains of the six CD3 chains associated to the TCR [Purbhoo et al., 2001]. Phosphorylation of the tyrosines of the CD3 ITAMs by LCK initiates active TCR signalling events [Boggon and Eck, 2004]. CD4 and CD8 lineage specificity arises during thymocyte development [Germain, 2002].

CD28 is a T cell specific transmembrane homodimer with an Ig-like extracellular domain [Acuto et al., 2003] [Chen and Flies, 2013]. It recognises CD80 and CD86 which is upregulated on the surface of activated APC. Binding of CD28 to its ligands alone does not support the activation of T cell effector functions or clonal expansion. Yet, the induction of CD28-downstream signalling pathways provide synergistic signals to reinforce the amplitude and duration of TCR signals [Kalland et al., 2011] [Chen and Flies, 2013]. TCR triggering in the absence of CD28 leads to T cell anergy and cell death because of the lack of CD28-activated anti-apoptotic and cell cycle progression signals. CD28 thus poses an important second signal besides the TCR signal which determines T cell activation [Acuto and Michel, 2003]. During T cell triggering, CD28 co-locates with the TCR in the cSMAC area of the IS [Chen and Flies, 2013]. While CD28 does not induce signalling through ZAP-70 and the LAT-SLP-76 complex, it has been shown to induce the activity of kinases

LCK, PI3K, Vav1, Akt and MAPK, anti-apoptotic BcL-X_L and transcription factors NF-AT and NF-$\varkappa$B [Acuto et al., 2003]. Important results of CD28 signalling are the potent induction of IL-2 transcription and release. $CD28^-$ $CD8^+$ cells only release IL-2 following extremely strong stimulation by for example PMA-ionomycin [Topp et al., 2003]. Furthermore, the expression of IL-2R α-chain (CD25), IL-12R, the chemokine receptor CXCR5 and co-stimulatory molecules OX-40, ICOS and CD40L are also increased through CD28-dependent signalling responses [Acuto and Michel, 2003].

Similarly to CD28, CD2 is involved in priming naive T cells towards full activation [Chen and Flies, 2013]. CD2 recognises the APC surface protein CD58 and augments cell adhesion [Kalland et al., 2011]. Furthermore, CD2 signalling along the ZAP-70 signal pathway assists proximal TCR signalling [Kalland et al., 2011]. However, CD2 does not increase TCR signal strength to the same extent as CD28 and cannot initiate T cell activation on its own [Michel et al., 2001]. A further important adhesion molecule is LFA-1 which recognises ICAM-1 on the APCs' surface [Acuto and Michel, 2003].

CD45 is a heavily glycosylated tyrosine-specific phosphatase which is essential for effective TCR signalling [Janeway, 1992] [McNeill et al., 2007]. Up to eight isoforms of the CD45 extracellular domains are produced by alternative splicing and their expression is T cell subset-specific. The CD45RO isoform, for example, is primarily found in thymocytes and activated T cells whereas the CD45RA isoform is expressed by naive and memory T cells [Janeway, 1992] [Zamoyska, 2007]. Because of its large glycosylated extracellular domains, CD45 is thought to be excluded from cSMAC and is thus spatially prevented from de-phosphorylating and inhibiting the activity of TCR prox-

imal signalling molecules such as LCK (Figure 1.4) [Burroughs and van der Merwe, 2007].

The catalytic function of CD45 is found in its constant cytoplasmic domain. It dephosphorylates both the activating tyrosine-394 and the inactivating tyrosine-505 residues of LCK, its primary substrate. Thus it both positively and negatively regulates TCR signalling (Figure 1.8, inset box) [McNeill et al., 2007].

1.2.4 TCR triggering kinetics

Even though the TCR was discovered about 25 years ago, its precise mechanism of action remains unknown [Reinherz and Acuto, 2011]. The TCR is a unconventional and complex receptor whose ligand recognising α and β-chains have no cytoplasmic signal transducing function. Instead, TCR triggering is transmitted in an unknown manner to the cytoplasmic chains of the associated CD3 molecules. Signal transduction is initiated through the phosphorylation of the ITAM-tyrosines on the cytoplasmic CD3-chains [Germain, 2001]. TCR signalling results in T cell effector functions that are specific to the peptide encountered on MHC [Kuhns et al., 2006]. T cells have the potential to induce strong effector functions to any peptide presented. However, thymocytes which are highly reactive to self-derived peptides are eliminated during negative selection. Positively selected peripheral T cells interact weakly with self peptides. This interaction results in weak tonic signalling which maintains peripheral T cell homeostasis and self-tolerance [Morris and Allen, 2012]. However, the presentation of peptides of foreign

origin has the potential to induce strong T cell effector responses including the targeted cytolysis of the recognised target cell. This is dependent on the peptides' sequence. At resting state only 0.0003 to 0.001% of T cells will possess the TCR specificity towards a particular antigen [Blattman et al., 2002] [Obar et al., 2008] [Amsen et al., 2013].

Since self- and agonist peptides are potentially closely related structurally - their sequence could differ by as little as one amino acid - the specificity of the TCR is a remarkable feat [Morris and Allen, 2012]. The precise mechanism of how the TCR distinguishes qualitatively between different pMHC is still poorly understood. Effective T cell activation requires the TCR:pMHC interactions to fulfil four requirements: the recognition of agonist pMHC has to proceed with speed, be specific towards the agonist peptide's sequence, be robust to 'noise' from an abundance of self-peptide MHC and be sensitive to low agonist ligand densities [Burroughs and van der Merwe, 2007]. Precisely how various structural, spatial, stochastic and kinetic TCR:pMHC binding parameters contribute to T cell activation remains controversial [van der Merwe, 2001]. In the following chapter, I will provide an overview of the most common models towards the kinetics underlying TCR recognition of agonist pMHC.

Structural and spatial aspects of TCR triggering kinetics. The TCR is an unconventional receptor which has no kinase activity and X-ray analyses reveal no obvious structural mechanism to initiate the phosphorylation of CD3 ITAMs and thus activate TCR signalling [van der Merwe, 2001]. Many diverse theories attempt to explain TCR triggering structurally and

spatially. They all focus on three basic principles: aggregation, conformational change and segregation [Burroughs and van der Merwe, 2007] [Kuhns and Davis, 2012].

Aggregation of the TCR is thought to enhance signalling by increasing the dwell time of pMHC:TCR interactions through the cooperative binding of multiple TCRs and pMHC at once. On the T cell surface, about 45% of TCRs are thought to be in a monovalent state, while 30% associate into dimers or trimers and 10% form larger clusters [Schamel et al., 2005] [Lillemeier et al., 2010]. The formation of microclusters has been observed to occur simultaneously with Ca^{2+} signalling [Campi et al., 2005]. Protein islands of TCR clusters and their associated molecules contain up to 70 to 300 TCRs [Lillemeier et al., 2010]. Schamel et al., 2005, observed that microclusters formed linear complexes. TCR:pMHC interactions are likely to require an optimal half-time to induce active proximal signalling which is neither too long nor too short. Flexible binding kinetics allow the sequential association and dissociation of a pMHC molecule to neighbouring TCRs. This sequential engagement of the same of closely associated TCRs reinforces signalling pathways and results in sustained activation.

Conformational models

Conformational change models suggest that the TCR undergoes structural rearrangements upon pMHC engagements which transmits the cue to activation to the CD3 signal transducing complex [Gil et al., 2002]. The two-step model discussed earlier offers structural explanations towards how the TCR is able to distinguish between self- and agonist peptides [Krogsgaard and

Davis, 2005]. According to the two-step model, recognition of pMHC first proceeds in a lock-and-key type manner through binding of the poorly flexible CDR1 and 2 loops of the TCR V-domain. If this initial binding is of sufficient strength the flexible CDR3 loop folds around the peptide complex in a manner described as an induced fit [Krogsgaard and Davis, 2005] [Wu et al., 2002]. Yet, apart from the flexibility of the CDR chains, only minor conformational changes have been observed within the general TCR complex upon ligand binding in crystals. These changes are virtually the same between bound agonist, superagonist and non-agonist pMHC [van der Merwe, 2001]. It is difficult to envision how such small changes in structure could transmit subtle differences in binding quality to the CD3 signalling complex to initiate distinct T cell effector responses. One theory suggests that in the resting state the cytoplasmic tails of CD3ε and ζ are associated to acidic phospholipids of the plasma membrane [Risueño et al., 2008] [Gagnon et al., 2012]. Subtle twists in the TCR chains' structure leads to the reorientation of the CD3 cytoplasmic chains and their dissociation from the plasma membrane. This model explains both how structural changes could be transferred from the TCR to the CD3 signal transducing complex and how ITAM phosphorylation by pre-activated LCK only occurs after TCR triggering and not in resting T cells [Risueño et al., 2008] [Xu et al., 2008]. TCR triggering can also be induced by mechanical stresses. Both the TCR and pMHC molecules are tethered to the membranes of their respective cells. Molecular movements between the cell interfaces creates torque which induces a piston-like movement of the entire TCR-CD3 complex. Experiments with tweezers have shown that the mechanical stress induces TCR signalling and decreases the

half-time of the TCR:pMHC interactions [Kim et al., 2009] [Kim et al., 2012].

Kinetic models

The kinetic segregation model is based on the spatial arrangement of the TCR and its co-receptors after pMHC binding. The TCR and co-stimulatory molecules such as CD28 possess short ectodomains and the binding of these molecules to their ligands draws the T cell-APC interfaces into close localised proximity [Choudhuri et al., 2005] [Davis and van der Merwe, 2006] [Choudhuri and van der Merwe, 2007]. Co-inhibitory molecules such as the phosphatases CD45 and CD148 are excluded from the site of contact by large and bulky ectodomains (Figure 1.4). This removes the phosphatases from their substrates which are located to the TCR and promotes and reinforces tyrosine phosphorylation signalling events and ultimately T cell activation (Figure 1.4) [Choudhuri and van der Merwe, 2007] [Davis and van der Merwe, 2006].

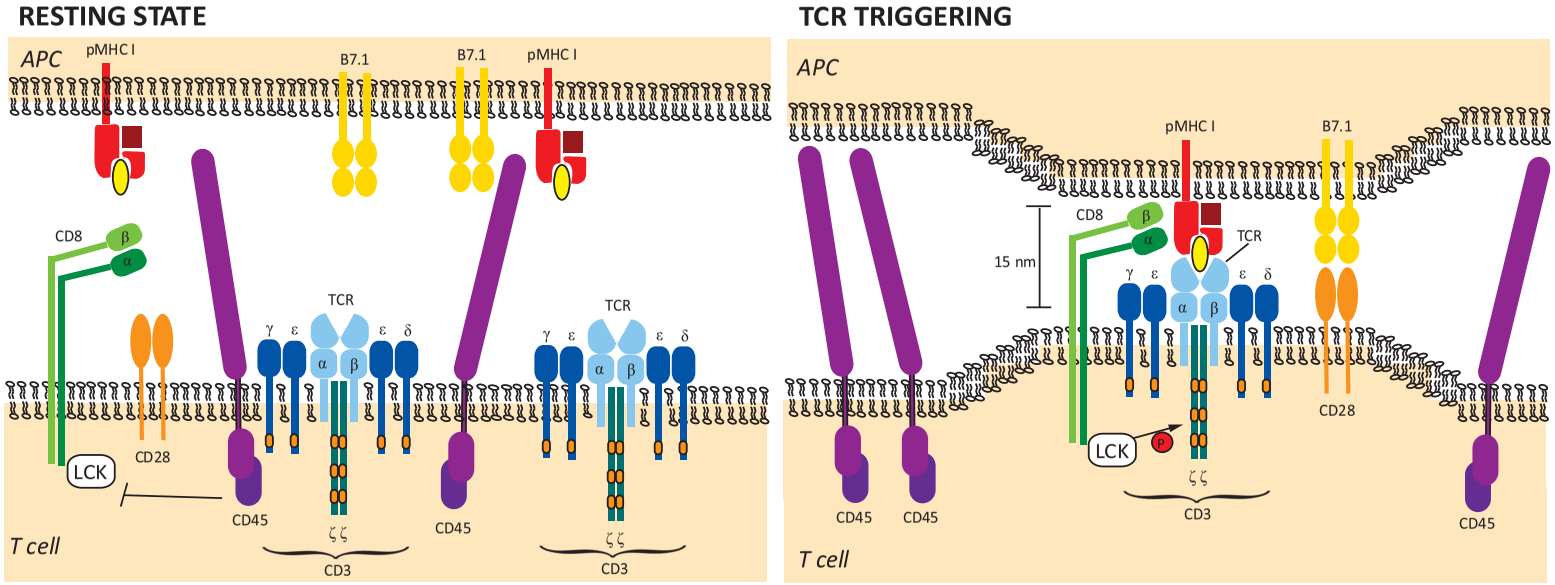

Figure 1.4: The kinetic segregation model. The kinetic segregation model suggests a spatial arrangement of the TCR and its co-receptors and co-signalling molecules. In the resting state, the TCR and its associated proteins are distributed in an unordered manner on the cell surface. TCR signalling is prevented by the close proximity of signal inhibiting phosphatases such as CD45. TCR triggering draws the T cell and APC surfaces into close proximity because of the short ectodomains of the TCR. Co-receptors and co-stimulatory molecules, including CD4, CD8 and CD28, and their ligands possess similarly short ectodomains. This allows them to associate to the TCR:pMHC interaction interface and enhance TCR signalling. Inhibitory phosphatases are excluded from their substrates at the TCR complex through their large ectodomains.

The structural and spatial requirements for TCR triggering and ultimately the activation of T cell effector functions remain ambiguous. Several valuable models have been proposed which are consistent with the available evidence. Yet in the light of the diversity of the data gathered and the lack of direct structural evidence within the TCR complex, the elucidation of the physical TCR triggering mechanism remains a challenge.

Kinetic parameters and models of TCR:pMHC binding The binding parameters governing TCR:pMHC binding which convey qualitative specificity are commonly determined in a 3D setting by SPR [Corr et al., 1994] [Lyons et al., 1996] [Zarnitsyna and Zhu, 2012]. Simplistically the kinetics of TCR:pMHC binding can be described as follows [Stone et al., 2009] [Dushek et al., 2011]:

$$TCR + pMHC \underset{k_{off}}{\overset{k_{on}}{\rightleftharpoons}} TCR:pMHC$$

This means that the affinity is described by::

$$K_D = k_{off} / k_{on}$$

And the half-time of the TCR:pMHC interactions is determined by:

$$t_{1/2} = ln2 / k_{off}$$

In this set-up the k_{on} represents the association rate in $M^{-1}sec^{-1}$ and the k_{off} the dissociation rate measured in sec^{-1}. Smaller values for the affinity

indicate more stable interactions between the TCR and pMHC. Besides the affinity, the half-time is also often used in the literature to describe the potency of TCR:pMHC interactions. It is measured in seconds.
TCR:pMHC interactions characteristically represent with slow k_{on}- and intermediate k_{off}-rates. The affinities between TCR and pMHC interactions are low and physiologically range between 1 and 50 μM to evoke T cell responses [Stone et al., 2009].
Various models for TCR triggering emphasize the role of particularly the off-rate and the affinity over the other kinetic constants in determining TCR activation thresholds.

Affinity model The affinity model describes TCR triggering as a function of the number of TCR:pMHC interactions formed at equilibrium [Lyons et al., 1996] [van der Merwe, 2001]. The effect of the affinity of ligand binding on T cell functions has been correlated in several studies [Chen et al., 2005] [Jenkins et al., 2009] [Chervin et al., 2009] [Schmid et al., 2010] [Irving et al., 2012]. According to these, the cognate affinities for TCR:pMHC interactions are very low. An optimal affinity plateau is reached around 1 μM. Supraphysiological affinities below 1 μM evoke either similar or even reduced T cell effector responses. Up to 10 μM the affinity is potent enough to induce T cell effector responses without the need for CD4 or CD8 co-stimulation [Stone et al., 2009]. Agonist interactions are evoked up to between 50 to 100μM [Davis et al., 1998] [Stone et al., 2009]. Very little data has been collected on the binding properties of self-peptides [Stone et al., 2009]. However, their affinity is estimated to be less than one order of a magnitude lower than ag-

onist affinities [Morris and Allen, 2012]. Affinity has also often been defined as the functional avidity referring to multiplexed TCR triggering models but it is generally measured in a 2D setting of pMHC monomers and TCR monomers by SPR. Thus intrinsic low level affinities are enhanced through the simultaneous engagement of several TCRs in a mode called functional avidity [Dutoit et al., 2002b].

The affinity of pMHC to the TCR is widely used as a measure for agonist potency in the literature and good correlations between binding affinity and the potency of the T cell responses were reported [Dutoit et al., 2002b] [Stone et al., 2011]. However, van der Merwe, 2001, pointed out that the affinity on its own poorly explains the triggering of T cell responses by agonist pMHC when present on the APC at low concentrations. In addition, the qualitative distinction of agonist and antagonist pMHC purely based on small differences between their K_Ds is potentially too simplistic [Dushek et al., 2011]. Hence, kinetic models based on binding $t_{1/2}$ which is related to the k_{off} (refer to formula in previous section) have been proposed that would describe the biological potency of antigen better.

Kinetic models The kinetic models focus on the half-time ($t_{1/2}$) and dissociation rate (k_{off}) of TCR:pMHC binding. The impact of the $t_{1/2}$ and the k_{off} on TCR triggering were explored in the closely related kinetic proofreading and productive hit rate models [McKeithan, 1995] [Aleksic et al., 2010]. The kinetic proofreading model postulates that a minimum dwell time of TCR:pMHC interactions is required for the TCR and its associated signalling machinery to undergo necessary modifications to initiate and propagate sig-

nals [McKeithan, 1995] [Carreño et al., 2007] [Rosette et al., 2001]. These modifications include any changes to the TCR which tranduce the signal across the membrane to the CD3 complex and phosphorylation events which initiate signalling events. Only once one step X_n is accomplished, the next step of the signalling casade can proceed to step X_{n+1} [McKeithan, 1995] [Carreño et al., 2007] [Rosette et al., 2001]. The activation of T cell responses is thus primarily dependent on the dissociation rate [Kalergis et al., 2001] [Rosette et al., 2001].

Kalergis et al., 2001, extended the kinetic proofreading model. The 'productive hit rate' model assumes two parameters: A single pMHC molecule would be able to evoke T cell responses by serially triggering multiple TCRs and these interactions require a minimum dwell time of TCR:pMHC interactions to cause T cell activation [Valitutti et al., 1995] [Itoh et al., 1999]. The repeated interactions of TCRs with agonist pMHC amplifies, reinforces and elongates the duration of the TCR signal [Irving et al., 2012]. Thus, dwell times which last too long will trigger fewer TCRs and ultimately result in short transient signal spike rather than sustained TCR signals over time [Kalergis et al., 2001] [Chervin et al., 2009] [Thomas et al., 2011] [Irving et al., 2012].

Constraints Recent studies have shown that neither the K_D nor the k_{off} described pMHC potency satisfactorily on their own [Aleksic et al., 2010]. This stems from the facts that purely kinetic models do not take structural and spatial modifications to the TCR complex such as TCR-CDRs flexibility or kinetic segregation into account. Mechanical stresses onto the TCR for

example affect the activation enthalpy of TCR:pMHC interactions and thus influences binding kinetics [Kim et al., 2009]. Serial engagement in turn is not only determined by the k_{off}. As re-binding of the TCR to pMHC is determined by the k_{on} which neither the kinetic proofreading nor the productive hit rate models have taken into account [Dushek et al., 2011].
Dushek et al, 2011, observed paradoxic results during their kinetic studies but ultimately preferred a productive hit rate model which related with potency (EC50) of the response to the K_D and the efficiency (maximal response E_{max}) of the T cell responses to the k_{off}.

However, a major constraint to the elucidation of the kinetic parameters governing TCR triggering might lie within the methodology used. Generally, the kinetics of TCR:pMHC binding are measured in 3D setting using SPR (Figure 1.5) [Corr et al., 1994] [Kalergis et al., 2001] [Carreño et al., 2007]. This approach might not provide sufficient resolution to measure the kinetic parameters accurately. Within a physiological setting the TCR and pMHC are tethered on apposing cell membranes in a 2D environment [Huang et al., 2010]. The 2D TCR:pMHC binding parameters have recently been determined using micropipettes and biomembrane force probes (Figure 1.5) [Zarnitsyna and Zhu, 2012]. The data revealed faster on- and off-rates in a 2D environment which confer high TCR triggering speed [Huang et al., 2010]. The broader dynamic range proposed in this model explains TCR sensitivity and favours a model of rapid antigen sampling and frequent re-binding of a TCR to the same pMHC [Huang et al., 2010] [Zarnitsyna and Zhu, 2012]. The determination of 2D binding kinetics is a powerful tool and

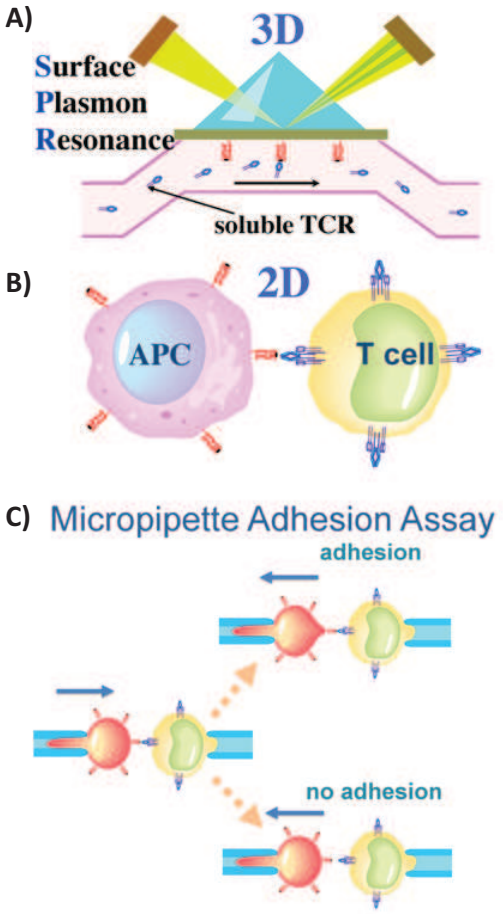

Figure 1.5: Comparison between SPR and wo 2D assays. (A) In SPR soluble TCR (blue) flows over (i.e. 3D) and binds to pMHCs (red) bound to a sensor chip surface, as detected by the change of resonance angle. (B) In reality, this interaction occurs on the interface (i.e. 2D) between two contacting membranes of a T cell and an APC on which the TCR and pMHC are respectively anchored. (C) In the Micropipette Adhesion Frequency Assay a pMHC-coated red blood cell (RBC) (red) is brought into contact with a T cell (yellow). Upon RBC retraction whether adhesion is present or not is detected by RBC elongation as shown top right versus bottom right. Adhesion frequency can be estimated from repeated contacts at a given contact duration.
Source: adapted from Zarnitsyna and Zhu, *Phys. Biol.*, 2012

in future studies is likely to be extended to more TCR:pMHC models and also co-receptors.

1.2.5 Clinical applications to TCR affinity studies

Adoptive T cell transfer immunotherapy for cancer The specificity of TCR recognition of foreign antigen and subsequent T cell functions are attractive to the treatment of cancers [Schumacher and Restifo, 2009]. The inherent genetic instability of cancer cell genomes carries the potential for the generation of diverse cancer-specific antigen [Restifo et al., 2012] [Harada et al., 2001]. Melanomas are particularly often enriched with T cells bearing anti-tumour specificity [Friedman et al., 2012]. In some contemporary clinical trials isolated cancer antigen-specific T cells were activated and expanded *ex vivo* and used to treat patients in conjuncture with chemotherapy. This process is called adoptive T cell transfer. Both naturally occurring and genetic engineered T cells are considered suitable for therapy [Schumacher and Restifo, 2009] [Rizzuto et al., 2009] [Restifo et al., 2012].

One of the hallmarks of cancer is the ability to evade immune responses [Hanahan and Weinberg, 2011]. Cancer cells employ various strategies to this end, including the downregulation of MHC class I expression and the release of immunosuppressive cytokines [Restifo et al., 2012]. Adoptive T cell transfer aims to introduce pre-activated T cells with heightened cancer immunogenicity to augment conventional therapies. During a recent clinical trial, the adoptive transfer of autologous T cells specific for the tumour antigen NY-ESO-1 [Robbins et al., 2011]. The treatment resulted in im-

proved T cell anti-tumour efficacy and showed 45% and 67% response rates in melanoma and synovial sarcoma patients respectively [Robbins et al., 2011].

The 1G4 - NY-ESO-1 system NY-ESO-1 is a cancer-testis antigen which is of particular interest to adoptive T cell transfer cancer therapies [Restifo et al., 2012]. If target antigens are not only expressed by cancer cells, the cross-reactivity of tumour antigens with normal tissue can lead to severe side effects of the adoptive transfer treatment approach. For instance, T cells engineered for reactivity for the carcinoembryonic antigen (CEA) mediate both the destruction of colon cancer cells and, transiently, of normal colonic mucosa [Restifo et al., 2012]. To circumvent side effects, cancer-testis antigen are interesting targets. These antigens are usually expressed in germline cells which do not express MHC class I or II molecules and are thus nor targeted by T cells [Restifo et al., 2012]. NY-ESO-1 is 17.9 kDa, 180 amino acid putative testicular antigen which is also expressed by a wide variety of cancers including myeloma, synovial sarcoma and breast, ovarian, thyroid and prostate cancers [Chen et al., 1997] [Robbins et al., 2011]. NY-ESO-1-positive cancer cells present on average 10 to 50 antigens per cell [Purbhoo et al., 2001]. This corresponds to the average presentation levels of individual self-antigens on the surface of cells. As few as ten antigen ligands are thought to be sufficient to activate effector functions under physiological conditions [Irvine et al., 2002].

The SLLMWITQC NY-ESO-$1_{156-165}$ peptide is recognised by, among others, the 1G4 TCR [Schmid et al., 2010]. The protruding amino acids 4Met and 5Trp are critical for the recognition of the peptide by the 1G4 TCR [Derré

et al., 2008] [Chen et al., 2005]. The monomeric affinity of the wild-type NY-ESO-$1_{156-165}$ peptide presented on HLA-A2 to the 1G4 TCR is 14 μM which is within the agonist affinity range up to 50 μM but below the optimal effector function inducing affinity of 1 to 10 μM [Aleksic et al., 2010] [Stone et al., 2009]. T cells bearing the 1G4 isolated from patients show weak immune responses to the antigen [Schmid et al., 2010] [Chen et al., 2005]. The NY-ESO-$1_{156-165}$-1G4 system has been used in *in vitro* studies and in clinical trials to investigate the effect of binding affinities on T cell effector function efficacy and the potential of using this research in cancer vaccine therapies. Professor Cerundolo's group uses variants of the NY-ESO-$1_{156-165}$ peptide to 'prime' 1G4 T cells to wild-type NY-ESO-$1_{156-165}$ peptides to create melanoma vaccine therapies [Chen et al., 2005] [Chen et al., 2010]. The binding characteristics of several NY-ESO-$1_{156-165}$ homologues with a wide range of physiologically activating affinities to the 1G4 TCR were determined by SPR (Figure 1.6) [Aleksic et al., 2010]. The higher 9V derivative was found to elicit higher T cell responses characterised by IFN-γ release, Ca^{2+} signalling and granule polarization than both the wild-type and lower affinity 9L NY-ESO-$1_{156-165}$ peptides [Chen et al., 2000] [Chen et al., 2005] [Chen et al., 2010].

pMHC		K_D	K_A	k_{off}	$t_{1/2}$	k_{on}	ΔG	ΔH	-TΔS	ΔC	EC_{50} (IFN-γ)	EC_{50} (CTL)
peptide name	peptide sequence	(μM)	(mM^{-1})	(s^{-1})	(s)	x10^3 ($M^{-1}s^{-1}$)	(kcal mol^{-1})	(kcal mol^{-1})	(kcal mol^{-1})	(kcal $mol^{-1}K^{-1}$)	(μg/ml pMHC)	x10^5 ($C_{40\%}$ dilution)
ESO-9C	SLLMWITQC	14 ± 1	69 ± 3	0.82 ± 0.01	0.84 ± 0.01	57 ± 3	-6.9 ± 0.0	-8.7 ± 0.3	2.0 ± 0.3	-0.58 ± 0.02	115 ± 14	
ESO-9L	SLLMWITQL	56 ± 6	18 ± 2	0.93 ± 0.05	0.74 ± 0.04	17 ± 2	-6.0 ± 0.1	-8.0 ± 0.6	2.2 ± 0.6	-0.47 ± 0.05	426 ± 113	
ESO-9V	SLLMWITQV	7.2 ± 0.5	139 ± 10	0.33 ± 0.01	2.12 ± 0.08	45 ± 4	-7.3 ± 0.0	-10.1 ± 0.9	2.9 ± 0.9	-0.64 ± 0.05	180 ± 19	2777 ± 854
ESO-3A	SLAMWITQV	6.6 ± 0.5	152 ± 12	0.31 ± 0.01	2.26 ± 0.05	47 ± 4	-7.4 ± 0.0	-13.4 ± 0.4	6.1 ± 0.5	-0.70 ± 0.04	70 ± 15	979 ± 330
ESO-3I	SLIMWITQV	17 ± 1	58 ± 3	0.61 ± 0.04	1.14 ± 0.07	35 ± 3	-6.8 ± 0.0	-10.3 ± 0.2	3.7 ± 0.2	-0.60 ± 0.01	94 ± 16	241 ± 91
ESO-3M	SLMMWITQV	9.2 ± 0.2	109 ± 3	0.38 ± 0.01	1.81 ± 0.04	42 ± 1	-7.1 ± 0.0	-11.5 ± 0.6	4.4 ± 0.6	-0.63 ± 0.02	48 ± 7	946 ± 227
ESO-3Y	SLYMWITQV	30 ± 1	33 ± 1	1.15 ± 0.04	0.60 ± 0.02	38 ± 1	-6.4 ± 0.0	-5.3 ± 0.4	-0.85 ± 0.37	-0.37 ± 0.03	240 ± 50	129 ± 26
ESO-4D	SLLDWITQV	252 ± 12	4.0 ± 0.2	2.59 ± 0.15	0.27 ± 0.02	10 ± 1	-5.1 ± 0.0	-12.1 ± 0.6	6.8 ± 0.6	-0.60 ± 0.03	661 ± 85	2.3 ± 0.5
ESO-6V	SLLMWVTQV	18 ± 0	57 ± 1	0.85 ± 0.03	0.81 ± 0.03	49 ± 2	-6.8 ± 0.0	-10.9 ± 0.9	4.1 ± 0.8	-0.60 ± 0.05	45 ± 5	310 ± 85
ESO-6T	SLLMWTTQV	101 ± 5	9.9 ± 0.4	1.30 ± 0.03	0.53 ± 0.01	13 ± 1	-5.7 ± 0.0	-11.0 ± 0.3	5.4 ± 0.3	-0.53 ± 0.02	228 ± 62	111 ± 30
ESO-7H	SLLMWIHQV	100 ± 8	10.0 ± 0.8	1.73 ± 0.09	0.40 ± 0.02	17 ± 2	-5.7 ± 0.0	-7.3 ± 0.8	1.8 ± 0.8	-0.44 ± 0.06	526 ± 201	19 ± 6
A2-R65	SLLMWITQV	112 ± 4	8.9 ± 0.3	1.93 ± 0.13	0.36 ± 0.02	17 ± 1	-5.6 ± 0.0	-8.8 ± 3.3	3.4 ± 3.4	-0.49 ± 0.27	479 ± 12	
A2-H70	SLLMWITQV	84 ± 3	12 ± 0	0.22 ± 0.01	3.10 ± 0.09	2.7 ± 0.1	-5.8 ± 0.0	-11.3 ± 0.9	5.6 ± 1.1	-0.65 ± 0.08	151 ± 19	
A2-H74	SLLMWITQV	26 ± 1	39 ± 2	0.49 ± 0.01	1.41 ± 0.02	19 ± 1	-6.5 ± 0.0	-8.0 ± 0.2	1.9 ± 0.3	-0.63 ± 0.02	107 ± 12	
A2-R75	SLLMWITQV	17 ± 1	59 ± 3	0.39 ± 0.00	1.80 ± 0.02	23 ± 1	-6.8 ± 0.0	-11.7 ± 0.1	5.1 ± 0.1	-0.58 ± 0.01	99 ± 12	
A2-V76	SLLMWITQV	22 ± 1	46 ± 2	0.67 ± 0.01	1.04 ± 0.01	31 ± 2	-6.6 ± 0.0	-10.3 ± 0.1	3.8 ± 0.1	-0.47 ± 0.01	146 ± 38	
A2-K146	SLLMWITQV	20 ± 2	50 ± 4	0.48 ± 0.01	1.43 ± 0.02	24 ± 2	-6.7 ± 0.1	-11.8 ± 0.3	5.3 ± 0.3	-0.61 ± 0.02	179 ± 23	

pMHC		$\Delta G^{\ddagger}_{diss}$	$\Delta H^{\ddagger}_{diss}$	$-T\Delta S^{\ddagger}_{diss}$	$\Delta C^{\ddagger}_{diss}$	$\Delta G^{\ddagger}_{ass}$	$\Delta H^{\ddagger}_{ass}$	$-T\Delta S^{\ddagger}_{ass}$	$\Delta C^{\ddagger}_{ass}$
peptide name	peptide sequence	(kcal mol^{-1})	(kcal mol^{-1})	(kcal mol^{-1})	(kcal $mol^{-1}K^{-1}$)	(kcal mol^{-1})	(kcal mol^{-1})	(kcal mol^{-1})	(kcal $mol^{-1}K^{-1}$)
ESO-9C	SLLMWITQC	18.1 ± 0.0	14.4 ± 0.4	3.6 ± 0.5	0.07 ± 0.04	11.4 ± 0.0	5.5 ± 0.5	5.9 ± 0.3	-0.51 ± 0.04
ESO-9L	SLLMWITQL	17.9 ± 0.0	16.6 ± 0.7	1.3 ± 0.7	0.12 ± 0.02	12.1 ± 0.1	9.4 ± 0.9	2.6 ± 0.6	-0.28 ± 0.05
ESO-9V	SLLMWITQV	18.7 ± 0.0	17.0 ± 0.4	1.8 ± 0.4	0.01 ± 0.00	11.6 ± 0.0	6.6 ± 1.0	5.0 ± 0.9	-0.66 ± 0.05
ESO-3A	SLAMWITQV	18.7 ± 0.0	16.5 ± 0.6	2.2 ± 0.6	0.04 ± 0.04	11.5 ± 0.1	3.1 ± 0.8	8.4 ± 0.5	-0.67 ± 0.06
ESO-3I	SLIMWITQV	18.2 ± 0.0	9.8 ± 0.1	8.4 ± 0.2	-0.05 ± 0.01	11.6 ± 0.0	-0.5 ± 0.2	12.1 ± 0.2	-0.65 ± 0.01
ESO-3M	SLMMWITQV	18.5 ± 0.0	20.1 ± 1.1	-1.6 ± 1.1	0.27 ± 0.08	11.5 ± 0.0	8.7 ± 1.2	2.8 ± 0.6	-0.36 ± 0.09
ESO-3Y	SLYMWITQV	17.7 ± 0.0	15.3 ± 0.1	2.4 ± 0.1	0.45 ± 0.01	11.5 ± 0.0	10.0 ± 0.4	1.5 ± 0.4	0.08 ± 0.03
ESO-4D	SLLDWITQV	17.7 ± 0.0	15.0 ± 0.0	2.7 ± 0.0	-0.04 ± 0.00	12.5 ± 0.0	2.9 ± 0.6	9.6 ± 0.6	-0.64 ± 0.03
ESO-6V	SLLMWVTQV	18.1 ± 0.0	10.7 ± 2.7	7.3 ± 2.8	-0.14 ± 0.15	11.3 ± 0.0	-0.2 ± 2.8	11.4 ± 0.8	-0.74 ± 0.16
ESO-6T	SLLMWTTQV	17.8 ± 0.0	8.1 ± 2.0	9.7 ± 2.0	0.02 ± 0.16	12.3 ± 0.0	-2.8 ± 2.0	15.1 ± 0.3	-0.51 ± 0.16
ESO-7H	SLLMWIHQV	17.7 ± 0.0	8.5 ± 3.1	9.2 ± 3.1	-0.05 ± 0.20	35.3 ± 0.1	26.2 ± 3.2	9.0 ± 0.9	0.13 ± 0.21
A2-R65	SLLMWITQV	17.6 ± 0.0	17.7 ± 0.7	-0.17 ± 0.68	0.18 ± 0.05	12.1 ± 0.0	8.9 ± 3.4	3.2 ± 3.4	-0.32 ± 0.27
A2-H70	SLLMWITQV	19.0 ± 0.0	22.6 ± 1.0	-3.6 ± 1.1	0.49 ± 0.09	13.2 ± 0.0	11.3 ± 1.4	1.9 ± 1.1	-0.15 ± 0.11
A2-H74	SLLMWITQV	18.6 ± 0.0	21.4 ± 0.5	-2.9 ± 0.5	0.35 ± 0.04	12.4 ± 0.0	13.4 ± 0.5	-1.0 ± 0.3	-0.28 ± 0.04
A2-R75	SLLMWITQV	18.8 ± 0.0	20.6 ± 0.9	-1.8 ± 0.8	0.21 ± 0.04	12.2 ± 0.0	8.9 ± 0.9	3.3 ± 0.1	-0.38 ± 0.04
A2-V76	SLLMWITQV	18.3 ± 0.0	20.3 ± 0.2	-1.9 ± 0.2	0.26 ± 0.00	11.9 ± 0.0	10.0 ± 0.2	1.9 ± 0.1	-0.21 ± 0.01
A2-K146	SLLMWITQV	18.5 ± 0.0	21.3 ± 0.2	-2.7 ± 0.2	0.30 ± 0.01	12.0 ± 0.1	9.5 ± 0.3	2.6 ± 0.3	-0.31 ± 0.03

Figure 1.6: Biophysical and functional characterisation of 1G4 TCR interaction with pMHC variants. Binding affinity, kinetics and thermodynamics of 1G4 TCR to various peptide and MHC mutants were measured at 37 °C by SPR. Activation potency of each pMHC in IFNγ release assay and cytotoxicity assay is presented by EC50 value. Mean values of at least three independently performed experiments are shown with standard error of mean (SEM). Source: Aleksic et al., *Immunity*, 2010.

1.3 Complexity of the T cell activation process

1.3.1 Dynamic interactions of T cells with APCs and IS formation

T cells are highly mobile cells within the peripheral lymphoid tissues, moving at an average directional speed of 10 to 15 μm/min in an amoeboid fashion [Miller et al., 2002] [Miller et al., 2003]. The high motility allows the T cell to interact with many pMHC-presenting APC [Mempel et al., 2004]. von Andrian proposed that two phases of activation events seem to exist *in vivo* [Mempel et al., 2004] [Mrass et al., 2006]. One in which multiple brief contacts with APCs provide signalling but not T cell arrest on the APC. The second is characterised by long duration interactions between the T cell and the APC. This was determined using two photon microscopy *in vivo* [Mempel et al., 2004] [Mrass et al., 2006]. Upon the recognition of cognate antigen, TCR:pMHC interactions and CD28 ligation activate integrins and LFA-1 to promote cell-cell adhesion and suppress cell motility [Dustin, 2008] [Lam Hui et al., 2012]. A stable association of APC and T cells induces the formation of an immunological synapse (IS). At high density of peptide agonist this event is driven by the accumulation of TCR-enriched microclusters into central supramolecular activation clusters (cSMACs) at the cell-cell interface with in a few minutes of T cell binding [Dustin, 2008] [Campi et al., 2005]. The cSMAC is surrounded by two segregated bulls-eye-shaped zones (Figure 1.7): the peripheral pSMAC defined by of LFA-1-ICAM-1 interactions

and the distal dSMAC defined by the presence of the phosphatases CD45 and CD148 (Figure 1.7) [Huppa and Davis, 2003] [Dustin, 2008]. The IS has various functions. Its formation stops T cell motility and promotes T cell adhesion to the APC. Furthermore, it mediates the directed secretion of cytokines and lytic granules through an f-actin-depleted central secretory domain [Dustin, 2008]. The IS acts as a seal allowing CTLs to specifically target cell lysis by granzymes such as perforin at virally infected cells [Jenkins et al., 2009] [Sanderson et al., 2012]. Lytic granules are delivered to the IS via microtubules. Target cell killing is more strongly induced with high avidity stimulation [Jenkins et al., 2009].

Surprisingly, the cSMAC is not the major site of proximal phospho-tyrosine signalling events [Dustin, 2008] [Campi et al., 2005]. In fact, the earliest signalling events are traceable to TCR microclusters at the periphery of the IS which co-localise with active LCK, ZAP-70 and LAT within 30 seconds of APC-T cell adhesion; before the formation of the IS [Lee et al., 2002] [Lillemeier et al., 2010]. The TCR and LAT molecules remain in physically separated microclusters which most likely concatenate to protein islands through the activity of ZAP-70. Within a few minutes the TCR microclusters move towards the cSMAC while ZAP-70, LAT and SLP-76 domains remain in the pSMAC. This segregation is independent of kinase activity but depends on f-actin polymerisation [Campi et al., 2005] [Jenkins et al., 2009] [Lillemeier et al., 2010].

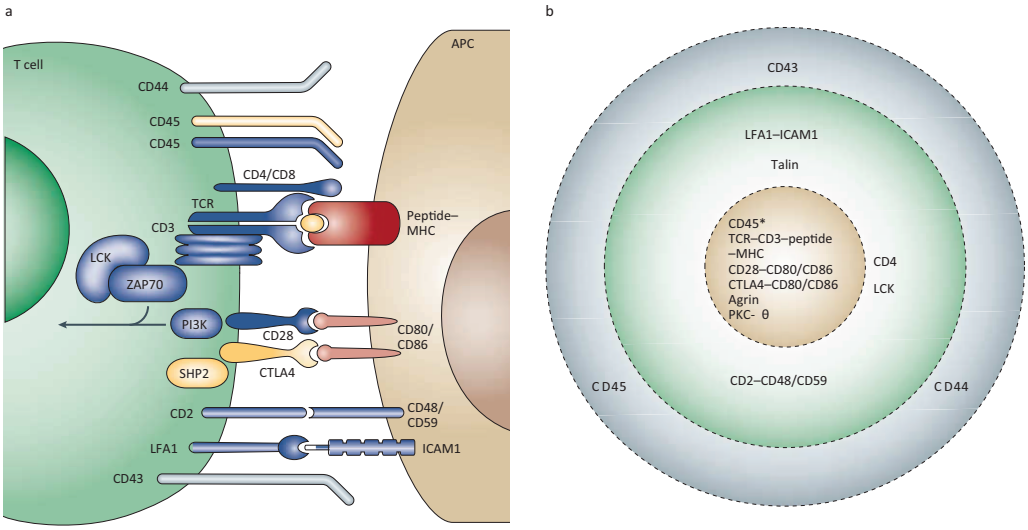

Figure 1.7: Overview of a mature T-cell synapse. (A) A profile view showing a selection of the key ligand pairs and signalling molecules that are involved in T-cell recognition. The stimulatory peptideMHC molecule is shown in red, activating/co-stimulatory molecules are blue, inhibitory molecules are yellow and molecules that are not contributing to signalling are grey. The arrow indicates converging signals that lead to T-cell activation. (B) The face on view of the synapse with the characteristic 'bulls-eye' zone pattern, including the central region of the supra-molecular activation complex (cSMAC) (yellow), the peripheral ring surrounding the cSMAC (pSMAC, green) and the region distal to the synapse outside the pSMAC (dSMAC, grey) as well the molecules/ligand pairs that are found enriched within.
Source: adapted from Huppa and Davis, *Nat. Rev. Immunol.*, 2003

1.3.2 Formation of TCR proximal signalling complexes drive T cell activation

TCR signal initiation T cell activation is mediated through a cascade of phospho-tyrosine kinases following TCR:pMHC interactions (Figure 1.8) [Acuto et al., 2008]. TCR triggering results in the initiation of a multitude of biochemical modifications which activates multiple signalling pathways to cause dramatic changes in cell morphology, lamellopodia protrusion,

cell adhesion, gene expression, the expression and release of cytokines and chemokines, cell proliferation and the killing of target cells [Kindt et al., 2007] [Murphy et al., 2008].

The TCR is non-covalently associated to three CD3 dimers whose cytoplasmic domains contain the signal-transducing ITAMs as discussed in earlier chapters. TCR triggering results in the recruitment of the Src-kinase LCK to the TCR:CD3 complex via CD4 and CD8 which are required to induce signalling by low affinity pMHC (Figure 1.9). The activity of LCK is tightly regulated through the phosphorylation of two crucial tyrosines (Figure 1.8, inset box). Phosphorylation of LCK at tyrosine 505 (pY505) locks LCK into a closed inactive conformation. The pY505 phosphorylation is mediated by Src-specific kinase Csk [Boggon and Eck, 2004]. CD45 mediates the de-phosphorylation of LCK at both pY505 and pY394 and thus both pos-

---

Figure 1.8 *(following page)*: TCR signalling pathways. T cell activation is the result of sequential phospho-protein signalling events. Upon TCR-pMHC binding, the Src-family kinase LCK phosphorylates immunotyrosine activating motifs (ITAMs) on the CD3 chains. LCK activity is regulated by phosphorylation and de-phosphorylation events to its two regulatory tyrosines at positions 394 and 505 (inset box). The phosphorylation of the ITAMs recruits Zap70 which is activated by LCK. Zap70 phosphorylates LAT which in conjunction with SLP-76 acts as a platform for further propagation and diversification of the signal which initiates diverse T cell responses to TCR triggering. PLCγ1 catalyses the hydrolysis of $PtdIns_{(4,5)}P_2$ to $InsPP_3$ and DAG. $InsPP_3$ initiates the influx of Ca^{2+} ions which in turn activates calcineurin and calmodulin. This ultimately results in the activation of the transcription factors NFAT and NF-$\varkappa$B and gene expression. DAG activates both PKC- and Ras-mediated pathways to initiate NF-$\varkappa$B activity and ERK-mediated activation of AP-1, respectively. ERK signalling results in increased cell survival and proliferation. Cytoskeletal rearrangements and increased adhesion of activated T cells to target cells via integrins are controlled through signalling via VAV and ADAP.

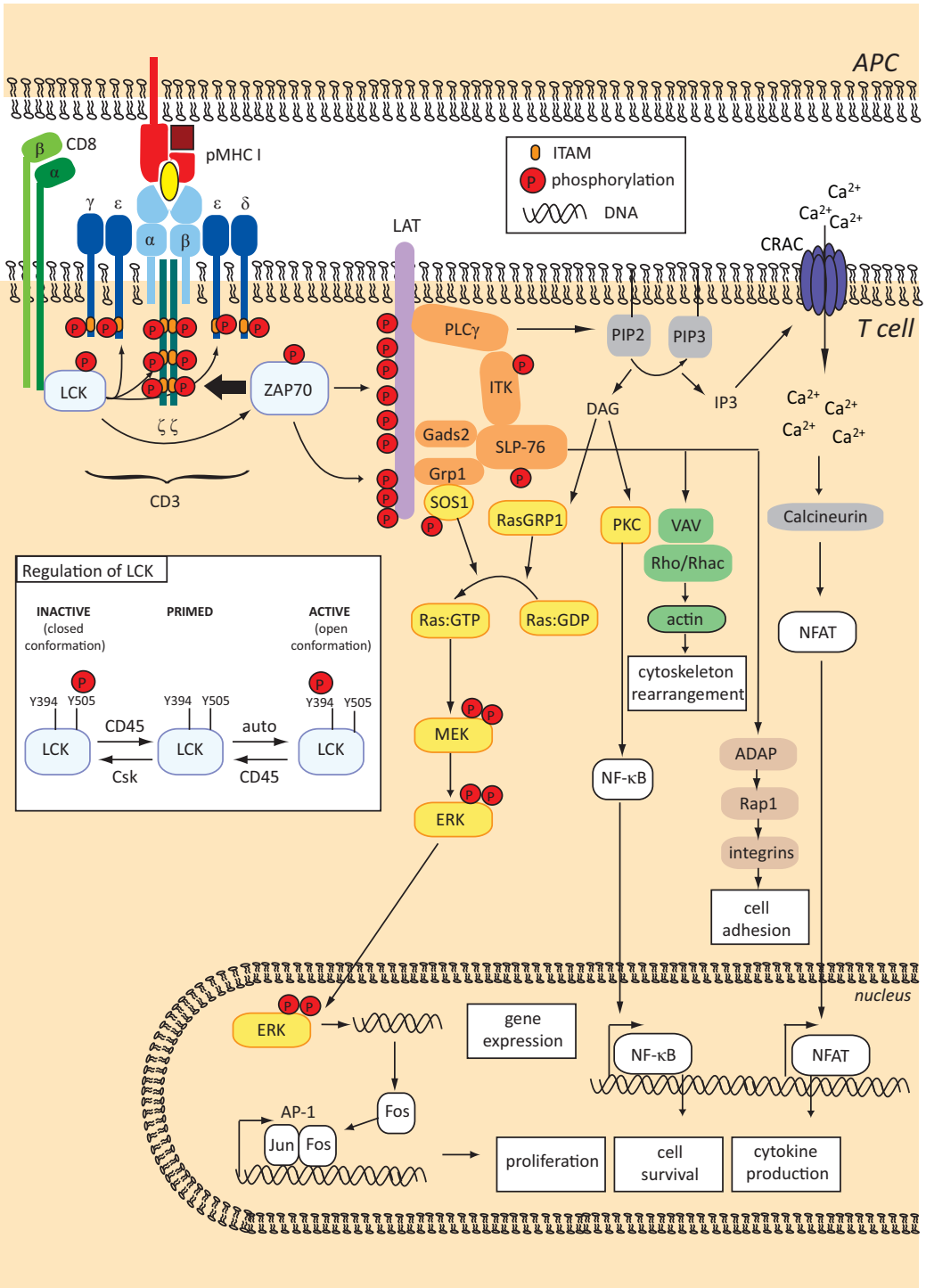
APC
CD8
pMHC I
ITAM
phosphorylation
DNA
LAT
CRAC
T cell
PLCγ
PIP2
PIP3
ITK
DAG
IP3
LCK
ZAP70
ζ ζ
CD3
Gads2
SLP-76
Grp1
SOS1
RasGRP1
PKC
VAV
Rho/Rhac
actin
cytoskeleton rearrangement
Calcineurin
NFAT
Ras:GTP
Ras:GDP
MEK
ERK
NF-κB
ADAP
Rap1
integrins
cell adhesion
Regulation of LCK
INACTIVE (closed conformation)
PRIMED
ACTIVE (open conformation)
Y394 Y505
CD45
Csk
auto
nucleus
gene expression
AP-1
Jun
Fos
proliferation
cell survival
cytokine production

itively and negatively regulates LCK activity [Thomas and Brown, 1999]. Autophosphorylation activates LCK at tyrosine 394 (pY394) which subsequently adopts an open conformation [Boggon and Eck, 2004] [Nika et al., 2010]. Up to 40% of LCK is pre-activated in resting T cells, yet phosphorylation of the CD3 ITAMs only ensues after TCR triggering. The mechanism which translates TCR triggering into CD3 ITAM phosphorylation is still unknown [Nika et al., 2010]. Theories discussed earlier suggest that conformational changes in the TCR:CD3 complex render the ITAMs accessible to active LCK [Risueño et al., 2008] [Gagnon et al., 2012].

The phosphorylation of CD3-ITAMs recruits the Syk family tyrosine kinase ZAP-70 to the CD3ζ ITAMs [Huby et al., 1997] [Brdicka et al., 2005]. ZAP-70 binds to the doubly phosphorylated ITAMs via its tandem SH2 domains (Figure 1.9). The activation loop of ZAP-70 contains two tyrosines at positions 492 and 493 which are phosphorylated following the phosphorylation of regulatory tyrosine 319 that connects the tandem SH2-domains to the kinase domain [Di Bartolo et al., 1999]. After ZAP-70 binds CD3ζ LCK proceeds to phosphorylate ZAP-70 at tyrosine 493 [Huby et al., 1997]. Subsequently Y492 is auto-phosphorylated [Brdicka et al., 2005]. Subsequently, ZAP-70 progresses to phosphorylate the scaffold proteins linker for activation of T cells (LAT) and Src homology (SH) 2 domain-containing leukocyte phosphoprotein of 76 kDa (SLP-76) [Williams et al., 1998].

LAT complex and signal diversification LAT is an essential transmembrane scaffold protein in the T cell signalling cascade. It belongs to the type-III transmembrane proteins and has a short extracellular domain

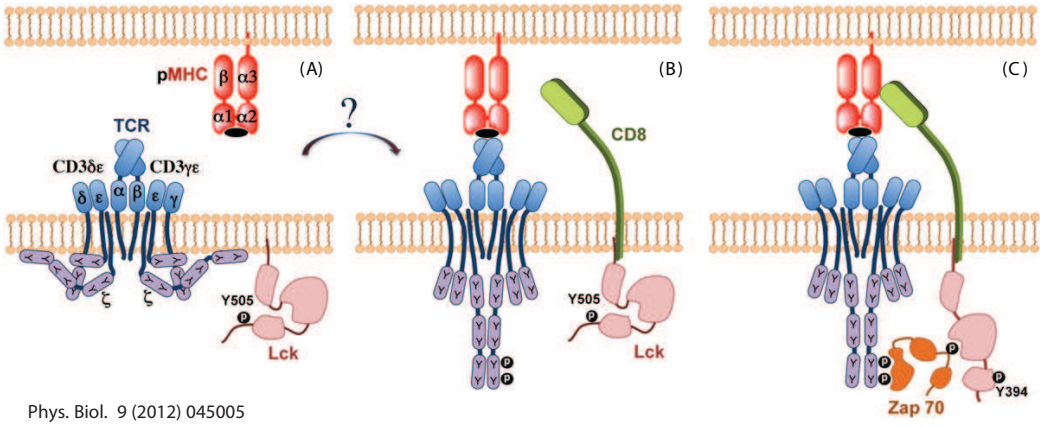

Figure 1.9: Early steps in T cell triggering. Interaction space between opposing membranes of a T cell (bottom) and an APC (top) is shown. (A) Resting state with no interaction between the αβ TCR (blue) and the pMHC (MHC in red, inserted peptide in black). The cytoplasmic tails of both CD3ε and TCR-CD3ζ of the TCR complex are buried in the cell membrane. ITAMs on CD3δε, CD3δε and ζζ cytoplasmic domains are shown as violet ovals with their two tyrosines marked (Y-Y). (B) Binding of TCR with agonist pMHC leads to phosphorylation of tyrosine residues in ITAMs. Coreceptor CD8 is shown in two shades of green and is associated with LCK (pink). LCK molecules are shown in two states: free-state (A) and CD8-bound state (B), (C) and in two conformations: inactive (A), (B) with its inhibitory Y505 residue phosphorylated and active (C) with its activation Y394 residue phosphorylated. Phosphorylated residues are shown as black circles with white letter P inside. (C) Assembly of a functional TCR:pMHC:CD8 trimolecular complex. ZAP-70 (orange) is recruited and activated by CD8-bound LCK. The mechanisms by which the information encoded in binding of a pMHC to the αβ TCR transmits to the CD3 and TCR-CD3ζ signalling units to cause ITAMs phosphorylation remain to be elucidated, as indicated by the question mark.
Source: adapted from Zarnitsyna and Zhu, *Phys. Biol.*, 2012

and a long unstructured cytosolic tail without catalytic capacity [Samelson, 2002]. The cytosolic tail contains nine conserved tyrosines which are phosphorylated by ZAP-70 upon TCR triggering [Samelson, 2002] [Smith-Garvin et al., 2009]. LAT is post-translationally palmitoylated which locates it to glycolipid-enriched membrane microdomains (GEMs) [Shim et al., 2011]. To-

gether with the adaptor molecule SLP-76, LAT forms a diversification platform for the TCR signal onto varied signalling pathways to induce complex and diverse cellular outcomes (Figure 1.8). The loss of either molecule results in the near complete abrogation of TCR signal transduction [Clements et al., 1998] [Finco et al., 1998] [Zhang et al., 1999]. The phosphorylation of LAT upon TCR triggering recruits several signalling components including adaptor and scaffold proteins and enzymes. These associate to the LAT complex via their SH2 domains [Shim et al., 2011]. The adaptor protein Grb-2 (growth factor receptor-bound protein 2), phospholipase (PLC)-γ1 and PI3K-p85 all associate directly to LAT via its phosphorylated tyrosines 132, 171 and 191 [Sommers et al., 2002] [Shim et al., 2011] [Smith-Garvin et al., 2009]. Furthermore, LAT indirectly interacts with the E3 ubiquitin protein ligase Cbl, the Rho/Rac guanine nucleotide exchange factor (GEF) for Ras Vav1 and the GEF SOS (son of sevenless) through Grb-2 [Shim et al., 2011] [Smith-Garvin et al., 2009]. SLP-76 is an adaptor protein and associates to LAT indirectly via Grb2-related adaptor downstream of Shc (Gads) [Liu et al., 1999] [Jackman et al., 1995]. The adaptor functions of SLP-76 is mediated through the three protein-protein interaction domains. These include three N-terminal tyrosine which form SH2-binding sites, a proline-rich central region and a C-terminal SH2 domain [Jackman et al., 1995] [Fang et al., 1996] [Motto et al., 1996]. SLP-76 associated directly to Vav-1, the adaptor NCK, the Tec family kinase ITK (IL2-induced tyrosine kinase), Gads, PLC-γ1, the adaptor ADAP and the kinase HPK1 (hematopoeitic progenitor kinase 1) [Kliche et al., 2006] [Di Bartolo et al., 2007] [Acuto et al., 2008]. The association of SLP-76 to HPK1 mediates a negative feedback release SLP-76 and

Gads from LAT and thus abrogate the TCR signal [Di Bartolo et al., 2007] [Lasserre et al., 2011].

PLC-γ1 and calcium signalling PLC-γ1 activation leads to the initiation of three independent signalling pathways which all involve the influx of Ca^{2+} and the production of the second messenger diacylglycerol (DAG) (Figure 1.10).

Firstly, the regulatory p85 subunit of PI3K appears to interact with the acidic N-terminal region of SLP-76. Membrane-targeting the catalytic subunit p110 initiates the generation of phosphatidylinositol 3,4,5-triphosphate (PIP_3) from phosphatidylinositol 4,5-triphosphate (PIP_2) [Ward and Cantrell, 2001]. Subsequently, ITK recruited to SLP-76 via phosphatidylinositol-binding pleckstrin homology (PH) domain which bind to PIP_3 and locates ITK to the plasma membrane. PLC-γ1 is a substrate of ITK and phosphorylation of PLC-γ1 results in its activation. Active PLC-γ1 hydrolyses PIP_2 to inositol 1,4,5-triphosphate (IP_3) and DAG [Smith-Garvin et al., 2009] [Rhee and Bae, 1997]. The generation of DAG results in the activation of the Ras-GEF RasGRP1 and serine-threonine protein kinase C (PKC) which will be discussed below [Smith-Garvin et al., 2009]. IP_3 difuses into the endoplasmic reticulum (ER) and binds to calcium-permeable ion channel IP_3 receptors (IP_3R) which causes the release Ca^{2+} from the ER into the cytoplasm (Figure 1.10) [Feske, 2007]. This leads to a transient increase in intracellular Ca^{2+} concentrations which triggers the sustained influx of extracellular Ca^{2+} through Ca^{2+}-release activated calcium (CRAC) channels [Lewis, 2007] [Hogan et al., 2010]. The increase of intracellular calcium concentrations activates sev-

eral calcium-dependent molecules. These include the serine-threonine phosphatase calcineurin, the kinase CaMK (Ca^{2+}-calmodulin-dependent kinase) and several transcription factors including NFAT (nuclear factor of activated T cells), CREB (cyclic-AMP-repsonsive element binding protein) and MEF2 (myocyte enhancer factor 2) (Figure 1.10) [Macian, 2005] [Oh-hora and Rao, 2008].

Firstly, calmodulin is activated by the increase in intracellular Ca^{2+} concentrations which proceeds to activate calcineurin. The dephosphorylation of NFAT by calcineurin induces a conformational change which causes the nuclear translocation of NFAT. Several genes upregulate their expression through the activity of NFAT. This includes the expression of the cytokines interleukin-2 (IL-2), IL-4, IL-10, interferon (IFN)-γ and tumour necrosis factor (TNF) [Macian, 2005] [Oh-hora and Rao, 2008].

DAG-dependent activation of PKC PKC isoforms play crucial roles in the activation of T cells. There are three PKC subgroups: The first are called conventional PKC and are require both DAG and Ca^{2+} for their activation and includes the isoforms α, $\beta 1$, $\beta 2$ and γ. The activation of novel PKCs (nPKCs) δ, ε, ϑ and η is DAG-dependent only. The third class of PKCs, called atypical, ζ and ι/λ are both DAG and Ca^{2+}-independent [Genot et al., 1995] [Spitaler and Cantrell, 2004]. PKCϑ is recruited to the IS during TCR triggering and it is crucial for the activation of NF-$\varkappa$B [Monks et al., 1997]. In the following paragraph, I will focus on the activation of PKCϑ and NF-$\varkappa$B. PKCϑ is expressed in lymphocytes and muscle and PKCϑ-deficient mice show dramatic defects in T cell proliferation and IL-2 production after

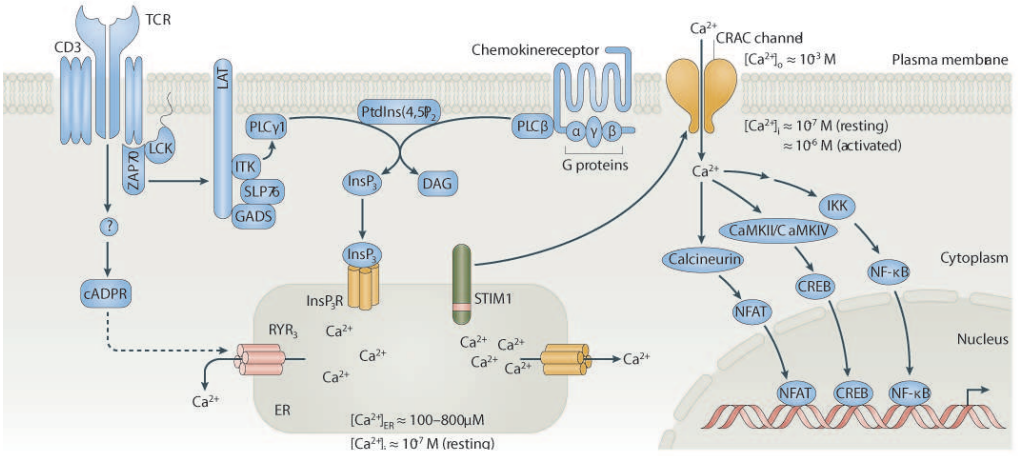

Figure 1.10: Calcium signalling in T cells. In resting T cells, a steep gradient in Ca^{2+} concentrations exists between the cytoplasm and the extracellular space, as well as between the cytoplasm and the lumen of the ER. The intracellular Ca^{2+} concentrations in T cells is tightly regulated and kept between 100 nM in resting cells and 1 μM following TCR stimulation. TCR triggering results in the activation of protein tyrosine kinases, such as LCK and ZAP70, which initiate phosphorylation events of adaptor proteins, such as SLP76 and LAT. This leads to the recruitment and activation of the TEC kinase ITK and PLCγ1. Similarly, binding of G-protein-coupled chemokine receptors results in the activation of PLCβ. PLCβ and PLCγ1 catalyse the hydrolysis of the membrane phospholipid $PtdIns_{(4,5)}P_2$ to $InsPP_3$ and DAG. $InsPP_3$ binds to and opens $InsPP_3$ receptors in the membrane of the ER, resulting in the release of Ca^{2+} from intracellular Ca^{2+} stores. A decrease in the Ca^{2+} content of the ER is 'sensed' by STIM1, which in turn activates CRAC channels in the plasma membrane. Ca^{2+} influx though CRAC channels and elevated intracellular Ca^{2+} concentration activate Ca^{2+}-dependent enzymes, such as calcineurin, and thereby transcription factors, such as NFAT, NF-κB and CREB.
Source: adapted from Feske, *Nat Rev Immunol*, 2007

TCR/CD28-mediated cell activation [Altman et al., 2004].

The activation of PLC-γ1 following TCR triggering results in the increase of DAG concentrations. This recruits PKC isoforms to the plasma membrane via their DAG-binding C1 domains. At the plasma membrane, PDK1 (3-phosphoinositide-dependent protein kinase 1 phosphorylates PKCs [Spitaler and Cantrell, 2004]. PKCϑ is key for the activation of several transcription factors: AP-1 is composed of a Jun and/or Fos dimer and synergistically with NFAT contributes towards the initiation of IL-2 expression. PKCϑ activates IKKβ which phosphorylates and activates the transcription factor NF-κB. In conjunction with NFAT and AP-1, NF-κB is essential to the production of IL-2. PKCϑ also protects T cells from activation-induced cell death by protecting the cell from Fas-mediated apoptosis [Altman et al., 2004] [Genot et al., 1995].

DAG-dependent and -independent activation of Ras Ras is a membrane-bound GTPase whose activity is controlled by guanine nucleotide exchange factors (GEFs) [Genot and Cantrell, 2000]. In its inactive state, Ras is bound to GDP. GEFs promote the dissociation of Ras from GDP and the binding to GTP [Roose and Weiss, 2000]. The GTP-bound active form of Ras is an important signal transduction protein which activates several serine-threonine kinases and ultimately influences changes in gene expression patterns. Within the TCR signalling cascade, the activity of Ras is triggered in a DAG-dependent and -independent manner (Figure 1.11) [Egan et al., 1993] [Ebinu et al., 2000] [Roose et al., 2005].

DAG generated by PLC-γ at the plasma membrane recruits the Ras GEF

RasGRP1 (Ras guanyl nucleotide releasing protein) to the membrane via its DAG/phorbol ester-binding C1 domain [Ebinu et al., 2000] [Roose et al., 2005]. The location of RasGRP1 to the plasma membrane recruits it into the vicinity of Ras. RasGRP1 is a GTPase-activating proteins (GAP) which catalyses the exchange of GDP for GTP by Ras and thus activates Ras functions (Figure 1.11). The loss of RasGRP1 has been shown to impair ERK activation and thymocyte differentiation [Dower et al., 2000] [Kortum et al., 2013].

The DAG-independent Ras activation pathway involves the LAT-binding adaptor protein Grb2 and its associated GEF SOS. Grb2 and SOS form a complex through the SH3-domains of Grb2 and the proline rich region of SOS [Simon et al., 1993] [Sondermann et al., 2004]. Grb2 binds to the tyrosines 171, 191 and 226 of LAT which is phosophorylated after TCR triggering [Zhang et al., 2000]. This process locates Grb2-SOS to the plasma membrane and into the proximity of Ras. SOS acts similarly to RasGRP1 to catalyse the GDP-GTP exchange from Ras and thus activates Ras (Figure 1.11) [Roose and Weiss, 2000]. RasGRP has been was suggested to act within a positive feedback loop to enhance Ras signalling by priming SOS with RasGTP to facilitate SOS-mediated Ras activation [Roose et al., 2007] [Das et al., 2009]. However, recent data have questioned this model [Kortum et al., 2013]. SOS1 and SOS2 do not seem to play a role in thymocyte positive selection, whereas both RasGRP1 and, to a lesser extent, SOS1 are required for negative selection [Kortum et al., 2013].

The best characterised target of Ras-GTP is the serine-threonine kinase Raf-1 [Rebollo and Martinez-A, 1999]. Through interactions with Raf-1, Ras

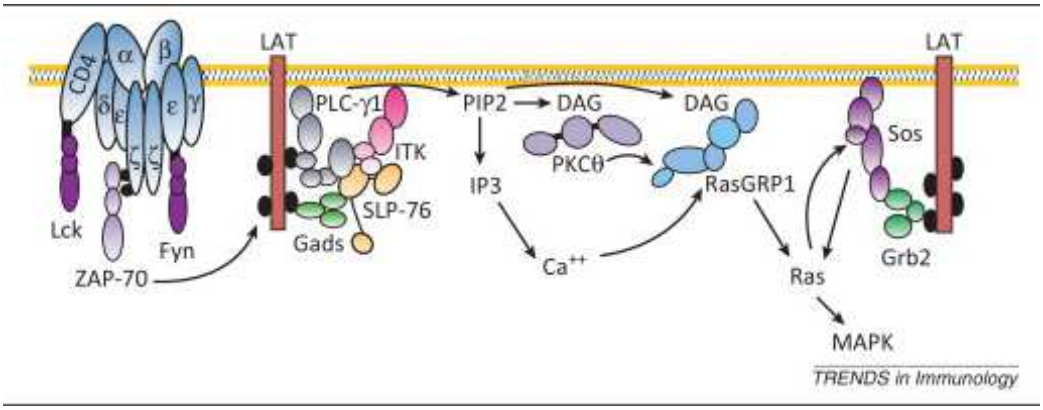

Figure 1.11: DAG-dependent and -independent activation of Ras. After TCR binding and engagement of the upstream kinases LCK and Fyn, activated ZAP-70 triggers phosphorylation of LAT. Phosphorylated LAT associates with two molecular complexes that regulate Ras activation: PLC-γ1, GADS, SLP-76 and Grb2-SOS. On LAT, activated PLC-γ1 cleaves PIP_2 generating IP_3, which stimulates release of calcium from intracellular stores and DAG that then recruits PKCϑ and RasGRP1 to the membrane, and the combined actions of Ca^{2+}, DAG, and PKCϑ activate RasGRP1. The Ras guanine nucleotide exchange factors (GEFs) SOS1 and SOS2 are also recruited to LAT via the adapter Grb2. SOS proteins have basal RasGEF activity, which can be enhanced by the binding of activated Ras (Ras-GTP) to an allosteric binding pocket on SOS. Ras-GTP binding to SOS potentially allows for the engagement of a positive feedback loop, primed by either RasGRP1 or basal SOS activity, to produce high levels of Ras activation. Ras signals to multiple downstream eector pathways including the Raf-MAPK/ERK kinase (MEK)-ERK kinase cascade.
Source: adapted from Kortum et al., *Trends in Immunology*, 2013

activates a cascade of the mitogen-activated protein kinase (MAPK) group of serine-threonine protein kinases. Initially, Raf-1 acts as a MAPK kinase kinase (MAPKKK) to phosphorylate and activate the serine-threonine kinase MEK1/2, a MAPK kinase (MAPKK). MEK1/2 in turn activates the MAPK ERK1/2 (extracellular signal-related kinase) by phosphorylation at threonine 202 and tyrosine 204 [Genot and Cantrell, 2000] [Alberola-Ila and Hernández-Hoyos, 2003]. ERK1/2 is a highly conserved protein found in many different cell types and it fulfils a crucial role in TCR signalling to influence diverse T cell functions including as proliferation, differentiation, cell migration and survival [Karlsson et al., 2006]. Upon activation ERK translocates to the nucleus which is essential to induce growth factor-induced gene expression and cell cycle entry. Furthermore, ERK contributes to the activation of AP-1 (activator protein-1) transcription complex. AP-1 is a heterodimer of Fos and Jun. ERK upregulates the expression of Fos by activating the transcription factor Elk-1 [Smith-Garvin et al., 2009]. Additionally, ERK induces the transcriptional activation of STAT3 (signal transducer and activator of transcription 3) which promotes T cell survival [Smith-Garvin et al., 2009] [Oh et al., 2011].

1.4 Themis

1.4.1 Themis identification and isotypes

Since the discovery of the TCR in 1983, the molecules involved in T cell activation and their interactions have been extensively studied. It was generally

assumed that all essential components involved in TCR proximal signalling were known.

However, in 2009 three independent groups of investigation identified an uncharacterised protein exclusively expressed in the T cell lineage [Fu et al., 2009] [Lesourne et al., 2009] [Johnson et al., 2009]. Two further studies identified Themis later during the same year by similar methods [Patrick et al., 2009] [Kakugawa et al., 2009]. The protein was called Themis for '**t**hymus-**e**xpressed **m**olecule **i**nvolved in **s**election'. Fu et al. and Lesourne et al. identified Themis using cDNA subtraction libraries from TCRα-deficient ($Tcra^{-/-}$) and Rag1-deficient ($Rag1^{-/-}$) thymocytes and from multipotent progenitor and T cell lineage-committed foetal liver CD4 CD8 DN thymocyte subsets respectively. Additionally, Dr. Oreste Acuto's laboratory started to collaborate with Dr Nick Gascoigne's laboratory (Scripps Research Institute, La Jolla, USA) after they identified Themis independently during a proteomics study in 2007 [Brockmeyer et al., 2011]. Johnson et al. discovered Themis by an ethylnitrosourea (ENU)-induced nonsense mutation which resulted in an abnormal response to immunisation, anti-nuclear autoantibodies, low proliferation to anti-CD3/CD28-antibody stimulations.

Themis is highly conserved among vertebrates (Figure 1.13). In the human, two isotypes of Themis are expressed, Themis1 and Themis2. Themis1 (subsequently referred to as Themis) was identified from the uncharacterised protein C6orf190 and is highly and exclusively expressed in the T cell lineage. Themis expression appears to be more prominent in CD8-positive peripheral T cells than in the CD4-positive lineage (Figure 1.12). The database of BioGPS gives no data on the expression of human Themis within thymo-

cytes.

Themis2 was identified by BLAST from the open reading frame position C1orf38. Themis1 and Themis2 are mutually exclusively expressed in the hematopoietic cell lineage and they share 33% identity and 51% homology. Themis2 is mostly expressed in dendritic cells, monocytes, NK cells and CD33-positive myeloid cells (Figure 1.12). The function of Themis2 in these cells is still unknown.

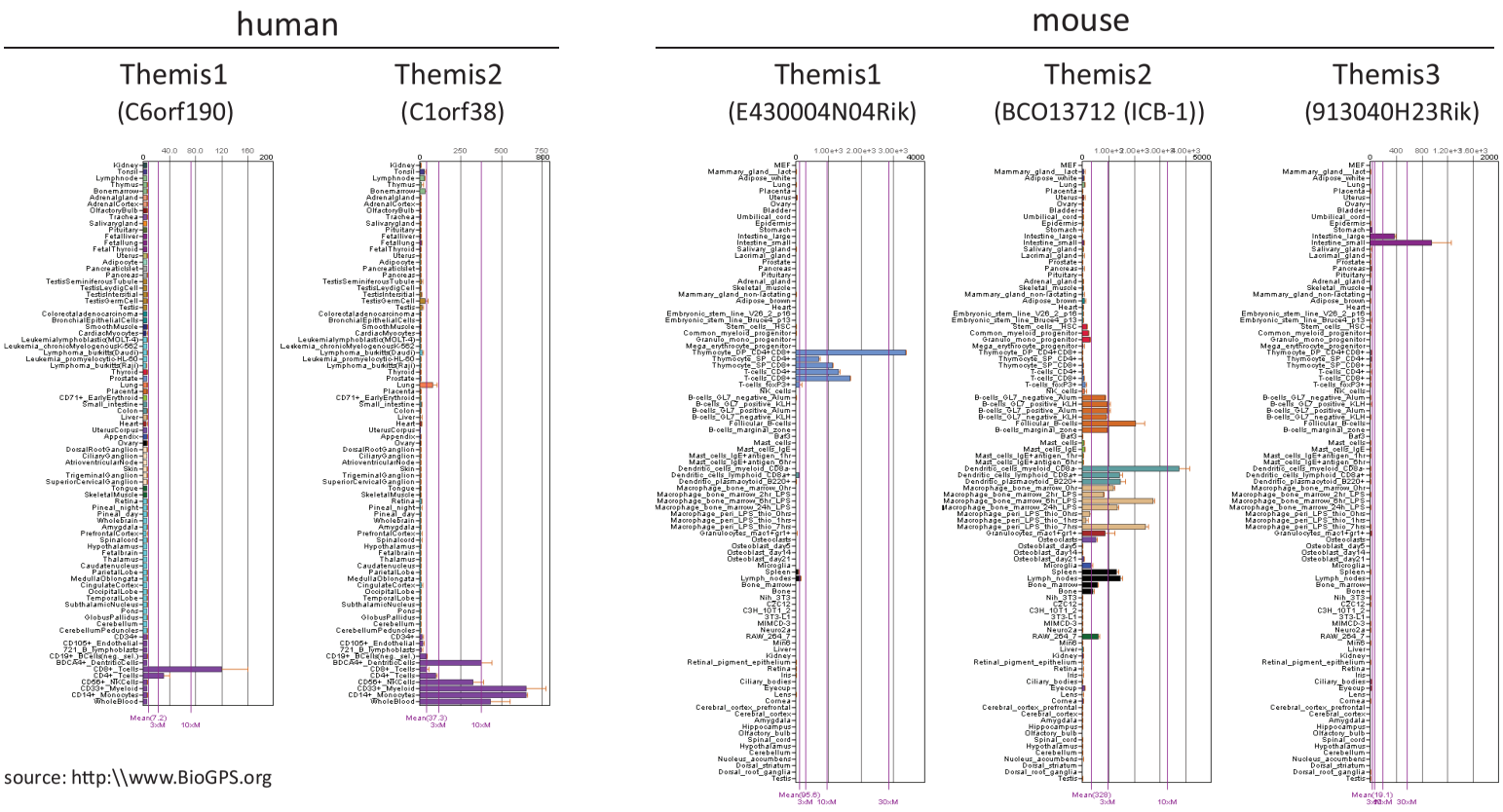

Figure 1.12: Human and murine Themis gene expression patterns. Themis and its murine homologue E430004N04Rik are primarily expressed in the T cell lineage in human and the mouse. The highest expression of Themis is found in thymocytes. The Themis2 isotype (called Icb-1 in mice) is mainly expressed in dendritic and myeloid lineage cells. The mouse isoform 9130404H23Rik or Themis3 is expressed in intestinal tissues only.
Source: http://www.BioGPS.org.

The mouse orthologue E430004N04Rik to the human Themis1 was identified which shares 76% identity and 83% homology with the human Themis1. Comparatively to its human homologue, the murine Themis is also expressed mainly in the T cell lineage. Its expression levels are particularly high in DP thymocytes (Figure 1.12). More precisely, Themis expression is low in DN1 and DN2 thymocytes but upregulated in the DN3 stage of thymocyte development. Themis levels remain elevated throughout the immature pre-selection DP stage and are subsequently downregulated in post-positive-selection thymocytes which have moved from the cortex towards the medulla [Fu et al., 2009] [Lesourne et al., 2009]. The expression levels in peripheral T cells is reduced by about 3-fold in comparison to DP thymocytes (Figure 1.12). As in the human, Themis is mainly expressed in conventional murine T cells.

In the mouse, two further isotypes of Themis1, Themis2 (Icb-1) and Themis3 (9130404H23Rik) have been identified. Themis2 is expressed in a variety of hematopoetic cells including B cells and macrophages (Figure 1.12). The molecular function is conserved between Themis1 and Themis2. Both proteins have similar domain structures and share the same interaction partners. In mice, Themis2-expression is capable of restoring the original phenotype in Themis$^{-/-}$ thymocytes [Lesourne et al., 2012]. Themis2 probably fulfils similar functions the BCR signalling cascade as Themis1 does in T cells. Finally, Themis3 is mainly expressed in the intestine and little is known about its function.

1.4.2 Themis structure and molecular function

Themis is a 72 kDa, 636 amino acid protein of unknown molecular function which is highly conserved in vertebrates (Figure of Fu et al.) [Fu et al., 2009].

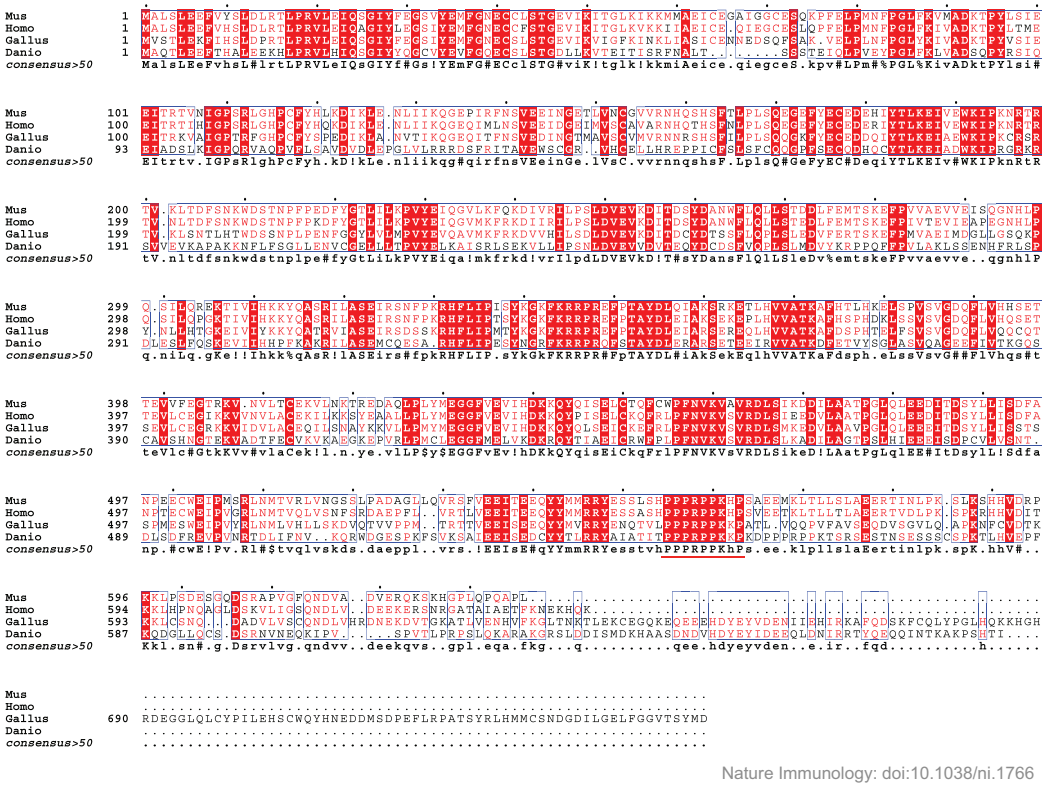

Figure 1.13: Themis protein alignment. Alignment of Themis protein sequences from mouse (*Mus musculus*), human (*Homo sapiens*), chicken (*Gallus gallus*) and zebrafish (*Danio rerio*). Amino acid identities are shown in white-on-red and similarities in red. The proline-rich region of Themis is underlined in red.
Source: Fu et al., *Nat Immunol*, 2009

In Oreste Acuto's laboratory, the bioinformatics tools PFAM and SMART were used to some features of the molecular structure of Themis. Alignments identified two conserved folded regions (CABIT1 and 2 as termed by [Johnson et al., 2009]): an apparent bipartite nuclear localisation signal

(NLS, resides 330-346) and a poorly structured C-terminal proline-rich region (PRR, residues 555-563) with the atypical SH3-binding motif PxRPxK (Figure 1.14) [Fu et al., 2009] [Paster et al., 2013]. Furthermore, Johnson et al. 2009, identified two homologous tandem C-terminal globular domains belonging to a previously uncharacterised domain family. The domains have been called 'cysteine-containing all-β in Themis', or 'CABIT'. The structure of the domains are predicted to contain either an extended β-sandwich-like fold or two six-stranded β-barrels. The function of CABIT domains is unknown [Johnson et al., 2009]. Unpublished data (C. Brockmeyer, P. Roversi, O. Acuto) indicated that each CABIT domain seems to be formed by two similar modular domains which bore resemblance to SH3 domains. However, the critical residues that confer binding to proline-rich sequences were missing.

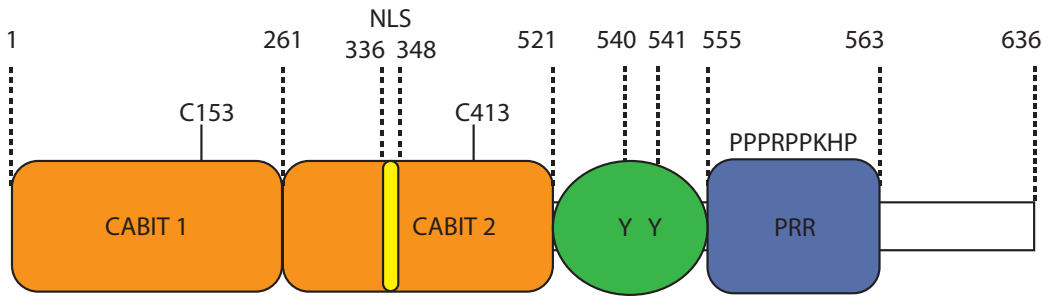

Figure 1.14: Molecular structure of Themis. Themis is a 72 kDa, 636 amino acid protein. It is predicted to contain two C-terminal CABIT domains with conserved cysteines at positions 153 and 413. The second CABIT domain hosts a NLS region. Two tyrosines at positions 540 and 541 are phosphorylated by LCK. The C-terminal PRR region associates to the SH2-domain of Grb2. CABIT: cysteine-containing all-β in Themis. NLS: nuclear localisation sequence. PRR: proline rich region.

The lack of known catalytic domains within the protein sequence leaves from for speculation towards the molecular function of Themis. While Themis

contains an NLS sequence and while the protein has been found by biochemical criteria within both the cytosol and the nucleus, it displays no apparent transcription factor functions. The SH3-binding PRR suggests interactions with other proteins. Indeed, Themis has been found to interact directly with GRB2 as discussed in more detail in the following section [Fu et al., 2009]. It is possible, that Themis acts as a scaffold protein to TCR proximal signalling proteins associated with the LAT complex [Allen, 2009].

1.4.3 Themis in thymocyte selection

All three papers of 2009 which identified Themis as a new and uncharacterised protein of the TCR signalling chain, uniformly reported defective thymocyte development at the double-positive stage in Themis$^{-/-}$ mice [Fu et al., 2009] [Johnson et al., 2009] [Lesourne et al., 2009].

In comparison to the wild-type strains, Themis$^{-/-}$ mice showed strong reductions of CD4- and CD8-SP thymocyte and CD8- and particularly CD4-positive peripheral T cells numbers. Themis$^{-/-}$ mice expressing a transgenic TCR for both class I and class II had essentially no SP thymocytes or peripheral T cells. [Fu et al., 2009] [Johnson et al., 2009] [Lesourne et al., 2009]. Yet, the numbers of DP thymocytes were slightly but significantly raised [Fu et al., 2009]. Furthermore, Johnson et al. and Fu et al. reported a small decrease in the number of CD4^{+}Foxp3^{+} regulatory T cells. Recently, Fu et al. (Nature, 2013, submitted) showed that NKT development and numbers in Themis$^{-/-}$ mice are almost normal.

The cellular loss in Themis$^{-/-}$ T cells was progressive throughout thymo-

cyte development from the DP stage to the SP peripheral T cells which clearly indicates a block in late positive selection. At this stage, DP cells with re-arranged αβTCR interact with pMHC class I and II molecules on cortical thymic epithelial cells. DP thymocytes that react too strongly to self-peptide MHC die and are negatively selected while unresponsive thymocytes die as they are unable to recognise pMHC. Only DP thymocytes which moderately react to self-peptide MHC progress in development and begin to downregulate CD8 expression in the following developmental stage before committing to either the CD4- or the CD8SP lineage. Themis$^{-/-}$ mice have fewer CD4+CD8^{int} thymocytes [Fu et al., 2009]. Decreasing the expression of Themis in Jurkat cells showed a defect in IL-2 production after anti-CD3ε-CD28-stimulation [Fu et al., 2009]. The initial three studies were divided on the effect of Themis on TCR signalling. C. Brockmeyer showed that Themis was phosphorylated at tyrosine residues within 30 sec of TCR engagement [Fu et al., 2009] [Brockmeyer et al., 2011]. However, overall no TCR proximal signalling defect per se was observed [Lesourne et al., 2009] [Johnson et al., 2009]. No obvious differences in the phosphorylation of ZAP-70, PLC-γ and Itk were observed. However, the lack of Themis resulted in some reduced phosphorylation of Erk in thyocytes [Fu et al., 2009] and Jurkat cells [Brockmeyer et al., 2011]. Critically, in both of these systems, the cells were stimulated with anti-CD3ε antibodies that induce strong TCR signals. It was thus difficult to see subtle responses of Themis$^{-/-}$ cells to low agonist stimulation as is important in thymocyte development and selection. Since the initial three reports, contradicting data on the actions of Themis on proximal TCR signalling has been published. The defect of ERK signalling is

only present in SP but not in DP thymocytes. In contrast, one study showed Themis to increase ERK signalling in Jurkat cells in response to low but not high avidity ligands [Brockmeyer et al., 2011].

Themis appears to reside mostly in the cytosol but small amounts of it are located in the nucleus. Translocation into the nucleus requires the NLS domain located in the CABIT2 domain [Lesourne et al., 2009] [Lesourne et al., 2012]. However, thymocyte stimulation does not alter the cytosol/nucleus distribution pattern of Themis [Lesourne et al., 2012]. Nevertheless, the expression of 325 genes was affected in Themis (Y498X) mutant murine DP thymocytes and uncommitted $CD4^{+}CD8^{lo}TCR\beta^{hi}CD24{+}MHCI^{lo}$ cells. Gene targets downstream of pERK or NFAT signalling pathways were not affected. However, apoptosis-related genes were downregulated. These genes included the ERK-signalling mediator B-Raf which is essential for T cell development beyond the DP stage. Furthermore cell survival genes involved in carbohydrate and vitamin metabolism were downregulated. The expression of further cell survival and cell cycle progression genes *Ccnb1*, *Cdc2* and *E2f1* was reduced. Finally, even though Notch target genes in thymocytes are unaffected by Themis, *Notch1* gene expression was downregulated [Johnson et al., 2009].

The effect of Themis on the negative selection of thymocytes is more controversial [Gascoigne and Palmer, 2011]. Negative selection appeared to be reduced and less efficient in thymocytes of male $Themis^{-/-}$ thymocytes [Fu et al., 2009] [Lesourne et al., 2009]. However, more recent studies suggest that $Themis^{-/-}$ thymocytes are unable to distinguish between negative and positive selection inducing ligands and that no defect in negative selection

can be observed (Fu et al., 2013, Nature, submitted).

All current studies indicate that Themis is an important checkpoint regulator involved in positive thymocyte selection and the generation of the TCR repertoire of peripheral T cells. In this function, it is likely to affect the proximal TCR signalling threshold which determines the positive or negative selection of thymocytes [Fu et al., 2009] [Brockmeyer et al., 2011].

1.4.4 Interaction partners

The lack of any conserved catalytic domains has led to much speculation about the molecular function of Themis. The presence of two CABIT domains of no known catalytic function and a C-terminal PRR domain could suggest that Themis fulfils an adaptor or linker protein function [Allen, 2009]. In this context, the atypical SH3-binding domain PxRPxK within the PRR domain is of particular interest [Paster et al., 2013]. Several independent studies have shown that Themis associates to the SH3-domain of Grb2 through the PRR domain (Figure 1.15) [Fu et al., 2009] [Patrick et al., 2009] [Brockmeyer et al., 2011] [Johnson et al., 2009]. The SH3-binding motif within Themis resembles that of SLP-76 and Gabs which also associate to Grb2 SH3-domains [Paster et al., 2013]. Grb2 is a protein-interaction-mediating scaffold molecule with an SH3-SH2-SH3 motif [Johnson et al., 2009]. The expression of Grb2 is crucial to the positive selection of thymocytes. Both downstream p38 and JNK and upstream LCK and ZAP70 activation is reduced in $Grb2^{-/-}$ cells [Jang et al., 2010]. Grb2 constitutively binds Themis through at least one SH3-domain. While Themis has been shown to bind

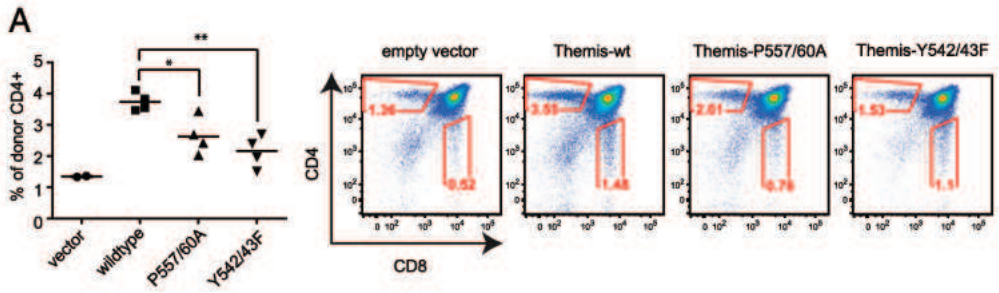

Figure 1.15: Critical role of the THEMISGrb2 complex for thymocyte development. The development of wt or PRR1-mutant THEMIS expressing thymocytes in bone marrow chimeric mice. Irradiated B6.SJL recipient mice (CD45.1$^+$) were reconstituted with *Themis*$^{-/-}$ bone marrow cells (CD45.2$^+$) transduced with a bicistronic GFP-based retroviral vector harbouring either no insert, muTHEMIS-wt, muTHEMIS-PRR1 (P557/560A), or muTHEMIS-Y542/43F. Four mice were injected per experiment. Eight weeks post-reconstitution, only recipient mice bearing 0.5% CD45.2$^+$GFP$^+$ thymocytes were included and analysed by flow cytometry. In the far left scheme, each symbol represents an individual mouse. Shown are CD4 versus CD8 stains after gating on CD45.2$^+$GFP$^+$ (transgene expressing) thymocytes. Mutations of the PRR domain and tyrosines 542 and 543 resulted in defects in thymocyte development.
Source: adapted from Paster et al., *J Immunol*, 2013

to both SH3 domains of Grb2, Patrick et al. 2009 and Paster et al. 2012 have shown contradicting preferences of Themis binding to either the N- or C-terminal SH3 domain respectively. Upon TCR triggering Grb2 is recruited to the LAT complex. Paster formally demonstrated that Themis binds constitutively to the C-terminal SH3-domain of Grb2 via the conserved PRR [Paster et al., 2013]. This association locates Themis to the LAT signalosome and thus the immunological synapse. Grb2 is essential for interactions of Themis with LAT and is required for thymocyte development and positive selection [Paster et al., 2013]. Together with Itk, LCK and ZAP-70 control most of the tyrosine phosphorylation in TCR proximal signalling. A Y540/541F Themis Src-phosphorylation site mutation abolishes Themis-Grb2 associations [Paster et al., 2013].

Themis associates to a variety of LAT-SPL-76 complex associated proteins through Grb2 (Figure 1.16). Similarly, the interactions with SLP-76 are not constitutive but depend on the presence of Grb2. SLP-76 phosphorylates Themis to a lesser extent than LCK or ZAP-70 [Brockmeyer et al., 2011]. Upon phosphorylation Themis furthermore associates to Itk which is involved in the phosphorylation and activation of PLC-γ which shows low but constitutive binding to Themis [Brockmeyer et al., 2011]. PLC-γ activates the DAG-RasGRP1 pathway which also initiates ERK signalling and plays an important role in thymocyte positive selection as discussed in previous chapters [Labrecque et al., 2011].

While Themis interacts with a multitude of proteins upstream, within and downstream of the LAT-SLP76 complex, its molecular function remains elusive.

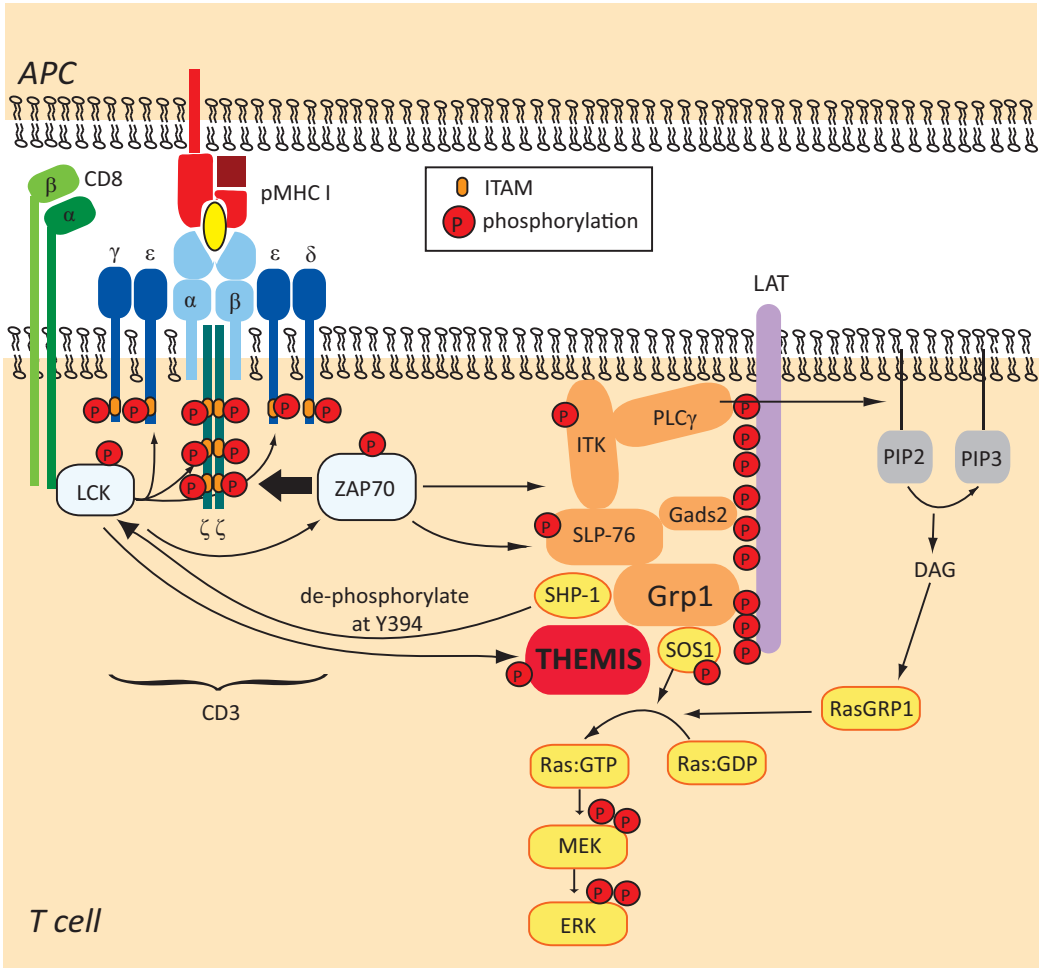

Figure 1.16: Themis in proximal TCR signalling. Themis locates to the LAT-SLP76 complex through the interactions of its proline rich region with Grb2. LCK phosphorylated Themis on tyrosines 542 and 543. Themis associates indirectly to LAT, SLP-76 and Itk through its interactions with Grb2. Further possible interactors associated to the LAT signalosome are currently under investigation.

1.5 Aims and objectives

T cell activation is a complex and diverse subject. While the mechanics of TCR ligation and the sequence of T cell signalling responses following TCR triggering have been well researched over the last 25 years, many questions still remain unanswered. The TCR is an unusual receptor with extraordinary properties. It has no known signal transduction capabilities itself and the mechanism by which TCR ligation is translated into signal propagation by the CD3 chains remains ambiguous. Even more remarkable is the TCR's ability to qualitatively respond to short structurally related peptide sequences and remain either inactive or mount immune responses accordingly.

The effect of different ligand affinities and off-rates on cellular effector outcomes has been described by several studies [Kalergis et al., 2001] [Carreño et al., 2007] [Dushek et al., 2011]. This includes the observations that beyond a threshold the analogue input of the strength of TCR:pMHC interactions results in distinct digital effector responses such as cytotoxicity. Translating a graded instruction into a distinct response allows T cells to effectively discriminate infected or transformed cells from healthy tissues and mount a cytotoxic immune response to one while tolerating the other [Daniels et al., 2006] [Gascoigne and Palmer, 2011]. Recently, a protein prominently expressed in tymocytes, Themis, has been shown to modulate TCR signalling thresholds determining positive and negative selection [Fu et al., 2009] [Brockmeyer et al., 2011] [Paster et al., 2013].

The aim of this study was to gain an understanding of how qualitative dif-

ferences in TCR:pMHC binding are conveyed through the TCR proximal signalling cascade, modulated by downstream signalling molecules and translated into ultimately functionally distinct outcomes. In order to correlate T cell signalling accordingly to the affinity of the TCR stimulation, I employed an *in vitro* system using a panel of four NY-ESO-$1_{156-165}$ peptide derivates presented on HLA-A2 pMHC and Jurkat cells expressing the 1G4 TCR. NY-ESO-$1_{156-165}$ is a nine amino acid peptide derivative of a protein expressed by 80% of synovial cell sarcomas and 25% of melanomas and has been used to develop cancer vaccines in clinical trials [Chen et al., 1997] [Robbins et al., 2011]. The 1G4 TCR recognised NY-ESO-$1_{156-165}$-pMHC and induces mild T cell responses against the peptide. Single amino acid substitutions in the peptide's sequence have been shown to influence both the TCR:pMHC binding kinetics and the resulting T cell effector functions [Aleksic et al., 2010] [Chen et al., 2010].

The major objectives of my thesis were:

1. Produce a panel of NY-ESO-$1_{156-165}$ pMHC monomers of distinct and known monomeric binding properties to the 1G4 TCR and test their tetrameric binding properties to 1G4 TCR-expressing Jurkat cells (Chapter 3).

2. Characterize the 1G4 TCR-expressing Jurkat cells and test the efficacy of TCR triggering by NY-ESO-$1_{156-165}$ tetramers *in vitro* (Chapter 4).

3. Analyse early proximal signalling kinetics in response to stimulation

with NY-ESO-$1_{156-165}$ pMHC tetramer of different affinities in a qualitative and quantitative manner using flow cytometry (Chapter 5).

4. Investigate the effect of Themis expression on proximal 1G4 cell TCR signalling responses to stimulation with different affinity NY-ESO-$1_{156-165}$ pMHC tetramers (Chapter 6).

Investigating the proximal TCR signalling responses to stimulation of different affinities provides insights into how T cells sense qualtitative differences of agonist and self-peptide ligands. The use of TCR- or antigen-engineered cytotoxic T cell vaccines are an attractive approach to treating cancer. Understanding the signalling events which drive or attenuate T cell effector in response to stimulation with particular affinities could help in the design of more effective treatment approaches.

Chapter 2

Materials and Methods

2.1 Materials

2.1.1 Chemicals and consumables

Chemical or consumable	Abbreviation	Source
β-mercaptoethanol		Sigma
10x Perm/Wash buffer		BD Bioscience
15% acrylamide/ 0.4% Bis-acrylamide		National Diagnostics
3,3,5,5-tetramethylbenzidine	TMB	Sigma
4-(2-hydroxyethyl)-1-piperazineethanesulfonic acid	HEPES	Sigma
adenosine triphosphate	ATP	Fluka Biochimika

ammonium persulfate	APS	Sigma
ampicillin	AMP	Sigma
apoptosis wash buffer		ImmunoChemistry Technologies
BirA enzyme		Avidity
bovine serum albumin	BSA	Fisher Chemicals
bromophenol blue		Sigma
calcium chloride	$CaCl_2$	Fluka
camptothecin		Sigma
carboxyfluorescein succinimidyl ester	CFSE	Invitrogen
chloroquine		Sigma
Coomassie-based Instant Blue™		expedon
D-biotin		Sigma
dextrose		Sigma
dimethyl sulfoxide	DMSO	Sigma
disodium phosphate	Na_2HPO_4	VWR Internaional, AnalaR®
dithiothreitol	DTT	Sigma
Dulbecco modified Eagle's minimal essential medium	DMEM	PAA
ethanol		Sigma

ethylenediaminetetraacetic acid	EDTA	Sigma
Fix buffer I		BD Bioscience
fluorescent labelled inhibitor of caspases	FLICA®	ImmunoChemistry Technologies
fluorocarbonylcyanide phenylhydrazone	FCCP	AbCam
foetal calf serum	FCS	Thermo
glutathione (oxidised)		Sigma
glutathione (reduced)		Sigma
glycerol		Fisher Chemicals
glycine		Sigma
hydrogen peroxidase	H_2O_2	Sigma
isopropanol		Sigma
isopropyl β-D-1-thiogalactopyranoside	IPTG	Melford
L-arginine hydrochloride		Sigma
magnesium chloride	$MgCl_2$	AnalaR®
methanol		VWR International
monopotassium phosphate	KH_2PO_4	Fisher Chemicals
n-dodecyl-β-D-maltoside	LM	Calbiochem

Odyssey buffer		Li-Cor Biosciences
penicillin-streptomycin	pen-strep	PAA
peroxidase streptavidin	Extravidin	Sigma
pervanadate	Na_3VO_4	Sigma
phenylmethanesulfonyl-fluoride	PMSF	Fluka Biochimika
phorbol 12-myristate 13-acetate	PMA	Sigma
potassium chloride	KCl	VWR Internaional, AnalaR®
protein phosphatase 2	PP2	Calbiochem
proteinase cocktail tablets		Roche
puromycin		Gibco
Quick-Start 1x Bradford reagent		BioRad
Roswell Park Memorial Institute medium	RPMI-1640	PAA
sodium azide	NaN_3	Acros Organics
sodium chloride	NaCl	VWR Internaional, AnalaR®
sodium dodecyl sulfate	SDS	VWR Internaional
sterile phosphate buffered saline	sterile PBS	Gibco

streptavidin-phycoerythrin	streptavidin-PE	Fluka
tetramethylethylenediamine	TEMED	Sigma
tetramethylrhodamine, ethyl ester, perchlorate	TMRE	AbCam
Tris		MP Biochemicals, LLC
Triton X-100		
Tween		VWR International
urea		VWR Internaional, AnalaR®

Table 2.1: Chemicals and Consumables

2.1.1.1 Immunoblotting

- Transfer buffer

  38 mM glycine, 50 mM Tris, 20% methanol

- Blocking buffer

  50% Odyssey buffer (Li-Cor Biosciences)

- 10x wash buffer

  10x PBS, 1% Tween

- Primary antibody solution

  PBS, 0.1% Tween, 3% BSA, 0.01% NaN_3

- Secondary antibody solution

  50% Odyssey buffer (Li-Cor Biosciences), 0.5% PBS, 0.01% Tween

2.1.1.2 Flow cytometry

- Wash buffer

  PBS, 1% BSA, 2 mM EDTA, 0.01% NaN_3

- Fixation buffer

  Fix buffer I (BD Bioscience, containing paraformaldehyde)

- Saponin-based permeabilisation buffer

  10x Perm/Wash Buffer I (BD Bioscience, containing saponin, FBS and 0.09% NaN_3)

2.1.1.3 Other buffers

- Cell lysis buffer

  20 mM Tris pH 7.5, 150 mM NaCl, 1% n-dodecyl-β-D-maltoside, 4 mM Na_3VO_4, 1 mM PMSF

- 2x HEPES buffered saline (HBS)

  273 mM NaCl, 10 mM KCl, 1.5 mM Na_2HPO_4-$2H_2O$, 11 mM dextrose, 42 mM HEPES

2.1.2 Antibodies

Antigen	Phospho-site	Fluoro-chrome	Host	Clone	Source
Actin	n/a	n/a	rabbit	n/a	Sigma
Akt	S473	Alexa647	rabbit	n/a	Cell Signaling Technologies
CD3ε	n/a	n/a	mouse	UCHT1	eBioscience
CD3ε	n/a	PE	mouse	UCHT1	BD Biosciences
CD4	n/a	PE	mouse	RPA-T4	BD Biosciences
CD8	n/a	APC	mouse	LT8	AbD Serotec
CD28	n/a	PE	mouse	CD28.2	BD Biosciences
CD45	n/a	PE	mouse	HI30	BD Biosciences
CD69	n/a	APC	mouse	CH/4	Invitrogen
CD69	n/a	APC	mouse	L78	BD Biosciences
CD247	n/a	n/a	mouse	6B10.2	Santa Cruz Biotechnologies
CD247	Y142	n/a	rabbit	n/a	Epitomics
CD247	Y142	Alexa647	mouse	K25-407.69	BD Biosciences
IgG1 $\varkappa$	n/a	PE	mouse	MOPC-21	BD Biosciences
IgG1 $\varkappa$	n/a	FITC	mouse	MOPC-21	BD Biosciences
LAT	n/a	n/a	rabbit	n/a	Millipore
LAT	Y226	Alexa647	mouse	J96	BD Biosciences

LCK	n/a	n/a	mouse	3A5	Santa Cruz Biotechnologies
LCK	n/a	Alexa647	mouse	MOL 171	BD Biosciences
LCK (Src family)	Y394 (Y416)	n/a	rabbit	n/a	Cell Signaling Technologies
LCK	Y505	n/a	rabbit	n/a	Cell Signaling Technologies
MAPK (ERK1/2)	n/a	n/a	mouse	3A7	Cell Signaling Technologies
MAPK (ERK1/2)	T202/Y204	n/a	mouse	E10	Cell Signaling Technologies
MAPK (ERK1/2)	T202/Y204	Alexa647	mouse	E10	Cell Signaling Technologies
phospho-tyrosine	Y	n/a	mouse	4G10	Millipore
SOS1/2	n/a	n/a	rabbit	n/a	Santa Cruz Biotechnologies
Themis	n/a	n/a	rabbit	n/a	Sigma
Themis	n/a	PE	mouse	Q13-1103	BD Biosciences
ZAP-70	n/a	n/a	mouse	L1E5	Cell Signaling Technologies
ZAP-70	Y319	n/a	rabbit	n/a	Cell Signaling Technologies

ZAP-70	Y493	n/a	rabbit	n/a	Cell Signaling Technologies

Table 2.2: Antibodies

2.1.3 Plasmids and constructs

To knock-down Themis in cells in culture, short-hairpin RNA (shRNA) against Themis were obtained from Sigma Aldrich. The sequences for the shRNAs and the corresponding TRC numbers to the constructs are shown in the table below. The stalk region of the short-hairpin is highlighted in bold.

Identity	TRC number	Sequences
non-mammalian shRNA control plasmid DNA	SHC002	CCGG**CAACAAGATGA AGAGCACCAA**CTCGA G**TTGGTGCTCTTCAT CTTGTTG**TTTTTTG
Themis	128476	CCGG**GAGATCACTGA AGAGCAATAT**CTCGA G**ATATTGCTCTTCAG TGATCTC**TTTTTTG
Themis	130264	CCGG**CCCATAGTGAC TGAAGTCATA**CTCGA G**TATGACTTCAGTCAC TATGGG**TTTTTTG

Table 2.3: Themis shRNA sequences.

The lentiviral expression vector used in this study was the pLKO-1-puro which besides the shRNA construct also contains a puromycin resistance vector. This allows the selection of transduced cells *in vitro* (Figure 2.1).

Identity	Sequences
wildtype target sequence to 128476	GAGATCACTGAAGAGCAATAT
shRNA resistant target site	GAGATCAC**C**GA**G**GAGCAATAT
translation of target site	EITEEQY

Table 2.4: Themis shRNA target sequences and mismatch mutation resistances.

To overexpress Themis full-length cDNA encoding human Themis was obtained from Open Biosystems. This sequence contains a resistance against the 128476-shThemis target sequence. This allows the expression of the full-length Themis construct even on the background of an endogenous knock-out. The resistance is achieved through mismatch mutations that maintain the protein sequence (Table 2.4). Themis overexpression studies were performed with the aid of the lentiviral helper plasmid psPAX2 (Addgene 10703) and pMD2.G (Addgene 12259). These were provided by Dr Didier Trono (Ecole Polytechnique Fédérale de Lausanne, Switzerland).

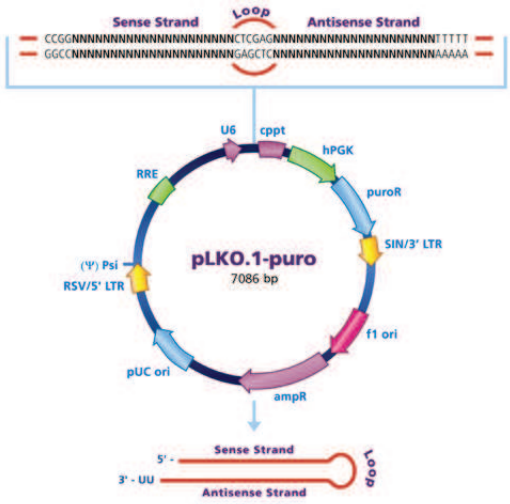

Figure 2.1: pLKO1-puro vector obtained from Sigma Aldrich.

2.2 Methods

2.2.1 Cell culture techniques

2.2.1.1 Cells and culture conditions

The human leukaemic Jurkat T cell lines C20 (subclone 20, $CD4^+$), J.RT3-T3.5 which was stably transduced with the human 1G4 TCR (kind gift of Prof Vincenzo Cerundolo [Davis et al., 2012]). and the 1G4 TCR-expressing J.RT3-T3.5 which was stably transduced with CD8α(kind gift of Prof Anton van der Merwe) were maintained at in RPMI-1640 supplemented with 10% FCS at 37 °C in a humidified 5% CO_2 atmosphere.
Human embryonic kidney epithelial cells (HEK293) were maintained in DMEM supplemented with 10% FCS under the same conditions.

2.2.1.2 Cell freezing and thawing

To freeze cells, 9 x 10^6 cells were harvested and centrifuged at 100 xg for 5 min at room temperature (RT) The medium was aspirated and the cells were resuspended in 1 ml sterile freezing medium (FCS + 10% DMSO) and transferred to cryovials. The cells were transferred to storage at −80 °C on dry ice.
Cells were gradually thawed with a total of 10 ml pre-warmed culture medium. Cells were spun down, resuspended in fresh culture medium and transferred to fresh cell culture flasks.

2.2.1.3 Lentiviral particle production and cell transduction

HEK293 cells were transfected by standard calcium phosphate precipitation. One day before transfection, HEK293 cells were plated in 10 ml DMEM +10% FCS at 3 x 10^6 cells per 10 cm culture dish. Each transfection contained a total of 20 µg DNA (10 µg pHR-SIN-BX-IRES-Emerald lentiviral expression vector and 5 µg of each packaging plasmid psPAX2 and pMDG2). The vectors were supplemented with 850 µl deionised water (dH_2O) and, under vortexing, with 122 µl 2 M $CaCl_2$. Under vortexing, 1 ml 2x HBS was added dropwise. The solution was incubated at RT for 13 min. 5 min prior to adding the DNA complexes to the HEK293 cells, chloroquine was added to the culture dish at a final concentration of 25 µM. Dropwise the DNA complexes were distributed onto the cells.

After three hours of incubation at 37 °C, the medium was exchanged for fresh DMEM + 10% FCS and the cells were returned to the incubator.

48 hours after transfection viral supernantants were harvested, filtered and used to transduct 3 x 10^6 at a 1:3 ratio of viral supernantant and RMPI + 10% FCS in the presence of in a 6-well. After three hours the medium was exchanged for fresh RPMI + 10% FCS and after overnight culture the cells were transferred into small culture flasks.

Where appropriate, puromycin selection was applied at 1 µg/ml 48 hours post transduction.

2.2.2 NY-ESO-1 pMHC monomer and tetramer preparation

Culture of *E. coli* expressing the MHC A2 heavy chain and β2M light chain Residues 1278 of the A2 heavy chain with the COOH-terminal BirA tag and β2M were expressed in *Escherichia coli*. Initial bacterial stocks were a kind gift of Prof Vincenzo Cerundolo. The stocks were derived from 0.5 ml bacterial overnight culture and 0.5 ml sterile glycerol and were stored at −80 °C.

From frozen stocks, bacterial cultures were streaked onto agar plates supplemented with 100 μg/ml ampicillin (AMP) (Sigma) and incubated overnight at 37 °C. A colony of each plate was picked and inoculated in 10 ml lysogeny broth (LB) with 0.1 mg/ml AMP at 37 °C shaking for 6 hours. 1 ml of this inoculation was further incubated in 200 ml LB+AMP at 37 °C shaking overnight.

50 ml of the overnight bacterial cultures were transferred into 1 L LB with 0.1 mg/ml AMP and incubated at 37 °C shaking for approximately 2 hours or until OD_{600} absorption levels equalled between 0.4 and 0.6. 1 ml of this pre-induction culture was removed and stored at −20 °C. A2 and β2M expression was induced with 0.5 mM isopropyl β-D-1-thiogalactopyranoside (IPTG) for 4 hours at 37 °C shaking.

At the end of the incubation, 1 ml of the medium was removed and the OD_{600} of the sample was measured. This post-induction sample was also stored at −20 °C.

The bacteria were harvested by centrifugation at 5,000 xg for 30 min at 4 °C

and resuspended in 25 ml ice-cold PBS supplemented with proteinase inhibitors (1 tablet of complete EDTA-free proteinase inhibitor cocktail (Roche) in 25 ml PBS) and stored at −20 °C.

Induction analysis The bacteria in the pre- and post-induction samples were thawed and pelleted at 20,000 xg for 5 min. The supernantant was discarded and the bacterial pellets of each sample was re-suspended in LB at a volume in µl corresponding to 100x OD_{600} measured to equalise protein levels between different samples. The samples were boiled for 5 min and 10 µl per sample were run on a 15% SDS-PAGE gel. Protein induction was assessed by staining of the gel with Coomassie blue.

Extraction of A2 and β2M from *E.coli* The bacterial resuspensions were thawed and the inclusion bodies containing A2 or β2M were extracted by sonication on ice and pelleted at 20,000 xg for 30 min at 4 °C. To wash the inclusion bodies from cellular debris, the resulting pellet was repeatedly resuspended in 25 ml ice-cold Triton wash buffer with the help of a homogeniser and centrifuged at 27,000 xg for 15 min at 4 °C.

The includion bodies were washed off detergents by resuspension in ice-cold resuspesion buffer and centrifugation at 27,000 xg for 15 min at 4 °C.

To extract the proteins from the inclusion bodies, the inclusion body pellets were resuspended in 5 ml ice-cold 8 M urea buffer and rotated at overnight 4 °C.

The extracts were centrifuged at 27,000 xg for 30 min at 4 °C and the supernatant was collected. A 50 µl sample was taken for Coomassie protein

gel analysis and the protein concentration within the extract was measured by Bradford assay. The extracted A2 heavy chain was diluted to 3.2 mg/ml and the extracted β2M to 2.6 mg/ml in 8 M urea buffer. The samples were stored at −80 °C in 100 µl aliquots.

Refolding of pMHC monomers NY-ESO-$1_{156-165}$ pMHC monomer refolds were usually set up in volumes of 200 or 300 ml. Aliquots of the NY-ESO-$1_{156-165}$ peptides, the A2 heavy chain and β2M were kept in aliquots suitable for 100 ml refolds.

The refold buffer was prepared as described in section 2.1.2.2, filtered through a 0.45 µm membrane and cooled at 4 °C stirring in the cold room. One aliquot per 100 ml of refold buffer of NY-ESO-$1_{156-165}$ peptides, β2M and the A2 heavy chain was added in this sequence dropwise to the refold buffer while stirring. The refold was stirred gently for 40 hours at 4 °C.

The refold was kept on ice for all following steps. The solution was filtered through a 0.45 µm membrane to purify it from protein aggregations. The refolds were concentrated to 2.5 ml in Centricon®Plus-70 (Millipore) centrifugal filters at 3,500 xg at 4 °C.

Desalting and biotinylating pMHC monomers The concentrated refold solution was de-salted using the manufacturer's gravity protocol on PD-10 de-salting columns (GE Healthcare). The PD-10 columns were equilibrated five times with Tris-buffered saline (TBS). The concentrated refold solution was added to the column and allowed to enter the column bed completely. The sample was eluted with 3.5 ml TBS.

The biotinylation buffer (section 2.1.2.2) was prepared at RT. For this adenosine triphosphate (ATP) was first added to TBS. D-biotin (Sigma) stocks were prepared in 200 mM pH-unadjusted Tris base. 3.5 ml of the desalted refold solution was added to the biotinylation mix. 5 µl BirA enzyme (Avidity) was added last. The solution was incubated overnight at RT on a roller.

Monomer purification by fast protein liquid chromatography (FPLC) After the biotinylation, the refold mix was filtered through a 0.45 µm membrane. To purify the monomers, the refold mix was loaded on a HiLoad^{TM} 16/600 Superdex^{TM} 200 pg column (GE Healthcare). A 5 ml loading loop was used to load the sample. 1 ml fractions were collected. The program used to control the FPLC method and data collection was Unicorn 5.11 (General Electric Company). Fractions corresponding to peaks were pooled and a small 50 µl aliquot was collected for Coomassie protein gel analysis. Peak samples corresponding to the monomer fraction were concentrated to 1 mg/ml using AmiconUltra-15 centrifugal filter devices (Millipore) at 3,500 xg at 4 °C.

Monomer storage Aliquots of NY-ESO-$1_{156-165}$ monomers in Lo-Bind Eppendorfs contained 66.6 µl at 1 mg/ml. The aliquots were stored at −80 °C.

2.2.2.1 pMHC tetramer preparation

Streptavidin contains four biotin binding sites. For the tetramerisation of previously prepared NY-ESO-$1_{156-165}$ pMHC monomers, streptavidin linked

to phycoerythrin (PE) (Fluka) was used. The concentration of biotin on the monomers and streptavidin biotin binding sites was calculated with reference to [Altman and Davis, 2003]:

1. Calculate the total moles of biotinylated MHC (about 50 kDa) in the purified 100 µl stocks:

$$0.1ml * 1\frac{mg}{ml} * 1000\frac{ml}{l} * \frac{1mol}{50000g} * 100\% = 2 * 10^{-9}mol$$

2. Calculate the concentration of biotin binding sites (BBS) in the streptavidin-PE stock (streptavidin-PE conjugate: 300,000 g/mol; stock concentration: 1 mg/ml):

$$1\frac{mg}{ml} * \frac{1g}{1000mg} * 1000\frac{ml}{l} * \frac{1mol}{300000g} * 4\frac{BBS}{mol} = 1.33 * 10^{-5}\frac{mol}{l}$$

3. Calculate the volume of streptavidin-PE needed to tetramerise 100 µl pMHC monomers at a ratio of 1:1 biotin:BBS:

$$\frac{2.9 * 10^{-9}molbiotin.pMHCmonomers}{1.33 * 10^{-11}\frac{molBBS}{\mu lstreptavidinPE}} = 150.38\mu lstreptavidinPE$$

4. Calculate the total volume after tetramerisation of pMHC monomers with streptavidin-PE:

$$100\mu l\, monomers + 150.38\mu l\, streptavidin PE = 250.38ml\, tetramers$$

5. Calculate the pMHC monomer concentration within the pMHC tetramer stock solution:

$$\begin{aligned} 2 * 10^{-9} mol/250.38ml &= 7.98 * 10^{-6} mol/l \\ &= 7.98 * 10\mu mol/l \\ &\approx 0.399 g/l \\ &\approx 399 mg/l \end{aligned}$$

6. Tetramer stock concentration (4 pMHC sites/tetramer):

$$\begin{aligned} monomer\, concentration/4 &= tetramer\, concentration \\ 7.98 * 10^{-6}\mu mol/l/4 &= 1.995\mu mol/l \\ &\approx 2\mu M \\ 399 mg/l/4 &= 99.75 mg/ml \\ &\approx 100 mg/ml \end{aligned}$$

This means that 100 µl streptavidin-PE needs to be added to 66.6 µl of monomer solution. Streptavidin-PE was added stepwise in 10 µl per 10 min increments to a monomer surplus at RT under agitation in a mixer.
As quality control a biotin ELISA was performed. This assays for free biotin of surplus monomers within the tetramer solution.
Tetramers were stored at 4 °C.

2.2.3 Biochemistry

2.2.3.1 Stimulation of cells

anti-CD3ε antibodies Jurkat cells were stimulated 1 x 10^7 cells/ml in solution at 1 µg/ml anti-CD3ε (clone UCHT1) at 37 °C in RMPI on a heating block under agitation.

pMHC tetramers Jurkat cells were stimulated in solution at 1 x 10^7 cells/ml with 200 to 0.2 nM NY-ESO-$1_{156-165}$ pMHC tetramers at 37 °C in RMPI on a heating block under agitation. The NY-ESO-$1_{156-165}$ peptides used are outlined in Figure 1.9 and 3.1. For apoptosis and CD69 assays, 1G4 Jurkat cells were stimulated with 20 nM NY-ESO-$1_{156-165}$ pMHC tetramers at 37 °C in RMPI + 10% FCS

plate-bound pMHC monomers NY-ESO-$1_{156-165}$ monomers were plated at a serial dilution from 100 to 6.25 µM in 100 µl sterile PBS on streptavidin-coated microplates (Thermo). The plates were incubated at 37 °C for 60 min. The plates were washed three times with sterile PBS. Jurkat cells were plated out at 0.2 x 10^6 per well in RPMI + 10% FCS and incubated for 20 hours at 37 °C, 5% CO_2

PMA Jurkat cells were stimulated at 1x 10^7 cells/ml with 2.5 µg/ml PMA for 2 min at 37 °C in RMPI on a heating block under agitation.

Na_3VO_4 Jurkat cells were stimulated at 1 x 10^7 cells/ml with 1 µM freshly-prepared Na_3VO_4 for 2 min at 37 °C in RMPI on a heating block under agitation.

PP2 Jurkat cells were stimulated at 1 x 10^7 cells/ml with 25 µM PP2 for 15 min at 37 °C in RMPI on a heating block under agitation.

2.2.3.2 SDS-PAGE

For analyses based on SDS-PAGE, Jurkat cells were quickly lysed with ice-cold 2x lysis buffer and incubated for 15 min on ice. Cell debris was pelleted by centrifugation at 4 °C at 20,000 xg for 15 min. Lysates were mixed with 2x sample buffer and vortexed. The samples were boiled for 5 min and loaded on 10%, 12% or 15% self-cast gels or Novex 4-12% Bis-Tris pre-cast gels (Life Technologies) together with 2-5 µl Precision Plus Protein® Standards pre-stain protein ladder (BioRad). Electrophoresis was carried out at 175 V for approximately 65 min. Gels were further used for immunoblotting or protein content by Coomassie blue staining.

non-reducing PAGE To analyse samples on PAGE in non-reducing conditions, SDS was excluded from the sample buffer. The procedure to lyse the samples, run the gel and analyse it by Coomassie blue analysis or immunoblotting was the same as for SDS-PAGE.

2.2.3.3 Coomassie protein gel analysis

SDS- or Native PAGE gels were removed from their tanks and submerged in Coomassie-based Instant Blue™ (expedon) staining solution and placed on a rocker. The solution was removed when clear blue protein bands were visible on the gels. The gels were washed several times with dH_2O before being scanned on an Odyssey® near-infrared imager (Li-Cor Biosciences). For

analysis the Odyssey®infrared imaging system application software version 3.0 was used.

2.2.3.4 Immunoblotting

Before transfer, nitrocellulose membranes were submerged first in dH_2O and then in transfer buffer. Proteins were transferred onto the membranes in semi-dry transfer units (BioRad) at 25 V over 55 min.

Transferred membranes were blocked in 50% Odyssey blocking buffer (Li-Cor Biosciences) for 30 min and then washed in PBS-Tween for 5 min.

Primary antibodies were usually diluted in 1:1000 in primary antibody dilution buffer. Membranes were incubated with primary antibodies for 60 min at RT or overnight at 4 °C. Membranes were subsequently washed for 30 min in PBS-Tween at RT with the buffer being changed at least three times.

Secondary antibodies were diluted 1:10,000 in secondary antibody dilution buffer. Membranes were incubated with secondary antibodies for 30 min at RT and then washed for 30 min with PBS-Tween at RT. The wash buffer was changed at least 3 times during this time. The secondary antibodies are fluorescently-labelled with IRDye® infrared dyes (Li-Cor Biosciences).

Membranes were scanned on an Odyssey® near-infrared imager (Li-Cor Biosciences). The Odyssey® allows simulatenous two infra-red colour detection and quantitation on the same membrane. Anti-rabbit secondary antibodies are labelled with a fluorochrome excited at 580 nm and appear red on the scanner while anti-mouse secondary antibodies are labelled with a fluorochrome excited at 660 nm and appear green. Thus, for example, a mouse monoclonal ERK antibody and a rabbit polyclonal phospho-ERK antibody

can be detected and analysed quantitatively at the same time. For analysis the Odyssey®infrared imaging system application software version 3.0 was used.

2.2.3.5 Bradford assay

To determine protein concentrations within a solution, 5 µl of diluted or undiluted protein solution were assayed with 200 µl Quick-Start 1x Bradford reagent (BioRad) per well of a 96-well flat-bottomed ELISA plate. A standard curve with a minimum R^2 of 0.98 made of 0.1, 0.2, 0.4, 0.6 and 0.8 mg/ml BSA was used to determine sample protein concentrations. After 5 min incubation the plate was measured against a blank sample at 595 nm in a Biotek µQuant microplate spectrophotometer.
To determine monomer concentrations, monomer solutions were diluted 1:2, 1:4 and 1:8. the protein concentration in the undiluted and diluted samples was measured and an average concentration calculated.

2.2.3.6 Biotin ELISA

To determine the successful biotinylation of NY-ESO-$1_{156-165}$ pMHC monomers and tetramerisation of the same, 1 µg of pMHC monomers (note, tetramer volumes needed to be adjusted for their extra volume) were added to 100 µl PBS onto flat-bottomed Nunc maxisorb ELISA plate and double diluted at least eight times. The plate was incubated for one hour at 37 °C and subsequently washed six times in PBS. The samples were blocked with 200 µl 1% BSA-PBS for 15 min at 37 °C. Peroxidase streptavidin (Extravidin, Sigma) was diluted 1:1000 in blocking solution and 100 µl thereof were added

to the samples. After 30 min incubation at RT in the dark, the plate was washed ten times in 200 µl PBS. To determine the amount of free biotin of the pMHC monomers, the plate was assayed for bound Extravidin by adding 100 µl TMB substrate (3,3,5,5-tetramethylbenzidine - Sigma) per well. The colour was developed for 5 min at RT. The plate was measured against a blank sample at 540 nm in a Biotek µQuant microplate spectrophotometer.

2.2.4 Flow Cytometry

2.2.4.1 Cell surface staining

1 x 10^6 Jurkat cells per sample were harvested and washed three times in PBS supplemented with 1% BSA and 0.01% azide (PBS-BSA-azide) and transferred to U-bottomed 96-well plates. Antibody staining was performed in 50 or 100 µl PBS-BSA-azide for 1 hour at RT in the dark. Antibody concentrations used varied according to manufacturer's instructions. The plate was washed three times with PBS-BSA-azide by pelleting the cells at 1,200 xg for 2 min. Subsequently the samples were resuspended in a total of 300 µl of PBS and transferred to flow cytometry tubes.

Flow cytometry was performed on a FACS Calibur (Becton Dickinson) and the experiment was analysed using FlowJo (Tree Star, Inc.). Statistics were performed using GraphPad Prism.

2.2.4.2 Intracellular phospho-protein staining

5 x 10^5 Jurkat cells were stimulated with UCHT1, tetramers, PMA, PP2 or Na_3VO_4 in RPMI at 37 °C under agitation in as described earlier. 50 µl per

sample were transferred immediately into wells of U-bottomed 96-well plate. The wells contained 150 µl pre-warmed paraformaldehyde-based Fix Buffer 1 (BD Biosciences) to fix the cell immediately after stimulation. Fixation was performed for 10 min at 37 °C in the dark.

Samples were washed three times with PBS-BSA-azide by pelleting the cells at 1200 xg for 2 min and subsequent resuspension before permeabilisation with 200 µl saponin-based Perm/Wash Buffer (BD Biosciences) on ice for 30 min in the dark. Cells were pelleted once and the permeabilisation buffer was discarded.

Antibody staining was performed in 50 µl saponin-based Perm/Wash Buffer 1 (BD Biosciences) for 1 hour at RT in the dark. Antibody concentrations varied according to manufacturer's instructions. The plate was washed three times with PBS-BSA-azide. The samples were resuspended in a total of 300 µl of PBS and transferred to flow cytometry tubes.

Flow cytometry was performed on a FACS Calibur (Becton Dickinson) and the experiment was analysed using FlowJo (Tree Star, Inc.). Statistics were performed using GraphPad Prism.

2.2.4.3 CD69 expression assays

2 x 10^5 1G4 Jurkat cells per sample were incubated with 2 nm pMHC tetramers or 2 µg/ml anti-CD3ε(clone UCHT1, eBioscience) for 5 hours at 37 °C in RPMI with 10% FCS supplemented with 1 µg/ml puromycin (Gibco) and penicillin-streptomycin (PAA). The cells were stained with APC-conjugated anti-CD69 (clone CH/4, Invitrogen). Flow cytometry was performed on a FACS Calibur (Becton Dickinson) and the experiment was anal-

ysed using FlowJo (Tree Star, Inc.). Statistics were performed using GraphPad Prism.

2.2.4.4 Apoptosis assays

1G4 Jurkat cells were plated at a concentration of 1 x 10^6 cells/ml in 200 µl pre-warmed RMPI + 10% FCS + 1 µg/ml puromycin (Gibco) + 1 µg/ml penicillin-streptomycin (PAA) into a sterile 96-well cell culture plate. The cells were stimulated with either 20 nM PE-labelled NY-ESO-$1_{156-165}$ pMHC tetramers or 2 µg/ml camptothecin for 24 hours at 37 °C in the dark
[Rybakin and Gascoigne, 2012]. FAM- or far-red FLICA (ImmunoChemistry Techonologies) dyes were prepared according to manufacturer's instructions: The FLICA stain was reconstituted in 50 µl DMSO. The stock solution was either stored at −20 °C or further diluted in 200 µl PBS.
After incubation cells were stained within the 96-well plate with 7 µl FAM- or far-red-FLICA to 200 µl medium for 60 min at 37 °C in the dark. Samples were washed twice by centrifugation at 1200 xg for 2 min and resuspension in 1x Apoptosis Wash Buffer (ImmunoChemistry Techonologies). Cells were resuspended in a total of 300 µl PBS.
Flow cytometry was performed on a FACS Calibur (Becton Dickinson) and the experiment was analysed using FlowJo (Tree Star, Inc.). Statistics were performed using GraphPad Prism.

2.2.5 Data and statistical analysis

Statistical analysis were based on data acquired by flow cytometry in the form of geometric means or percentage of cells activated. For statistical analyses, experiments were performed in triplicate at least. All data was analysed and graphs drawn using GraphPad Prism® version 5.04 (GraphPad Software, Inc.). Graphs show the standard error of mean (SEM) between the samples. Statistical significance was calculated using the unpaired two-tailed student t-test. In all cases ns = $P > 0.05$, * = $P < 0.05$, ** = $P < 0.01$, *** = $P < 0.001$.

Chapter 3

NY-ESO-1 pMHC monomer and tetramer production and composition

3.1 Introduction

3.1.1 Ligand recognition by T cells

CD8- and CD4-classed T cells are a critical part of the adaptive immunity of higher vertebrates. Each mature T cells bears about 40,000 clonal αβ T cell receptor (TCR) molecules of unique specificity on the cell surface [Labrecque et al., 2001]. T cells respond through the TCR to antigen peptides bound to major histocompability complex (pMHC) class I or II molecules. The general affinity of the TCR for pMHC is low, ranging only between 1 and 50 μM [Krogsgaard and Davis, 2005]. The surface of each cells displays over 10^5

MHC molecules [Yewdell et al., 2003]. They bind to peptides which derive from both "self" proteins and proteins of pathogenic origin. The sequences of "self" and "foreign" peptides might only differ by one amino acid. Yet despite the overwhelming abundance of self peptides, TCR signalling responds sensitively and specifically to the binding of as few as 5 to 10 foreign peptide MHC [Germain, 2001] [Altman and Davis, 2003] [Irvine et al., 2002].

3.1.2 pMHC *in vivo* production and processing

T lymphocytes are classed into CD4- and CD8-subsets. CD4-classed T cells activate effector functions in other cells of the immune system. They bind to MHC class II molecules displayed by professional antigen-presenting cells including B cells, dendritic cells and macrophages [Kobayashi and van den Elsen, 2012] [Murphy et al., 2008].

Viruses and other pathogens infect host cells and replicate within the cytosol or the nuclear compartment [Murphy et al., 2008]. CD8-classed T cells recognise infected cells by binding MHC class I molecules presenting pathogen peptides [Kindt et al., 2007]. CD8 T cell activation results in the killing of the infected cells. MHC class I molecules are constitutively expressed on most nucleated cells [Murphy et al., 2008] [Kobayashi and van den Elsen, 2012].

MHC class I and II molecules are generated by distinct pathways but both consist of a heavy α and a light β2M-chain [Bouvier, 2003]. In this study I will focus on pMHC class I molecules only. Cellular proteins are continuously degraded and replaced within the cell. Degradation by the proteasome is a

ubiquitin-dependent pathway and results in the production of antigenic peptides of nine amino acids in length. The peptides are actively transported into the endoplasmic reticulum (ER) via transporter associated with antigen processing-1 and -2 (TAP-1 and -2) proteins [Rock et al., 2002] [Kobayashi and van den Elsen, 2012].

The newly synthesized heavy α-chain is transported into the endoplasmic reticulum and bind to the chaperone calnexin in a partly folded state [Kobayashi and van den Elsen, 2012]. Binding to the light β2M-chain causes the dissociation from calnexin and association of a partly folded α:β2M heterodimer with calreticulin. Tapasin, a TAP-associated protein, connects the TAP and the incomplete MHC class I molecules. Binding of antigenic peptides onto the MHC class I molecules results in the release of fully folded pMHC class I molecules from the TAP complex. The pMHC class I molecules are transported to the cell surface through the Golgi apparatus [Kobayashi and van den Elsen, 2012]. Without peptide-binding mediated by TAP, MHC class I proteins do not fold fully and are retained in the ER [Murphy et al., 2008] [Kobayashi and van den Elsen, 2012].

3.1.3 Analysis of T lymphocytes using pMHC multimers

Single TCRs recognise a variety of MHC complexes bound to potentially structurally related self or foreign peptides. Both molecules are naturally membrane-bound to T cells and target or APC cells. Thus, it is difficult to measure precise and direct kinetic properties of specific TCR:pMHC interac-

tions and the resulting immune responses [Davis et al., 1998]. Within the last decade, soluble pMHC complexes have become an essential tool to identify, enumerate, isolate and stimulate T cell populations specifically [Klenerman et al., 2002] [Alanio et al., 2010]. Plate-bound pMHC monomers have been used to measure TCR:pMHC affinities by surface plasma resonance (SPR) [Corr et al., 1994] [Kalergis et al., 2001] [Carreño et al., 2007]. This method was employed to determine the affinities of the 1G4 TCR to the NY-ESO-$1_{156-165}$ peptide derivatives which are used in this study [Aleksic et al., 2010]. In their soluble form, monomeric pMHC are poor stimulants. Because of the low affinities of TCR:pMHC interactions, pMHC monomers rapidly dissociate from T cells and fail to illicit activation [Davis et al., 1998]. Instead, multimeric pMHC complexes, usually tetramers, bind more than one TCR simultaneously [Stone et al., 2011]. Because of the higher avidity, pMHC tetramers have slower dissociation rates and their interactions to TCRs are thought to approximate cell-cell surface interactions [Stone et al., 2011].

To produce pMHC multimers, monomers are first enzymatically biotinylated and then tetramerised by streptavidin [Altman and Davis, 2003]. Fluorescent tags to the streptavidin moiety allow the identification and isolation of clonal T cell populations by flow cytometry [Altman and Davis, 2003]. Already the first experiments using pMHC class I multimers showed a correlation of tetramer binding efficiency and CD8-T cell cytoxicity [Altman et al., 1996]. Within the last decade pMHC multimers have become an essential tool to detect specific T cell populations sensitively and combine these phenotypic experiments with functional assays such as cytokine release or apoptosis assays [Altman et al., 1996] [Klenerman et al., 2002].

3.1.4 The 1G4:NY-ESO-$1_{156-165}$ TCR:pMHC system

The 1G4 TCR has been isolated from T cells of melanoma patients which recognised the NY-ESO-$1_{156-165}$ peptide [Chen et al., 1997]. The NY-ESO-1 protein is a germline prostate protein which has been found to be expressed in a variety of cancer cells. In the clinic, 1G4-TCR bearing T cells only mount weak immune responses to cancer [Chen et al., 2000]. In attempts to enhance T cell responses to the NY-ESO-$1_{156-165}$ peptides, both variants of the TCR which recognise the same peptides and variants of the NY-ESO-$1_{156-165}$ peptides which are recognised by the same TCR have been used to increase the TCR:pMHC interactions [Chen et al., 2005] [Schmid et al., 2010] [Chen et al., 2010] [Robbins et al., 2011]. Our collaborators at the van der Merwe laboratory investigated the binding parameters of a panel of NY-ESO-$1_{156-165}$ peptides to the 1G4 TCR which I used as a basis to this study [Aleksic et al., 2010]. Two NY-ESO-$1_{156-165}$ peptide variants in particular have been used in parallel studies: the high affinity 9V and the low affinity 9L variants [Chen et al., 2005] [Chen et al., 2010]. The 9V variants affinity is twice as high as the wild-type peptide and induced stronger Ca^{2+} signalling responses as well as high levels of IFN-γ cytokine release [Chen et al., 2005] [Chen et al., 2010]. The lower affinity 9L peptide in turn elicited weaker T cell responses than the wild-type peptide [Chen et al., 2005] [Chen et al., 2010]. Based on these observations, I investigated the effects on T cell responses to the different affinities of a wider panel of NY-ESO-$1_{156-165}$ peptide variants on proximal T cell signalling events which confer T cell response sensitivity.

3.2 Aims

The TCR signalling pathway and the molecules involved have been well researched. To investigate proximal signalling events, T cells are often stimulated by CD3ε monoclonal antibodies. This method stimulates T cells indiscriminately to the TCR clone expressed.

In this chapter, I produced NY-ESO-$1_{156-165}$ pMHC class I monomers and tetramerised them. NY-ESO-$1_{156-165}$ pMHC molecules are the natural ligands to the 1G4 TCR. I produced a panel of four NY-ESO-$1_{156-165}$ peptide derivate MHC tetramers to stimulate 1G4 TCR-expressing Jurkat cells specifically in solution. The four pMHC monomer species range from 7.2 to 252 μM in affinity to the 1G4 TCR [Aleksic et al., 2010].

3.3 Results

3.3.1 Production of NY-ESO-1 pMHC monomers and tetramers

The 1G4 TCR recognises the NY-ESO-$1_{156-165}$ melanoma-derived peptide. Aleksic et al., (2010), determined the kinetic properties of a range of NY-ESO-$1_{156-165}$ pMHC monomers to the 1G4 TCR by SPR. Based on their affinity parameters, I selected four peptides from this panel (Figure 3.1).

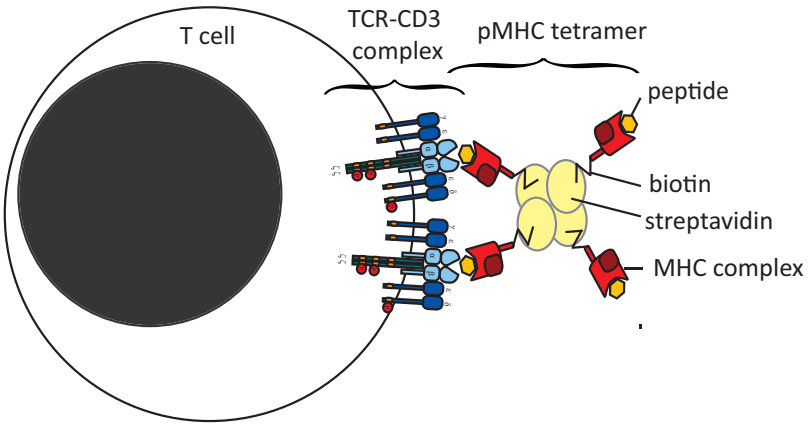

NY-ESO-$1_{157-165}$ pMHC		K_D (μM)	k_{off} (μM)	k_{on} x10^3 ($M^{-1}s^{-1}$)	$t_{1/2}$ (s)	ΔG (kcal mol^{-1})	EC50 (IFN-γ) (μg/ml pMHC)
peptide name	peptide sequence						
9C (wt)	SLLMWITQC	14 ± 1	0.82 ± 0.01	57 ± 3	0.84 ± 0.01	-6.9 ± 0.0	115 ± 14
9V	SLLMWITQV	7.2 ± 0.5	0.33 ± 0.01	45 ± 4	2.12 ± 0.08	-7.3 ± 0.0	180 ± 19
6V	SLLMWVTQV	18 ± 0	0.85 ± 0.03	49 ± 2	0.81 ± 0.03	-6.8 ± 0.0	45 ± 5
9L	SLLMWITQL	56 ± 6	0.93 ± 0.05	17 ± 2	0.74 ± 0.04	-6.0 ± 0.1	426 ± 113
4D	SLLDWITQV	252 ± 12	2.59 ± 0.15	10 ± 1	0.27 ± 0.02	-5.1 ± 0.0	2.3 ± 0.5

Figure 3.1: NY-ESO-1 pMHC monomer affinities to the 1G4 TCR. Schematic representation of NY-ESO-1 pMHC tetramers binding to 1G4 TCRs on the surface of 1G4 Jurkat cells. Table of the NY-ESO-1 peptides, their amino acid sequence and monomeric binding properties to the 1G4 TCR as determined by SPR by Aleksic et al., 2010.

The four peptides purposefully range from 7.2 to 252 μM in their affinity to the 1G4 TCR which lie within and outside the affinity range of 1 to 50 μM that has been reported to induce T cell effector functions [Krogsgaard and Davis, 2005]. This panel of peptides is to be used in all later chapters to analyse the proximal signalling responses to stimulation with different affinities. The NY-ESO-$1_{156-165}$ peptides presented here were chosen based on their affinity to mimic T cell responses to agonistic, intermediate wild-type and naturally inert low affinity pMHC.

The wild-type NY-ESO-$1_{156-165}$ was excluded from the panel because the peptide's nine amino acid sequence, SLLMTWITQC, contains a cysteine at the ninth position of the peptide. Cysteinylation and dimerisation of the cysteines of wild-type 9C NY-ESO-$1_{156-165}$ pMHC monomers caused reduced antigenicity [Chen et al., 2000]. Instead, the panel included the 9V (valine substitution from the wild-type at position nine) peptide whose affinity is twice as high as the wild-type NY-ESO-$1_{156-165}$ peptide. With an affinity of 7.2 μM this peptide lies well within the TCR:pMHC affinity range of 1 to 50 μM which elicits T lymphocyte responses. Indeed, the affinity of 9V should be high enough to induce T cell activation independently of CD8 co-stimulation [Stone et al., 2009]. The 9V pMHC monomer is used as an agonist to the 1G4 TCR in all following experiments. At 18 μM the 6V peptide's affinity is close to the wild-type 9C affinity of 14 μM. Thus 6V is excepted to elicit similar responses to the wild-type peptide. In melanoma patients, the expression of wild-type 9C pMHC on the surface of the cancer cells elicits only weak T cell responses [Chen et al., 2010]. 6V was selected to mimic the wild-type peptide's responses in 1G4 T cells. The affinity of

9L (56 μM) is close to the threshold affinity of 50 μM which is still able to induce T cell activation. The 9L peptide serves as a model for low affinity stimulation which is likely to be tolerated by peripheral 1G4 T cells. 4D has the very low affinity of 252 μM for the 1G4 TCR and thus acts in lieu of a null peptide. The peptides were produced off-site at Cambridge Peptides Ltd.

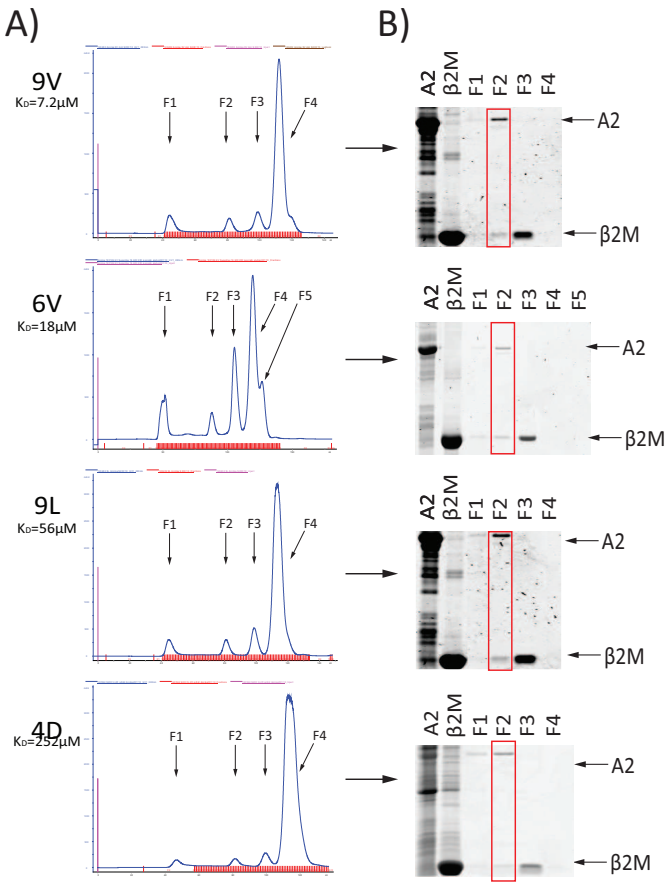

Figure 3.2: NY-ESO-1 monomer production FPLC traces. (A) NY-ESO-1 pMHC monomers were purified over an S200 FPLC column and fractions were collected every minute. Graphs show the 280 nm trace. (B) Peaks identified on the FPLC trace were analysed on Coomassie blue-stained protein gels. By comparison with previously isolated A2 and B2M chains were used as positive controls. Identified monomer fractions are boxed in red.

The production of NY-ESO-$1_{156-165}$ pMHC monomers followed the protocol by Altman et al, 2003. pMHC A2 and B2M chains were expressed in and isolated from bacterial cultures. The pMHC refolding process was carried out for 40 hours at 4 °C in the presence of 0.5 M urea. The refold was filtered, concentrated and separated over an S200 FPLC column. Typical FPLC read-outs for each pMHC monomer species is shown in Figure 3.2. In sequence of elution the FPLC fractions contained aggregations (F1), pMHC monomers (F2), free B2M (F3) and free biotin (F4) as determined on protein gels against previously isolated A2 and B2M (Figure 3.1 B). The molecular weight of free biotin and free peptides were usually too low to be visible on 15% SDS-PAGE. Since biotin was added in excess, the peak corresponding to the free biotin fraction can be attributed with confidence despite varying peak intensity. The monomer containing fraction was concentrated to 1 mg/ml which was determined in triplicate by Bradford Coomassie blue assay.

Monomers were tetramerised using streptavidin. The streptavidin used was linked to phycoerythrin to monitor tetramer binding (occupancy) using flow cytometry (Figure 3.3A). Streptavidin is a 52.9 kDa protein of four subunits. The protein contains four biotin binding sites to which two subunits each contribute equally [Howarth et al., 2006]. Streptavidin binds biotin at very high affinity (10^{14} μM) [Green, 1975] [Howarth et al., 2006]. The number of biotin sites present on streptavidin had to be carefully matched with the number of biotinylated pMHC monomers [Altman and Davis, 2003]. Tetramerisation was performed in stepwise addition of streptavidin in excess of pMHC monomers. Successful tetramerisation and successful biotinyla-

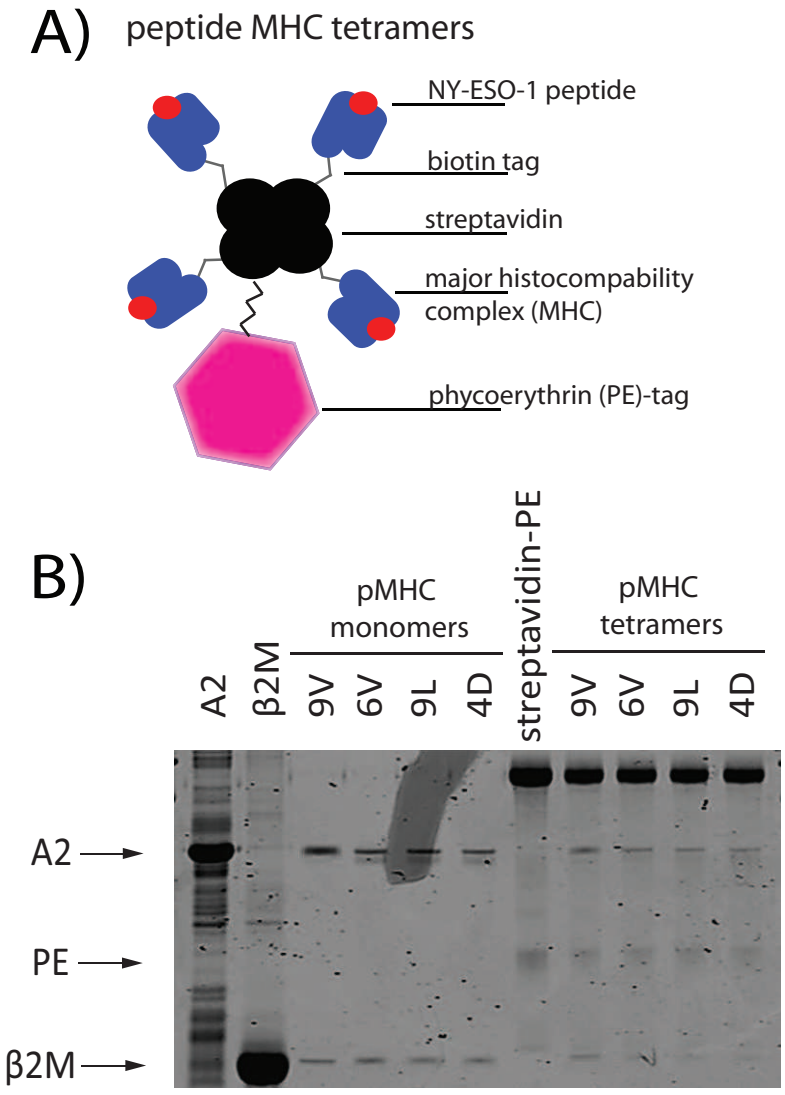

Figure 3.3: NY-ESO-1 pMHC tetramer structure. (A) Schematic structure of NY-ESO-1 pMHC tetramers. Four NY-ESO-1 pMHC monomers are linked to streptavidin-PE through a biotin moiety. (B) pMHC monomer and tetramer compositions were compared against A2 and B2M isolates using Coomassie blue stained protein gels.

tion of monomers was tested using an ELISA to detect free biotin (data not shown). Tetramer composition was determined using SDS-PAGE which was stained with Coomassie Blue (Figure 3.3 B). Tetramer occupancy was assessed using flow cytometry (Figure 3.4). Occupancy was related to tetramer concentration and tetramer affinity. The highest affinity tetramer achieved highest occupancy and binding saturation levels. Even at high concentrations, lower affinity 9L tetramers did not reach equal occupancy as high or intermediate affinity 9V or 6V tetramers. 4D tetramers showed background levels of pMHC binding to the 1G4 TCR. Monomers were stored at $-80\,^{\circ}\mathrm{C}$ while tetramers were stored at $4\,^{\circ}\mathrm{C}$.

In this chapter, I produced a panel of NY-ESO-$1_{156-165}$ peptide MHC class I tetramers which form the basis for the specific stimulation experiments of all later chapters of this thesis. The method of pMHC tetramer production was previously not established in the host laboratory. The produced pMHC tetramers were assessed for composition, biotinylation and concentration and bound to 1G4 TCR-expressing Jurkat cells. This occupancy is not equal to all tetramers at the same concentrations but rather correlates to the affinity and off-rates of the NY-ESO-$1_{156-165}$ peptides to the 1G4 TCR.

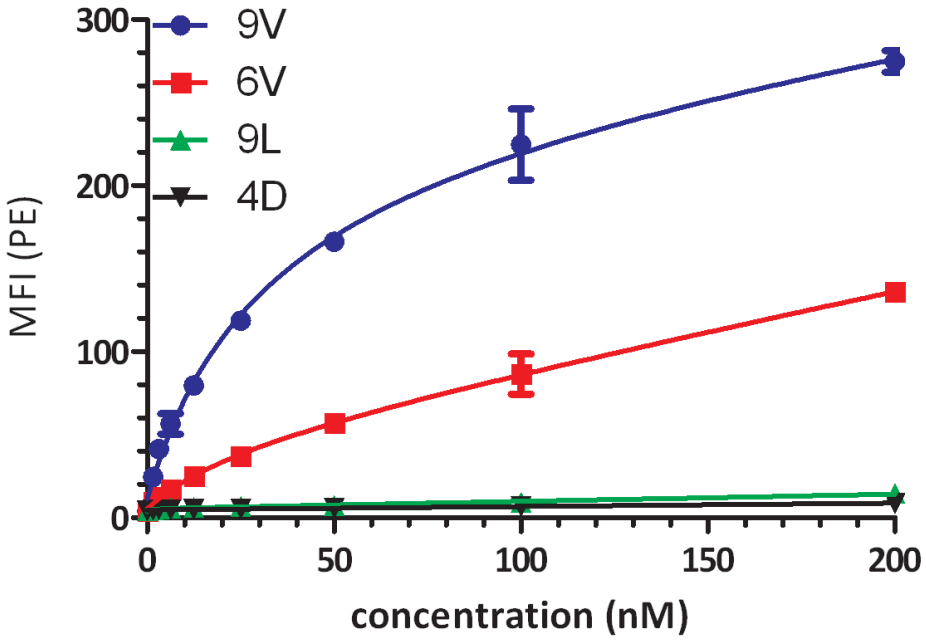

Figure 3.4: Analysis of tetramer occupancy. 1G4 cells were stimulated with different concentrations of the four NY-ESO-1 pMHC TCR for 30 min and were washed twice with PBS-BSA-azide before analysis by flow cytometry. The experiment was repeated three time and the error bars show the SEM.

3.4 Discussion

T cell activation follows pMHC-TCR interactions at the T cell:antigen-presenting cell interface. The peptides' sequence determines the affinity with which the pMHC complex binds to a particular TCR. Whether a T lymphocyte is activated after encountering a particular pMHC molecule or is tolerant to its presence is determined by the affinity with which the pMHC binds to the TCR. The binding affinity of TCRs are very low and are within a range of 1 to 50 μM [Krogsgaard and Davis, 2005].

The 1G4 TCR recognises the nine amino acid NY-ESO-$1_{156-165}$ peptide which derives from a germline prostrate protein of the same name which is expressed in a variety of cancers [Restifo et al., 2012]. T cells against this antigen have been identified in melanoma or prostate cancer patients [Chen et al., 2010]. In the collaborating Cerundolo laboratory, a panel of NY-ESO-$1_{156-165}$ variants, including the 9V and 9L variants used in this study, were utilised to sensitise patients' T cells to kill previously tolerated cancer cells [Chen et al., 2010].

In order to investigate the different signalling kinetics evoked by a range of pMHC of different binding affinities to the 1G4 TCR, I produced 9V, 6V, 9L and 4D NY-ESO-$1_{156-165}$ pMHC tetramer variants. The selected pMHC monomers bind to the 1G4 TCR with affinities between 7.2 and 252 μM as determined by SPR [Aleksic et al., 2010]. The affinity of the 9V peptide is twice as high as that of the wild-type peptide and 9V stimulations have been reported to result in higher Ca^{2+} signals and cytokine release responses [Chen et al., 2005] [Chen et al., 2010]. In this thesis, 9V stimulation as an

agonist pMHC which is expected to induce strong T cell responses. The wild-type peptide SLLMTWITQC was excluded from the study because its N-terminal cysteine residue has been reported to cause tetramer aggregations [Chen et al., 2005]. This could affect the avidity and thus the dose of tetramers received by the 1G4 cells stimulated. Thus the dose of tetramers would not comparable to other NY-ESO-$1_{156-165}$ pMHC tetramer variants. Instead of the wild-type 9C NY-ESO-$1_{156-165}$ peptide the 6V variant was selected. The affinity of the 6V monomer is within 4 μM of that of the wild-type 9C pMHC. The low affinity peptide, 9L, is expected to induce either low or no T cell responses. Its affinity of 56 μM is at the threshold of the 1 to 50 μM range within which T cell responses to pMHC have been reported [Krogsgaard and Davis, 2005]. 4D with its extremely weak affinity, which is 5-times lower than that of 9L, is not expected to induce any 1G4 cell response. It acts as a null peptide which would be tolerated by T cells and thus acts as a negative control in this study.

Occupancy is a function of pMHC tetramer affinity. The streptavidin of the pMHC tetramers is linked to a phycoerythrin moeity which allows pMHC occupancy to 1G4-TCR bearing cells to be monitored by flow cytometry. High affinity 9V tetramers showed higher levels of occupancy than the lower affinity tetramers. This phenomenon has been observed previously [Dutoit et al., 2002a]. The potency of a ligand is dependent on the affinity (K_D) and the dissociation rate (k_{off}). Low potency ligands with fast dissociation rates fail to bind to the TCR long enough to achieve significant levels of occupancy. Thus, the occupancy recorded is a measure of the stability of the TCR:pMHC interactions formed and an indication towards the potency of

the ligand [Dutoit et al., 2002a].

pMHC tetramers have been used to elicit T cell effector functions such as CD69 expression upregulation or cytokine release assays. A correlation of tetramer affinity and the extent of late effector function has been observed [Altman et al., 1996] [Klenerman et al., 2002]. TCR triggering is transduced across the plasma membrane to cause the phosphorylation of CD3-ITAMs and initiate a sequential cascade of proximal TCR signalling events mediated by protein phosphorylation. Qualitative differences in TCR engagement have to be transduced through the signalling cascade to result in the differential later T cell effector responses observed in previous studies. In following chapters the presented NY-ESO-$1_{156-165}$ tetramers are used in solution to stimulate 1G4 cells and analyse the effect of ligand affinity on very early TCR phospho-signalling events to elucidate how qualitative differences of TCR triggering by different affinity ligands are translated into specific and sensitive TCR proximal signalling events.

Chapter 4

Activation of 1G4 Jurkat cells by pMHC tetramers

4.1 Introduction

4.1.1 Proximal TCR signalling events

The activation of T cell effector functions depends on the preceeding interactions between agonist pMHC and cognate TCRs. This interaction triggers a series of signalling events which ultimately result in T cell adhesion, proliferation and the production and release of cytokines and cytotoxins [Acuto et al., 2008].

Remarkably the αβ TCR and its short intracellular domains contain no catalytic function [Kuhns et al., 2006]. The TCR is closely but non-covalently associated to three CD3-dimers, γε, δε and ζζ [Call et al., 2006]. The intracellular domains of the CD3 dimers contain ITAM motifs of the sequence

YxxL/Ix$_{(6-8)}$YxxL/I. The CD3$\varepsilon\gamma\delta$-chains contain one ITAM each and the CD3ζ-chain contains three. Thus, a total of ten ITAMs are associated to the TCR through the three CD3 dimers. The tyrosines of the ITAMs are phosphorylated by LCK upon TCR:pHC engagement. This event initiates the activation of a proximal signalling cascade. Firstly, ZAP-70 binds to the phosphorylated ITAMs via its tandem SH2 domains. Bound ZAP-70 is phosphorylated and activated by LCK [Huby et al., 1997]. Upon activation, ZAP-70 phosphorylates the scaffold proteins LAT and SLP-76 which are associated to each other via Gads. The LAT-SLP-76 complex serves as a platform for the diversification of the TCR signal into Ca^{2+}, PKC and Ras signals which coordinately regulate cytoskeletal rearrangements and gene expression to mediate cell activation. Further downstream, RasGRP1 and SOS1 activate Ras which in turn initiate the MAPK cascade. RasGRP1 and SOS are both GEF and facilitate the exchange of Ras-GDP to Ras-GTP. SOS associates to Grb2 and the LAT complex while RasGRP1 is a cytosolic protein whose activity is controlled by DAG, PKCϑ and Ca^{2+} signals [Kortum et al., 2013]. The activation of the MAPK cascade, which includes ERK, by Ras-GTP results in the T cell proliferation and cell survival [Warnecke et al., 2012].

4.1.2 Co-stimulating molecules assisting T cell activation

TCR:pMHC interactions serve as the primary trigger towards T cell activation [Kuhns et al., 2006]. Co-receptors such as CD4, CD8 and co-signalling

molecules CD28 and CD45 augment, regulate and facilitate TCR signalling and T cell activation [Hutchinson et al., 2003] [Germain, 2002] [Janeway, 1992].

CD4 and CD8 are T cell subset-defining molecules. They are first expressed during thymocyte development. CD4 expression commits the T cell to the helper or tolerant T cell subsets. CD8-expressing cells are cytotoxic T cells [Germain, 2002].

Both CD4 and CD8 belong to the immunoglobulin gene superfamily and display similar functions. Yet their structure is very different [Janeway, 1992]. CD4 is a monomeric transmembrane protein with four extracellular immunoglobulin domains which bind MHC class II molecules. CD8 consists of either αα or αβ dimers. CD8αα T cells are found in the intraepithelial T cells in the gut, NK and DC cells. CD8αβ is the major dimer found on conventional T cells. While both dimers bind to MHC class I with equal affinity, CD8αβ is the more efficient facilitator to TCR signalling, probably through its co-localisation with the TCR to GEM rafts by palmitoylation of the β subunit [Sun and Kavathas, 1997] [Rybakin et al., 2011] [Walker et al., 2013].

Despite their large structural differences, CD4 and CD8 are both glycoproteins and associate via their conserved cysteine motif CxCP to the CxxC motif within the unique N-terminal domain of LCK [Shaw et al., 1990] [Turner et al., 1990]. Both CD4 and CD8 bind to pMHC molecules with very low affinities. The K_D of CD4 to pMHC class II is only 150 to 200 μM and the interactions display rapid off-rates [Krummel et al., 2000]. Similarly, CD8 dimers bind pMHC class I molecules with a K_D between 65 to 200 μM and

also possess rapid binding kinetics ($k_{off} = 18\,sec^{-1}$) [Kern et al., 1999] [Wyer et al., 1999]. The function of CD4 and CD8 was suggested to include the stabilisation of TCR:pMHC interactions. But the rapid off-rate kinetics of CD4 and CD8 to the TCR:pMHC complex argue against this notion [Artyomov et al., 2010]. In fact, pMHC complexes which bind to TCRs with an affinity at or below 10 μM can also signal independently of co-receptors [Stone et al., 2009]. More importantly CD4 and CD8 recruit and direct cytoplasmic LCK to the TCR:CD3 complex. CD4 and CD8 thus contribute to increase the sensitivity of the TCR by facilitating LCK approximation to the TCR ITAMs to initiate cell activation [Artyomov et al., 2010].

CD28 interacts with CD80 and CD86 on the surface of APCs. This activates a complementary signalling pathway to the TCR signalling cascade which involves the activation of PKCϑ and NF-ϰB [Topp et al., 2003]. The activation of the CD28 signalling pathway results in sustained production and release of the autocrine growth factor interleukin-2 (IL-2), upregulation of the anti-apoptotic BcL-X_L and ultimately cell proliferation [Topp et al., 2003] [Kalland et al., 2011].

CD45 is a heavily glycosylated tyrosine-specific membrane-bound phosphatase which is a major regulator of LCK activation and is essential for effective TCR signalling [McNeill et al., 2007]. Up to eight isoforms of the CD45 extracellular domains are produced by alternative splicing and their expression is T cell subset-specific. The CD45RO isoform, for example, is primarily found in thymocytes and central and effector memory T cells whereas the CD45RA isoform is expressed by naive and some effector memory T cells [Zamoyska, 2007].

The catalytic function of CD45 is found in its constant cytoplasmic domain. It dephosphorylates both the activating tyrosine-394 and the inactivating tyrosine-505 residues of LCK, its primary substrate. Thus it both positively and negatively regulates TCR signalling [McNeill et al., 2007].

4.2 Aims

pMHC tetramers are powerful tools to investigate specific interactions between pMHC complexes and a particular clonotypic TCR. I previously selected and produced a panel of four NY-ESO-$1_{156-165}$ pMHC tetramers (Figure 1.12 and 3.1). The melanoma NY-ESO-$1_{156-165}$ peptide is recognised *in vivo* by the 1G4 TCR [Chen et al., 2005]. The 1G4 TCR α- and β-chains were expressed by lentiviral transduction into the recipient J.RT3-T3.5 Jurkat cells that lacks the transcript of the β-chain of the TCR [Alajez et al., 2006]. The resulting T cell line is named 1G4 [Davis et al., 2012]. The cells do not express CD3 at the cell surface. The expression of the 1G4 αβTCR should as well result in the re-expression of the CD3 in complex with the αβTCR.

The aim of the presented work in this chapter was to assess the faithfulness of the activation response to pMHC of different affinities to the 1G4 TCR and the contribution of the CD8αα co-receptor to activation. Furthermore, I investigated the binding efficacy of pMHC tetramers to 1G4 cells. Protein phosphorylation is a key post-translational modification which mediates the initiation of cell signalling. Immunoblotting was initially used to determine whether the stimulation with 9V or 9L NY-ESO-$1_{156-165}$ pMHC tetramers

results in quantifiable differences in proximal phosphorylation-mediated signalling in 1G4 cells.

4.3 Results

4.3.1 1G4 cell surface phenotype

I prepared a panel of MHC tetramers bound to one of four NY-ESO-$1_{156-165}$ peptide variants. These complexes have affinities for the 1G4 TCR ranging from 7.2 to 252 μM (Figure 3.1). The pMHC tetramers were used to investigate the effect of affinity on early proximal signalling events.

Although TCR:pMHC interactions are the primary trigger to T cell activation, co-receptors regulate and augment T cell activation [Kuhns et al., 2006]. Thus, I compared tetramer binding and activation events in 1G4 and 1G4-CD8α^+ cell lines. I also compared the 1G4 cell surface phenotype against that of another Jurkat cell line, clone 20, which has been widely used for signalling studies within the host laboratory (Figure 4.1). 1G4 cells express levels of CD3 which are comparable with clone 20. This is an indication that the 1G4 cells express the TCR well after the transduction of the 1G4 TCR α- and β-chains because CD3 is only expressed on the surface of T cells in complex with the TCR [Murphy et al., 2008]. However, 1G4 cells express the endogenous TCRα-chain of the J.RT3-T3.5 cells. This α-chain could potentially pair with the 1G4 TCRβ-chain to express a second TCR on the 1G4 surface. While this TCR is unlikely to respond to NY-ESO-$1_{156-165}$ pMHC tetramers, it is important to measure the expression levels of the 1G4 TCR in particular. The pMHC tetramers are linked to the fluorochrome phycoerythrin which allows to visualise 1G4 TCR expression specifically using flow cytometry.

1G4 cells lack the expression of co-stimulatory subset-defining molecules CD4

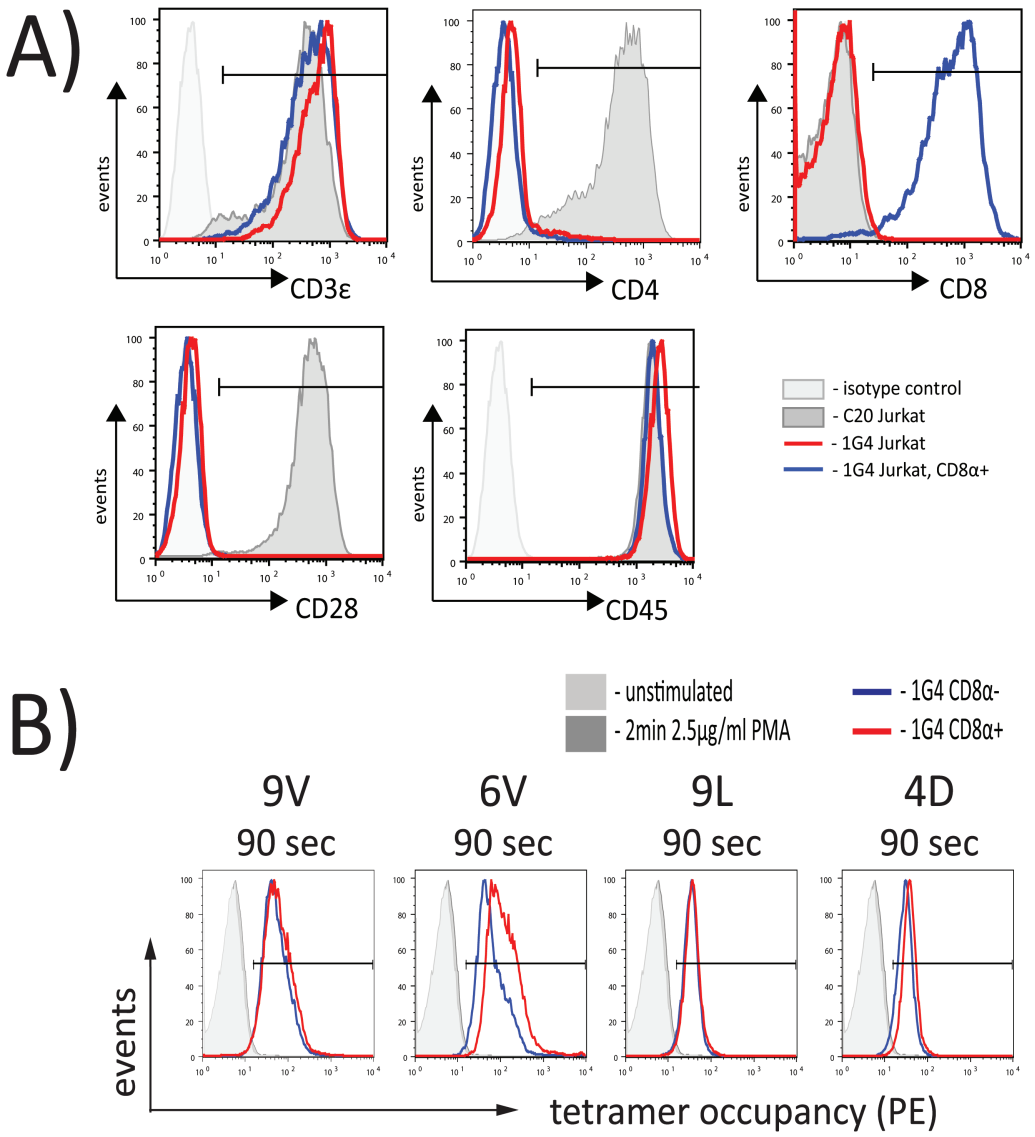

Figure 4.1: 1G4 cell surface phenotype. (A) The expression of the TCR, CD3ε-chains and co-stimulatory surface proteins CD4, CD8, CD28 and the phosphatase CD45 on 1G4 and C20 Jurkat cells was evaluated by flow cytometry. 1G4 cells were stably transfected with CD8-αα by Dr Shaun-Paul Cordoba. (B) Effect of the presence of CD8α on tetramer occupancy on 1G4 cells. Cells were incubated with 200 nM tetramers at 37 °C for 30 min. The samples were washed with PBS-BSA-azide before being analysed using flow cytometry. An example of three experiments in shown.

or CD8 molecules. Their expression facilitates TCR signalling by stabilising TCR-pMHC interactions and by recruiting LCK to the TCR complex [Artyomov et al., 2010]. Dr Shaun-Paul Cordoba (van der Merwe laboratory, Sir William Dunn School Pathology, University of Oxford, Oxford) stably transfected 1G4 cells with CD8α (Figure 4.1). Both CD8αβ and CD8αα are found in T cells. Both dimers bind to the TCR and the pMHC class I molecule with equal affinity and associate to LCK via the α subunit [König, 2002]. The CD8αβ dimer is expressed more widely in T cells and enhances TCR sensitivity over CD8αα [Rybakin et al., 2011]. The presence of CD8 increases the occupancy, particularly of 6V (Figure 4.1 B). The presence of CD8 has been shown to stabilise TCR:pMHC interactions by lowering the k_{off} rate [Neveu et al., 2006]. The occupancy of high and very low affinity pMHC tetramers is largely unchanged by the presence of CD8. Binding of high affinity tetramers is strong enough that low level stabilisation of TCR:pMHC interactions by CD8 seems not to alter the tetramer occupancy levels significantly.

1G4 cells also express equally high levels of CD45 compared to clone 20 cells (Figure 4.1). The co-stimulatory molecule CD28 is not expressed by 1G4 cells. IL-2 release is commonly measured as a T cell effector function output. To achieve this, T cells are stimulated with peptide-pulsed APC or with anti-CD3ε-CD28-antibody beads and IL-2 release is measured by ELISA. 1G4 cells released no IL-2 in response to stimulation (data not shown), possibly because of the lack of CD28 [Topp et al., 2003].

4.3.2 Initial activation events in 1G4 cells

Recruitment of LCK to the TCR:CD3 complex by CD8 facilitates signal induction by LCK-mediated CD3ζ ITAM phosphorylation. Resting 1G4 cells contain four-times less pre-activated pY394-LCK and half as much pY505-LCK than clone 20 Jurkat cells (Figure 4.2 A and B). Stimulation with 1 μg/ml UCHT1 does not change pY394 levels in C20 cells. 1G4 Jurkat cells show a 3-fold increase in Y394-LCK phosphorylation over 2 min (Figure 4.2 A and B).

The CD8α subunit binds to LCK via its intracellular CxCP motif [Shaw et al., 1990]. The expression of CD8αα could increase local LCK concentrations as two LCK molecules are able to bind to one CD8 dimer. This could enhance LCK cross-auto-phosphorylation at tyrosine 394 and thus LCK activation. This effect could be furthermore reinforced by the tetramers' ability to cross-link multiple TCRs at once and thus recruit and heighten local CD8 and LCK concentrations. To address whether CD8αα influences the activation of LCK, I investigated the phosphorylation at tyrosine-394 and -505 at steady-state and after stimulation with high affinity 9V and low affinity 9L tetramers (Figure 4.3 A and C). I used the LICOR Odyssey® infrared imaging system to blot for phosphorylated and total LCK simultaneously and thus normalise for loading differences. The ratios of phosphorylated to total LCK indicates that basal levels of pY394 and pY505 are comparable between CD8αα-negative and -positive 1G4 cells. The levels of inactivating Y505-LCK phosphorylation was unchanged by 9V and 9L stimulation or CD8αα expression (Figure 4.3 B and D). These data suggest that stimulation

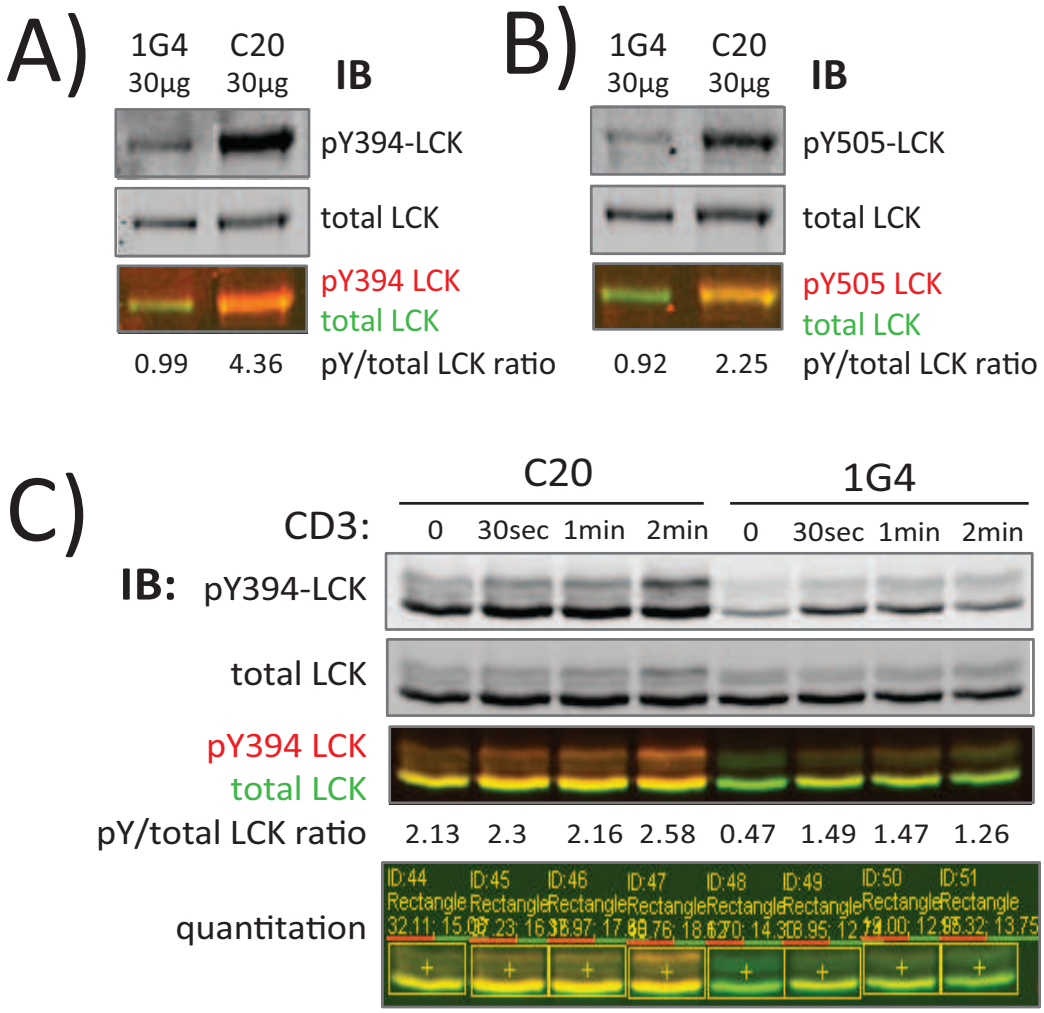

Figure 4.2: Basal levels of phosphorylated LCK are low in 1G4 cells. Levels of pY394 activated LCK and pY505 inactivated LCK in 1G4 and C20 cell lines were investigated using immunoblotting. The levels of phosphorylated LCK was normalised against the total expression of LCK. 1G4 cells show low levels of basal phosphorylation of (A) activating tyrosine 394 and (B) inactivating tyrosine 505 in comparison to C20 cells. (C) Stimulation with 1 ug/ml anti-CD3ε monoclonal antibody UCHT1 increases LCK Y394 phosphorylation in 1G4 cells. The intensity of bands visible on the immunoblots were obtained using Odyssey infrared imaging system application software version 3.0. All data shown is exemplary of three individual experiments.

causes the activation of LCK in 1G4 cells. This is in apparent contradiction to the observations of Nika et al., 2010, who found no pY394 increase upon antigen-specific stimulation of T cells with anti-CD3ε antibodies, tetramers, superantigen and peptide-loaded APC on clone 20 cells and primary T cells [Nika et al., 2010]. An increase in pY394 active LCK is likely to belong to 'primed' LCK which is phosphorylated in both Y394 and Y505 [Nika et al., 2010]. While an increase in LCK activation after 1G4 TCR engagement could increase the levels of downstream proximal signalling, this apparent contradiction observed with 1G4 cells requires further investigation in future experiments with higher statistical accuracy.

4.3.3 Early activation events in 1G4 cells stimulated by pMHC tetramers

Activation of CD8-positive T cells proximal signalling requires the interactions of the TCR with agonist pMHC class I molecules on APC. The extent of the response is largely dependent on the affinity and off-rate of the TCR-pMHC interactions (Figure 1.12) [Dushek et al., 2011].

1G4 Jurkat CD8-negative Jurkat cells were stimulated with 200 nM 9V or 9L NY-ESO-$1_{156-165}$ pMHC class I tetramers. Samples were taken between 10 sec and 20 min post-stimulation. The samples were lysed immediately and the proteins were separated using SDS-PAGE. Immunoblotting was used to investigate the phosphorylation and thus activation of CD3ζ-chain (through pY142 and total p-Y using monoclonal antibody clone 4G10), LAT (through total p-Y using antibody clone 4G10) and ERK1/2 (through pT202 and

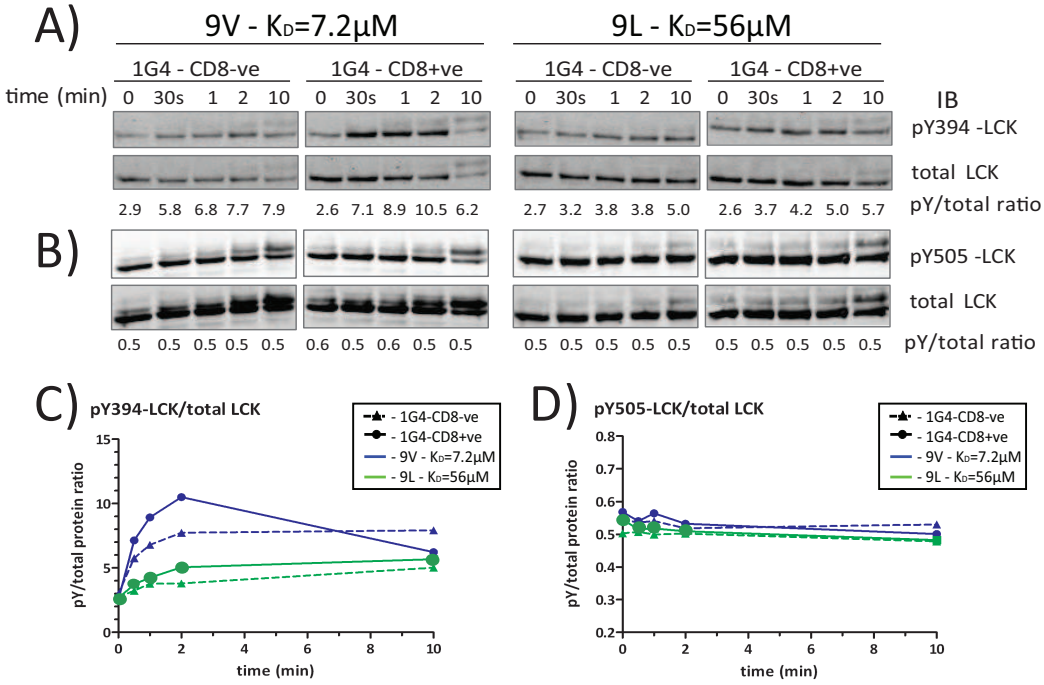

Figure 4.3: Activation of LCK in 1G4 cells after tetramer stimulation. (A) Levels of pY394 activated LCK and pY505 inactivated LCK in CD8αα-negative and -positive 1G4 cells over a 10 min timecourse of 200 nM 9V or 9L NY-ESO-1 pMHC tetramer stimulation were investigated using immunoblotting. The levels of phosphorylated LCK was normalised against the total expression of LCK. The intensity of bands visible on the immunoblots were obtained using Odyssey infrared imaging system application software version 3.0. (B) The normalised levels of pY394 LCK after 9V and 9L stimulation against the total level of LCK for both cell lines were analysed using GraphPad Prism. (C) The normalised levels of pY505 LCK after 9V and 9L stimulation against the total level of LCK for both cell lines were analysed using GraphPad Prism. Shown is an individual experiment exemplary of three experiments.

pY204, using antibody clone E10). Immunoblotting of total CD3ζ, LAT, ERK1/2 and actin were used as loading controls (Figure 4.4). The quantitation of total and phospho-protein levels was performed using Odyssey® infrared imaging system application software version 3.0.

CD3ζ-chain phosphorylation was initiated within 10 to 30 sec of stimulation with either 9V or 9L. CD3ζ phosphorylation peaked at about 2 min and decreased between 2 and 20 min to almost background levels. Stronger affinity stimulation with 9V caused up to 10-fold higher phosphorylation of pY142-CD3ζ than 9L stimulation. Overall 9V stimulation increased CD3ζ-phosphorylation by 3- to 4-fold over 9L stimulations (Figure 4.4, A-C).

9V stimulation caused a sharp spike of phospho-LAT activation at 1 to 2 min. Subsequently the signal decreased rapidly to background levels. 9L stimulation caused a delayed but sustained activation of LAT which reached maximum after 5 min. The maximum was maintained past 20 min post-stimulation. The maximal activation of LAT by 9V stimulation was approximately 3x higher than the 9L stimulation but the 9L-induced signal was more sustained (Figure 4.4, A and D). This is reminiscent of the Ca^{2+} signalling signatures in response to strong and weak stimulations in DP thymocytes

---

Figure 4.4 *(following page)*: Activation of CD3zeta , LAT and ERK in 1G4 cells by 9V and 9L tetramers. (A) 1G4 cells were stimulated using 200 nM 9V or 9L NY-ESO-1 pMHC class I tetramers over a timecourse of 20 min. Samples were analysed by immunoblotting. The quantitation of total and phospho-protein levels was performed using Odyssey infrared imaging system application software version 3.0. Activation by phosphorylation were investigated for pY142 CD3ζ (B), total phosphorylated CD3ζ (C), phosphorylated LAT (D) and phospho-T202.Y204 ERK (E). Shown is an individual experiment exemplary of three experiments.

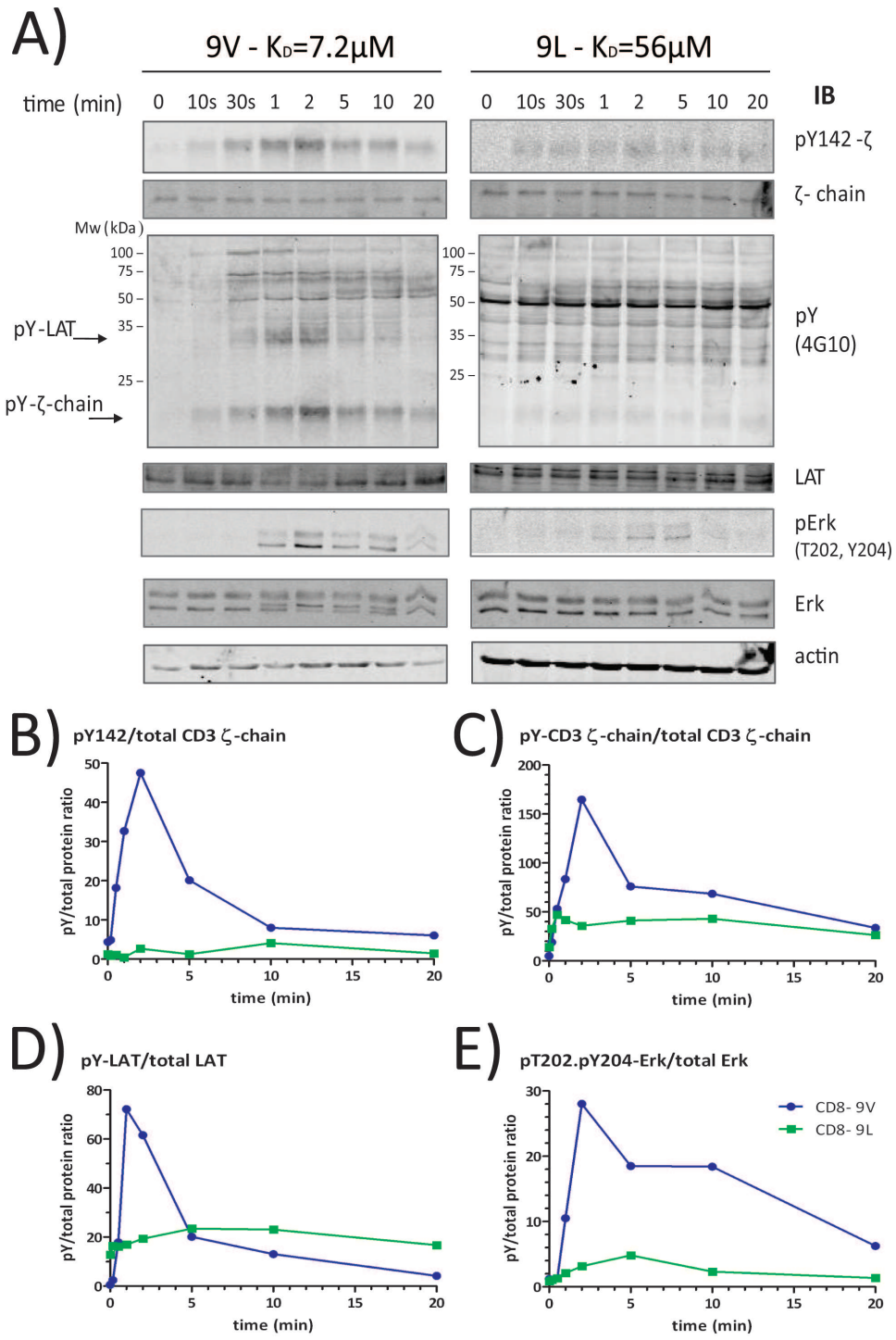
A)
9V - KD=7.2µM
9L - KD=56µM
time (min)
0 10s 30s 1 2 5 10 20
IB
pY142 -ζ
ζ- chain
Mw (kDa)
100
75
50
35
25
pY-LAT
pY-ζ-chain
pY (4G10)
LAT
pErk (T202, Y204)
Erk
actin
B)
pY142/total CD3 ζ-chain
pY/total protein ratio
time (min)
C)
pY-CD3 ζ-chain/total CD3 ζ-chain
D)
pY-LAT/total LAT
E)
pT202.pY204-Erk/total Erk
CD8- 9V
CD8- 9L

[Bhakta et al., 2005]

pT202.pY204-ERK activation peaked after 2 min 9V stimulation and was sustained at a lower level until 20 min post-stimulation. The 9L-induced signal was consistently 4-fold lower (Figure 4.4, A and E)

This data is consistent with the hypothesis that TCR:pMHC binding affinity is positively correlated to increases in the amplitude of TCR proximal signalling. This correlation of affinity and T cell response has been shown for 9V and 9L tetramer stimulations at later stages within the signalling cascade. For example Ca^{2+} signals and cytokine release were increased and more sustained after 9V stimulations [Chen et al., 2010]. The data presented here corroborates these earlier observations and validates the system used to investigate early signalling events.

The expression of CD8αα increases tetramer occupancy on the surface of 1G4 cells [Leishman et al., 2001]. CD8αα is thought to facilitate TCR proximal signalling by recruiting LCK to the TCR:pMHC interface [Shaw et al., 1990] [Turner et al., 1990]. In previous experiments, I showed that in 1G4 cells, stimulation with UCHT1 and NY-ESO-$1_{156-165}$ tetramers increases the levels of activated LCK (Figures 4.2 and 4.3). The extent to which this might quantitatively influence further proximal TCR signalling is not well understood.

To address this function, CD8αα-negative and -positive 1G4 cells were stimulated with 200 nM 9V or 9L NY-ESO-$1_{156-165}$ pMHC class I tetramers. Samples were taken between 30 sec and 10 min post-stimulation and analysed using immunoblotting as before. The phosphorylation and thus activation of CD3ζ-chain (total p-Y, using monoclonal antibody clone 4G10),

LAT (through total p-Y, using antibody clone 4G10) and ERK1/2 (through pT202 and pY204, using antibody clone E10) was monitored. Immunoblotting of total CD3ζ, LAT and ERK1/2 were used as loading controls (Figure 4.5). The quantitation of total and phospho-protein levels were performed using Odyssey® infrared imaging system application software version 3.0.
As I observed in the experiment presented in Figure 4.4, the high affinity 9V tetramer induced more pronounced activation of CD3ζ , LAT and ERK than 9L. Sharp spikes of CD3ζ and LAT activation as in Figure 4.4 were not observed. Generally, the expression of CD8αα increased the strength of the low affinity 9L-induced signal at least two-fold. This effect could be due to the introduction of CD8αα to the system. The phospho-ERK signal was increased 6-fold at most. CD8αα expression had no influence on CD3ζ activation after 9V stimulation but increased LAT activation two-fold. Phospho-ERK levels were decreased in CD8αα-positive 1G4 cells, although this is not immediately apparent from the immunoblot itself. Repeats of the experiment showed an increase of phospho-ERK levels in CD8αα-positive 1G4 cells (data not shown).
Although immunoblotting is a powerful method to detect phospho-protein kinase activation, it is prone to variations between experiments. Quantitations also vary largely between experiments.

In all further experiments, 1G4-CD8αα-positive cells were used. They are referred to as 1G4 cells.

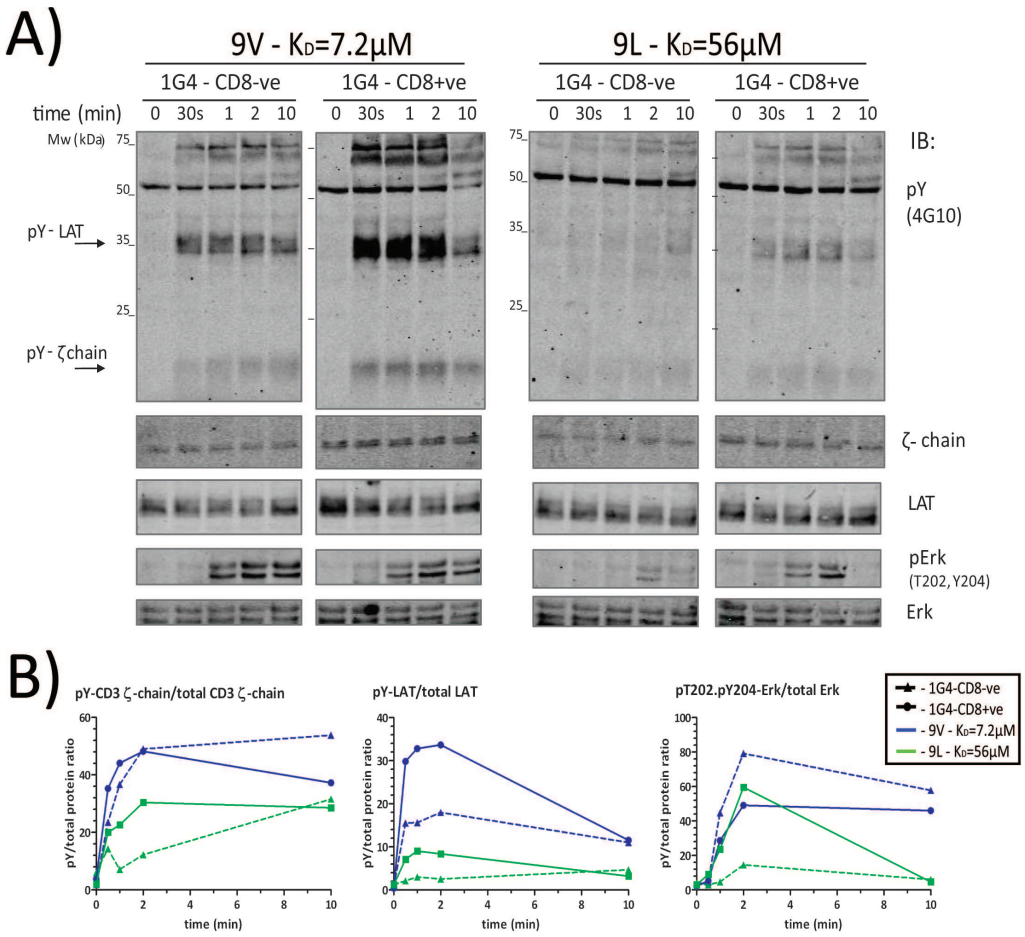

Figure 4.5: CD8αα expression enhances proximal TCR signalling. CD8αα-positive 1G4 cells were stimulated with 200 nM 9V or 9L pMHC class I tetramers over a timecourse of 10 min. (A) Immunoblotting of total and phosphorylated TCR proximal signalling proteins CD3ζ , LAT and ERK. The quantitation of total and phospho-protein levels was performed using Odyssey infrared imaging system application software version 3.0. (B) Ratios of phosphorylated to total proteins quantitated in A were analysed using GraphPad Prism. Shown is an individual experiment exemplary of three experiments.

4.4 Discussion

1G4 cells derive from J.RT3-T3.5 Jurkat cells which do not express endogenous TCR molecules because they lack the TCR-β-chain transcript [Davis et al., 2012] [Alajez et al., 2006]. On the surface, 1G4 cells express high levels of CD3 and the co-receptors CD45 and, after transduction high levels of CD8αα. The cells do not express CD4 or CD28. Expression of CD3 indicates the successful transfection of the 1G4 TCR. However, because of the endogenous J.RT3-T3.5 α-chain it is important to assess the levels of the 1G4 TCR as opposed to the expression of the TCRα and TCRβ 1G4. This is not easy to assess but through flow cytometry I could demonstrate a constitutive binding of the pMHC tetramers to the surface of the cells. This indicates the substantial expression of CD3-complexed to the 1G4 αβTCR. The inherent specificity of TCRs to particular pMHC means it is very unlikely that a 1G4β-J.RT3-T3.5α chimeric TCR would bind the pMHC tetramers efficiently. CD45 is an essential TCR signalling phosphatase which positively and negatively regulates LCK activity. 1G4 cells were poor IL-2 producers in response to stimulation (data not shown). CD28 co-stimulation is known to be important to the production of IL-2 by T cells [Topp et al., 2003] [Acuto and Michel, 2003]. Without CD28 co-stimulation, the release of IL-2 is not an effective method to assess 1G4 cell effector functions after TCR activation. Thus only events relatively proximal to the TCR signalling cascade could be measured in this experimental system.

The expression of CD4 or CD8 is mutually exclusive on the surface of

mature T cells [Murphy et al., 2008]. Generally two functions are attributed to CD4 and CD8: Firstly, binding of the extracellular domains of CD4 and CD8 to the invariant regions of the pMHC molecule stabilize TCR-pMHC binding and enhance the duration of the interactions [Stefanová et al., 2003]. Secondly and more importantly, the co-receptors associate to the unique N-terminal domain of LCK via their cytoplasmic tails and thus enhance the spatial delivery of the Src-family kinase LCK to the site of TCR-pMHC engagement [Stefanová et al., 2003] [Van Laethem et al., 2007]. The spatial recruitment of LCK closer to the TCR through CD4 and CD8 during TCR:pMHC engagements increases the phosphorylation and activation of the CD3 chains by LCK. This results in stronger downstream signal transduction [Artyomov et al., 2010]. The expression of CD8 enhanced the responses of 1G4 cells to tetramer stimulations at any stage of the signalling cascade (Figure 4.3 and 4.5).

1G4 cells expressed low levels of pre-phosphorylated LCK at positions Y394 and Y505 at steady state in comparison to clone 20 Jurkat. Inactivated LCK levels are unchanged after tetramer stimulation. Activated pY394 LCK is increased upon UCHT1 and tetramer stimulation. Nika et al., 2010, reported that up to 40% of LCK is pre-activated at Y394 in resting Jurkat clone 20 and primary T cells. The amount of pre-activated LCK was not altered upon primary T cell or clone 20 Jurkat activation with superantigen, anti-CD3ε monoclonal antibodies, pMHC tetramer or peptide-pulsed APC. These observations suggest that LCK is not activated upon TCR triggering and that thus spatial re-organisations and structural changes among the TCR supercomplex are more likely to induce TCR proximal signalling. The

palmitoylation of LCK and CD8β-subunit localise these two molecules to the same GEM as the TCR [Boggon and Eck, 2004] [Rybakin et al., 2011]. Rearrangements of the cytoplasmic CD3 chains upon TCR triggering could be the step which initiates LCK phosphorylation of the CD3-ITAMs and thus TCR signalling [Risueño et al., 2008].

The phenotype observed in 1G4 cells apparently contradicts Nika at al., 2010's observations in Jurkat clone 20 and primary T cells for unknown reasons. Jurkat cells are derived from acute T cell leukaemia cells [Schneider et al., 1977]. While they are good models for essential T cell signalling *in vitro*, there are differences between cell lines and primary T cells. Nika et al., observed no changes in active LCK ratios in clone 20 and primary T cells. It is possible that because 1G4 cells derive from a CD4-, CD8- and TCR-negative cell line, that LCK is less active in the cells' resting state and more readily phosphorylated upon TCR triggering. The engagement of multiple TCRs through pMHC tetramer could bring LCK into a higher localised concentration which causes its increased autophosphorylation. This effect could be enhanced by the introduction of CD8αα which, as a dimer, contains two LCK binding sites [Shaw et al., 1990]. Thus the higher local concentration of LCK through binding to CD8αα dimers and the further increase of this concentration through the triggering of multiple TCRs by tetramers might cause the cross-auto-phosphorylation of LCK and thus the increased levels of pY394-LCK observed in Figures 4.2 and 4.3. The increases in phosphorylation of downstream signalling molecules was slight. In following chapters, I am investigating the effect of increased levels of pY394-LCK after TCR triggering on downstream signalling events more closely and quantitatively

using flow cytometry.

Further downstream signalling events also confirm the hypothesis that higher TCR:pMHC binding affinities result in stronger induction of signalling events and ultimately, as observed outside this study, stronger T cell effector functions [Chen et al., 2005]. High affinity 9V stimulations generally resulted in increased proximal TCR signalling. Binding of 9L provides a weak stimulus only. CD3ζ is only poorly phosphorylated after stimulation with 9L. Positive feedback loops might enhance phosphorylation of downstream kinases such as LAT and ERK whose activations shows higher intensities on immunoblots than CD3ζ activation. A similar effect is seen after high affinity 9V pMHC tetramer stimulation. This could indicate an amplification of the signal down the cascade. Positive feedback loops might be initiated through multiple dissociation and rebinding events of the TCR and its ligand [Boggon and Eck, 2004]. It is also possible that an amplification of the signal is rather an artefact of the antibodies used and the different binding properties to epitopes on the proteins which the antibodies detect.

In this chapter, I showed the faithful response of 1G4 cells to increasing affinity of pMHC tetramer stimulations. pMHC tetramers induced strong TCR signalling responses detectable by immunoblotting. Very early signalling events including CD3ζ-phosphorylation and ERK-activation were induced strongly within seconds after NY-ESO-$1_{156-165}$ pMHC class I tetramer stimulation. Higher affinity NY-ESO-$1_{156-165}$ pMHC tetramer stimulation resulted in more pronounced proximal signalling responses.

The expression of CD8αα augmented the signalling responses to pMHC tetramers

at all stages of the cascade. While immunoblotting is a powerful tool to investigate proximal TCR signalling responses, I used flow cytometry in subsequent work as it allows investigating signal events in a more detailed and semi-quantitative manner.

Chapter 5

Influence of pMHC binding affinity to TCR on proximal signalling in 1G4 cells

5.1 Introduction

5.1.1 TCR signalling kinetics

Full T cell activation *in vivo* requires two stimuli: TCR:pMHC interactions and co-stimulation. The best characterized co-stimulatory molecule is CD28 whose engagement results in enhanced proliferation and cytokine release [Acuto and Michel, 2003]. The variable nature of TCR:pMHC interaction is the primary trigger to T cell activation and confer specificity and sensitivity to T cell responses. The sensitivity of the responses to the ligands is determined by the TCR:pMHC binding kinetics and by TCR downstream

signalling machinery which include sequential proximal protein phosphorylation events and positive and negative feedback regulatory loops [Acuto et al., 2008]. Some cellular responses are discrete and of a digital on/off nature. This includes the phospho-ERK and cytotoxicity responses [Burroughs and van der Merwe, 2007] [Das et al., 2009]. The initiation of these signals is dependent on the TCR:pMHC binding parameters overcoming an activating threshold. The affinity model allows for the rapid detection of minimal stimuli. The time-integrated model focuses on the off rate and dwell time of ligands to the TCR. Prolonged dwell time or high ligand density results in the amplification of downstream signals [Kalergis et al., 2001] [Gottschalk et al., 2012]. A time-integrated model explains the quantitative functional output of cellular functions such as cytokine release or proliferation and confers good control over specificity and sensitivity of T cell responses [Burroughs and van der Merwe, 2007]. Dushek et al., 2011, showed that while the K_D relates to the potency of T cell responses, the k_{off} corresponded to the maximal efficacy and the importance of both towards T cell activation. Regardless of the TCR triggering model, TCR signalling is characterised by very high speed of signal transduction and propagation, high specificity for the agonist, extreme capability to discriminate between signals of close affinity, robustness to noise to prevent autoimmunity and extreme sensitivity to low ligand density in spite of vast excess of self-peptide MHC [Burroughs and van der Merwe, 2007].

The affinity and the off-rate are especially implicated in determining an activation threshold [Dushek et al., 2011]. The affinity model proposes that the TCR:pMHC affinity is the determining parameter for T cell activation.

The affinities of several TCRs to pMHC monomer in solution have been determined using SPR [Stone et al., 2009] [Aleksic et al., 2010]. Monomeric TCR:pMHC binding kinetics in solution and measured by SPR are different from the physiologic setting of two cell interfaces. Yet, one study noted that TCR multimer off-rates and T cell function correlated well with monomeric affinities [Schmid et al., 2010]. There are two approaches to studying T cell responses to different TCR:pMHC affinities: varying the sequence of the peptide presented or varying the sequence of the TCR. Studies with primary $CD8^+$ lymphocytes transfected a panel of TCRs of different affinities to the same NY-ESO-$1_{156-165}$ melanoma-derived peptide revealed an optimal affinity for efficient functional responses between 1 and 5 μM [Schmid et al., 2010] [Irving et al., 2012]. Supra-physiological affinities above this threshold decreased T cell activation [Irving et al., 2012]. Affinities below the threshold decreased functionality gradually. The wild-type 1G4 TCR interaction was determined to be 21.4 μM which is lower in this study than in the kinetic study by Aleksic et al., 2010 (14 μM) [Schmid et al., 2010]. Patients with the 1G4 TCR only show weak T cell responses to the NY-ESO-$1_{156-165}$ melanoma-derived peptide which is why in the studies by Schmid and Irving, the 1G4 TCR was defined to represent neutral T cell functions [Chen et al., 2000]. These studies showed very well-defined and concise ranges of affinities which confer efficient optimal T cell function. However, models using different TCR systems, for example the 2C TCR system, reported that TCR affinities up to 10 μM induced strong responses independent from CD4 or CD8 co-stimulation and agonist interactions were observed with affinities as low as 100 μM [Kalergis et al., 2001] [Stone et al., 2009]. Morris et al.,

2012, distinguish between agonists and partial or positively selecting peptide ligands. Non-agonist- and self-peptides are recognised with an affinity a magnitude lower than agonist binding [Morris and Allen, 2012].

Considering the published studies using the 1G4:NY-ESO-$1_{156-165}$ system, the peptides used in this studies are expected to yield the following T cell responses: The 9V peptide with an affinity of 7.2 μM lies just outside the affinity plateau inducing optimal T cell function reported by Schmid, 2010, and Irving 2012, but within the boundaries of strong agonists set by Stone, 2009. Chen et al, 2005 and 2010, reported strong T cell responses to the 9V peptide. Thus, in this study, strong agonist reposes are to be expected from 1G4 cells to 9V stimulation. The intermediate 6V peptide with an affinity of 18 μM is close in affinity to the wt peptide and thus would be expected induce weak or neutral T cell responses. The affinity of the 9L peptide is at the low end of agonist interactions with 56 μM affinity for the 1G4 TCR. Typically these interactions are higher than 100 μM in affinity [Stone et al., 2009]. In general, very little is known about the more precise affinities and binding kinetics of self-peptide MHC and TCRs and how these interactions drive peripheral T cell homeostasis [Stone et al., 2009]. All T cells must respond to self-peptide MHC for development and peripheral homeostasis even if only few T cells encounter foreign antigens and mount effector function to control infection. The 4D NY-ESO-$1_{156-165}$ pMHC tetramers have a very low affinity for the 1G4 TCR at 252 μM and is not expected to induce T cell responses. In this study it is used as a null peptide. Besides weak TCR signals, T cell homeostasis also requires IL-2, IL-7 and IL-15 signalling [Morris and Allen, 2012].

As detailed above, T cell responses are not homogeneous but can confirm both a specific digital all-or-nothing response to ligand potency and a sensitive analogue response [Burroughs and van der Merwe, 2007]. While immunoblotting is a powerful tool to investigate the induction of signalling responses, it is an not fully adequate to provide accurate indication of the responses of specific populations of T cells because the signal obtained is an average of a large, pooled cell population. Furthermore, the technical restrictions of immunoblotting are unsuitable to conducting time-courses, dose responses and accurate quantitations and repeats in order to obtain kinetic data with associated statistical confidence [Haas et al., 2008].

In recent years, flow cytometry of phosphorylated intracellular proteins has been established as a powerful comparative, semi-quantitative tool to investigate cellular signalling events at population level [Haas et al., 2008].

5.2 Aims

The results of the previous chapter showed that high affinity 9V NY-ESO-$1_{156-165}$ pMHC tetramers initiated stronger activation of proximal signalling events than the low affinity 9L peptide.

The aim of the work in this chapter was to extend the panel of NY-ESO-$1_{156-165}$ pMHC tetramers to also include the intermediate affinity 6V and non-agonist/self-peptide 4D tetramers. To investigate the effect of tetramer potency on early TCR proximal signalling events, I used flow cytometry of several phospho-proteins simultaneously in time-course and dose-response experiments. This high throughput quantitative approach provides new details

of how TCR:pMHC affinities correlate with proximal signalling and confers T cell effector functions. The presented flow cytometry approach aims to overcome some of the limitations of immunoblotting to achieve a more quantitative appreciation of TCR signalling events.

5.3 Results

5.3.1 Signalling kinetics in response to tetramer affinity.

In response to TCR stimulation a series of intracellular kinases are phosphorylated and thus activated. Previous experiments have shown the 9V and 9L NY-ESO-$1_{156-165}$ pMHC tetramers stimulate 1G4 cells with different strengths. To achieve higher resolution of the stimulation kinetics invoked by pMHC tetramers of different affinities, I stimulated 1G4 cells with four species of NY-ESO-$1_{156-165}$ pMHC tetramers at 200 nM over a 4 hour timecourse (Figure 5.1). Cells were stimulated at 37 °C in solution, fixed immediately with 4% paraformaldehyde without removing excess pMHC and permeabilised with 10% saponin. Cells were analysed using intracellular phosphoflow cytometry for activated ERK phosphorylated at threonine 202 and tyrosine 204 (pT202.pY204-ERK) and activated LCK phosphorylated at tyrosine 394 (pY394-LCK) simultaneously through its fluorochrome conjugates to the indicated antibodies. Occupancy was also simultaneously measured through the streptavidin phycoerythrin. Sodium pervanadate and PMA served as positive controls for strong LCK and ERK activation, respectively. Unstimulated cells served as background phosphorylation controls.

Occupancy of NY-ESO-$1_{156-165}$ tetramers detectable at the first measured timepoint and reaches saturation by 10 min (Figure 5.1 A and B). The degree of occupancy is dependent on the affinity of the tetramer. Occupancy of 9L and 4D remain about 80% lower than occupancy levels of 9V and 6V.

In order to record precise and consistent timings in regards to the signalling events, the cells were not washed before fixation. A correlation of occupancy to tetramer binding affinity and potency was reported previously [Kalergis et al., 2001] [Neveu et al., 2006]. The off-rate is critical to this binding. For example the binding half-time of 9L is 2.8 times lower than that of 9V (Figure 1.12). 9L thus reaches a binding-dissociation equilibrium at a much lower level of occupancy.

Even though occupancy levels differed by a factor of five between tetramers, the phosphorylation of LCK on its activating tyrosine 394 was only very slightly and elevated after tetramer stimulation (Figure 5.1 C). Similar effects were already observed using immunoblotting (Figure 4.2 and 4.3). The rise of activated LCK was only slight and statistically insignificant on flow cytometry: about 1.2-fold to the unstimulated control. The affinity of the tetramers did not influence the degree of LCK-activation significantly. The affinity of 4D for example, is 35-times lower than that of 9V and their occupancy levels differ by 3- to 4-fold. 9V also causes marked pT202.pY204-ERK

Figure 5.1 *(following page)*: 4 hour tetramer stimulation timecourse. 1G4-CD8αα cells were stimulated with 200 nM pMHC tetramer for up to 4 hours. (A) Histogram flow cytometry read-out. Data represented is an example of three separate experiments. Tetramer occupancy, pY394-LCK and pT202.pY204-ERK were recorded simultaneously through the use of distinct fluorochromes. (B) Individual data of three experiments of tetramer occupancy was analysed using the geometric mean. (C) LCK activation over 4 hours expressed as percentage of the maximal response achieved by the positive control, sodium pervanadate. (D) ERK activation over 4 hours expressed as percentage of the maximal response achieved by the positive control, PMA. All analysis was performed with data from the histograms shown in A using GraphPad Prism. All error bars show the SEM of three individual experiments.

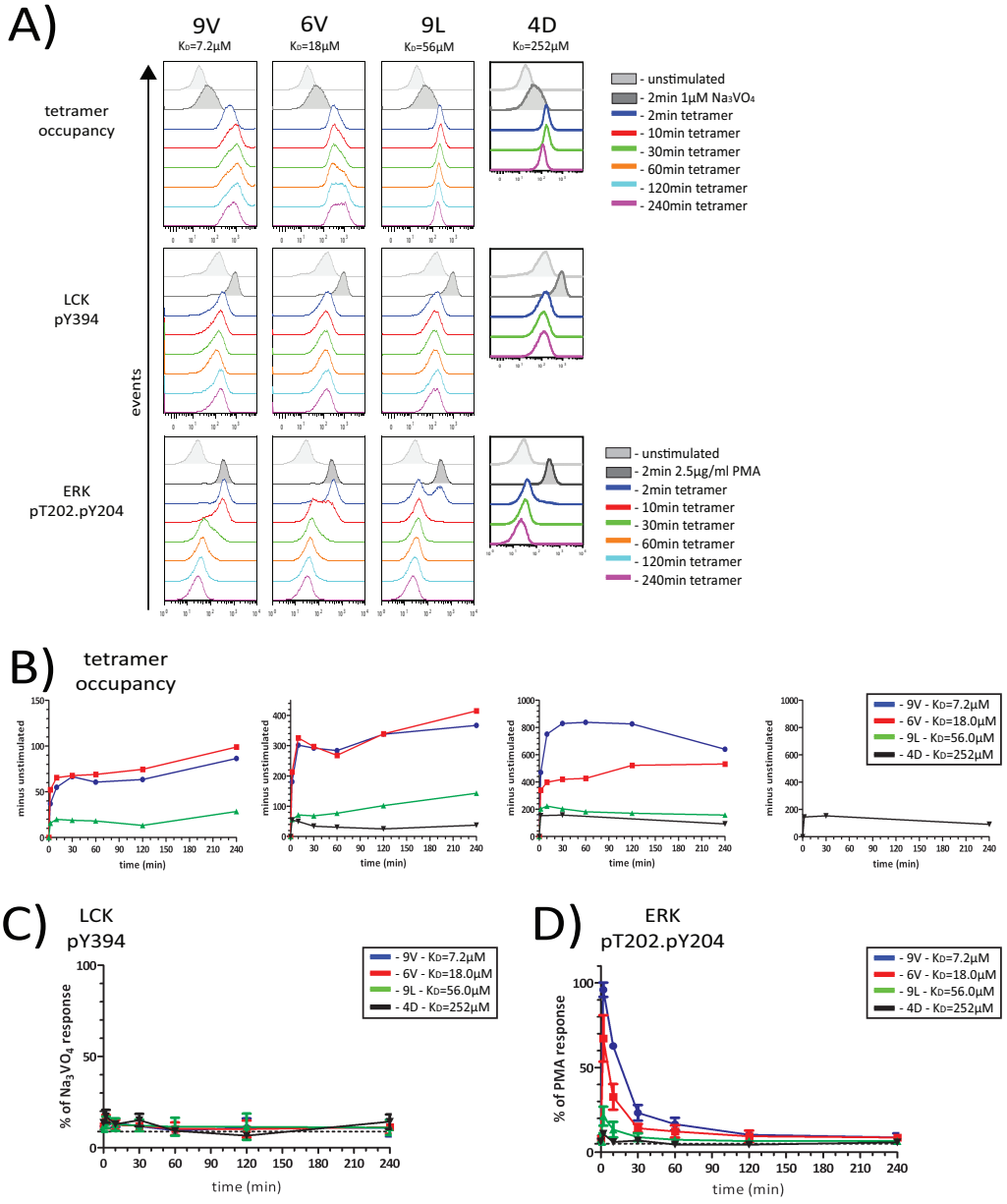
A)
9V
KD=7.2μM
6V
KD=18μM
9L
KD=56μM
4D
KD=252μM
tetramer occupancy
LCK pY394
ERK pT202.pY204
events
- unstimulated
- 2min 1μM Na3VO4
- 2min tetramer
- 10min tetramer
- 30min tetramer
- 60min tetramer
- 120min tetramer
- 240min tetramer
- unstimulated
- 2min 2.5μg/ml PMA
- 2min tetramer
- 10min tetramer
- 30min tetramer
- 60min tetramer
- 120min tetramer
- 240min tetramer
B)
tetramer occupancy
minus unstimulated
time (min)
- 9V - KD=7.2μM
- 6V - KD=18.0μM
- 9L - KD=56.0μM
- 4D - KD=252μM
C)
LCK pY394
% of Na3VO4 response
time (min)
- 9V - KD=7.2μM
- 6V - KD=18.0μM
- 9L - KD=56.0μM
- 4D - KD=252μM
D)
ERK pT202.pY204
% of PMA response
time (min)
- 9V - KD=7.2μM
- 6V - KD=18.0μM
- 9L - KD=56.0μM
- 4D - KD=252μM

activation whereas 4D elicits no responses (Figure 5.1). Yet, LCK-activation does not differ significantly between the two tetramers. Thus, it seems unlikely that the elevation of pY394-LCK observed after TCR engagement by pMHC tetramers contributes to changes in proximal signalling based on the affinity of the ligands.

In contrast, activation of ERK through the phosphorylation of threonine 202 and tyrosine 204 is pronounced. Maximum activation is reached within 2 min of stimulation. The largest differences between tetramer stimulations is also seen at this timepoint. 9V elicits the highest pERK response while cells stimulated with 4D remain unresponsive. In all stimulations, the pERK signal decayed rapidly after reaching full activation and the rate of the signal's decay correlated to the affinity of the stimulation.

The flow cytometry histograms for 9V reveal a complete switch of the entire cell population from resting to activated. After 2 min of 9L stimulation the histogram shows two populations. By comparison to the unstimulated and positive controls, the lower intensity peak corresponds to an unresponsive cell population and the higher intensity peak to a population actively signalling through pT202.pY204-ERK. This indicates that the activation of phospho-ERK displays a digital, switch-like nature and corroborates previous findings observed after anti-CD3ε stimulations [Das et al., 2009]. How many cells are pERK-responsive is dependent on the affinity of the pMHC tetramer. It is likely that the decision for discrete cell activation must have been made at a further upstream signalling protein.

After the peak at 2 min the pERK signal decreases steadily until background

levels are reached again after 2 hours of stimulation. This was observed despite the continuing exposure to tetramers in the experimental set-up.

In this initial analysis of proximal T cell signalling after pMHC tetramer stimulation by flow cytometry, I could measure tetramer occupancy as well as LCK and ERK activation simultaneously. The analysis showed that the degree of occupancy is dependent on the affinity of the pMHC complex. This has been reported before and is most likely due to the faster off-rates of low affinity ligands. LCK phosphorylation was slightly but insignificantly increased at activating tyrosine 394 upon pMHC binding. This effect was seen independently of ligand affinity. 1G4 cells have low resting activated LCK concentrations and it is conceivable that the binding of the pMHC tetramers to CD8αα results in the clustering of LCK molecules and increased cross-auto-phosphorylation. In this case, the increase of pY394-LCK levels is independent of the pMHC binding affinity and unlikely to contribute to downstream signalling kinetics which are dictated by them. The strength phospho-ERK response in contrast was clearly dependent on pMHC binding affinity. Higher affinity stimulation resulted in higher amplitude and longer sustained ERK signals. The ERK signal was defined by a sharp peak rather than a sustained signal. It is possible that the lack of CD28 expression and thus possible co-stimulation contributes to the shape of the pERK response and that particularly low affinity signals might be enhanced in amplitude and duration by co-stimulation.

The peak of the pERK signal was observed after 2 min of stimulation (Figure 5.1). Thus I investigated the pT202.pY204-ERK, pY394-LCK, pY142-CD3ζ and pY493-ZAP-70 responses in a more detailed timecourse from 10 sec to

2 min (Figures 5.2 and 5.3). Samples were taken at 10 second intervals until 1 min and then at 15 second intervals until 2 min. Stimulation conditions were the same as detailed before.

Tetramer occupancy is visible within 10 sec. In Figure 5.1, occupancy reached saturation after about 10 min of stimulation. Thus it is expected that the occupancy of 9V and 6V in particular do not reach saturation within the 2 minute timecourse. However, 9L and 4D occupancy levels are less than half of the 9V occupancy observed and remain constant over the timecourse (Figure 5.2).

ERK phosphorylation shows clearly a digital pattern over 2 min in Figure 5.2, as suggested by Figure 5.1. The digital pattern is shown in two clear populations which represent an pERK unresponsive and a responsive population of 1G4 cells. To assess the degree of ERK activation induced by tetramer stimulation, I analysed what percentage of all events collected by flow cytometry were recorded in the activated pT202.pY204-ERK peak. No pERK activation is observed for the lowest affinity tetramer, 4D. 9V induces

---

Figure 5.2 *(following page)*: 2 minute phospho-ERK activation by NY-ESO-1 tetramers. 1G4 cells were stimulated with 200 nM pMHC tetramer for up to 2 min. (A) Histogram flow cytometry read-out. Data represented is an example of three separate experiments. Tetramer occupancy and pT202.pY204-ERK were recorded simultaneously through the use of distinct fluorochromes. (B) Tetramer occupancy over three experiments were analysed using GraphPad Prism. (C) ERK activation displays as two distinct peaks correlating to an unresponsive and an activated fraction of cells. ERK activation was evaluated by the percentage of cells activated. (D) Half-times to the graphs of C. (E) The geometric means of the unresponsive (1) and ERK-activated (2) fractions were compared over the 2 min timecourse. All graphs show the SEM and are representative of three individual experiments.

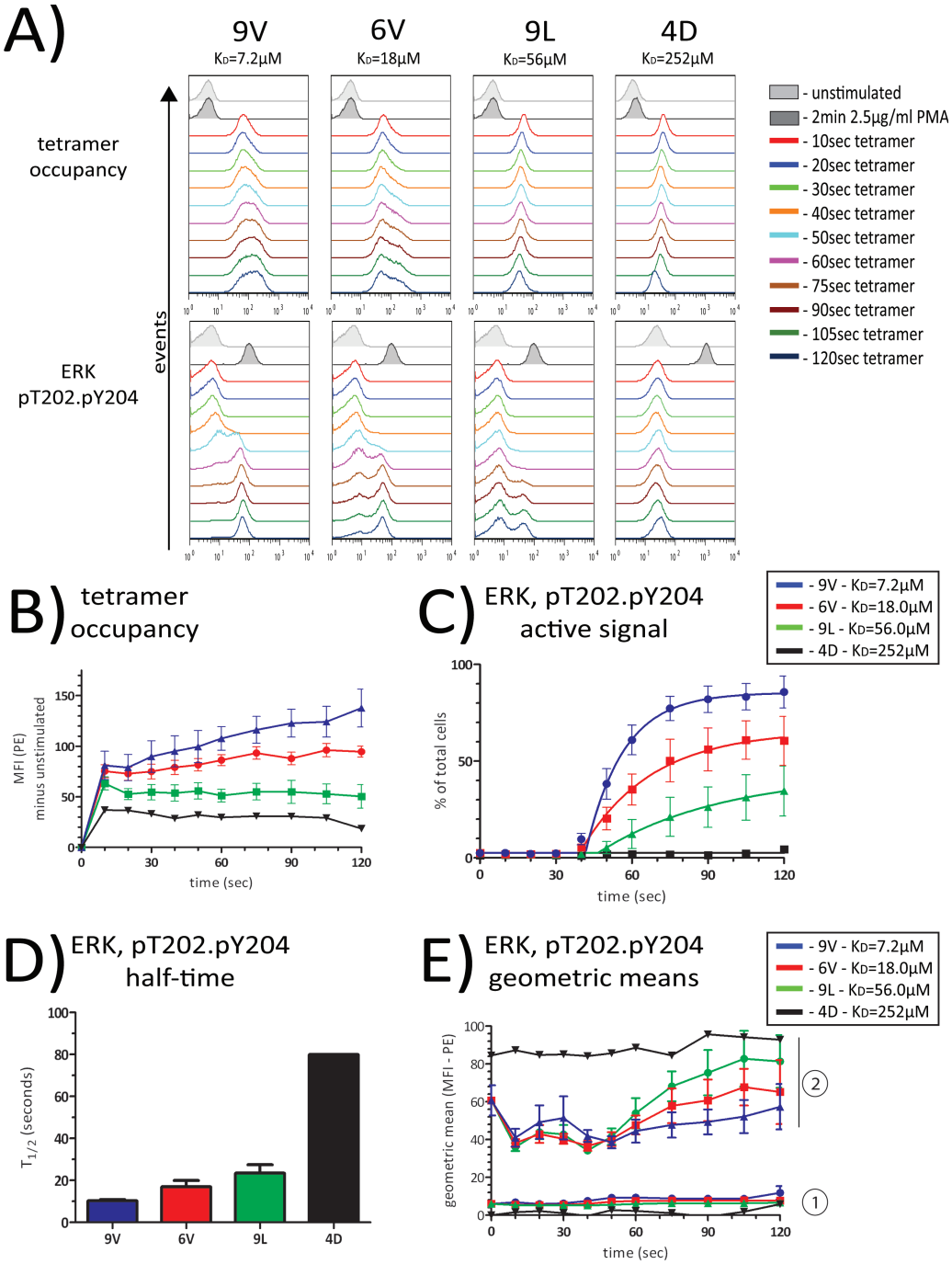
A)
9V
KD=7.2μM
6V
KD=18μM
9L
KD=56μM
4D
KD=252μM
tetramer occupancy
ERK pT202.pY204
events
- unstimulated
- 2min 2.5μg/ml PMA
- 10sec tetramer
- 20sec tetramer
- 30sec tetramer
- 40sec tetramer
- 50sec tetramer
- 60sec tetramer
- 75sec tetramer
- 90sec tetramer
- 105sec tetramer
- 120sec tetramer
B) tetramer occupancy
MFI (PE) minus unstimulated
time (sec)
C) ERK, pT202.pY204 active signal
- 9V - KD=7.2μM
- 6V - KD=18.0μM
- 9L - KD=56.0μM
- 4D - KD=252μM
% of total cells
time (sec)
D) ERK, pT202.pY204 half-time
T1/2 (seconds)
9V
6V
9L
4D
E) ERK, pT202.pY204 geometric means
- 9V - KD=7.2μM
- 6V - KD=18.0μM
- 9L - KD=56.0μM
- 4D - KD=252μM
geometric mean (MFI - PE)
time (sec)
2
1

pT202.pY204-ERK activity at 50 seconds and by 70 seconds all cells are actively signalling (Figure 5.2 A and C). 6V also induces pERK activity at 50 seconds but the percentage of cells signalling is significantly lower at about 70% (Figure 5.2 A and C). This is observed despite the occupancy of 9V and 6V being very similar. The occupancy of 9V and 6V could be similar because the cells are stimulated with high tetramer concentrations and 200 nM of pMHC tetramers might saturate the system. The signalling differences observed despite the similar levels of occupancy shows that the amplitude of intracellular signalling events is governed by qualitative differences between the peptides' affinities. 9L induces pERK signalling but it is delayed and only less than 50% of cells are active. The different kinetics of pT202.pY204-ERK activation induced by the different pMHC tetramer binding properties is expressed in the half-time of the signal reaching its maximum (Figure 5.2 D).

In all cases of tetramer stimulation the digital nature of the pERK signal is evident. The peaks have been labelled (1) for the quiescent population and (2) for the responding population in Figure 5.2 D. For the timecourse, the geometric means of both peaks were plotted in the same graph. It shows that there is significant distinction between unresponsive and active peaks. But once active, all pERK signals reach similar levels. This shows the distinct switch-like nature of the signal.

The digital nature of the pERK signal is very informative and shows that TCR signalling along this pathway leads to a discrete decision towards activation based on the binding qualities of the TCR:pMHC interactions. To investigate whether earlier signal molecules are able to transmit qualitative

differences between pMHC tetramers, I performed the same timecourse as in Figure 5.2 and stained for pY394-LCK, pY142-CD3ζ and pY493-ZAP-70 (Figure 5.3). These experiments were co-stained with the results shown in Figure 5.2.

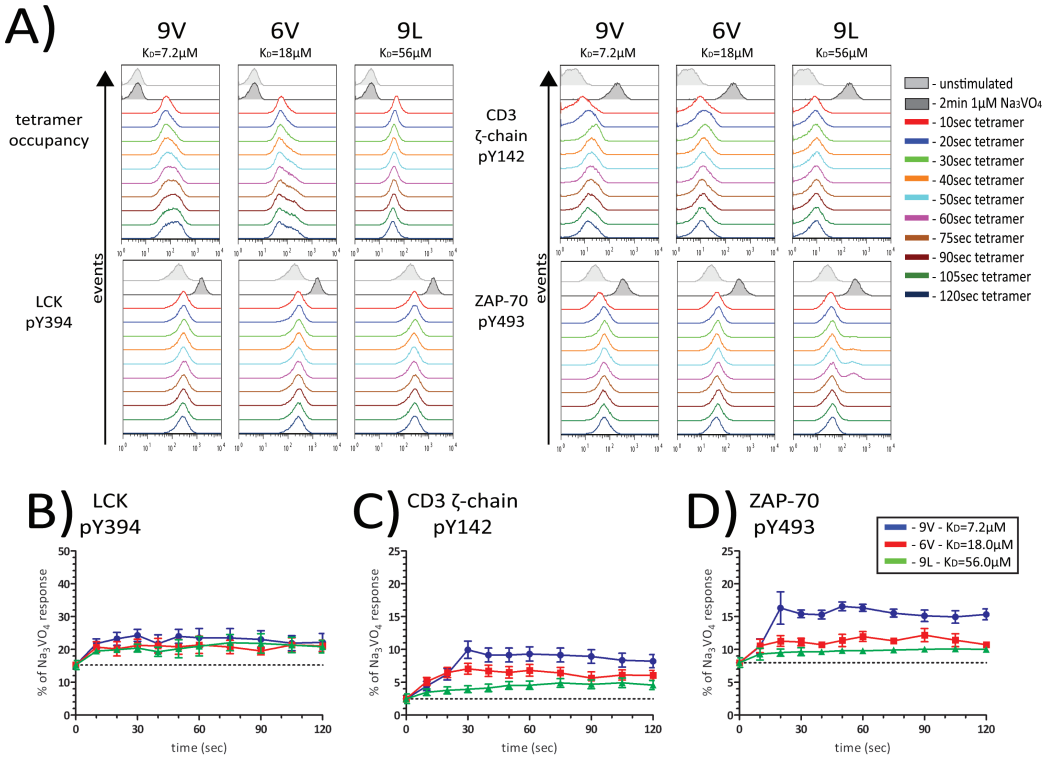

Figure 5.3: 2 minute phospho-LCK, -CD3ζ and -ZAP-70 phosphorylation and activation by NY-ESO-1 tetramers. 1G4 cells were stimulated with 200 nM of the indicated NY-ESO-1 tetramers over 2 min as in Figure 5.2. As normalisation between experiments all graphs express phospho-protein activation as the percentage of the sodium pervanadate positive control. (A) Histogram flow cytometry read-out. Data represented is an example of three separate experiments. (B) pY142-CD3ζ phsphorylation over three experiments. Error bars show SEM. (C) pY493-ZAP-70 activation over three experiments. Error bars show SEM. (D) pY394-LCK activation over three experiments. Error bars show SEM.

As observed and discussed in Figures 4.2 and 3 and 5.2, pY394-LCK levels were slightly elevated following tetramer stimulation (Figure 5.3 A and B).

This phenomenon was independent from tetramer binding affinity or occupancy and thus unlikely to govern the differences of pERK signalling observed between different NY-ESO-$1_{156-165}$ pMHC tetramers observed in Figure 5.2. pY142 CD3ζ levels reach maximum within 20 to 30 seconds which is much earlier than the pERK response (Figure 5.3 A and C). There is a clear and significant distinction in the level of CD3ζ-phosphorylation and tetramer affinity. Higher binding affinity correlates to the stronger the CD3ζ-phosphorylation. This was determined by calculating the degree of the tetramer-induced CD3ζ response in relation to the sodium pervanadate positive control. A similar pattern of activation induction is observed for pY493-ZAP-70 (Figure 5.3 A and D). In both cases, the differences in activation after stimulation with different affinities are not instantly recognisable from the flow cytometry histograms as is the case for the pERK response. Signals of CD3ζ and ZAP-70 phosphorylation are mild in comparison to the pERK response and analogue in nature while the pERK response is discrete and digital. Much higher levels of CD3ζ and ZAP-70 activity are recorded with the sodium pervanadate positive controls. This might indicate that although tetramer occupancy is very high and engages a high number of TCRs, tetramer stimulation does not achieve the efficient phosphorylation of all CD3ζ and ZAP-70 molecules. If this was the case, then the engagement of few TCRs is sufficient to induce maximal pERK activity. The maximum reached for pY142-CD3ζ and pY493-ZAP-70 seems to correspond with the likelihood of pT202.pY204-ERK activation further downstream (Figure 5.4). I assessed the link between the analogue signals observed in more TCR proximal signalling in Figure 5.3 and the digital signal observed in the pERK response in Figure

5.2. I quantified the analogue signal by determining the area underneath the timecourse's graph and subtracting the background of Figure 5.3 (Figure 5.4 A-C). I determined the strength of the pERK signal by calculating the maximal response of cells. This was expressed in the maximum fraction of cells activated by a particular stimulus (Figure 5.4 D). In Figure 5.4 E I correlated the parameters of the analogue and digital signals determined in the previous sections of the figure. This showed that stronger analogue pY142-CD3ζ and pY493-ZAP-70 signals resulted in the induction of a stronger and more discrete digital pT202.pY204-ERK signal. A similar correlation can be observed in Figure 5.4 F for the affinity of the stimulating NY-ESO-$1_{156-165}$ pMHC tetramer and the degree of the analogue pY142-CD3ζ and pY493-ZAP-70 responses. Thus, the analogue signal conveyed by pY142-CD3ζ and pY493-ZAP-70 is able to communicate qualitative differences of the binding ligand to further downstream signalling molecules which convert the signal into a discrete all-or-nothing response.

5.3.2 Tetramer concentration affects signalling

At the same concentrations, the four pMHC tetramers display different levels of occupancy. This has been attributed to differences in the dissociation rate [Neveu et al., 2006]. To investigate how the occupancy and thus the dose of tetramer stimulation received by the 1G4 Jurkat cells accounts for differences in proximal signal strength, I performed dose response stimulations with all four tetramers. Samples were taken at 3 min of stimulation. At this timepoint, maximal pT202.pY204-ERK responses are established. The manner

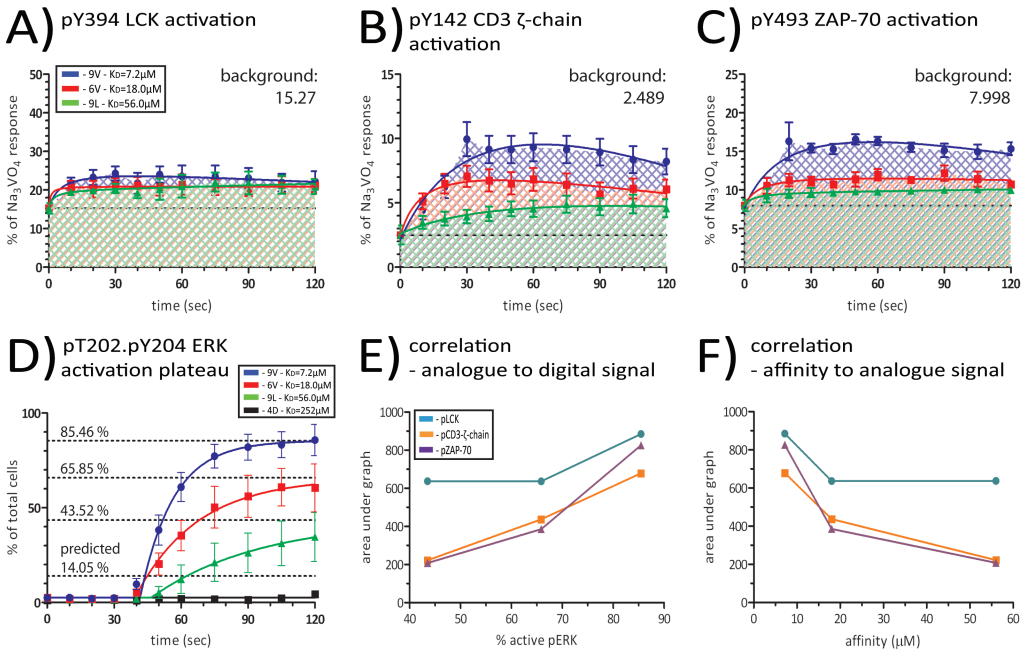

Figure 5.4: Affinity and early proximal analogue signal strength determines later digital T cell activation. Analysis of the timecourse data of Figure 5.2 and 5.3. (A-C) The activation of pY394-LCK (A), pY142-CD3ζ (B) and pY493-ZAP-70 (C) of Figure 5.3 were quantified by the area underneath the graphs. (D) The strength of the pT202.pY204-ERK response was expressed as the maximal percentage of cells actively signalling through pERK. (E) The effect of the analogue signal strength on the discrete pERK signal was analysed as the activation plateau of pERK determined in D against the quantification of the analogue signals determined in A-C. (F) The effect of the NY-ESO-1 pMHC tetramer affinity on the analogue signal strength as determined in A-C. All analyses were performed using GraphPad Prism.

of stimulation and preparation for flow cytometry was the same as before. Samples were investigated for occupancy and pT202.pY204-ERK simultaneously (Figure 5.5).

Occupancy decreases starkly with lower tetramer concentrations. Background levels of detection are reached at a tetramer concentration of 1 nM. The qualitative difference of stimulatory potency between the different tetramer is evident. 9V stimulation induces strong pT202.pY204-ERK signals at all concentrations (Figure 5.5 A and C). No fewer than 70% of cells are activated even by the lowest concentrations of 9V (Figure 5.5 C). At 1 nM, 9V occupancy is undetectable on flow cytometry through the phycoerythrin-tag. This shows that few tetramers of strong affinity are able to induce strong T cell activation.

At lower tetramer affinities, tetramer dose affects the potency of the pERK signal induced more strongly. Activation levels drop by 30% during both 6V and 9L dose responses (Figure 5.5 C). For 6V two distinct populations become more clearly visible with decreasing dosage. Decreasing doses of 9L attenuates the pERK signal. This indicates that reinforcement of intermediate and low signals might be important in triggering T cell responses. Although higher 9L concentrations increase the TCR signals elicited by this pMHC tetramer, the increased occupancy does not result in TCR signals comparable to higher affinity stimulations with 9V or 6V. Thus, increased 9L occupancy is unable to compensate for lower affinity of the ligand. A level of occupancy which causes 40% of pERK activity in 9L-stimulated cells, results in 78% and 90% activity in 6V- or 9V-stimulated cells respectively (Figure 5.5 E). 9V and 6V had very similar levels of occupancy. Still, 9V

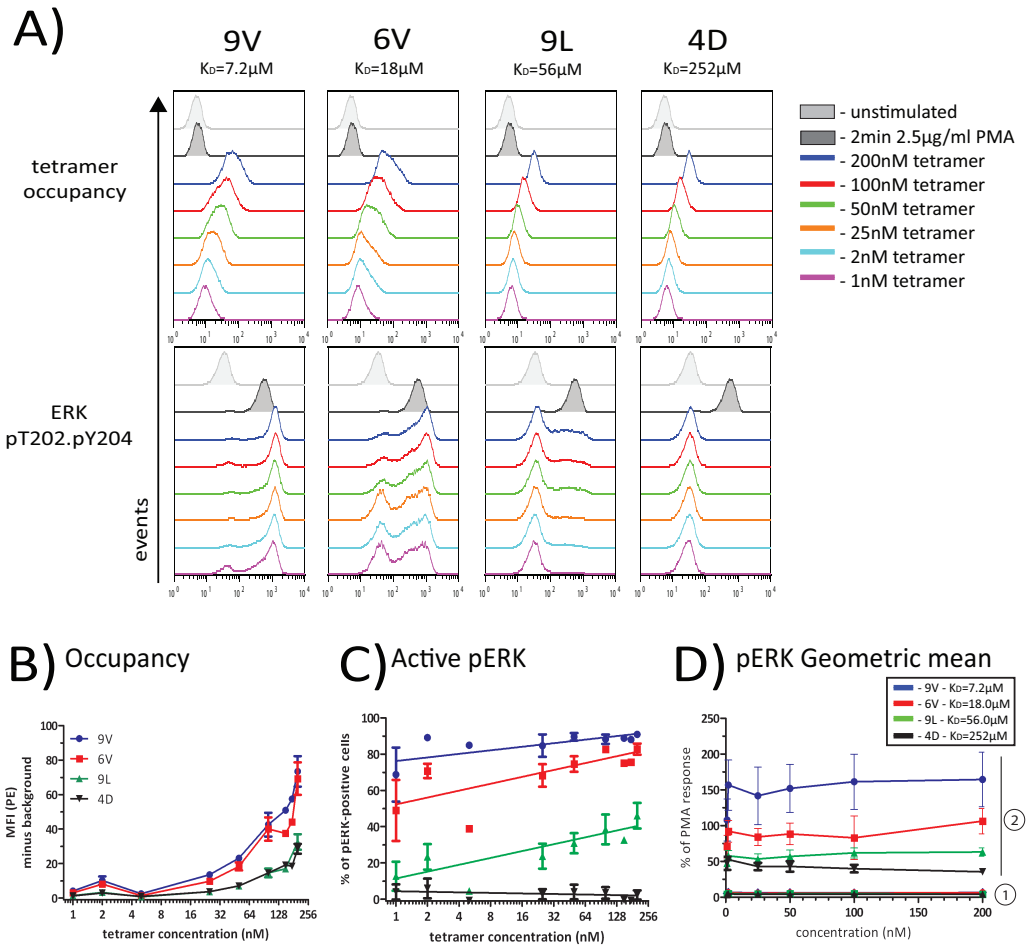

Figure 5.5: pERK response to NY-ESO-1 pMHC tetramer dose. 1G4 cells were stimulated for 3 min with 1 to 200 nM of the indicated NY-ESO-1 tetramers. The pT202.pY204-ERK response was recorded and PMA was used as positive control. (A) Histogram flow cytometry read-out. Data represented is an example of three separate experiments. Tetramer occupancy and pT202.pY204-ERK were recorded simultaneously through the use of distinct fluorochromes. (B) Occupancy of NY-ESO-1 pMHC tetramers. Error bars show SEM. (C) Activation of pT202.pY204-ERK expressed as percentage of cells activated as determined from the histograms in A. Error bars show SEM. (D) The geometric means of the unresponsive (1) and ERK-activated (2) fractions were compared over the dose response. All graphs show the SEM and are representative of three individual experiments.

stimulation activated at least 5 to 10% more cells than 6V. 80% of cells are pERK-active after stimulation with 2.1 nM 9V. The same level of activity is reached with 128 nM 6V. This is a 60-fold difference which is surprising since the K_D differs only 2-fold between the tetramers and the k_{off} differs only 2.6-fold. Elevated occupancy and thus tetramer concentration is partially able to compensate for decreased affinity. However, occupancy density and ligand affinity are clearly not interchangeable variables and affinity is the more dominant parameter determining the strength of downstream signalling. Possible positive and negative feedback loops act to enhance and amplify strong 9V signals and dampen more effectively weaker 6V signals, respectively.

To investigate if the concentration of NY-ESO-$1_{156-165}$ pMHC tetramers affects further parameters of T cell signalling kinetics despite the maximal response, I stimulated 1G4 cells with four 9V doses over 3 min timecourses. 9V concentrations ranged from 200 nM to 2 nM. Stimulations and flow cytometric analyses were carried out as before.

At 2 nM 9V occupancy is undetectable by flow cytometry. There is no difference in the maximum percentage of pT202.pY204-ERK responding cells between 200 nM and 40 nM of 9V even though occupancy differs by about 3-fold (Figure 5.6 A-C). This indicates that the system has reached saturation at these concentrations and a maximal response is induced at both concentrations. At both concentrations the pERK signal is induced after about 1 min and reaches its maximum by 90 sec. Both concentrations are able to induce pERK activity in up to 90% of cells. Lower concentrations show occupancy two magnitudes lower than the highest concentration. At

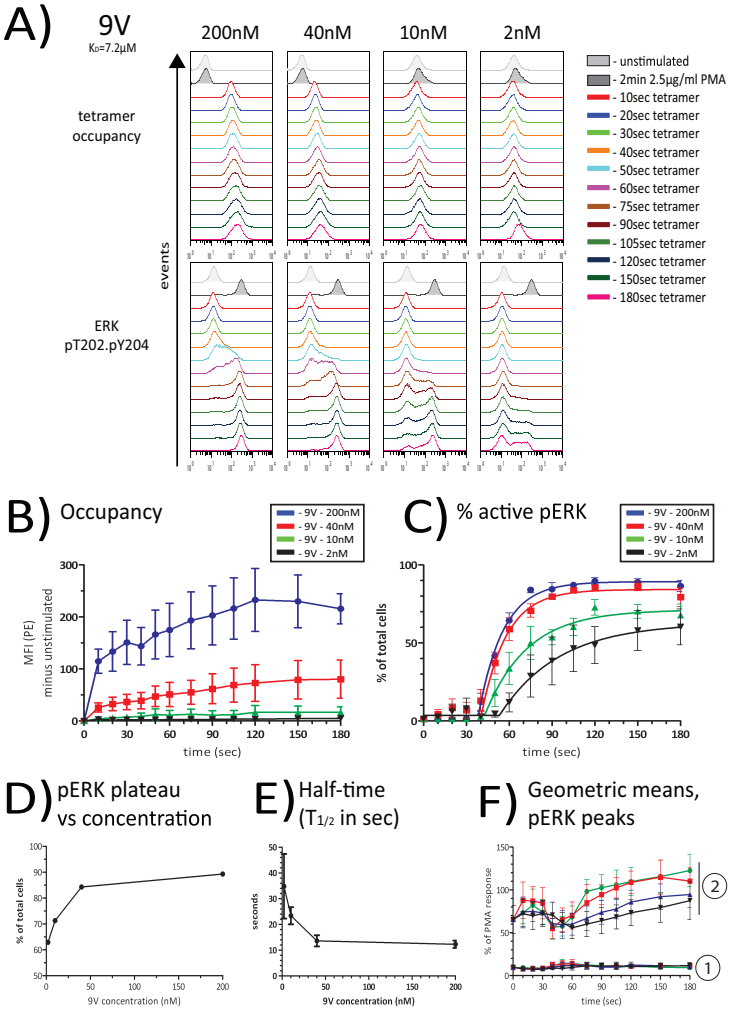

Figure 5.6: pERK activity to 3 min 9V NY-ESO-1 tetramer dose response. 1G4 cells were stimulated over 3 min with 2 to 200 nM of 9V NY-ESO-1 tetramer. The pT202.pY204-ERK response was recorded and PMA was used as positive control. (A) Histogram flow cytometry read-out. Tetramer occupancy and pT202.pY204-ERK were recorded simultaneously through the use of distinct fluorochromes. (B) Occupancy of NY-ESO-1 pMHC tetramers. (C) Activation of pT202.pY204-ERK expressed as percentage of cells activated as determined from the histograms in A. (D) the maximal response of pERK expressed in the percentage of cells actively signalling pERK was determined in B and plotted against 9V concentration. (E) The half-time of the activation curve presented in B in dependence of tetramer concentration. (F) The geometric means of the unresponsive (1) and ERK-activated (2) fractions were compared over the dose response. All graphs show the SEM of four individual experiments.

10 nM up to 72% of cells are pERK active despite the occupancy being close to undetectable. At 2 nM 9V still more than 60% of cells actively signal through pERK. This shows the efficiency of the 9V stimulation. In comparison, while 2 nM of 9V activate ERK in 60% of cell, only up to 40% are activated after being stimulated with 200 nM of 9L (Figure 5.5). This means that a 100-fold increase in ligand concentration is unable to compensate for a 7-fold difference in affinity (Figure 3.1). Figure 5.6 A and C show that decreasing tetramer concentration results in a delay of the pERK response. This coincides with a decrease in the maximal fraction of cells actively signalling through pERK after 3 min. Even though empirically the process of pERK activation is completed by 3 min, it cannot be excluded that even the lowest concentrations would be able to stimulate more cells in a longer timecourse. The half-time of the pERK activation decreases by up to 3-fold with decreasing concentrations. In comparison to earlier figures this shows that 2 nM of 9V stimulate 1G4 cells comparatively to 200 nM 6V in regards to the maximum signal achieved and to 200 nM 9L in regards to the speed of the signal (Figure 5.2 and Figure 5.6 C-E). However, at the lowest concentrations the variation between experiments is high. This could be due to factors such as the duration of cell culture. Nevertheless, once activated even with low concentrations, 9V responses show little variation in the extent of the ERK activation. The geometric means between the two peaks are distinctly separate showing that there are two distinct states of ERK - inactive and active as shown by Figure 5.6 F.

To investigate whether earlier signalling proteins are able to sense differences of tetramer occupancy, I performed the same timecourse as in Figure 5.6

and stained for pY394-LCK, pY142-CD3ζ and pY493-ZAP-70 (Figure 5.7). These experiments were co-stained with the results shown in Figure 5.6.

pY394-LCK levels were slightly and insignificantly elevated within 20 sec following stimulation with different 9V doses (Figure 5.7 A and B). The levels of pY394-LCK subsequently levelled. The dose of 9V had no influence on the extent of apparent LCK activation. This phenomenon is similar to the apparent LCK-activation observed earlier with different affinity pMHC including the 'null-agonist' 4D. The degree of pY394-LCK activation is hardly affected by 9V concentration and also hardly corresponds to the likelihood of further downstream pT202.pY204-ERK activation (Figure 5.8 A, D-F).

pY142-CD3ζ levels reached a maximum within 20 to 30 seconds (Figure 5.7 A and C). The extent of pY142-CD3ζ phosphorylation was determined by calculating the degree of the tetramer-induced CD3ζ response in relation to the sodium pervanadate positive control. 9V dose results in no clear difference in pY142-CD3ζ phosphorylation or pERK activation between 40 nM and 200 nM of 9V. The system appears to be saturated at this range of concentration and a maximum response is achieved by the 9V tetramers. Stimulation with lower concentrations of 10 nM and particularly 2 nM 9V

Figure 5.7 *(following page)*: LCK, CD3ζ and ZAP-70 phosphorylation and activity over 3 min 9V NY-ESO-1 tetramer dose response. 1G4 cells were stimulated with 2 nM, 10 nM, 40 nM or 200 nM of 9V NY-ESO-1 tetramers over 3 min as in Figure 5.6. To normalise the experiments all graphs express phospho-protein activation as the percentage of the sodium pervanadate positive control. All graphs show the SEM of three individual experiments. (A) Histogram flow cytometry read-out. (B) pY142-CD3ζ phosphorylation over three experiments. (C) pY493-ZAP-70 activation. (D) pY394-LCK activation.

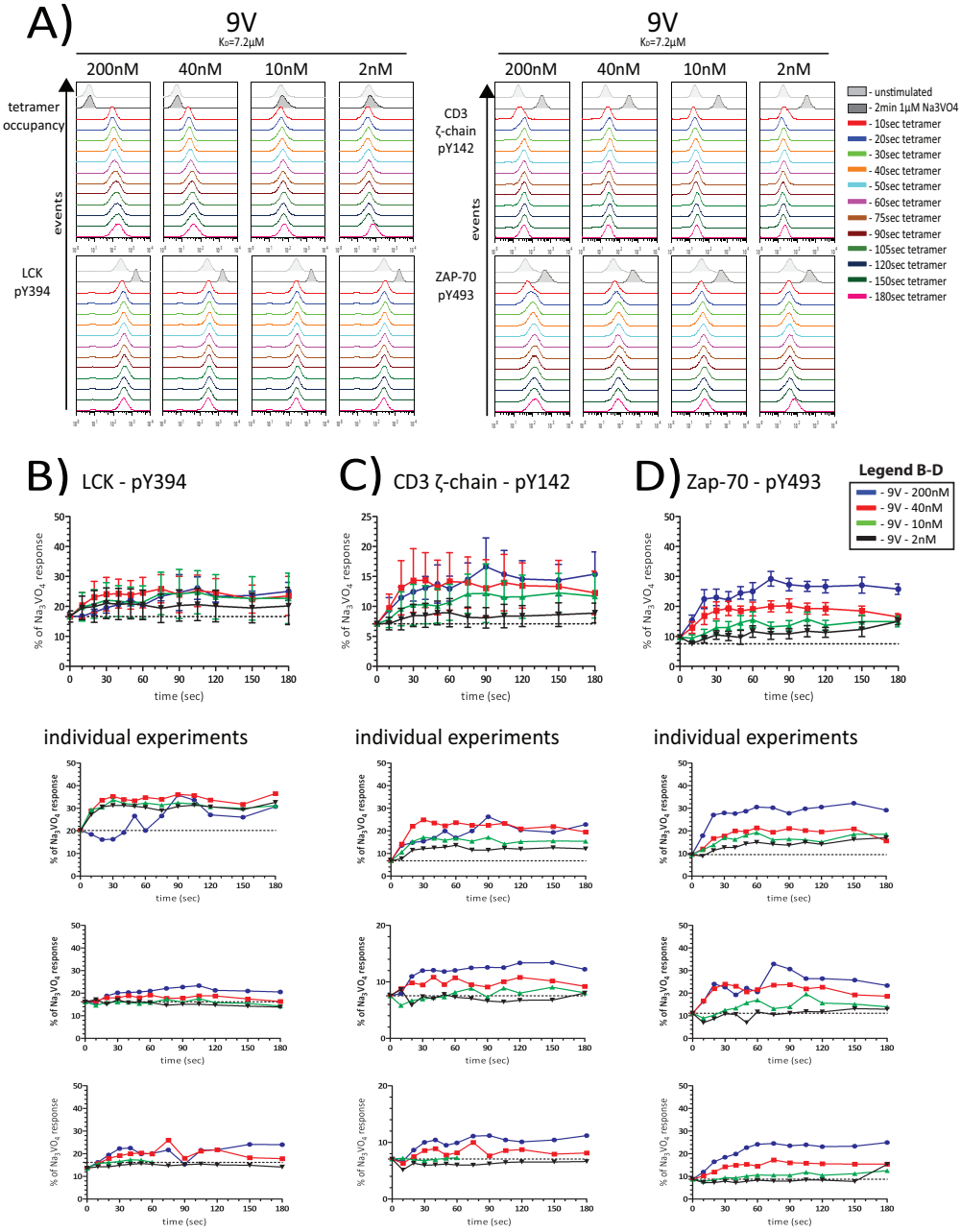
A)
9V
KD=7.2μM
200nM
40nM
10nM
2nM
tetramer occupancy
events
LCK pY394
CD3 ζ-chain pY142
ZAP-70 pY493
- unstimulated
- 2min 1μM Na3VO4
- 10sec tetramer
- 20sec tetramer
- 30sec tetramer
- 40sec tetramer
- 50sec tetramer
- 60sec tetramer
- 75sec tetramer
- 90sec tetramer
- 105sec tetramer
- 120sec tetramer
- 150sec tetramer
- 180sec tetramer
B) LCK - pY394
C) CD3 ζ-chain - pY142
D) Zap-70 - pY493
Legend B-D
- 9V - 200nM
- 9V - 40nM
- 9V - 10nM
- 9V - 2nM
% of Na3VO4 response
time (sec)
individual experiments

result in lower phosphorylation of pY142-CD3ζ. A similar but more clearly defined pattern of activation in response to tetramer dose is observed for pY493-ZAP-70 (Figure 5.7 A and D). Higher binding affinity correlates to stronger the ZAP-70 phosphorylation which possibly means that the degree of ZAP-70 phosphorylation represents an important analogue threshold to further downstream digital pERK activation.

In both cases, phosphorylation of CD3ζ and ZAP-70 are mild and analogue in nature while the pT202.pY204-ERK response is distinct and digital (Figure 5.6).

The maximum of pY142-CD3ζ reached corresponds to the likelihood of further downstream pT202.pY204-ERK activation (Figure 5.8 B and E). The same phenomenon is more pronounced with regards to pY493-ZAP-70 activation (Figure 5.8 C-F). This shows that analogue signals are sensitive to quantitative differences in ligand binding that is binding affinity and to a lesser extent ligand dose. This sensitivity results in a decisive on/off activation of pT202.pY204-ERK which confers distinct ligand discrimination. There might be a threshold ligand concentration and affinity beyond which TCR signals are passed downstream.

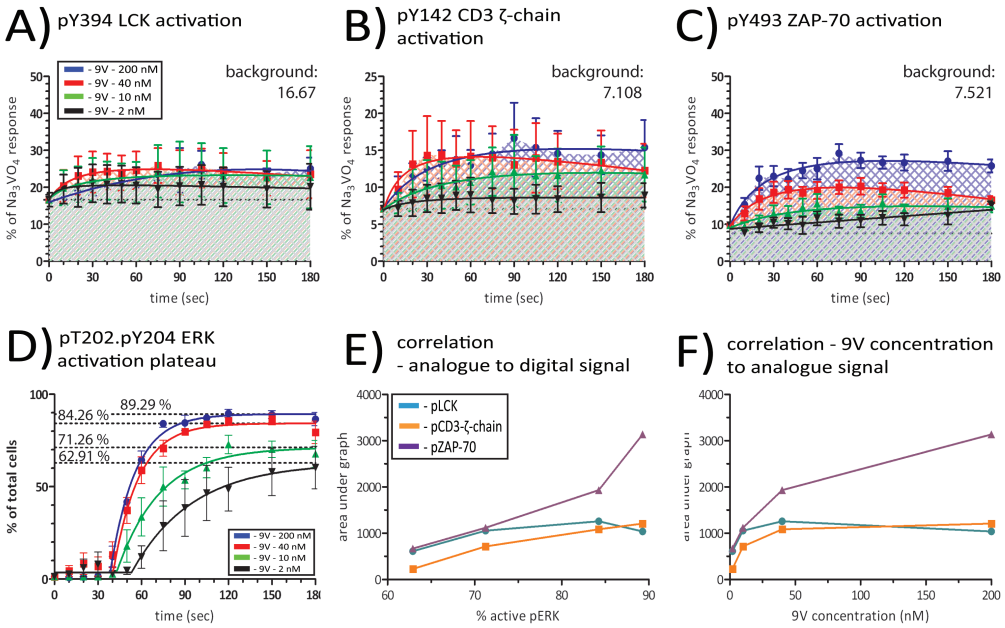

Figure 5.8: Occupancy and early proximal analogue signal strength determines later digital T cell activation. Analysis of the 9V dose response data over 3 min of Figure 5.6 and 5.7. (A-C) The activation of pY394-LCK (A), pY142-CD3ζ (B) and pY493-ZAP-70 (C) of Figure 5.7 were quantified by the area underneath the graphs. (D) The strength of the pT202.pY204-ERK response was expressed as the maximal percentage of cells actively signalling through pERK. (E) The effect of the analogue signal strength on the discrete pERK signal was analysed as the activation plateau of pERK determined in D against the quantification of the analogue signals determined in A-C. (F) The effect of the 9V NY-ESO-1 pMHC concentration on the analogue signal strength as determined in A-C.

5.4 Discussion

T cells are able to recognise and eradicate foreign infectious agents while maintaining tolerance to self. As few as 10 virus-derived antigenic peptides displayed on MHC molecules which are recognised by TCRs among an abundance of self-peptide-displaying MHC molecules are sufficient to induce T cell activation and elimination of the affected cell [Germain, 2001] [Altman and Davis, 2003] [Irvine et al., 2002].

Mature T cells recognise self-peptides with very low affinity that evoke 'tonic' TCR signals without which T cells would die by neglect [Tanchot et al., 1997]. Self-peptide-MHC bind to TCR with monomeric affinities lower than 100 μM. The exact signalling kinetics and binding affinity ranges are largely unknown. Yet, T cells must recognise and maintain homeostatic signals induced by self-peptide-MHC interactions in the periphery for survival [Stone et al., 2009]. Only rare T cells will usually encounter agonist pMHC and mount an immune responses. At any one time, only between 0.0003 to 0.001% of peripheral T cells will display a particular TCR [Obar et al., 2008] [Amsen et al., 2013]. The optimal monomeric binding affinity for pMHC and TCRs to induce T cell activation in solution is about 1 μM in the 1G4:NY-ESO-1 system [Schmid et al., 2010] [Irving et al., 2012]. But affinities up 10 μM have been shown to induce strong T cell responses and T cell activation is observable after stimulation with ligands of affinities up to 100 μM [Stone et al., 2009]. At which point in the signalling cascade a T cell "decides" to induce activation in response to TCR engagement is unknown. To address this question, I performed detailed timecourse flow cytometry studies with pMHC tetramers

of four different affinities and investigate the pLCK, pZETA, pZAP-70 and pERK responses elicited. The tetramer affinities ranged from 7.2 to 252 μM. The strongest affinity peptide elicits T cell signalling responses independent from CD8-coreceptor expression. The intermediate affinity peptide is close in affinity to the wild-type peptide which elicits weak immune responses *in vivo*. It lies within the agonist-partial agonist affinity range. The low strength 9L peptide's affinity lies at the threshold of agonist-non-agonist range while the 4D peptide's affinity is comparable to that of self-peptides. This peptide elicits no evident T cell response.

pT202.pY204-ERK signalling proved to be particularly suited to the investigation. The flow cytometry signal from pERK staining is strong and the signal was shown to be of digital nature. Thus, flow cytometry histograms of pERK signal activation showed two distinct peaks corresponding to the unresponsive and activated cell populations.

pERK signals were induced 60 sec after tetramer stimulation and reach maximum within 90 sec. The signal gradually reduces after 5 to 10 min until it reaches background levels within 2 hours post-stimulation. Tetramer affinity has a profound affect on the intensity of the pERK signal. High affinity peptides stably induce pERK activity of close to 100% of cells while low affinity peptides only induce a small fraction of cells to signal through pERK. The dose of the NY-ESO-1 pMHC tetramer stimulation compensated only mildly for reduced binding affinity. Increasing the concentrations of 9L 200-fold resulted in a rise of pERK signalling cells from 15 to 40%. Yet, even at the lowest concentration tested (1 nM) 9V induced pERK activity in 80% of cells. Investigating this observation from a different angle, I find that at

the same level of occupancy, 9V induces pERK activation in 90% of stimulated cells, while only 78% and 40% of cells were activated through 6V and 9L stimulations, respectively. Strong 9V-mediated TCR:pMHC interactions induced stronger pERK responses even at concentrations, which were below the occupancy detection level than 9L at highest concentrations. It has been suggested that not only the binding parameters per se but also the dose of the ligand presented influence TCR signal strength. This means that low binding affinity can be compensated for with high ligand density [Gottschalk et al., 2012]. The diverse T cell effector responses to TCR triggering have been shown to be diverse in their responsiveness to signal dose. Cytokine release for example follows an analogue response pattern which is sensitive to ligand dose. Digital effector functions such as the pERK signal, directed cytotoxicity and cell proliferations are on the other hand more sensitive to ligand specificity and ligand density is unable to compensate for low affinity [Gottschalk et al., 2012]. These findings correlate well to the 1G4:NY-ESO-1 system. While the magnitude of the IFN-γ responses were dependent on pMHC concentration [Aleksic et al., 2010], I show that the proximal signalling events, and especially pERK activation, is highly discriminatory towards specific ligands based on their TCR binding parameters.

Signal strength of further upstream signalling molecules pY142-CD3ζ and pY493-ZAP-70 is also governed by tetramer affinity to the 1G4 TCR. These signals develop very rapidly and unlike pT202.pY204-ERK have not been investigated previously in greater detail by flow cytometry. The amplitude of the phosphorylation of CD3ζ and ZAP-70 signals are not as pronounced as the pERK signal. I found that pCD3ζ and pZAP-70 signals analogue in

nature. Clearly, between the induction of the signal at the TCR and its progression down the cascade to ERK, the analogue TCR:pMHC binding signal is translated into a distinct all-or-nothing digital response. The precise position within the signalling pathway where the switch is made from an analogue to a digital signal remains unknown. Speculation would favour a location surrounding the LAT-complex where the signal diversifies. The Ras-ERK pathway is activated through the activity of the GEFs RasGRP1 and SOS1 (Figure 1.11) [Kortum et al., 2013]. Negative feedback loop acting on this pathway have been suggested to translate analogue proximal signals into a digital ERK response. RasGRP1 has been reported to be the dominant determinant for ERK activation while SOS1 activity was most important during thymocyte selection [Kortum et al., 2011] [Warnecke et al., 2012]. This activation of Ras and ultimately ERK through RasGRP1 is analogue [Das et al., 2009]. However, the digital response of ERK could be shaped by positive feedback mechanisms of Ras and ERK onto SOS. Three to four serine phosphorylation sites on SOS have been implicated in the regulation of SOS by ERK [Kamioka et al., 2010]. The feedback loops create a sharp discriminatory signalling thresholds which could induce either positive or negative selection of thymocytes [Alberola-Ila et al., 1996] [Das et al., 2009] [Kortum et al., 2011] [Kortum et al., 2012]. Furthermore, it has been suggested that an analogue negative feedback loop of SHP-1 which de-activates LCK at tyrosine 394 and a digital positive feedback loop through ERK which prevents LCK-deactivation are suspected to govern a sharp ligand discrimination threshold [Stefanová et al., 2003] [Altan-Bonnet and Germain, 2005]. However, very recent studies have disputed this hypothesis [Johnson et al., 2013]. This CD4

T cell-specific SHP-1 knock-down showed no effect on thymocyte selection or TCR sensitivity in the periphery [Johnson et al., 2013]. The feedback mechanism influencing TCR signal strengths and possibly ligand discrimination are very complex and still intensely investigated and debated.

In this chapter I studied the activation of proximal TCR signalling molecules LCK, CD3ζ, ZAP-70 and ERK in a detailed semi-quantitative manner using intracellular flow cytometry. The method allowed me to correlate simultaneous signalling events. I showed that very early proximal signalling events, for example the phosphorylation of CD3ζ and ZAP-70 progressed in an analogue fashion, further downstream ERK signalling events showed a distinct digital mode of activation. The likelihood of ERK activation and thus supposedly further downstream T cell effector functions was governed by the degree of the previous analogue signal. This indicates that there must be a threshold affinity above which T cell responses are activated. While its identity is yet unknown it is likely that molecules associated to the LAT complex and positive and negative feedback loops influence the switch-like activation if ERK.

Chapter 6

Themis - an attenuator of TCR signal strength

6.1 Introduction

6.1.1 Signalling thresholds in thymocyte development

The T cell's ability to eradicate invading pathogens while retaining tolerance towards self is primarily determined by selection processes of the expressed TCR repertoire taking place during thymocyte development [Morris and Allen, 2012].

Thymocytes develop from committed lymphoid progenitor cells which derive in the bone marrow and travel to the thymus via the blood [Germain, 2002]. In the outer cortex of the thymus, the precursors develop into double-negative T cell precursors which express neither CD4 nor CD8. Throughout differentiation, the thymocytes travel gradually from the outer cortex of the thymus

to the inner cortex and the medulla [Germain, 2002] [Carpenter and Bosselut, 2010]. There are four sequential stages of DN thymocyte development during which the potential for multipotency beside the T cell lineage is gradually lost. These stages are defined by the levels of CD25 and CD44 surface expression [Carpenter and Bosselut, 2010]. During the DN1 and DN2 developmental stages thymocytes proliferate extensively. In the DN3 stage, proliferation halts and somatic recombination and selection of the TCRβ-chain ensues. The rearranged βTCR-chain associates with the pre-αTCR and the CD3-chains to form the pre-TCR on the cell surface [Germain, 2002] [Murphy et al., 2008]. Signals through the pre-TCR finalise TCRβ-rearrangement and trigger proliferation of thymocytes through the DN4 stage and differentiation into CD4-CD8 double-positive (DP) thymocytes [Carpenter and Bosselut, 2010]. Cells that do not successfully rearrange the βTCR and fail to signal through the pre-TCR die by neglect [Germain, 2002]. During the DP stage thymocytes begin α locus rearrangement. After successful rearrangement DP thymocytes express low levels of the αβTCR [Carpenter and Bosselut, 2010]. The thymocytes interact with the cortical epithelial cells of the thymus which express self-pMHC I and II at high density. Lack of resulting signals through the TCR:pMHC interactions result in death by neglect [Germain, 2002]. Strong binding interactions result in strong transient pERK activation and death of the thymocytes. This process is known as negative selection [Werlen et al., 2000] [Labrecque et al., 2011]. It prevents autoimmunity and is a direct result of the avidity of TCR:pMHC interactions [Hwang et al., 2012]. Thymocytes which react mildly to the TCR:pMHC interactions through low level but sustained pERK signals are positively selected

[Labrecque et al., 2011] [Werlen et al., 2000]. These thymocytes develop into either CD4- or CD8-single-positive (SP) T cells [Morris and Allen, 2012]. Similarly to negative and positive selection the CD4 and CD8 lineage decision is based on the affinity of the TCR:pMHC interactions. Stronger signals result in CD4-positive T cells; weaker signals in CD8-positive ones. This last step of T cell differentiation occurs in the thymic medulla [Germain, 2002]. Subsequently, SP T cells emigrate into the periphery where within three weeks they mature from recent thymic emigrants into naive peripheral T cells [Houston et al., 2012].

6.1.2 Themis - a crucial checkpoint protein in positive thymocyte selection

The signalling thresholds associated with the development and selection of thymocytes are finely tuned. Already a two-fold difference in affinity has been shown to influence whether a TCR is positively or negatively selected for [Daniels et al., 2006] [Gascoigne and Palmer, 2011]. Furthermore, the strength of the TCR signal received determines whether DP thymoctes develop into CD4- or CD8-positive cells [Germain, 2002].

In 2009 three separate groups independently and via different methodological approaches discovered the thymocyte-expressed molecule involved in selection (Themis) [Fu et al., 2009] [Johnson et al., 2009] [Lesourne et al., 2009] [Brockmeyer et al., 2011]. Themis is a 73 kDa, 641 amino acid protein of unknown molecular function [Fu et al., 2009] [Allen, 2009]. Its expression is highly conserved in vertebrates and restricted to the T cell lineage. Themis

is most highly expressed in DP thymocytes. It is also expressed in high levels in mature thymocytes and peripheral T cells [Fu et al., 2009].

Themis contains no known catalytic or protein:protein interaction domains [Fu et al., 2009]. Based on multiple sequence alignment Themis is predicted to contain two conserved N-terminal globular β-stranded cysteine-containing, all-β in Themis (CABIT) domains of unknown function and an N-terminal proline-rich region with the atypical SH3-binding motif of the sequence PxR-PxK [Paster et al., 2013] [Johnson et al., 2009]. The second CABIT domain contains a nuclear-localisation signal (NLS) and Themis is expressed both in the cytoplasm and the nucleus. The distribution between nuclear and cytoplasmic Themis does not change following TCR triggering [Allen, 2009]. Two PRR-proximal tyrosines at positions 540 and 541 are phosphorylated by LCK and ZAP-70 within 30 sec of TCR engagement. The effect of phosphorylation on the function of Themis is yet unknown. Themis associates to the C-terminal SH3-domain of Grb2 via its PRR which is essential for the function of Themis. The deletion of the PRR region results in the abrogation of Grb2 binding and a severe reduction in CD4-positive thymocytes and peripheral T cells [Paster et al., 2013]. Grb2 is a SH3-SH2-SH3 adaptor molecule. Through its direct association to Grb2, Themis also indirectly associates to LAT, Itk, SLP-76 and PLCγ [Paster et al., 2013] [Johnson et al., 2009] [Brockmeyer et al., 2011].

Themis is necessary for thymocytes to progress through the positive selection checkpoint [Fu et al., 2009]. Themis$^{-/-}$ mice display a block in early positive selection which results in fewer total peripheral T cells but increased numbers of regulatory T cells [Fu et al., 2009]. An effect on negative selection is con-

troversial [Gascoigne and Palmer, 2011]. No major signalling defect has been shown in Themis$^{-/-}$ murine thymocytes. Instead, small changes in pERK and Ca^{2+} signalling in response to low avidity but not high avidity signals were observed [Brockmeyer et al., 2011] [Fu et al., 2009]. These observations were controversial as well. While Brockmeyer et al, 2011, observed a decrease in pERK activity in Themis$^{-/-}$ cells, Fu et al., 2013, show Themis to be an attenuator of low strength signals.

6.2 Aims

Themis has been shown to have a profound effect on thymocyte development and was thought to influence pERK signalling through an unknown mechanism [Brockmeyer et al., 2011] [Fu et al., 2009]. In this chapter, I address the effect of Themis expression on 1G4 cell signalling. I knocked-down Themis in 1G4 cells. The use of 1G4 cells enables the use of NY-ESO-$1_{156-165}$ pMHC tetramers for TCR triggering instead of high affinity CD3ε antibodies. I studied the effect of ligand affinity and Themis expression on proximal signalling. Themis is downregulated about 5-fold after DP thymocyte development but it is not absent from peripheral T cells. The effect of Themis on peripheral T cell signalling has not been studied. 1G4 cells also serve as a model towards peripheral T cells rather than thymocytes. I investigated the effect of Themis on CD3ζ, ZAP-70 and ERK activity.

6.3 Results

6.3.1 Phosphorylation of CD3ζ and ERK are elevated in Themis-knock-down cells

Themis expression was knocked-down using transduction of lentiviral particles. Two shRNA vectors were used to knock-down Themis. These target different sequences within the Themis mRNA and result in different efficacies of the knock-down. Themis was stably knocked-down in 1G4 cells to 90% and 70% (Figure 6.1). The stable Themis-k/d cell lines were cultured under puromycin selection in RPMI and stocks were frozen at −80 °C.

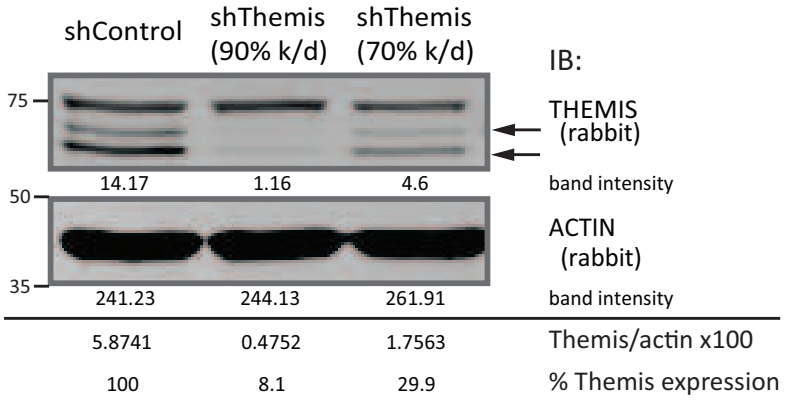

Figure 6.1: Lentiviral knock-down of Themis in 1G4 cells. The efficiency of the lentiviral Themis knock-down in 1G4 cells was assessed using immunoblotting. 5 x 10^5 cells were lysed and assessed for Themis expression. Themis was knocked-down by 90% and 70% compred to the control short-hairpin.

Themis-k/d and control 1G4 cells were stimulated with 10 ng/ml UCHT1 CD3ε-antibody for 60 and up to 300 sec at 37 °C (Figure 6.2). The cells were tested for pT202.Y204-ERK activation using flow cytometry. At 60 and

300 sec of stimulation, pERK levels are elevated in Themis-k/d 1G4 cells. At 60 sec the pERK signal first emerges and develops (Figure 6.2). Themis appears to delay the initiation of the pERK signal. Between 90 and 180 sec the maximum of the pERK signal is reached. It is possible that UCHT1 stimulates the cells to such an extent that maximal possible pERK activation is achieved in both Themis-positive and -negative cells. Thus, no difference between the cell lines is seen at these timepoints. At 300 sec the pERK signal begins to decline (Figure 6.2). The lack of Themis appears to strengthen the pERK signal and delay its attenuation (Figure 6.2 B). ERK signalling governs important downstream cellular responses such as proliferation and cell survival. Thus, even though its functions subtly change ERK signalling, the effects of Themis on T cell activation and behaviour might be profound. Themis was suggested to enhance pERK signalling in response to low avidity stimulation [Brockmeyer et al., 2011]. To investigate the effect of stimulation with different affinity NY-ESO-$1_{156-165}$ pMHC tetramers, Themis-k/d of 90% and 70% and control 1G4 cells were stimulated with 200 nM NY-ESO-$1_{156-165}$ pMHC tetramers for 60, 90 and 180 sec in solution at 37 °C (Figure 6.3). Cells were tested for occupancy and pY202.pT204-ERK activation using simultaneous staining on flow cytometry (Figure 6.3 A and B). No difference can be seen between the Themis-k/d and control cell lines after high affinity 9V pMHC tetramer stimulation. Intermediate 6V pMHC tetramer stimulation caused a significant higher pT202.pY204-ERK response in Themis-k/d 1G4 cells than in controls throughout the time-course. A similar effect was seen after low affinity 9L stimulation but only after 180 sec. 4D stimulation caused no pERK activation in any cell line (Figure 6 C).

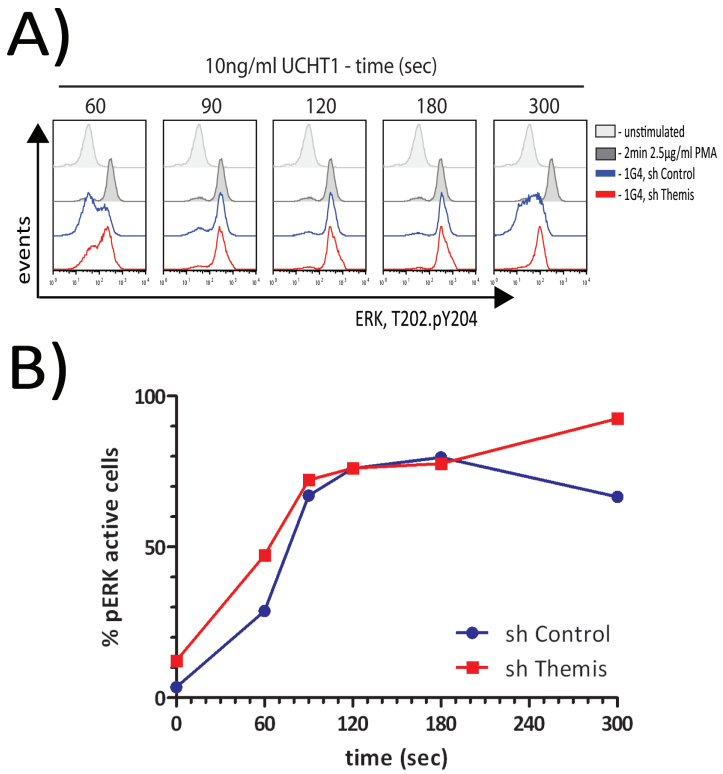

Figure 6.2: Themis-k/d 1G4 cells stimulated with UCHT1. Themis-k/d (shThemis) and control 1G4 cells were stimulated with 10 ng/ml anti-CD3ε monoclonal antibody UCHT1 for up to 300 sec. Cells were investigated for pT202.pY204-ERK activation using flow cytometry. (A) Example flow cytometry histograms of the timecourse. (B) Analysis of the flow cytometry histogram data using Graph Pad Prism. The experiment was repeated twice.

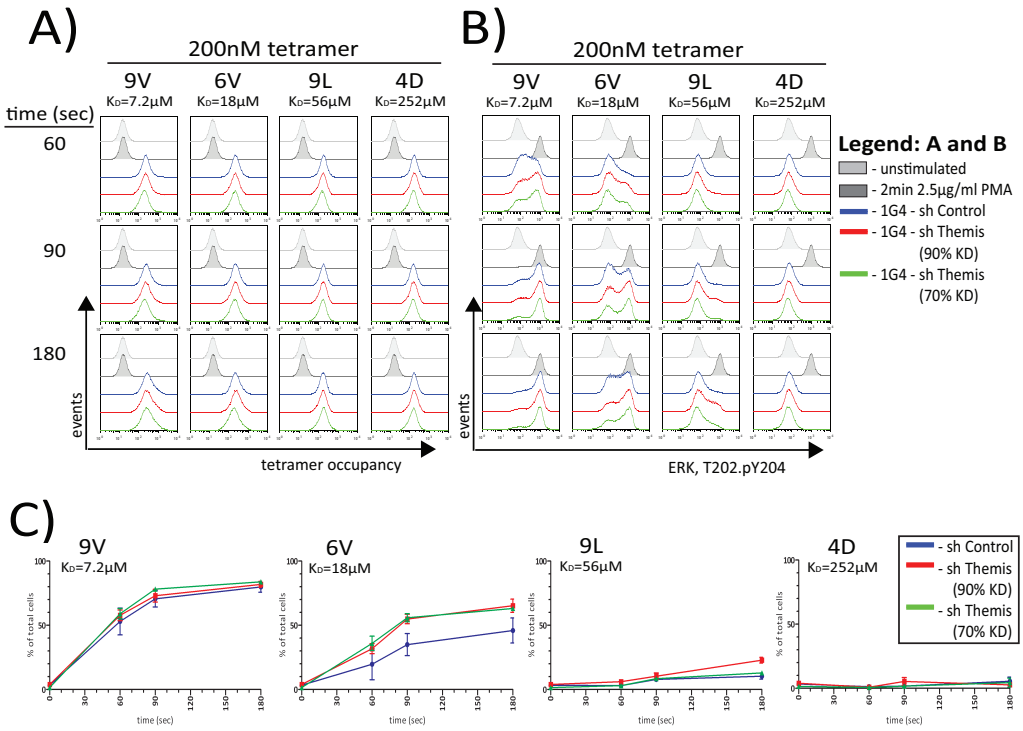

Figure 6.3: The effect of Themis expression on pERK signalling in response to different affinities. Themis-k/d of 90% and 70% and control 1G4 cells were stimulated with 200 nM NY-ESO-1 pMHC tetramers for 60, 90 and 180 sec in solution as before. Shown data is exemplary for three individual experiments. The cells were tested for occupancy (A) and pY202.pT204-ERK activation (B) using simultaneous staining on flow cytometry. (C) The data acquired was expressed as percentage of total cells which actively signal pERK as determined from the flow cytometry histograms of A and B. Data was analysed from three individual experiments using GraphPad Prism. Graphs show the SEM.

Themis is recruited to the LAT signalosome via Grb2 upstream from ERK in the TCR proximal signalling cascade [Paster et al., 2013]. Since its function is yet unknown, I investigated whether Themis also influences the function of further upstream, more TCR-proximal signalling molecules via potential feedback mechanisms.

Themis-k/d (90%) and control 1G4 cells were tested for pY142-CD3ζ activation between 10 and 60 sec under the same conditions as used in Figure 6.3 (Figure 6.4). The cells were tested for occupancy and pY142-CD3ζ activation using simultaneous staining on flow cytometry (Figure 6.4 A and B). No difference can be seen between the Themis-k/d and control cell lines after low and very low affinity 9L and 4D pMHC tetramer stimulation. High and intermediate 9V and 6V pMHC tetramer stimulation caused a significant higher pY142-CD3ζ response in Themis-k/d 1G4 cells than in controls throughout the timecourse (Figure 6.4 C).

The extent of analogue pY142-CD3ζ activation dictates the likelihood of digital pT202.pY204-ERK activation (Figure 5.4).

The Themis-k/d 1G4 cells show slight increases in pERK and CD3ζ phosphorylation levels. I investigated how Themis expression affects the correlation between the analogue pY142-CD3ζ signal and further downstream digital pT202.pY204-ERK response (Figure 6.5). I quantified the analogue pY142-CD3ζ signal by calculating the area underneath the graphs obtained from three experiments in Figure 6.4 C. To quantify the digital pT202.pY204-ERK signal, I determined the maximal percentage of cells which are activated by pMHC tetramer stimulation (Figure 6.5 B). The data obtained from Figures 6.5 A and B were combined in C to investigate how analogue signal strength

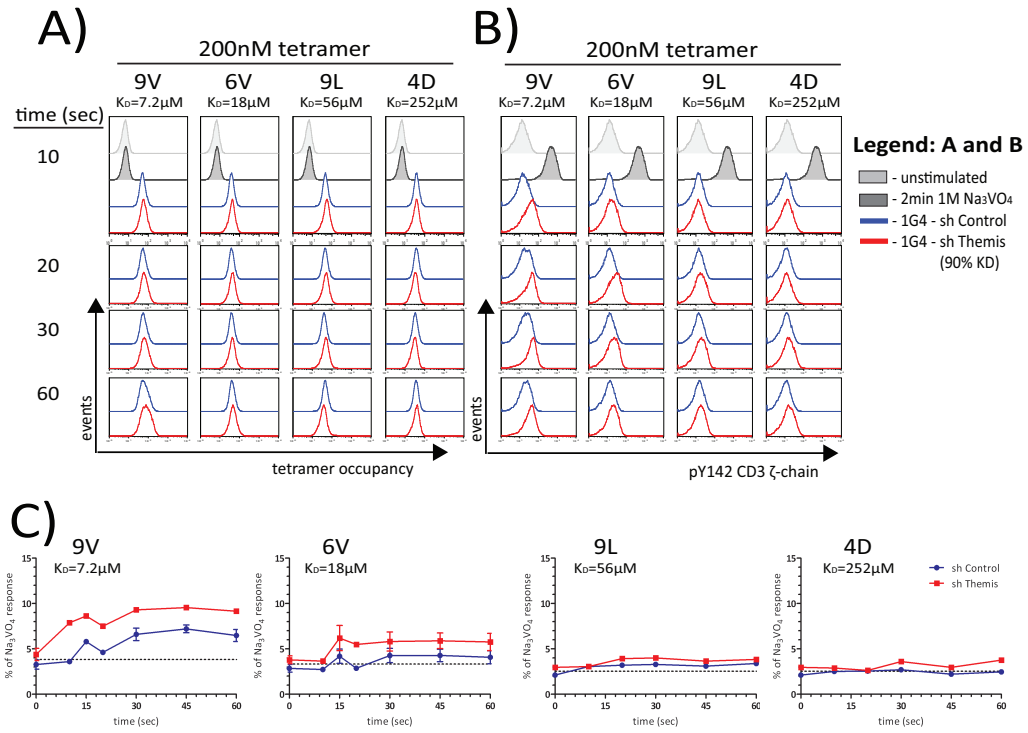

Figure 6.4: Effect on Themis on pY142-CD3ζ phosphorylation. Themis-k/d of 90% and control 1G4 cells were stimulated with 200 nm NY-ESO-1 pMHC tetramers between 10 and 60 sec in solution as before. Shown data is exemplary for three individual experiments. The cells were tested for occupancy (A) and pY142-CD3ζ phosphorylation (B) using simultaneous staining on flow cytometry. (C) The results of three individual experiments were analysed using GraphPad Prism. The data acquired was expressed as percentage of the positive control sodium pervanadate response. Error bars shown express the SEM.

influences the likelihood of further downstream digital pERK signals. Figure 6.5 C and D show that the higher pY142-CD3ζ signal observed in Themis-k/d cells correlates to increased downstream digital pT202.pY204-ERK signals and that the affinity of the pMHC tetramers determines the degree of the analogue pY142-CD3ζ signal. Themis-k/d 1G4 cells had a higher analogue response to the same affinity stimulation as the control 1G4 cells (Figure 6.5 D). The knock-down of Themis increased signalling overall. This indicates that Themis acts on the entire proximal signalling cascade and even governs upstream signalling events. If Themis only affects downstream signalling events, one would expect the analogue signals to remain unchanged but observe a boost in the digital ERK signal. This shows that Themis is an attenuator of global proximal signalling.

In earlier studies, Themis was shown to alter the signal strength of low avidity signals. In Figures 6.3 to 6.5, I showed that Themis-k/d cells responded mostly to high and intermediate affinity NY-ESO-$1_{156-165}$ pMHC tetramers. To investigate whether the effect of Themis-k/d is potentiated through dose, I stimulated Themis-k/d (90% and 70%) and control 1G4 cells with decreasing concentrations of 9V and 6V NY-ESO-$1_{156-165}$ pMHC tetramers before and monitored the pT202.pY204-ERK (Figure 6.6) and pY142-CD3ζ (Figure 6.7) by flow cytometry.

pT202.pY204-ERK responses were analysed after 60 sec. At this time point pERK signals first appears and develops and allows an insight into the speed of the signal induction process (Figure 5.2). Already, the emergence of the typical digital two-peak response of pERK can be seen in the flow cytometry histograms (Figure 6.6 A). Tetramer occupancy decreases dra-

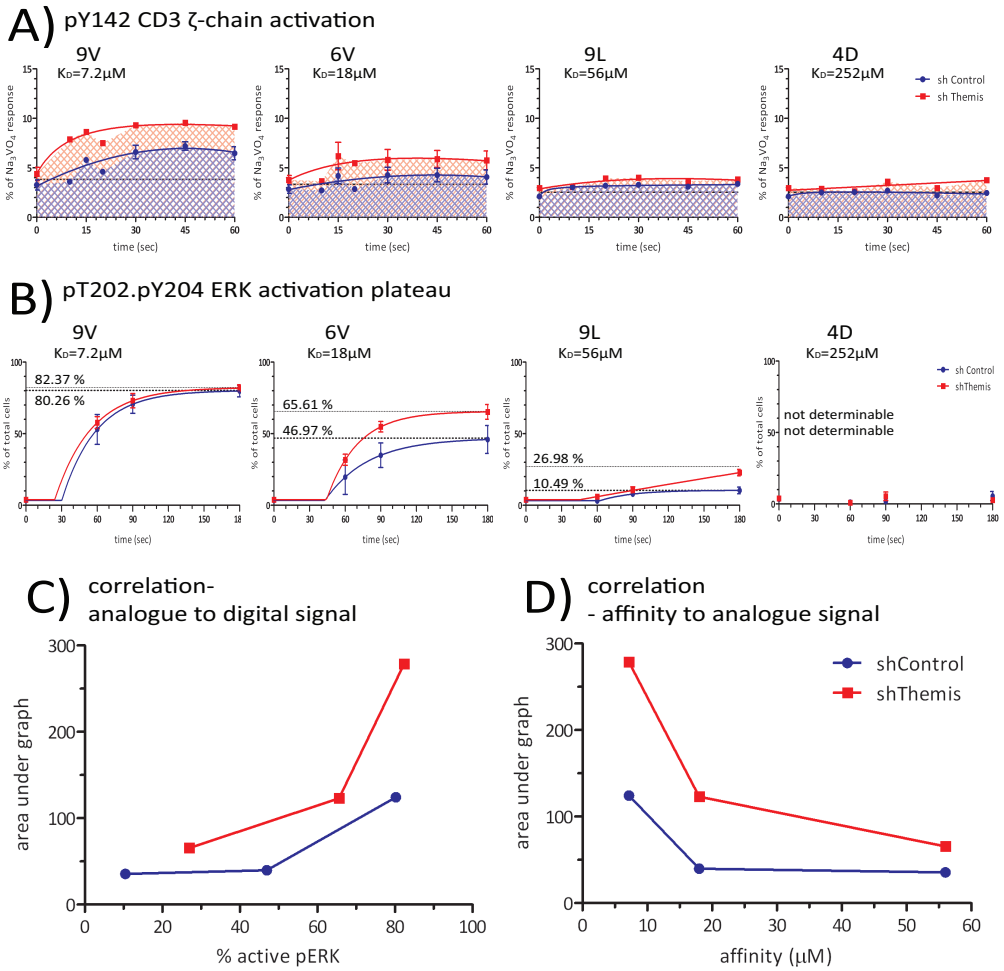

Figure 6.5: Themis expression levels alter the likelihood that analogue signals result in digital pERK activation. Analysis of the NY-ESO-1 pMHC tetramer timecourse data of Figure 6.3 and 6.4. Data of Themis-k/d (90%) and control 1G4 cells were analysed. (A) The graphs of pY142-CD3ζ phosphorylation of Figure 6.4 were quantified by the area underneath the graphs. (B) The strength of the pT202.pY204-ERK response determined in Figure 6.3 was expressed as the plateau of the maximal percentage of cells actively signalling through pERK. (C) The effect of the analogue signal strength on the discrete pERK signal was analysed as the activation plateau of pERK determined in B against the quantification of the analogue signals determined in A. (D) The effect of the NY-ESO-1 pMHC tetramer affinity on the analogue signal strength as determined in A.

matically with decreasing NY-ESO-$1_{156-165}$ pMHC tetramer concentrations. Themis-k/d and control 1G4 cells bind NY-ESO-$1_{156-165}$ pMHC tetramers to the same extent (Figure 6.6 A and B). 90% Themis-k/d 1G4 cells display stronger pT202.pY204-ERK signals after 9V and 6V NY-ESO-$1_{156-165}$ pMHC tetramer stimulation than the lower level knock-downs or the control cells (Figure 6.6 C). The pERK signal is distinctly digital with the quiescent fraction visible on the flow cytometry histograms being labelled as (1) and the signalling cell fraction being labelled as (2). The strengths of signals reached do not significantly differ between cell lines (Figure 6.6 A and D).

pY142-CD3ζ responses were analysed after 45 sec. The pY142-CD3ζ signal develops within the first 10 sec after stimulation and is established within 20 sec post-stimulation. At 45 sec the maximal pY142-CD3ζ response is visible (Figure 5.4). As before, differences in the pY142-CD3ζ signals are analogous and slight in comparison to the sodium pervanadate positive control (Figure 6.7 A). Tetramer occupancy decreases dramatically with decreasing NY-ESO-$1_{156-165}$ pMHC tetramer concentrations. Themis-k/d and control 1G4 cells bind NY-ESO-$1_{156-165}$ pMHC tetramers to the same extent (Figure 6.7 A and B). 90% Themis-k/d 1G4 cells display stronger pY142-CD3ζ signals after 9V and 6V NY-ESO-$1_{156-165}$ pMHC tetramer stimulation than the lower level knock-downs or the control cells (Figure 6.7 C).

In accordance with previous results, the analogue pY142-CD3ζ signal determines the likelihood of a digital all-or-nothing pT202.pY204-ERK response (Figure 6.8). Themis, by an unknown mechanism, has an attenuating effect on both downstream pERK and upstream pCD3ζ responses. To have such effects on upstream targets immediately after TCR engagement, Themis

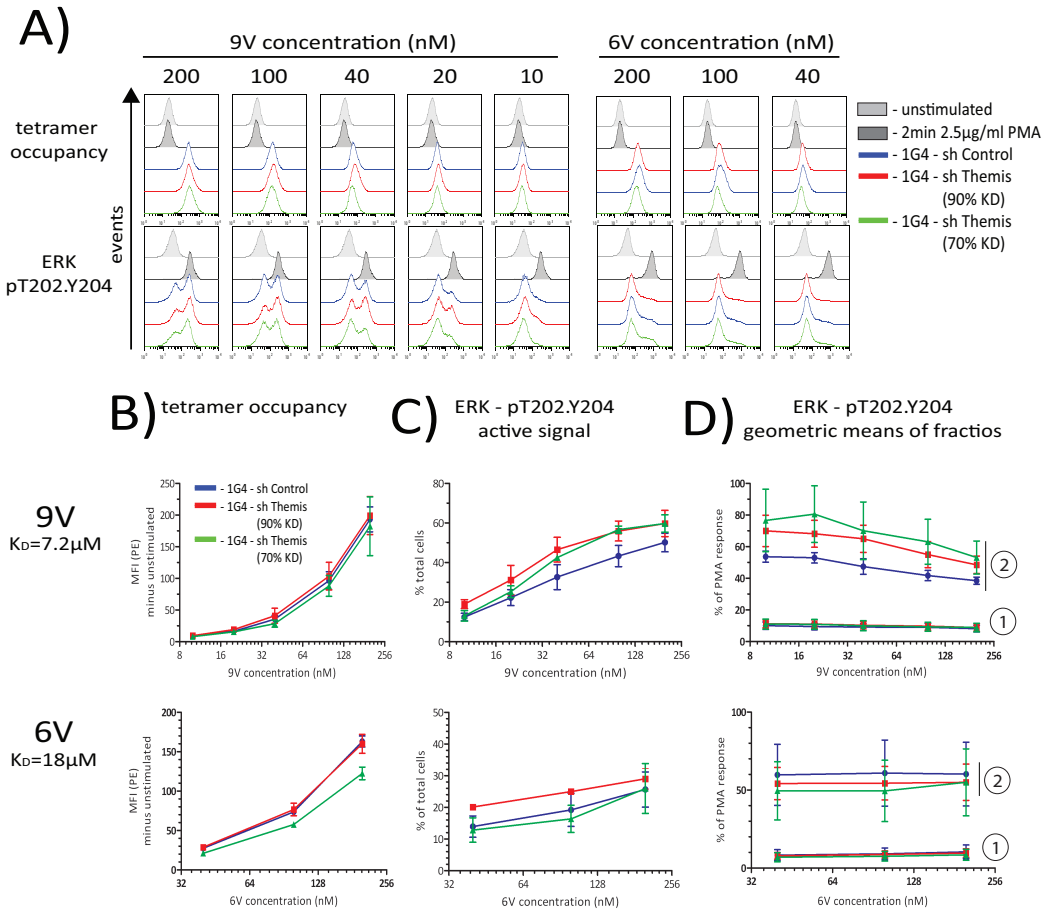

Figure 6.6: pMHC tetramer dose response and the effect of Themis expression on pERK signalling. Themis-k/d of 90% and 70% and control 1G4 cells were stimulated with between 10 and 200 nM 9V NY-ESO-1 pMHC tetramers and 40 to 200 nM 6V pMHC tetramers for 60 sec. The data shown is exemplary for three individual experiments. (A) The cells were tested for occupancy and pY202.pT204-ERK activation using simultaneous staining on flow cytometry. (B) Tetramer occupancy was analysed using data from the histograms of A. (C) The pERK histogram data acquired was expressed as percentage of total cells which actively signal pERK. (D) The geometric means of the two individual pERK peaks was expressed as percentage of the positive PMA control. (1) denotes the quiescent population and (2) the active pERK population. Data was analysed from three individual experiments using GraphPad Prism. Graphs show the SEM.

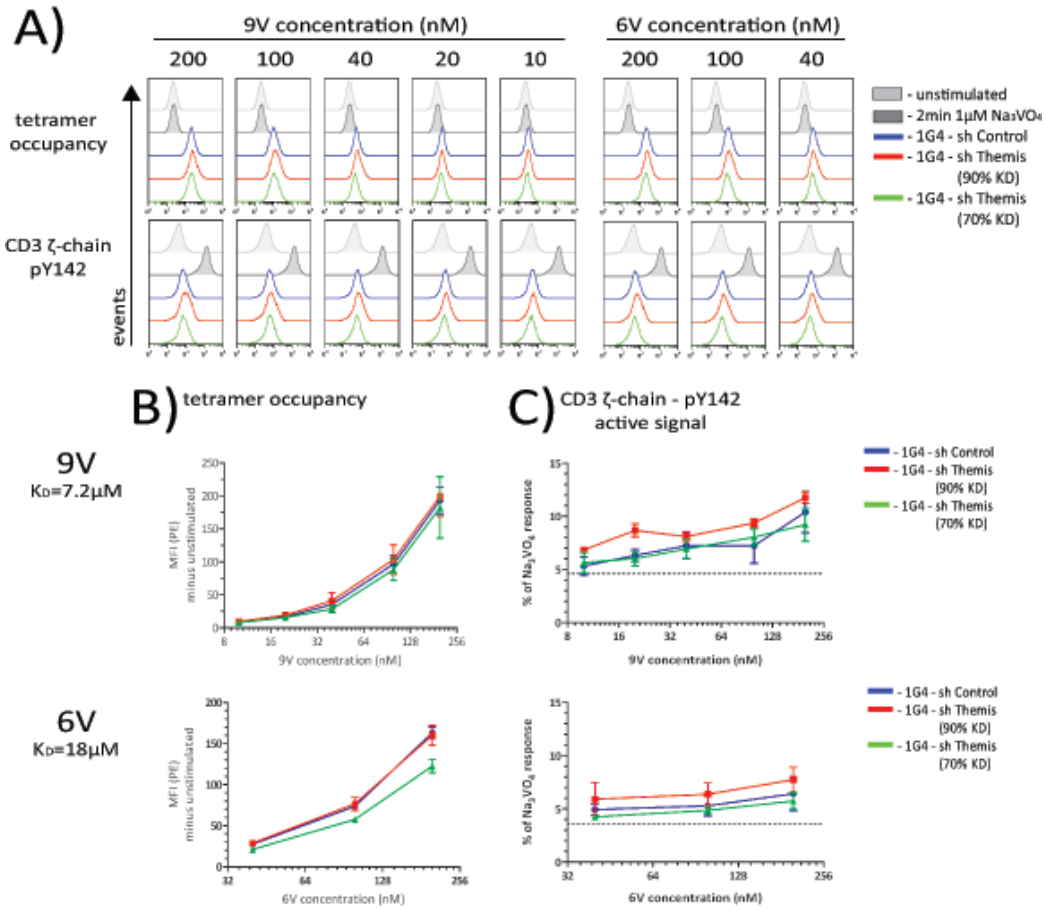

Figure 6.7: pMHC tetramer dose response and the effect of Themis on pY142-CD3zeta signalling. Themis-k/d of 90% and 70% and control 1G4 cells were stimulated with between 10 and 200 nM 9V NY-ESO-1 pMHC tetramers and 40 to 200 nM 6V pMHC tetramers for 45 sec. The data shown is exemplary for three individual experiments. (A) The cells were tested for occupancy and pY142-CD3ζ responses using simultaneous staining on flow cytometry. (B) Tetramer occupancy was analysed using data from the histograms of A. (C) The pCD3ζ histogram data acquired was expressed as activation in relation to the positive control sodium pervanadate. Data was analysed from three individual experiments using GraphPad Prism. Graphs show the SEM.

might work as a universal dampener of TCR signals in conventional T cells. Hypotheses for its function include that it could have phosphatase functions or recruit and activate a phosphatase which attenuates TCR proximal signals. Through facilitating negative feedback to the TCR, it could elevate the threshold affinity necessary to cause TCR triggering.

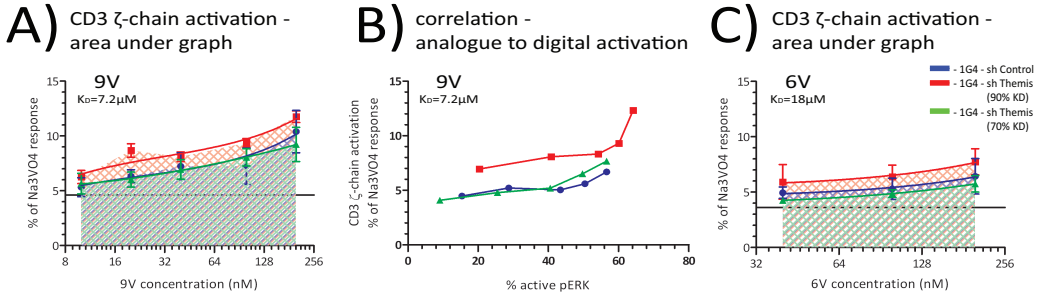

Figure 6.8: Analysis of Themis effect on link between analogue and digital signals. Analysis of the NY-ESO-1 pMHC tetramer timecourse data of Figure 6.6 and 6.7. Data of Themis-k/d (90%) and control 1G4 cells were analysed. (A) The graph of pY142-CD3ζ responses by 9V stimulation of Figure 6.4 was quantified by the area underneath the graphs. (B) The effect of 9V stimulation on of the analogue signal strength on the discrete pERK signal determined in Figure 6.6 was analysed. (C) The graph of pY142-CD3ζ activation by 6V stimulation of Figure 6.4 was quantified by the area underneath the graphs.

6.3.2 The effect of Themis on CD69 expression and apoptosis levels

In previous experiments Themis was shown to reduce the activation levels of upstream signalling molecules, for example CD3ζ. In this section, I investigated the effect of Themis on further downstream T cell effector functions such as the upregulation of CD69 surface expression and activation-induced

cell death (AICD).

CD69 is a C-lectin type II transmembrane cell surface activation marker on T cells. It has no known ligand [Marzio et al., 1999]. Cross-linking of CD69 enhances T cell proliferation, Ca^{2+} signalling and cytotoxicity. Even though it is expressed in thymocytes, it is absent from the cell surface of resting T cells. CD69 surface expression is upregulated within 30 to 60 min post-stimulation [Marzio et al., 1999]. Expression peaks after about 24 hours and can still be detected after up to 7 days. The ligand of CD69 is unknown. Cross-linking of CD69 activates signalling through RasGRP1 and Jak3/STAT5 pathway and results in increased T cell proliferation, cytokine release and cytotoxicity [Marzio et al., 1999].

Themis-k/d (90%) and control 1G4 cells were stimulated with 20 nM NY-ESO-$1_{156-165}$ pMHC tetramers at 37 °C in solution for 5 hours. Initially, the cells were stimulated for 24 hours but because of a high incidence of cell death especially in Themis-k/d 1G4 cells, CD69 expression was assessed at the earlier timepoint of 5 hours post-stimulation. Cells were monitored for CD69 surface expression using flow cytometry (Figure 6.11 A). Stimulation with 1 μg/ml UCHT1 anti-CD3ε monoclonal antibody was used as a positive control. As observed before, the level of tetramer occupancy depended on the tetramer's affinity (Figure 6.11 B). This can be explained by the variation in the off-rate between the different NY-ESO-$1_{156-165}$ pMHC tetramers and the 1G4 TCR [Carreño et al., 2007]. Although the mechanism of TCR activation is different, stimulation with UCHT1 anti-CD3ε antibodies also activates sequential TCR proximal signalling events. Thus, perturbations to signalling upstream of CD69 could result in decreased upregulation of CD69

in response to both UCHT1 and pMHC tetramer stimulations. To account for this effect, I analysed the level of CD69 surface in terms of fold-change to the unstimulated control and in terms of percentage of the positive control response (Figure 6.11 C and D). Higher NY-ESO-$1_{156-165}$ pMHC tetramer binding affinity corresponded with increased CD69 expression. Themis expression did not significantly affect the upregulation of CD69 on the surface of the cells. Different signals are thought to induce CD69 upregulation including TCR proximal signals and IL-2. The initial results seemed to indicate that the regulation of TCR proximal signalling which is influenced by Themis was not governing the upregulation of CD69 expression in this system. Recent unpublished indications seem to suggest that CD69 is upregulated in primary cells lacking Themis. This line of investigation is still being pursued in on-going work in the host laboratory.

In thymocyte development, strong signals cause negative selection through apoptosis to prevent autoimmunity in the periphery. In the periphery TCR stimulation by agonist pMHC is necessary to cause T cell activation and clonal expansion through proliferation. Once an infection is cleared, immune homeostasis is restored by activation-induced cell death (AICD) or activated cell-autonomous death (ACAD) to remove surplus T cells which remain after clonal expansion [Krammer et al., 2007]. Cytokine deprivation and the lack of survival signals induce ACAD [Li-Weber and Krammer, 2003]. ACAD is independent of cell death receptors and is mediated by BIM and PUMA which cause cytochrome C release from mitochondria and activation of the caspase cascade. AICD is induced by TCR re-stimulation within 4 to 7 days *in vitro* and the lack of IL-2 signals [Li-Weber and Krammer, 2003]. It can

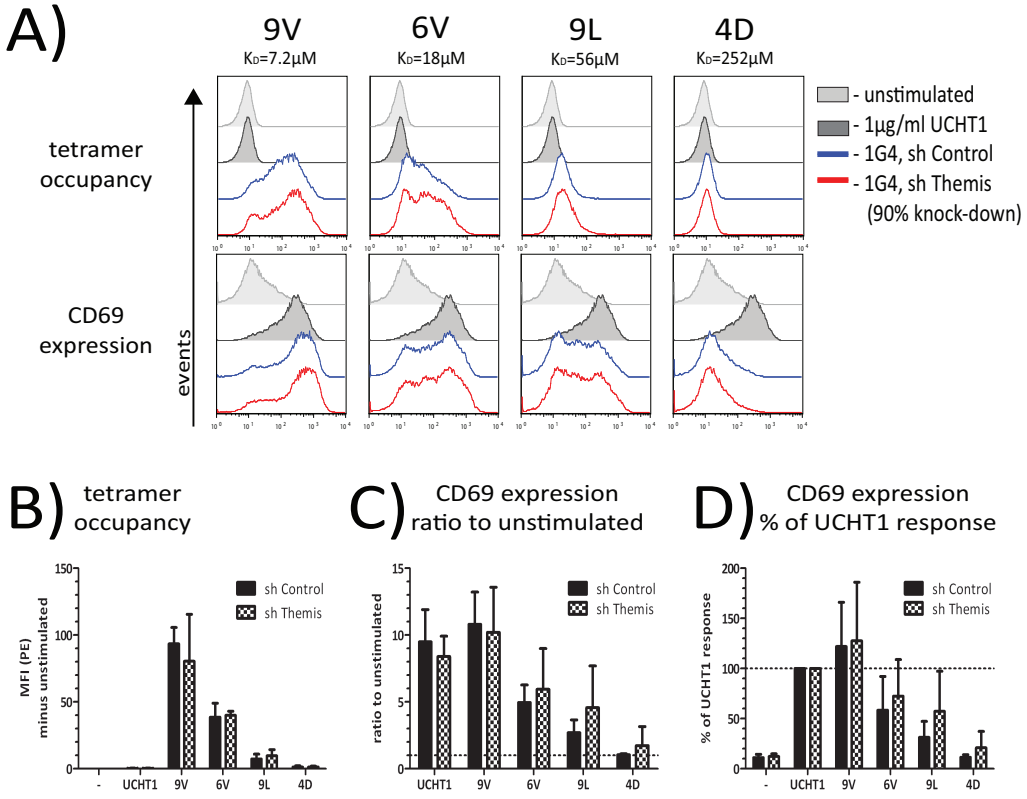

Figure 6.9: Effect of Themis on CD69 surface expression. Themis-k/d (90%) and control 1G4 cells were stimulated with 20 nM NY-ESO-1 pMHC tetramers in solution for 5 hours. (A) CD69 surface expression and tetramer occupancy were analysed simultaneously using flow cytometry. (B) Tetramer occupancy was analysed from the histogram geometric means of A. (C) CD69 surface expression analysis. Results are presented as a ratio to the unstimulated control (unstimulated control = 1). (D) CD69 surface expression analysis. Results are presented as a percentage of the positive control (UCHT1 control = 100%). All data was analysed from three individual experiments in GraphPad Prism. Error bars show the SEM.

also be induced through the engagement of surface proteins such as CD95L and TRAIL [Tartaglia et al., 1993] [Ashkenazi and Dixit, 1998] [Krammer, 2000]. AICD induces the formation of the death-inducing signalling complex (DISC) which includes pro-caspase 8 [Krammer, 2000]. In consequence, cytochrome c is released from the mitochondria through the actions of BAX [Muzio et al., 1998]. The release of cytochrome C results in the formation of the apoptosome and the activation of multiple caspases and ultimately the dismantling of vital cellular structures and cell death [Krammer et al., 2007]. Initial observations of the Themis-k/d and control 1G4 cells in culture indicated that the Themis-k/d cells were more susceptible to cell death. Moreover, experiments carried out in collaboration with Dr Wolfgang Paster in the host laboratory clearly indicated that primary T cell which were knocked down for Themis by retroviral transduction were dying by apoptosis in a TCR stimulation-dependent fashion (data not shown and see discussion) (Bruger, Paster, in preparation). To investigate the impact of Themis on T cell survival, I stimulated Themis-k/d (90%) and control 1G4 cells for 24 hours with 20 nM of the four NY-ESO-$1_{156-165}$ pMHC tetramers within the panel. Camptothecin, a cytotoxic quinoline alkaloid inhibitor of topoisomerase I, was used as a positive control [Liu et al., 2000]. Fluorescent Labeled Inhibitor of Caspases (FLICA®) detection probes were used to assess apoptosis induction by flow cytometry [Rybakin and Gascoigne, 2012]. The data shown in Figure 6.12 clearly demonstrate that Themis-k/d 1G4 cells were more prone to apoptosis than control cells. This is in accordance with data obtained in primary T cells (data not shown). Higher affinity stimulants induced a higher degree of apoptosis. Especially strong and intermediate

stimulation through 9V and 6V induced significantly more poly-caspase activity in Themis-k/d 1G4 cells (Figure 6.12 B). This implies an increased the incidence of apoptosis in Themis-k/d cells.

Apoptosis in T lymphocytes can be induced via the activation of surface death receptors, including CD95L and TCR engagement in the absence of IL-2. In previous experiments, Themis was shown to attenuate pT202.pY204-ERK activation in response to TCR stimulation with NY-ESO-$1_{156-165}$ pMHC tetramers. To assess whether the increased pERK activity causes the increase in apoptosis in Themis-k/d 1G4 cells, I stimulated Themis-k/d and control 1G4 Jurkat cells with 2 nM 9V NY-ESO-$1_{156-165}$ pMHC tetramer for 24 hours after pre-treating the cells with decreasing concentrations of the MEK inhibitor UO126 (Figure 6.13). MEK, the MAP kinase kinase, is a kinase within the mitogen activated protein kinase (MAPK) pathway and phosphorylates ERK at threonine 202 and tyrosine 204. U0126 is a noncompetitive inhibitor of MEK which probably binds to a unique site on the protein. It competes with neither ERK nor ATP for binding to MEK [Duncia et al., 1998]. Apoptosis was assessed by the flow cytometry forward scatter-side scatter dot plot. The live cell population is gated in red. Again, Themis-k/d cells show a basal and TCR-induced small but consistent increase in apoptosis. However, the addition of UO126 had no effect on apoptosis (Figure 6.12 B). pT202.pY204-ERK has been shown to be affected by Themis as seen in earlier data in this chapter. pERK activation is implicated in driving T cell survival and proliferation and antagonise apoptosis [Chen et al., 2001]. Thus, changes in pERK signalling should not be expected to affect activation-induced cell death. Indeed, pERK activation does not in-

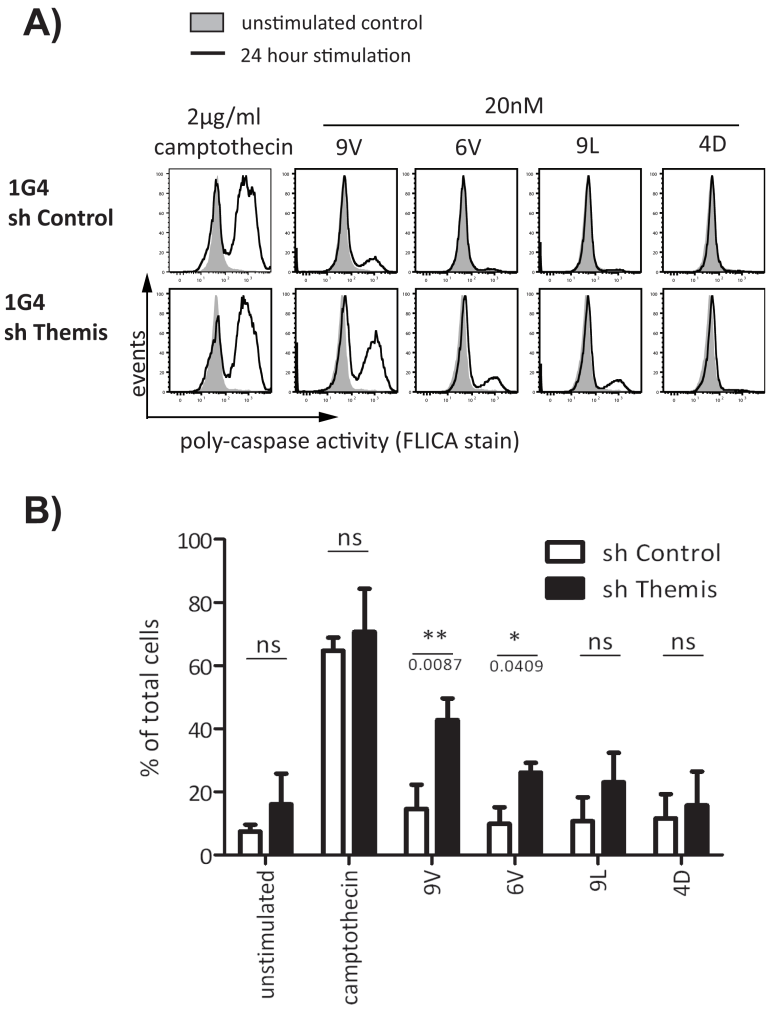

Figure 6.10: The effect of Themis on activation-induced cell death. Themis-k/d (90%) and control 1G4 cells for 24 hours with 20 nM of the four NY-ESO-1 pMHC tetramers within the panel. Camptothecin, a cytotoxic quinoline alkaloid inhibitor of topoisomerase I, was used as a positive control [Liu, 2000]. (A) Fluorescent Labeled Inhibitor of Caspases (FLICA) detection probes were used to assess apoptosis induction by flow cytometry [Rybakin, 2012]. The displayed flow cytometry histograms are example results of three individual experiments. (B) The degree of induced apoptosis was assessed using GraphPad Prism. Data of three experiments was used in the analysis. Error bars show the SEM. Statistical significance was calculated using the unpaired two-tailed student t-test. ns = $P > 0.05$, * = $P < 0.05$, ** = $P < 0.01$, *** = $P < 0.001$.

fluence Themis-dependent activation-induced cell death, it is possible that Themis affects parallel downstream signalling events which result in complex effects on T cell behaviour.

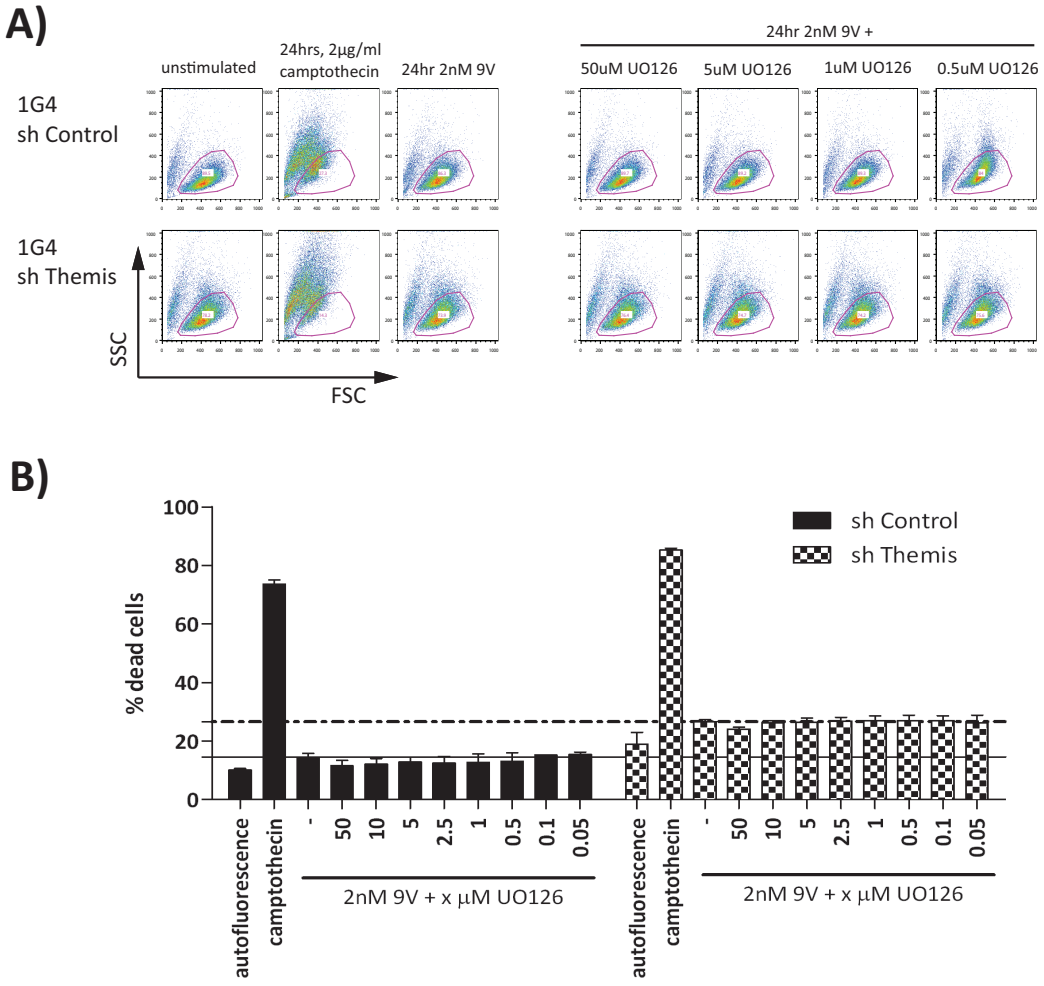

Figure 6.11: Effect of pERK signalling and Themis expression on signal-induced cell death. Themis-k/d (90%) and control 1G4 cells were stimulated with 2 nM 9V NY-ESO-1 pMHC tetramer for 24 hours. 2 µg/ml camptothecin was used as a positive control. To assess the effect of pERK on apoptosis, the cells were also incubated with decreasing concentrations of the MAPK inhibitor UO126. Cell death was assessed by flow cytometry (A) and by GraphPad Prism (B). The displayed flow cytometry histograms are example results of two individual experiments.

6.3.3 Themis overexpression

Themis is most highly expressed in thymocytes but is downregulated in peripheral T cells. To investigate if not only the lack of Themis but also its overexpression has an effect on proximal TCR signalling, I overexpressed Themis 7-fold in 1G4 cells (Figure 6.12 A).

As in the Themis-k/d 1G4 cells, I investigated the expression of the early activation marker CD69 in 1G4 cells which overexpress Themis following TCR triggering by NY-ESO-$1_{156-165}$ pMHC tetramers. Control and Themis-overexpressing 1G4 cells were stimulated with 20 nM NY-ESO-$1_{156-165}$ pMHC tetramers for 5 hours and were tested for CD69 surface upregulation (Figure 6.12 B). In earlier experiments (Figure 6.9), an increased incidence in cell death was observed in Themis-k/d cells after 24 hour incubations. Thus,

---

Figure 6.12 *(following page)*: The effect of Themis overexpression on 1G4 cell activation. (A) Themis overexpression was analysed using immunoblotting. Bands were quantified using Odyssey infrared imaging system application software version 3.0. (B) Themis-overexpressing and control 1G4 cells were stimulated for 5 hours with 20 nM NY-ESO-1 pMHC tetramers and were analysed for CD69 upregulation after stimulation using flow cytometry. (C) Themis-overexpressing and control 1G4 cells were stimulated between 60 and 300 sec with 5 μg/ml UCHT1 CD3ε monoclonal antibody and were analysed for pT202.pY204-ERK activation using flow cytometry. (D) The digital nature of the pERK signal produced through UCHT1 stimulation is shown by the distinct geometric means of the inactive pERK population (1) and the active pERK population (2). (E) Percentage of all cells acquired which actively signal through pERK after UCHT1 stimulation. F) Themis overexpressing and control 1G4 cells were stimulated between 30 and 180 sec with 20 nM high affinity 9V NY-ESO-1 pMHC tetramers and were analysed for pT202.pY204-ERK activation using flow cytometry. (G) The digital nature of the pERK signal produced through 9V stimulation is shown as in D. (H) Percentage of all cells acquired which actively signal through pERK after 9V stimulation.

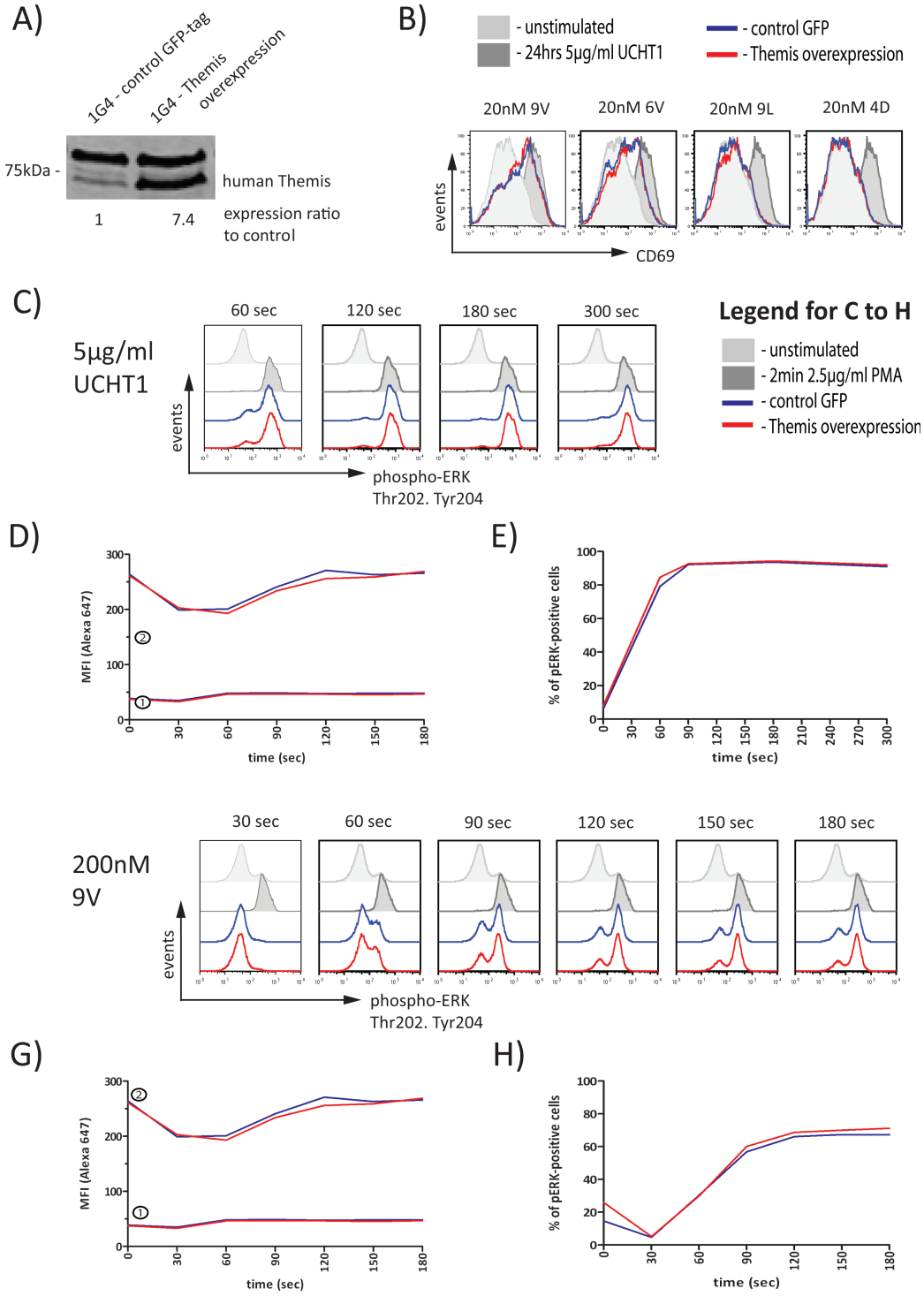
A)
1G4 - control GFP-tag
1G4 - Themis overexpression
75kDa -
human Themis
1
7.4
expression ratio to control
B)
- unstimulated
- 24hrs 5µg/ml UCHT1
- control GFP
- Themis overexpression
20nM 9V
20nM 6V
20nM 9L
20nM 4D
events
CD69
C)
5µg/ml UCHT1
60 sec
120 sec
180 sec
300 sec
events
phospho-ERK Thr202. Tyr204
Legend for C to H
- unstimulated
- 2min 2.5µg/ml PMA
- control GFP
- Themis overexpression
D)
MFI (Alexa 647)
time (sec)
E)
% of pERK-positive cells
time (sec)
200nM 9V
30 sec
60 sec
90 sec
120 sec
150 sec
180 sec
events
phospho-ERK Thr202. Tyr204
G)
MFI (Alexa 647)
time (sec)
H)
% of pERK-positive cells
time (sec)

as CD69 expression is already upregulated within 30 min post-stimulation [Marzio et al., 1999], the upregulation of CD69 was assessed after 5 hours of tetramer stimulation in this system. High NY-ESO-$1_{156-165}$ pMHC tetramer affinity corresponds with high expression of CD69. 9L and 4D stimulation caused very low surface expression of CD69. Themis overexpression had no effect on CD69 surface expression.

Control and Themis-overexpressing 1G4 cells were stimulated with either 5 µg/ml UCHT1 anti-CD3ε monoclonal antibodies or 200 nM 9V NY-ESO-$1_{156-165}$ pMHC tetramers and prepared for flow cytometry as described before. Timecourses of the stimulations up to 180 or 300 sec were performed (Figure 6.12 C-H). Both types of stimulation showed a rapid activation of pT202.pY204-ERK within 60 sec. The pERK signal was distinctly digital in both cases and displayed clear peaks denominating quiescent (1) and positively pERK signalling (2) cells (Figure 6.12 D and G). UCHT1 and 9V are both activate the pERK signalling pathway in 75 to 90% of cells stimulated (Figure 6.12 E and H). Themis overexpression had no effect on pERK signalling in any of the stimulations tested.

Themis expression is highest in thymocytes. During T cell maturation, Themis expression is downregulated. As seen in Figures 6.2 to 6.12, the lack of Themis increases pT202.pY204-ERK signalling strength and signal-induced apoptosis. Increased levels of Themis could have been expected to lower T cell signalling and further downstream responses. Instead it seems that the low expression of Themis already exhibits saturating effects on mature T cell signalling. It is conceivable that interaction partners or targets of

Themis-mediated regulation might be differentially expressed between thymocytes and our model Jurkat system.

6.4 Discussion

Themis is a recently discovered 72 kDa protein of unknown function which is exclusively expressed in the T cell lineage. Expression is particularly high in thymocytes and is subsequently downregulated in peripheral T cells [Fu et al., 2009]. Themis has been shown to be important as a checkpoint in thymocyte selection from the DP to the SP stages. Themis-k/d mice have reduced numbers of SP peripheral T cells [Fu et al., 2009]. The role of Themis in the periphery beyond thymocyte selection is still elusive.

I investigated the effect of Themis expression and TCR:pMHC interaction affinities on proximal TCR signals in 1G4 cells. Themis has been shown to both attenuate and enhance pERK signals in T cells [Brockmeyer et al., 2011]. The pERK signal is digital in nature and strongly implicated in the amplification of the proximal TCR signal and ligand discrimination [Altan-Bonnet and Germain, 2005].

Themis has been shown to associate with Grb2 and indirectly with LAT and SLP-76 and affects pERK signal as well as AP-1 and NFAT activation [Paster et al., 2013] [Brockmeyer et al., 2011]. The adaptor protein Grb2 interacts with SOS1 to activate Ras and mediate the Ras-MAPK activation pathway [Jang et al., 2010]. ERK signals are activated through upstream signalling events involving both the Ras and the DAG-RasGRP1 pathways [Warnecke et al., 2012].

Timecourse and dose-response experiments show that Themis attenuates agonist and partial agonist signals. These effects were most clearly observed with 9V and 6V tetramers. Data from experiments with thymocytes show

that Themis poses an important checkpoint in thymocyte development by governing signalling thresholds [Gascoigne and Palmer, 2011]. This is a crucial function of Themis because a shift in the signalling threshold which determines positive and negative selection could result in the increased positive selection of autoreactive thymocytes and could lead to autoimmunity [Chabod et al., 2012]. In the periphery, Themis could still exert modulating effects on T cell signalling although it seems to play a more important role in thymocytes. Themis is most highly expressed in DP thymocytes about to undergo positive or negative selection [Johnson et al., 2009]. The expression of Themis in the periphery is 5-fold lower. Yet, Themis overexpression had no effect on pERK signalling. This could indicate that either only minimal levels of Themis are able modulate peripheral activation thresholds or that one or more interaction partner of Themis are limiting factor for Themis function.

Contradicting effects of Themis on pERK signalling pathways have been reported [Carpenter and Bosselut, 2010]. It is yet unknown how Themis might affect further upstream signals from the LAT complex. Paster et al., 2013, showed that Themis is phosphorylated by LCK and ZAP-70 on tyrosines shortly upstream of the PRR1 domain. Through the PRR domain, Themis binds to the SH3 domain of Grb2 [Paster et al., 2013]. Mutations of the PRR domain abrogates Themis-Grb2 interactions and results in defective positive selection of thymocytes [Paster et al., 2013]. This firmly locates the activity of Themis to the LAT signalosome and not to the nucleus as might be suggested by the NLS sequence.

An additional feature of TCR signalling is the activation of positive and neg-

ative feedback loops to modulate TCR signalling [Acuto et al., 2008]. In particular, SHP-1 has been suggested to form a negative feedback loop by de-phosphorylating active pY394 LCK [Stefanová et al., 2003]. Although this theory has recently been disputed in T cell specific knock-down studies and attributed to major systemic inflammation caused by a global SHP-1 knock-down [Johnson et al., 2013], the attenuating effects of Themis could be linked to a similar system. It is conceivable that Themis might interact with a phosphatase or recruit one to the LAT signalosome which in turn exerts attentuating effects on the TCR signalling cascade. In current studies in the host laboratory, we are investigating possible further interactors of Themis which might elucidate some of the molecular functions of Themis.

CD69 expression is rapidly induced within 30 to 60 min post-activation [Marzio et al., 1999]. Consequently, CD69 is often used as an early activation marker for T cells. The extent of CD69 upregulation was sensitive to qualitative differences between the four NY-ESO-$1_{156-165}$ pMHC tetramers used. Neither the lack of Themis nor its overexpression affected the levels of CD69 upregulation. The signalling pathways which induce CD69 upregulation are not completely understood but the Ras/ERK pathway and Ca^{2+} signalling have been implicated in its upregulation [Cimo et al., 2013]. The expression of CD69 is rapidly induced after TCR engagement and independent of mRNA production [Hashemi et al., 1999]. Hence, an intracellular pool of CD69 or increased translation of mRNA of CD69 are thought to be translocated to the plasma membrane upon activation [Hashemi et al., 1999]. Phorbol ester and CD3ε-monoclonal antibody stimulations have been shown to induce CD69 upregulation through PKCϑ and Src-family protein kinase

signalling events [del Rio et al., 2004]. PKCϑ activates NF-ϰB [Isakov and Altman, 2012]. CD69 upregulation could be regulated independently from the distinct digital pERK signalling pathway and is unaffected by the actions of Themis in this system. Current work at the host laboratory is investigating the effect of Themis on CD69 expression in thymocytes.

Flow cytometry experiments with FLICA showed that Themis-k/d cells are significantly more prone to die by activation induced cell death. The increased rates of death are unconnected though to the effects of Themis on ERK activation suggested in previous publications [Fu et al., 2009] [Brockmeyer et al., 2011]. T cells die through signal-induced apoptosis to restore and maintain T cell homeostasis after an active T cell response to infection [Krammer et al., 2007]. These signals are mediated through repeated TCR engagements, especially in the absence of continuing co-stimulation [Krammer et al., 2007]. The 1G4 cells lack for example CD28-costimulatory molecules and might be more prone to accelerated death induction. Yet, unpublished observations report an increased incidence of apoptosis in Themis-negative thymocytes, arguing against a mechanism governed significantly by co-stimulatory molecules. Activation-induced cell death requires the activation of calcium and PKCϑ signalling. As described for CD69 upregulation, the PKCϑ signalling pathways runs in parallel to the RasGRP1-MAPK signalling pathway even though both are activated by DAG [Morris and Allen, 2012] [Roose et al., 2005]. In fact, pERK signals have been shown to promote cell survival and antagonize apoptotic signals [Chen et al., 2001]. Data in the host laboratory is currently indicating that activity through CD95L is not implicated in the higher incidence of apoptosis in Themis-k/d cells Bruger,

Paster, in preparation.

In this chapter, I have shown that Themis affects signalling in 1G4 Jurkat cell model on various levels. Themis is associated to Grb2 and thus may compete with SOS for Grb2 binding or Grb2-association to LAT. Surprisingly, no effect of Themis expression levels was seen on the expression of the early activation marker CD69 on the surface of stimulated 1G4 cells. CD69 upregulation is linked to pERK signalling and thus the reason for the lack of Themis influence on CD69 expression in this system is unknown [Cimo et al., 2013]. Previous studies had shown that while the lack of Themis did not cause an overall defect in TCR proximal signalling, Themis regulated signalling strengths subtly [Fu et al., 2009] [Brockmeyer et al., 2011]. However, the initial studies all used anti-CD3ε antibodies to stimulate cells. The use of pMHC tetramers of different affinities or the use of peptide-pulsed APC allow more refined investigation of subtle signalling events [Gascoigne and Palmer, 2011]. The effect of Themis on ERK signalling remained controversial after contradicting observations were published in thymocytes and Jurkat cells [Carpenter and Bosselut, 2010] [Brockmeyer et al., 2011]. In this study, I show that in 1G4 cells Themis acts to decrease the signalling strength of not only downstream ERK but also of upstream proximal signalling molecules CD3ζ and ZAP-70. Since the function of Themis is yet unknown, I can only speculate on the mechanism by which mediates Themis regulation on TCR signalling. It may be that Themis competes with SOS for binding of Grb2 and thus downregulates the activation of Ras and ERK further downstream [Roose et al., 2007] [Das et al., 2009]. However, SOS-knock-down studies I

performed showed no effect on ERK activation, arguing against the hypothesis that Themis might attenuate pERK signalling by competing with SOS for Grb2 binding (data not shown).

Alternatively, Themis could interact as a phosphatase or enhance the activity of a phosphatase which attenuates TCR signalling in a negative feedback loop upstream the cascade from the TCR. We are currently investigating the interactions and effects of Themis and phosphatases implicated in TCR signalling. SHP-1 is such a phosphatase. It associates to phosphorylated Grb2 has been suggested to de-phosphorylate LCK on Y394 and thus attenuate TCR signals by low affinity ligands especially [Zhang et al., 2000] [Stefanová et al., 2003]. SHP-1 could thus raise the TCR triggering threshold [Stefanová et al., 2003]. While recent data removes SHP-1 itself from this scenario, Themis might function as mediator between similar negative and positive feedback pathways and thus modulate TCR proximal signalling in thymocytes and in peripheral T cells. The overexpression of Themis had no effect on TCR signalling which could indicate that an interactor of Themis is rate-limiting the modulating actions of Themis.

Furthermore, activation-induced cell death was significantly increased in cells lacking Themis. The levels of activation-induced cell death were not dependent on ERK activity. This also indicates that Themis acts to attenuate TCR signalling on parallel signalling pathways to induce a variety of TCR effector responses.

Chapter 7

General Discussion

Even after more than 25 years of intensive research, some fundamental questions about T cell activation remain unanswered. One of these questions concerns how continuous and variable stimuli are translated into sensitive all-or-nothing biological responses and cell fate decisions. In the presented work I established a system of stimulating Jurkat cells expressing the 1G4 TCR in solution with NY-ESO-$1_{156-165}$ pMHC class I tetramers of different affinities to the 1G4 TCR. I used this system to study the transmission of quantitative and qualitative information about TCR ligand binding through proximal signalling events. This demonstrated in detail that the earliest signalling events are of analogue nature and that their signals' amplitudes determines the likelihood of later digital responses. I furthermore employed the 1G4 system to show that Themis attenuates global proximal TCR signalling by modulating the signal threshold required to activate digital ERK responses. Themis is an important checkpoint protein in thymocyte selection - a process which is governed by intricate signalling thresholds.

7.1 Controlled investigation of proximal TCR signalling kinetics using 1G4-TCR expressing Jurkat cells.

Mature peripheral T cells encounter antigen presented on the surface of APCs in the secondary lymphoid tissues. The priming of T cells by APCs is required for the efficient activation of both naive cytotoxic and naive helper T cells. The large diversity inherent to both the pMHC and the TCR ensures specific T cell functions but it also requires T cells to sample large populations of APC to recognise potential agonist pMHC. Within the T cell zones of lymph nodes, a DC interacts with up to 5000 T cells per hour [Dustin, 2008]. Each T cell expresses a clonotypic TCR. Hence, at any time, only between 0.0003 to 0.001% of T cells will display the same TCR [Blattman et al., 2002] [Obar et al., 2008] [Amsen et al., 2013]. Following clonal expansion after TCR triggering, up to 10% of the entire T cell repertoire possess the same antigen specificity [Blattman et al., 2002] [Obar et al., 2008] [Amsen et al., 2013]. Unlike the TCR, pMHC are not expressed clonally on APC. Each APC expresses about 100,000 MHC molecules on the surface which are bound to several peptides [Yewdell et al., 2003]. Ten or even less agonist pMHC among an 10^5 to 10^4-times higher concentrations of self-peptide MHC are sufficient to trigger T cell effector functions [Germain, 2001]. The short amino acid sequences of the presented peptides mean that self and agonist peptides are potentially closely related to each other in their structure [Stefanová et al., 2003]. Indeed, single amino acid substitutions to the sequence of peptides presented by MHC can

influence the TCR:pMHC binding kinetics and downstream T cell effector functions significantly [Altan-Bonnet and Germain, 2005]. One particular study reported that a single amino acid substitution resulted in the $2x10^4$-fold reduction of biological potency while the half-time of the TCR:pMHC interactions only decreased 5-fold [Kersh et al., 1998]. The sequence of the four NY-ESO-$1_{156-165}$ peptide MHC complexes used in this study differed by one or two amino acids. Yet the monomeric affinities to the 1G4 TCR diverged 2.5- to 35-fold [Aleksic et al., 2010]. In this study, I stimulated 1G4 cells in solution with NY-ESO-$1_{156-165}$ pMHC tetramers. *In vitro* produced, fluorochrome-linked pMHC tetramers are powerful tools in biochemical T cell research and were initially developed to identify T cells displaying a particular TCR within a diverse population of primary T cells [Klenerman et al., 2002] [Alanio et al., 2010]. In this study however, the TCR cross-linking and T cell stimulating properties of pMHC tetramers allowed me to assess TCR signalling in a controlled *in vitro* model. This allowed me to assess TCR signalling responses within seconds after stimulation and correlate occupancy directly to pMHC affinity and TCR signalling. Neither stimulation with plate-bound pMHC monomers, agonist peptide-pulsed APC nor CD3ε antibodies supported the experimental requirements of this investigation. The influence of valency on TCR:pMHC interactions and TCR triggering both in physiological and cell-free systems is an intensely discussed topic [Schamel et al., 2005] [Schrum et al., 2011] [Neveu et al., 2006] [Chervin et al., 2009] [Davis et al., 1998] [Stone et al., 2011]. The cross-linking of several TCR at once by one pMHC tetramer is thought to strengthen the TCR:pMHC interactions, lower the interactions' off-rates and reinforce downstream sig-

nalling responses in comparison to monovalent pMHC [Neveu et al., 2006] [Klenerman et al., 2002]. However, monomeric affinities have been shown to correlate well to the functional avidity of NY-ESO-$1_{156-165}$ pMHC tetramers which renders the described approach to investigate proximal TCR signalling kinetics viable [Dutoit et al., 2002a] [Chen et al., 2010] [Aleksic et al., 2010]. I established a method to investigate early proximal signalling events in response to different pMHC affinities in a detailed, controlled and repeatable fashion in the host laboratory whose success inspired later major lines of investigation in the laboratory.

7.2 The amplitude of early analogue TCR signals determine downstream activation of digital responses

The wide range of antigen encountered by T cells means that they are exposed to constant stimuli of variable strength and density. Some T cell effector responses, such as cytokine secretion, reflect both the qualitative and quantitative input [Burroughs and van der Merwe, 2007] [Aleksic et al., 2010]. However, the induction of other T cell fate decisions, such as proliferation and cytotoxicity, require a decisive activation threshold to be passed and the cells subsequently respond in a distinctly digital on/off manner [Ferrell and Machleder, 1998] [Burroughs and van der Merwe, 2007]. The ability to distinguish between agonist and self-peptides and mount effector responses to one but not the other requires exquisite TCR specificity and sensitivity.

The specificity of the pMHC recognition is conferred by the binding kinetics of the particular pMHC and TCR. Structural flexibility within the CDR3 chains of the TCR ensure the diversity of pMHC recognition [Krogsgaard and Davis, 2005]. The monomeric pMHC-TCR binding kinetics of the NY-ESO-$1_{156-165}$-1G4 system have been extensively studied before [Aleksic et al., 2010]. The sensitivity of T cell responses to agonist pMHC is additionally dependent on the intricate regulation of the TCR proximal signalling events. In this study, I investigated the properties of the signal transduction by LCK, CD3ζ, ZAP-70 and ERK in particular, and their effect on the qualitative distinction between different affinity ligands of known affinities. CD3ζ and ZAP-70 showed an analogue phosphorylation pattern to different affinity NY-ESO-$1_{156-165}$ pMHC stimulations. With a time delay of about one minute, this analogue signal was converted into a digital phospho-ERK signal. The extent of the analogue signal determined the stochastic likelihood and the extent of the later digital phospho-ERK response. Strong affinity stimulation resulted in higher CD3ζ and ZAP-70 signal amplitudes which increased the likelihood of digital ERK activation. The analogue signal amplitudes between CD3ζ phosphorylation and ZAP-70 activation already show a difference in definition. This might implicate ZAP-70 in not only linking the TCR-CD3 complex to the LAT signalosome but also indicate its importance in transferring qualitative information of ligand binding. The digital nature of ERK and its importance in cell fate decisions has been reported previously [Ferrell and Machleder, 1998]. In T cells, digital ERK signals govern cell proliferation and contribute to the control of IL-2 gene expression [Karlsson et al., 2006]. The ERK signal observed was highly amplified. A 60-fold

higher concentration of intermediate affinity 6V was required to achieve an ERK response comparable to high affinity 9V stimulation, even though both the affinity and off-rates of 9V and 6V differ by only 2.5-fold. The amplification of TCR signalling is achieved through a complex network of unknown feedback mechanisms [Acuto et al., 2008]. The interplay of feedback loops allows to define a sharp ligand discrimination thresholds and decisive T cell effector responses in response to ligand with close affinities.

My studies showed detailed investigations of simultaneous proximal TCR signalling events using flow cytometry and revealed close correlations between initial analogue signal amplitudes and further downstream digital ERK responses after the diversification of the TCR signal. In future experiments, this controlled experimental set-up and the detail of information about the TCR signals obtainable at different points of the cascade could help link kinetic TCR triggering models to downstream signalling events and help elucidate the mechanisms which confer T cell sensitivity to particular pMHC ligands. Furthermore, the 1G4:NY-ESO-$1_{156-165}$ system is used by our collaborators in cancer vaccination studies. Correlating very early proximal signalling strengths and later T cell activation to specific antigens could help shape the assessment and selection of pMHC molecules or transgenic TCRs which show potential for clinical applications.

7.3 Themis is a global attenuator of TCR signal events

One example of how TCR signalling contributes towards fine-tuning the specificity of T cell responses was demonstrated by the discovery of the protein Themis and its importance to governing thymocyte selection thresholds [Fu et al., 2009] [Lesourne et al., 2009] [Johnson et al., 2009]. Themis itself is a protein of unknown molecular function which associates to Grb2 and is phosphorylated by LCK and ZAP-70 [Paster et al., 2013]. The expression of Themis is specific to the T cell lineage and is most pronounced in thymocytes [Johnson et al., 2009]. In the absence of Themis, thymocyte positive selection is impaired; yet no clear defect in the TCR signalling networks was discovered [Fu et al., 2009] [Gascoigne and Palmer, 2011]. Work of the host laboratory have since established that the localisation of Themis to the LAT signalosome is essential for thymocyte development [Paster et al., 2013].
Further indications in the laboratory suggested that Themis might enhance ERK signalling [Fu et al., 2009] [Brockmeyer et al., 2011]. All signalling data at this point was acquired after stimulation of T cells with anti-CD3ε antibodies which causes strong stimulation of the T cells. Themis is implicated in modulating the threshold of positive selection in thymocytes [Fu et al., 2009]. Thus it is likely that function of Themis is sensitive to small differences in proximal signalling evoked by different affinity ligands. The system I established of stimulating cells in solution with a range of different affinity pMHC and the detail of the data acquired by flow cytometry meant that we were able to investigate the effect of Themis more accurately in a controlled

setting. My model cell line was also well suited to this investigation. Experiments with *ex vivo* cells may be subjected to artefacts of adaptations to the signalling machinery which are necessary to maintain the cells in absence of Themis. The *in vitro* system allows the controlled knock-down of Themis and the precise investigation of the resulting signalling irregularities.

In the 1G4 Jurkat cell system, the loss of Themis resulted in increased levels of both upstream CD3ζ and downstream ERK activity. This shows that Themis acts as a general attenuator of proximal TCR signalling and does not only affect downstream events (Bruger, Paster et al., in preparation). It is conceivable that Themis functions within a negative feedback loop which also affects the TCR:CD3 complex. As yet, possible mechanisms of Themis activity or interaction partners which might be involved in feedback signalling are open to speculation. Themis might act as a competitor to SOS1 for binding interactions with Grb2. SOS1 is a Grb2-associated GEF which along with GEF RasGRP1 activates Ras which in turn activates ERK [Roose and Weiss, 2000] [Das et al., 2009]. While RasGRP1 is thought to be the dominating signal necessary for ERK activation, SOS1 has been implicated in shaping the digital nature of the ERK signal and shape thymocyte selection [Alberola-Ila et al., 1996] [Stefanová et al., 2003] [Kortum et al., 2012].

However, data which is not presented here showed no effect of SOS1 on ERK activity while the knock-down of RasGRP1 significantly decreased ERK signalling. Current work in the host laboratory is aiming to identify possible further interactors of Themis which could also shed light on the effect of Themis to SOS and RasGRP1. Alternatively, Themis itself could possess phosphatase functions which regulate the TCR protein tyrosine kinase sig-

nalling cascade. However, sequence alignments do not reveal typical phosphatase catalytic domains [Johnson et al., 2009]. In the Acuto laboratory, we are currently working on obtaining structural data for the Themis protein which might elucidate Themis functions. Thirdly, Themis could represent an adaptor molecule which recruits phosphatases such as SHP-1 to the LAT signalosome and enhances their activity. We are in the process of investigating possible Themis-SHP-1 and -2 interactions and their effects on modulating TCR signalling. The effects of SHP-1 on TCR signalling are currently controversial. While it has been suggested that it forms a major negative feedlack loop from the LAT signalosome to LCK and attenuates signalling by low affinity ligands especially [Stefanová et al., 2003], recent T cell-specific data saw no influence of SHP-1 on peripheral TCR sensitivity [Johnson et al., 2013].

The overexpression of Themis had no effect on TCR signalling strength in 1G4 cells which mimic peripheral T cells rather than lymphocytes. Thymocytes express 5-times more Themis than peripheral T cells [Johnson et al., 2009]. The lack of a response of 1G4 cells to Themis overexpression might indicate that Themis interaction partners are the rate-limiting and catalytic factors to the TCR signal attenuating effects of Themis.

Themis itself or its interaction partners could also have signal attenuating activity on other TCR signalling branches besides the MAPK-signalling network. Cells lacking Themis are more prone to activation-induced cell death which was independent of ERK activity. Initial observations in primary T cells and 1G4 cells suggested such a phenotype. Closer investigation shows that Themis significantly protects 1G4 cells from apoptosis (Bruger, Paster et

al., in preparation). This *in vitro* work is of great importance and supports recent data of our collaborators in thymocytes. Themis$^{-/-}$ thymocytes showed increased TCR signalling which results in a defect in positive selection that is rescued by the knock-down of the pro-apoptotic Bcl-2 family protein Bim (Fu et al., Nature, submitted). The induction of activation-induced cell death is very complex and involves several pathways which include the activity of Ca^{2+}, PKCϑ and IKK signals [Krammer et al., 2007]. Whether Themis is directly involved in the government of activation-induced cell death pathways or whether its overall attenuation of TCR signals protects from apoptosis remains to be resolved but seems to resemble the hypothesis of present.
Future investigations to elucidate the molecular function of Themis are going to rely heavily on the 1G4:NY-ESO-$1_{156-165}$ system I established. It is a powerful tool which showed that Themis is an attenuator of general TCR proximal signalling and significantly protects T cells from TCR signal-induced cell death.

7.4 Future outlook and clinical context

In this study, I employed a system which tested the signalling responses induced in 1G4 TCR-expressing Jurkat cells to variants of the NY-ESO-$1_{156-165}$ HLA-A2 pMHC with different binding properties to the TCR. The 1G4 TCR was isolated from peripheral T cells of melanoma patients [Chen et al., 1997]. T cells expressing this TCR recognise cancer cells which express the testicular germline- and tumour-specific NY-ESO-1 protein; yet the T cells mount only mild immune responses against the tumour [Chen et al., 2005]. Inves-

tigating the signalling responses which govern T cell activation in response to the affinity of the ligand presented can help in the design and development of T cell-based cancer therapy approaches. The concept of using T cells to target and eradicate cancer cells is an elegant one. T cells have the inherent capabilities to specifically target particular transformed or infected cells and kill them without damaging the surrounding tissues [Offringa, 2009] [Restifo et al., 2012]. Programming T cells to recognise and eliminate cancer cells through the presentation of cancer-specific antigen to T cells could result in the efficient eradication of primary and secondary tumours without debilitating side effects [Offringa, 2009]. T cell activity against cancers could be induced in two ways: The use of peptide analogue adjuvants of greater affinity than the wild-type peptide could be used to induce greater antigen-specific CTL clone expansion and T cell sensitivity to the wild-type peptide-expressing target cancer cells [Chen et al., 2000] [Chen et al., 2005] [Chen et al., 2010]. Alternatively, T cells with genetically engineered TCRs of greater affinity for the cancer antigen could be reared and primed *in vitro* and transferred to the patient [Rosenberg et al., 1998] [Dutoit et al., 2002a] [Robbins et al., 2011]. One adoptive transfer clinical trial used genetically engineered T cells which targeted cancer cells expressing the NY-ESO-$1_{156-165}$ peptide and showed clinical responses in 45 to 67% of patients [Robbins et al., 2011]. Elucidating the mechanisms and kinetics of how T cells distinguish between antigens and translate these differences by TCR signalling into decisive T cell effector functions could help design more efficient and specifically targeted T cell-based therapies. *In vitro* TCR signalling studies could identify pMHC molecules or transgenic TCRs with therapeutic potential or help

predict the efficacy of T cell effector functions to a particular ligand based on the kinetic parameters of the TCR:pMHC interactions. Elucidating how molecules such as Themis are able to subtly yet significantly modulate the responses of T cells to different affinity ligands is also important for designing effective T cell vaccines.

Similarly to Goldilocks in the fairy tale, optimal T cell functions require the TCR:pMHC binding kinetics to fall within a range of optimal interaction affinity and dwell time. The knowledge of how TCR:pMHC binding parameters influence TCR signalling checkpoint thresholds, amplification loops and the signal's amplitude at different positions within the cascade is important to determine the optimal kinetic range for T cell functions against a particular antigen and design more efficient T cell-based vaccines.

Bibliography

[Acuto et al., 2008] Acuto, O., Di Bartolo, V., and Michel, F. (2008). Tailoring t-cell receptor signals by proximal negative feedback mechanisms. *Nat Rev Immunol*, 8(9):699–712.

[Acuto et al., 1983] Acuto, O., Hussey, R. E., Fitzgerald, K. A., Protentis, J. P., Meuer, S. C., Schlossman, S. F., and Reinherz, E. L. (1983). The human T cell receptor: appearance in ontogeny and biochemical relationship of alpha and beta subunits on IL-2 dependent clones and T cell tumors. *Cell*, 34(3):717–726.

[Acuto and Michel, 2003] Acuto, O. and Michel, F. (2003). Cd28-mediated co-stimulation: a quantitative support for tcr signalling. *Nature reviews. Immunology*, 3(12):939–951.

[Acuto et al., 2003] Acuto, O., Mise-Omata, S., Mangino, G., and Michel, F. (2003). Molecular modifiers of t cell antigen receptor triggering threshold: the mechanism of cd28 costimulatory receptor. *Immunological reviews*, 192:21–31.

[Acuto and Reinherz, 1985] Acuto, O. and Reinherz, E. L. (1985). The human T-cell receptor. Structure and function. *N. Engl. J. Med.*, 312(17):1100–1111.

[Alajez et al., 2006] Alajez, N. M., Eghtesad, S., and Finn, O. J. (2006). Cloning and expression of human membrane-bound and soluble engineered t cell receptors for immunotherapy. *Journal of biomedicine & biotechnology*, 2006(2):68091.

[Alanio et al., 2010] Alanio, C., Lemaitre, F., Law, H. K., Hasan, M., and Albert, M. L. (2010). Enumeration of human antigen-specific naive CD8+ T cells reveals conserved precursor frequencies. *Blood*, 115(18):3718–3725.

[Alberola-Ila and Hernández-Hoyos, 2003] Alberola-Ila, J. and Hernández-Hoyos, G. (2003). The ras/mapk cascade and the control of positive selection. *Immunological reviews*, 191:79–96.

[Alberola-Ila et al., 1996] Alberola-Ila, J., Hogquist, K. A., Swan, K. A., Bevan, M. J., and Perlmutter, R. M. (1996). Positive and negative selection invoke distinct signaling pathways. *J. Exp. Med.*, 184(1):9–18.

[Aleksic et al., 2010] Aleksic, M., Dushek, O., Zhang, H., Shenderov, E., Chen, J.-L., Cerundolo, V., Coombs, D., and van der Merwe, P. A. (2010). Dependence of t cell antigen recognition on t cell receptor-peptide mhc confinement time. *Immunity*, 32(2):163–174.

[Allen, 2009] Allen, P. M. (2009). Themis imposes new law and order on positive selection. *Nature immunology*, 10(8):805–806.

[Altan-Bonnet and Germain, 2005] Altan-Bonnet, G. and Germain, R. N. (2005). Modeling t cell antigen discrimination based on feedback control of digital erk responses. *PLoS Biol*, 3(11).

[Altman et al., 2004] Altman, A., Kaminski, S., Busuttil, V., Droin, N., Hu, J., Tadevosyan, Y., Hipskind, R. A., and Villalba, M. (2004). Positive feedback regulation of PLCgamma1/Ca(2+) signaling by PKCtheta in restimulated T cells via a Tec kinase-dependent pathway. *Eur. J. Immunol.*, 34(7):2001–2011.

[Altman and Davis, 2003] Altman, J. D. and Davis, M. M. (2003). Mhc-peptide tetramers to visualize antigen-specific t cells. *Curr Protoc Immunol*, Chapter 17.

[Altman et al., 1996] Altman, J. D., Moss, P. A., Goulder, P. J., Barouch, D. H., McHeyzer-Williams, M. G., Bell, J. I., McMichael, A. J., and Davis, M. M. (1996). Phenotypic analysis of antigen-specific t lymphocytes. *Science (New York, N.Y.)*, 274(5284):94–96.

[Amsen et al., 2013] Amsen, D., Backer, R. A., and Helbig, C. (2013). Decisions on the road to memory. *Advances in experimental medicine and biology*, 785:107–120.

[Arcaro et al., 2001] Arcaro, A., Grégoire, C., Bakker, T. R., Baldi, L., Jordan, M., Goffin, L., Boucheron, N., Wurm, F., van der Merwe, P. A., Malissen, B., and Luescher, I. F. (2001). Cd8beta endows cd8

with efficient coreceptor function by coupling t cell receptor/cd3 to raft-associated cd8/p56(lck) complexes. *The Journal of experimental medicine*, 194(10):1485–1495.

[Arcaro et al., 2000] Arcaro, A., Grégoire, C., Boucheron, N., Stotz, S., Palmer, E., Malissen, B., and Luescher, I. F. (2000). Essential role of cd8 palmitoylation in cd8 coreceptor function. *Journal of immunology (Baltimore, Md. : 1950)*, 165(4):2068–2076.

[Artyomov et al., 2010] Artyomov, M. N., Lis, M., Devadas, S., Davis, M. M., and Chakraborty, A. K. (2010). Cd4 and cd8 binding to mhc molecules primarily acts to enhance lck delivery. *Proc Natl Acad Sci U S A*, 107(39):16916–16921.

[Ashkenazi and Dixit, 1998] Ashkenazi, A. and Dixit, V. M. (1998). Death receptors: signaling and modulation. *Science (New York, N.Y.)*, 281(5381):1305–1308.

[Berkhout et al., 1988] Berkhout, B., Alarcon, B., and Terhorst, C. (1988). Transfection of genes encoding the T cell receptor-associated CD3 complex into COS cells results in assembly of the macromolecular structure. *J. Biol. Chem.*, 263(17):8528–8536.

[Bhakta et al., 2005] Bhakta, N. R., Oh, D. Y., and Lewis, R. S. (2005). Calcium oscillations regulate thymocyte motility during positive selection in the three-dimensional thymic environment. *Nature immunology*, 6(2):143–151.

[Bhandoola and Sambandam, 2006] Bhandoola, A. and Sambandam, A. (2006). From stem cell to t cell: one route or many? *Nature reviews. Immunology*, 6(2):117–126.

[Blattman et al., 2002] Blattman, J. N., Antia, R., Sourdive, D. J., Wang, X., Kaech, S. M., Murali-Krishna, K., Altman, J. D., and Ahmed, R. (2002). Estimating the precursor frequency of naive antigen-specific CD8 T cells. *J. Exp. Med.*, 195(5):657–664.

[Boggon and Eck, 2004] Boggon, T. J. and Eck, M. J. (2004). Structure and regulation of src family kinases. *Oncogene*, 23(48):7918–7927.

[Boursalian et al., 2004] Boursalian, T. E., Golob, J., Soper, D. M., Cooper, C. J., and Fink, P. J. (2004). Continued maturation of thymic emigrants in the periphery. *Nature immunology*, 5(4):418–425.

[Boursier et al., 1993] Boursier, J. P., Alcover, A., Herve, F., Laisney, I., and Acuto, O. (1993). Evidence for an extended structure of the T-cell co-receptor CD8 alpha as deduced from the hydrodynamic properties of soluble forms of the extracellular region. *J. Biol. Chem.*, 268(3):2013–2020.

[Bouvier, 2003] Bouvier, M. (2003). Accessory proteins and the assembly of human class I MHC molecules: a molecular and structural perspective. *Mol. Immunol.*, 39(12):697–706.

[Brdicka et al., 2005] Brdicka, T., Kadlecek, T. A., Roose, J. P., Pastuszak, A. W., and Weiss, A. (2005). Intramolecular regulatory switch in zap-70: analogy with receptor tyrosine kinases. *Molecular and cellular biology*, 25(12):4924–4933.

[Brockmeyer et al., 2011] Brockmeyer, C., Paster, W., Pepper, D., Tan, C. P., Trudgian, D. C., McGowan, S., Fu, G., Gascoigne, N. R. J., Acuto, O., and Salek, M. (2011). T cell receptor (tcr)-induced tyrosine phosphorylation dynamics identifies themis as a new tcr signalosome component. *The Journal of biological chemistry*, 286(9):7535–7547.

[Burroughs and van der Merwe, 2007] Burroughs, N. J. and van der Merwe, P. A. (2007). Stochasticity and spatial heterogeneity in t-cell activation. *Immunological reviews*, 216:69–80.

[Call et al., 2002] Call, M. E., Pyrdol, J., Wiedmann, M., and Wucherpfennig, K. W. (2002). The organizing principle in the formation of the t cell receptor-cd3 complex. *Cell*, 111(7):967–979.

[Call et al., 2006] Call, M. E., Schnell, J. R., Xu, C., Lutz, R. A., Chou, J. J., and Wucherpfennig, K. W. (2006). The structure of the zetazeta transmembrane dimer reveals features essential for its assembly with the t cell receptor. *Cell*, 127(2):355–368.

[Campi et al., 2005] Campi, G., Varma, R., and Dustin, M. L. (2005). Actin and agonist mhc-peptide complex-dependent t cell receptor microclusters as scaffolds for signaling. *The Journal of experimental medicine*, 202(8):1031–1036.

[Carpenter and Bosselut, 2010] Carpenter, A. C. and Bosselut, R. (2010). Decision checkpoints in the thymus. *Nature immunology*, 11(8):666–673.

[Carreño et al., 2007] Carreño, L. J., Bueno, S. M., Bull, P., Nathenson, S. G., and Kalergis, A. M. (2007). The half-life of the t-cell

receptor/peptide-major histocompatibility complex interaction can modulate t-cell activation in response to bacterial challenge. *Immunology*, 121(2):227–237.

[Chabod et al., 2012] Chabod, M., Pedros, C., Lamouroux, L., Colacios, C., Bernard, I., Lagrange, D., Balz-Hara, D., Mosnier, J. F., Laboisse, C., Vergnolle, N., Andreoletti, O., Roth, M. P., Liblau, R., Fournie, G. J., Saoudi, A., and Dejean, A. S. (2012). A spontaneous mutation of the rat Themis gene leads to impaired function of regulatory T cells linked to inflammatory bowel disease. *PLoS Genet.*, 8(1):e1002461.

[Chang et al., 2011] Chang, J. T., Ciocca, M. L., Kinjyo, I., Palanivel, V. R., McClurkin, C. E., Dejong, C. S., Mooney, E. C., Kim, J. S., Steinel, N. C., Oliaro, J., Yin, C. C., Florea, B. I., Overkleeft, H. S., Berg, L. J., Russell, S. M., Koretzky, G. A., Jordan, M. S., and Reiner, S. L. (2011). Asymmetric proteasome segregation as a mechanism for unequal partitioning of the transcription factor t-bet during t lymphocyte division. *Immunity*, 34(4):492–504.

[Chen et al., 2001] Chen, J., Fujii, K., Zhang, L., Roberts, T., and Fu, H. (2001). Raf-1 promotes cell survival by antagonizing apoptosis signal-regulating kinase 1 through a mek-erk independent mechanism. *Proceedings of the National Academy of Sciences of the United States of America*, 98(14):7783–7788.

[Chen et al., 2000] Chen, J. L., Dunbar, P. R., Gileadi, U., Jäger, E., Gnjatic, S., Nagata, Y., Stockert, E., Panicali, D. L., Chen, Y. T., Knuth, A., Old, L. J., and Cerundolo, V. (2000). Identification of ny-eso-1 peptide analogues capable of improved stimulation of tumor-reactive ctl. *Journal of immunology (Baltimore, Md. : 1950)*, 165(2):948–955.

[Chen et al., 2010] Chen, J.-L., Morgan, A. J., Stewart-Jones, G., Shepherd, D., Bossi, G., Wooldridge, L., Hutchinson, S. L., Sewell, A. K., Griffiths, G. M., van der Merwe, P. A., Jones, E. Y., Galione, A., and Cerundolo, V. (2010). Ca2+ release from the endoplasmic reticulum of ny-eso-1-specific t cells is modulated by the affinity of tcr and by the use of the cd8 coreceptor. *Journal of immunology (Baltimore, Md. : 1950)*, 184(4):1829–1839.

[Chen et al., 2005] Chen, J.-L., Stewart-Jones, G., Bossi, G., Lissin, N. M., Wooldridge, L., Choi, E. M. L., Held, G., Dunbar, P. R., Esnouf, R. M., Sami, M., Boulter, J. M., Rizkallah, P., Renner, C., Sewell, A., van der Merwe, P. A., Jakobsen, B. K., Griffiths, G., Jones, E. Y., and Cerundolo,

V. (2005). Structural and kinetic basis for heightened immunogenicity of t cell vaccines. *The Journal of experimental medicine*, 201(8):1243–1255.

[Chen and Flies, 2013] Chen, L. and Flies, D. B. (2013). Molecular mechanisms of T cell co-stimulation and co-inhibition. *Nat. Rev. Immunol.*, 13(4):227–242.

[Chen et al., 1997] Chen, Y. T., Scanlan, M. J., Sahin, U., Türeci, O., Gure, A. O., Tsang, S., Williamson, B., Stockert, E., Pfreundschuh, M., and Old, L. J. (1997). A testicular antigen aberrantly expressed in human cancers detected by autologous antibody screening. *Proceedings of the National Academy of Sciences of the United States of America*, 94(5):1914–1918.

[Chervin et al., 2009] Chervin, A. S., Stone, J. D., Holler, P. D., Bai, A., Chen, J., Eisen, H. N., and Kranz, D. M. (2009). The impact of tcr-binding properties and antigen presentation format on t cell responsiveness. *Journal of immunology (Baltimore, Md. : 1950)*, 183(2):1166–1178.

[Choudhuri and van der Merwe, 2007] Choudhuri, K. and van der Merwe, P. A. (2007). Molecular mechanisms involved in t cell receptor triggering. *Seminars in immunology*, 19(4):255–261.

[Choudhuri et al., 2005] Choudhuri, K., Wiseman, D., Brown, M. H., Gould, K., and van der Merwe, P. A. (2005). T-cell receptor triggering is critically dependent on the dimensions of its peptide-MHC ligand. *Nature*, 436(7050):578–582.

[Cimo et al., 2013] Cimo, A. M., Ahmed, Z., McIntyre, B. W., Lewis, D. E., and Ladbury, J. E. (2013). CD25 and CD69 induction by 41 outside-in signalling requires TCR early signalling complex proteins. *Biochem. J.*, 454(1):109–121.

[Clements et al., 1998] Clements, J. L., Yang, B., Ross-Barta, S. E., Eliason, S. L., Hrstka, R. F., Williamson, R. A., and Koretzky, G. A. (1998). Requirement for the leukocyte-specific adapter protein SLP-76 for normal T cell development. *Science*, 281(5375):416–419.

[Corr et al., 1994] Corr, M., Slanetz, A. E., Boyd, L. F., Jelonek, M. T., Khilko, S., al Ramadi, B. K., Kim, Y. S., Maher, S. E., Bothwell, A. L., and Margulies, D. H. (1994). T cell receptor-MHC class I peptide interactions: affinity, kinetics, and specificity. *Science*, 265(5174):946–949.

[Crotty, 2011] Crotty, S. (2011). Follicular helper CD4 T cells (TFH). *Annu. Rev. Immunol.*, 29:621–663.

[Daniels et al., 2006] Daniels, M. A., Teixeiro, E., Gill, J., Hausmann, B., Roubaty, D., Holmberg, K., Werlen, G., Holländer, G. A., Gascoigne, N. R. J., and Palmer, E. (2006). Thymic selection threshold defined by compartmentalization of ras/mapk signalling. *Nature*, 444(7120):724–729.

[Das et al., 2009] Das, J., Ho, M., Zikherman, J., Govern, C., Yang, M., Weiss, A., Chakraborty, A. K., and Roose, J. P. (2009). Digital signaling and hysteresis characterize ras activation in lymphoid cells. *Cell*, 136(2):337–351.

[Davis et al., 2012] Davis, L. C., Morgan, A. J., Chen, J.-L., Snead, C. M., Bloor-Young, D., Shenderov, E., Stanton-Humphreys, M. N., Conway, S. J., Churchill, G. C., Parrington, J., Cerundolo, V., and Galione, A. (2012). Naadp activates two-pore channels on t cell cytolytic granules to stimulate exocytosis and killing. *Current biology : CB*, 22(24):2331–2337.

[Davis et al., 1998] Davis, M. M., Boniface, J. J., Reich, Z., Lyons, D., Hampl, J., Arden, B., and Chien, Y. (1998). Ligand recognition by alpha beta t cell receptors. *Annu Rev Immunol*, 16:523–544.

[Davis and van der Merwe, 2006] Davis, S. J. and van der Merwe, P. A. (2006). The kinetic-segregation model: TCR triggering and beyond. *Nat. Immunol.*, 7(8):803–809.

[del Rio et al., 2004] del Rio, R., Rincón, M., Layseca-Espinosa, E., Fierro, N. A., Rosenstein, Y., and Pedraza-Alva, G. (2004). Pkctheta is required for the activation of human t lymphocytes induced by cd43 engagement. *Biochemical and biophysical research communications*, 325(1):133–143.

[Derré et al., 2008] Derré, L., Bruyninx, M., Baumgaertner, P., Ferber, M., Schmid, D., Leimgruber, A., Zoete, V., Romero, P., Michielin, O., Speiser, D. E., and Rufer, N. (2008). Distinct sets of alphabeta tcrs confer similar recognition of tumor antigen ny-eso-1157-165 by interacting with its central met/trp residues. *Proceedings of the National Academy of Sciences of the United States of America*, 105(39):15010–15015.

[Di Bartolo et al., 1999] Di Bartolo, V., Mege, D., Germain, V., Pelosi, M., Dufour, E., Michel, F., Magistrelli, G., Isacchi, A., and Acuto, O. (1999). Tyrosine 319, a newly identified phosphorylation site of ZAP-70, plays a critical role in T cell antigen receptor signaling. *J. Biol. Chem.*, 274(10):6285–6294.

[Di Bartolo et al., 2007] Di Bartolo, V., Montagne, B., Salek, M., Jungwirth, B., Carrette, F., Fourtane, J., Sol-Foulon, N., Michel, F., Schwartz,

O., Lehmann, W. D., and Acuto, O. (2007). A novel pathway down-modulating T cell activation involves HPK-1-dependent recruitment of 14-3-3 proteins on SLP-76. *J. Exp. Med.*, 204(3):681–691.

[Dower et al., 2000] Dower, N. A., Stang, S. L., Bottorff, D. A., Ebinu, J. O., Dickie, P., Ostergaard, H. L., and Stone, J. C. (2000). RasGRP is essential for mouse thymocyte differentiation and TCR signaling. *Nat. Immunol.*, 1(4):317–321.

[Duncia et al., 1998] Duncia, J. V., Santella, J. B., Higley, C. A., Pitts, W. J., Wityak, J., Frietze, W. E., Rankin, F. W., Sun, J. H., Earl, R. A., Tabaka, A. C., Teleha, C. A., Blom, K. F., Favata, M. F., Manos, E. J., Daulerio, A. J., Stradley, D. A., Horiuchi, K., Copeland, R. A., Scherle, P. A., Trzaskos, J. M., Magolda, R. L., Trainor, G. L., Wexler, R. R., Hobbs, F. W., and Olson, R. E. (1998). Mek inhibitors: the chemistry and biological activity of u0126, its analogs, and cyclization products. *Bioorganic & medicinal chemistry letters*, 8(20):2839–2844.

[Dushek et al., 2011] Dushek, O., Aleksic, M., Wheeler, R. J., Zhang, H., Cordoba, S.-P., Peng, Y.-C., Chen, J.-L., Cerundolo, V., Dong, T., Coombs, D., and van der Merwe, P. A. (2011). Antigen potency and maximal efficacy reveal a mechanism of efficient t cell activation. *Science signaling*, 4(176):ra39.

[Dustin, 2008] Dustin, M. L. (2008). T-cell activation through immunological synapses and kinapses. *Immunological reviews*, 221:77–89.

[Dustin and Long, 2010] Dustin, M. L. and Long, E. O. (2010). Cytotoxic immunological synapses. *Immunological reviews*, 235(1):24–34.

[Dutoit et al., 2002a] Dutoit, V., Guillaume, P., Cerottini, J. C., Romero, P., and Valmori, D. (2002a). Dissecting tcr-mhc/peptide complex interactions with a2/peptide multimers incorporating tumor antigen peptide variants: crucial role of interaction kinetics on functional outcomes. *Eur J Immunol*, 32(11):3285–3293.

[Dutoit et al., 2002b] Dutoit, V., Taub, R. N., Papadopoulos, K. P., Talbot, S., Keohan, M. L., Brehm, M., Gnjatic, S., Harris, P. E., Bisikirska, B., Guillaume, P., Cerottini, J. C., Hesdorffer, C. S., Old, L. J., and Valmori, D. (2002b). Multiepitope cd8(+) t cell response to a ny-eso-1 peptide vaccine results in imprecise tumor targeting. *J Clin Invest*, 110(12):1813–1822.

[Ebinu et al., 2000] Ebinu, J. O., Stang, S. L., Teixeira, C., Bottorff, D. A., Hooton, J., Blumberg, P. M., Barry, M., Bleakley, R. C., Ostergaard, H. L., and Stone, J. C. (2000). RasGRP links T-cell receptor signaling to Ras. *Blood*, 95(10):3199–3203.

[Egan et al., 1993] Egan, S. E., Giddings, B. W., Brooks, M. W., Buday, L., Sizeland, A. M., and Weinberg, R. A. (1993). Association of sos ras exchange protein with grb2 is implicated in tyrosine kinase signal transduction and transformation. *Nature*, 363(6424):45–51.

[Fang et al., 1996] Fang, N., Motto, D. G., Ross, S. E., and Koretzky, G. A. (1996). Tyrosines 113, 128, and 145 of SLP-76 are required for optimal augmentation of NFAT promoter activity. *J. Immunol.*, 157(9):3769–3773.

[Ferrell and Machleder, 1998] Ferrell, J. E. and Machleder, E. M. (1998). The biochemical basis of an all-or-none cell fate switch in xenopus oocytes. *Science (New York, N.Y.)*, 280(5365):895–898.

[Feske, 2007] Feske, S. (2007). Calcium signalling in lymphocyte activation and disease. *Nat. Rev. Immunol.*, 7(9):690–702.

[Finco et al., 1998] Finco, T. S., Kadlecek, T., Zhang, W., Samelson, L. E., and Weiss, A. (1998). LAT is required for TCR-mediated activation of PLCgamma1 and the Ras pathway. *Immunity*, 9(5):617–626.

[Fink and Hendricks, 2011] Fink, P. J. and Hendricks, D. W. (2011). Post-thymic maturation: young t cells assert their individuality. *Nature reviews. Immunology*, 11(8):544–549.

[Flajnik and Kasahara, 2010] Flajnik, M. F. and Kasahara, M. (2010). Origin and evolution of the adaptive immune system: genetic events and selective pressures. *Nature reviews. Genetics*, 11(1):47–59.

[Fremont et al., 1996] Fremont, D. H., Hendrickson, W. A., Marrack, P., and Kappler, J. (1996). Structures of an MHC class II molecule with covalently bound single peptides. *Science*, 272(5264):1001–1004.

[Friedman et al., 2012] Friedman, K. M., Prieto, P. A., Devillier, L. E., Gross, C. A., Yang, J. C., Wunderlich, J. R., Rosenberg, S. A., and Dudley, M. E. (2012). Tumor-specific cd4+ melanoma tumor-infiltrating lymphocytes. *Journal of immunotherapy (Hagerstown, Md. : 1997)*, 35(5):400–408.

[Fu et al., 2009] Fu, G., Vallée, S., Rybakin, V., McGuire, M. V., Ampudia, J., Brockmeyer, C., Salek, M., Fallen, P. R., Hoerter, J. A. H., Munshi, A., Huang, Y. H., Hu, J., Fox, H. S., Sauer, K., Acuto, O., and Gascoigne, N. R. J. (2009). Themis controls thymocyte selection through regulation of t cell antigen receptor-mediated signaling. *Nature immunology*, 10(8):848–856.

[Gagnon et al., 2012] Gagnon, E., Schubert, D. A., Gordo, S., Chu, H. H., and Wucherpfennig, K. W. (2012). Local changes in lipid environment of tcr microclusters regulate membrane binding by the cd3ϵ cytoplasmic domain. *The Journal of experimental medicine*, 209(13):2423–2439.

[Garcia et al., 1996] Garcia, K. C., Degano, M., Stanfield, R. L., Brunmark, A., Jackson, M. R., Peterson, P. A., Teyton, L., and Wilson, I. A. (1996). An alphabeta t cell receptor structure at 2.5 a and its orientation in the tcr-mhc complex. *Science (New York, N.Y.)*, 274(5285):209–219.

[Gascoigne et al., 1984] Gascoigne, N. R., Chien, Y., Becker, D. M., Kavaler, J., and Davis, M. M. (1984). Genomic organization and sequence of T-cell receptor beta-chain constant- and joining-region genes. *Nature*, 310(5976):387–391.

[Gascoigne and Palmer, 2011] Gascoigne, N. R. J. and Palmer, E. (2011). Signaling in thymic selection. *Current opinion in immunology*, 23(2):207–212.

[Genot and Cantrell, 2000] Genot, E. and Cantrell, D. A. (2000). Ras regulation and function in lymphocytes. *Curr. Opin. Immunol.*, 12(3):289–294.

[Genot et al., 1995] Genot, E. M., Parker, P. J., and Cantrell, D. A. (1995). Analysis of the role of protein kinase c-alpha, -epsilon, and -zeta in t cell activation. *The Journal of biological chemistry*, 270(17):9833–9839.

[Germain, 2001] Germain, R. N. (2001). The t cell receptor for antigen: signaling and ligand discrimination. *J Biol Chem*, 276(38):35223–35226.

[Germain, 2002] Germain, R. N. (2002). T-cell development and the cd4-cd8 lineage decision. *Nat Rev Immunol*, 2(5):309–322.

[Gil et al., 2002] Gil, D., Schamel, W. W., Montoya, M., Sanchez-Madrid, F., and Alarcon, B. (2002). Recruitment of Nck by CD3 epsilon reveals a ligand-induced conformational change essential for T cell receptor signaling and synapse formation. *Cell*, 109(7):901–912.

[Gottschalk et al., 2010] Gottschalk, R. A., Corse, E., and Allison, J. P. (2010). Tcr ligand density and affinity determine peripheral induction of foxp3 in vivo. *The Journal of experimental medicine*, 207(8):1701–1711.

[Gottschalk et al., 2012] Gottschalk, R. A., Hathorn, M. M., Beuneu, H., Corse, E., Dustin, M. L., Altan-Bonnet, G., and Allison, J. P. (2012). Distinct influences of peptide-mhc quality and quantity on in vivo t-cell responses. *Proceedings of the National Academy of Sciences of the United States of America*, 109(3):881–886.

[Gourley et al., 2004] Gourley, T. S., Wherry, E. J., Masopust, D., and Ahmed, R. (2004). Generation and maintenance of immunological memory. *Semin. Immunol.*, 16(5):323–333.

[Gratz et al., 2013] Gratz, I. K., Rosenblum, M. D., and Abbas, A. K. (2013). The life of regulatory t cells. *Annals of the New York Academy of Sciences*, 1283:8–12.

[Green, 1975] Green, N. M. (1975). Avidin. *Advances in protein chemistry*, 29:85–133.

[Haas et al., 2008] Haas, A., Weckbecker, G., and Welzenbach, K. (2008). Intracellular phospho-flow cytometry reveals novel insights into tcr proximal signaling events. a comparison with western blot. *Cytometry. Part A : the journal of the International Society for Analytical Cytology*, 73(9):799–807.

[Hanahan and Weinberg, 2011] Hanahan, D. and Weinberg, R. A. (2011). Hallmarks of cancer: the next generation. *Cell*, 144(5):646–674.

[Harada et al., 2001] Harada, M., Li, Y. F., El-Gamil, M., Ohnmacht, G. A., Rosenberg, S. A., and Robbins, P. F. (2001). Melanoma-reactive cd8+ t cells recognize a novel tumor antigen expressed in a wide variety of tumor types. *Journal of immunotherapy (Hagerstown, Md. : 1997)*, 24(4):323–333.

[Hashemi et al., 1999] Hashemi, B. B., Penkala, J. E., Vens, C., Huls, H., Cubbage, M., and Sams, C. F. (1999). T cell activation responses are differentially regulated during clinorotation and in spaceflight. *FASEB journal : official publication of the Federation of American Societies for Experimental Biology*, 13(14):2071–2082.

[Haskins et al., 1983] Haskins, K., Kubo, R., White, J., Pigeon, M., Kappler, J., and Marrack, P. (1983). The major histocompatibility complex-restricted antigen receptor on t cells. i. isolation with a monoclonal antibody. *The Journal of experimental medicine*, 157(4):1149–1169.

[Hogan et al., 2010] Hogan, P. G., Lewis, R. S., and Rao, A. (2010). Molecular basis of calcium signaling in lymphocytes: STIM and ORAI. *Annu. Rev. Immunol.*, 28:491–533.

[Hogquist et al., 2005] Hogquist, K. A., Baldwin, T. A., and Jameson, S. C. (2005). Central tolerance: learning self-control in the thymus. *Nat. Rev. Immunol.*, 5(10):772–782.

[Houston et al., 2012] Houston, E. G., Boursalian, T. E., and Fink, P. J. (2012). Homeostatic signals do not drive post-thymic t cell maturation. *Cellular immunology*, 274(1-2):39–45.

[Howarth et al., 2006] Howarth, M., Chinnapen, D. J.-F., Gerrow, K., Dorrestein, P. C., Grandy, M. R., Kelleher, N. L., El-Husseini, A., and Ting, A. Y. (2006). A monovalent streptavidin with a single femtomolar biotin binding site. *Nature methods*, 3(4):267–273.

[Hsieh et al., 2006] Hsieh, C.-S., Zheng, Y., Liang, Y., Fontenot, J. D., and Rudensky, A. Y. (2006). An intersection between the self-reactive regulatory and nonregulatory t cell receptor repertoires. *Nature immunology*, 7(4):401–410.

[Huang et al., 2010] Huang, J., Zarnitsyna, V. I., Liu, B., Edwards, L. J., Jiang, N., Evavold, B. D., and Zhu, C. (2010). The kinetics of two-dimensional TCR and pMHC interactions determine T-cell responsiveness. *Nature*, 464(7290):932–936.

[Huang et al., 2012] Huang, Y.-H., Sojka, D. K., and Fowell, D. J. (2012). Cutting edge: Regulatory t cells selectively attenuate, not terminate, t cell signaling by disrupting nf-κb nuclear accumulation in cd4 t cells. *Journal of immunology (Baltimore, Md. : 1950)*, 188(3):947–951.

[Huby et al., 1997] Huby, R. D., Iwashima, M., Weiss, A., and Ley, S. C. (1997). ZAP-70 protein tyrosine kinase is constitutively targeted to the T cell cortex independently of its SH2 domains. *J. Cell Biol.*, 137(7):1639–1649.

[Huppa and Davis, 2003] Huppa, J. B. and Davis, M. M. (2003). T-cell-antigen recognition and the immunological synapse. *Nat. Rev. Immunol.*, 3(12):973–983.

[Hutchinson et al., 2003] Hutchinson, S. L., Wooldridge, L., Tafuro, S., Laugel, B., Glick, M., Boulter, J. M., Jakobsen, B. K., Price, D. A., and

Sewell, A. K. (2003). The cd8 t cell coreceptor exhibits disproportionate biological activity at extremely low binding affinities. *The Journal of biological chemistry*, 278(27):24285–24293.

[Hwang et al., 2012] Hwang, S., Song, K.-D., Lesourne, R., Lee, J., Pinkhasov, J., Li, L., El-Khoury, D., and Love, P. E. (2012). Reduced tcr signaling potential impairs negative selection but does not result in autoimmune disease. *The Journal of experimental medicine*, 209(10):1781–1795.

[Irvine et al., 2002] Irvine, D. J., Purbhoo, M. A., Krogsgaard, M., and Davis, M. M. (2002). Direct observation of ligand recognition by t cells. *Nature*, 419(6909):845–849.

[Irving et al., 2012] Irving, M., Zoete, V., Hebeisen, M., Schmid, D., Baumgartner, P., Guillaume, P., Romero, P., Speiser, D., Luescher, I., Rufer, N., and Michielin, O. (2012). Interplay between t cell receptor binding kinetics and the level of cognate peptide presented by major histocompatibility complexes governs cd8+ t cell responsiveness. *J Biol Chem*, 287(27):23068–23078.

[Isakov and Altman, 2012] Isakov, N. and Altman, A. (2012). Pkc-theta-mediated signal delivery from the tcr/cd28 surface receptors. *Frontiers in immunology*, 3:273.

[Itoh et al., 1999] Itoh, Y., Hemmer, B., Martin, R., and Germain, R. N. (1999). Serial TCR engagement and down-modulation by peptide:MHC molecule ligands: relationship to the quality of individual TCR signaling events. *J. Immunol.*, 162(4):2073–2080.

[Jackman et al., 1995] Jackman, J. K., Motto, D. G., Sun, Q., Tanemoto, M., Turck, C. W., Peltz, G. A., Koretzky, G. A., and Findell, P. R. (1995). Molecular cloning of SLP-76, a 76-kDa tyrosine phosphoprotein associated with Grb2 in T cells. *J. Biol. Chem.*, 270(13):7029–7032.

[Janeway, 1992] Janeway, C. A. (1992). The t cell receptor as a multicomponent signalling machine: Cd4/cd8 coreceptors and cd45 in t cell activation. *Annual review of immunology*, 10:645–674.

[Jang et al., 2010] Jang, I. K., Zhang, J., Chiang, Y. J., Kole, H. K., Cronshaw, D. G., Zou, Y., and Gu, H. (2010). Grb2 functions at the top of the t-cell antigen receptor-induced tyrosine kinase cascade to control thymic selection. *Proceedings of the National Academy of Sciences of the United States of America*, 107(23):10620–10625.

[Jenkins et al., 2009] Jenkins, M. R., Tsun, A., Stinchcombe, J. C., and Griffiths, G. M. (2009). The strength of t cell receptor signal controls the polarization of cytotoxic machinery to the immunological synapse. *Immunity*, 31(4):621–631.

[Johnson et al., 2009] Johnson, A. L., Aravind, L., Shulzhenko, N., Morgun, A., Choi, S.-Y., Crockford, T. L., Lambe, T., Domaschenz, H., Kucharska, E. M., Zheng, L., Vinuesa, C. G., Lenardo, M. J., Goodnow, C. C., Cornall, R. J., and Schwartz, R. H. (2009). Themis is a member of a new metazoan gene family and is required for the completion of thymocyte positive selection. *Nature immunology*, 10(8):831–839.

[Johnson et al., 2013] Johnson, D. J., Pao, L. I., Dhanji, S., Murakami, K., Ohashi, P. S., and Neel, B. G. (2013). Shp1 regulates T cell homeostasis by limiting IL-4 signals. *J. Exp. Med.*, 210(7):1419–1431.

[Jorgensen et al., 1992] Jorgensen, J. L., Esser, U., Fazekas de St Groth, B., Reay, P. A., and Davis, M. M. (1992). Mapping T-cell receptor-peptide contacts by variant peptide immunization of single-chain transgenics. *Nature*, 355(6357):224–230.

[Joshi et al., 2007] Joshi, N. S., Cui, W., Chandele, A., Lee, H. K., Urso, D. R., Hagman, J., Gapin, L., and Kaech, S. M. (2007). Inflammation directs memory precursor and short-lived effector cd8(+) t cell fates via the graded expression of t-bet transcription factor. *Immunity*, 27(2):281–295.

[Kakugawa et al., 2009] Kakugawa, K., Yasuda, T., Miura, I., Kobayashi, A., Fukiage, H., Satoh, R., Matsuda, M., Koseki, H., Wakana, S., Kawamoto, H., and Yoshida, H. (2009). A novel gene essential for the development of single positive thymocytes. *Molecular and cellular biology*, 29(18):5128–5135.

[Kalergis et al., 2001] Kalergis, A. M., Boucheron, N., Doucey, M. A., Palmieri, E., Goyarts, E. C., Vegh, Z., Luescher, I. F., and Nathenson, S. G. (2001). Efficient t cell activation requires an optimal dwell-time of interaction between the tcr and the pmhc complex. *Nature immunology*, 2(3):229–234.

[Kalland et al., 2011] Kalland, M. E., Oberprieler, N. G., Vang, T., Taskén, K., and Torgersen, K. M. (2011). T cell-signaling network analysis reveals distinct differences between cd28 and cd2 costimulation responses

in various subsets and in the mapk pathway between resting and activated regulatory t cells. *Journal of immunology (Baltimore, Md. : 1950)*, 187(10).

[Kamioka et al., 2010] Kamioka, Y., Yasuda, S., Fujita, Y., Aoki, K., and Matsuda, M. (2010). Multiple decisive phosphorylation sites for the negative feedback regulation of SOS1 via ERK. *J. Biol. Chem.*, 285(43):33540–33548.

[Karlsson et al., 2006] Karlsson, M., Mandl, M., and Keyse, S. M. (2006). Spatio-temporal regulation of mitogen-activated protein kinase (MAPK) signalling by protein phosphatases. *Biochem. Soc. Trans.*, 34(Pt 5):842–845.

[Kasamatsu, 2013] Kasamatsu, J. (2013). Evolution of innate and adaptive immune systems in jawless vertebrates. *Microbiology and immunology*, 57(1):1–12.

[Kern et al., 1999] Kern, P., Hussey, R. E., Spoerl, R., Reinherz, E. L., and Chang, H. C. (1999). Expression, purification, and functional analysis of murine ectodomain fragments of cd8alphaalpha and cd8alphabeta dimers. *The Journal of biological chemistry*, 274(38):27237–27243.

[Kersh et al., 1998] Kersh, G. J., Kersh, E. N., Fremont, D. H., and Allen, P. M. (1998). High- and low-potency ligands with similar affinities for the TCR: the importance of kinetics in TCR signaling. *Immunity*, 9(6):817–826.

[Kim et al., 2012] Kim, S. T., Shin, Y., Brazin, K., Mallis, R. J., Sun, Z. Y., Wagner, G., Lang, M. J., and Reinherz, E. L. (2012). TCR Mechanobiology: Torques and Tunable Structures Linked to Early T Cell Signaling. *Front Immunol*, 3:76.

[Kim et al., 2009] Kim, S. T., Takeuchi, K., Sun, Z. Y., Touma, M., Castro, C. E., Fahmy, A., Lang, M. J., Wagner, G., and Reinherz, E. L. (2009). The alphabeta T cell receptor is an anisotropic mechanosensor. *J. Biol. Chem.*, 284(45):31028–31037.

[Kindt et al., 2007] Kindt, T. J., Goldsby, R. A., and Osborne, B. A. (2007). *Kuby Immunology*. W.H. Freeman and Company, New York.

[King et al., 2012] King, C. G., Koehli, S., Hausmann, B., Schmaler, M., Zehn, D., and Palmer, E. (2012). T cell affinity regulates asymmetric division, effector cell differentiation, and tissue pathology. *Immunity*, 37(4):709–720.

[Kjer-Nielsen et al., 2003] Kjer-Nielsen, L., Clements, C. S., Purcell, A. W., Brooks, A. G., Whisstock, J. C., Burrows, S. R., McCluskey, J., and Rossjohn, J. (2003). A structural basis for the selection of dominant alphabeta T cell receptors in antiviral immunity. *Immunity*, 18(1):53–64.

[Klenerman et al., 2002] Klenerman, P., Cerundolo, V., and Dunbar, P. R. (2002). Tracking t cells with tetramers: new tales from new tools. *Nature reviews. Immunology*, 2(4):263–272.

[Kliche et al., 2006] Kliche, S., Breitling, D., Togni, M., Pusch, R., Heuer, K., Wang, X., Freund, C., Kasirer-Friede, A., Menasche, G., Koretzky, G. A., and Schraven, B. (2006). The ADAP/SKAP55 signaling module regulates T-cell receptor-mediated integrin activation through plasma membrane targeting of Rap1. *Mol. Cell. Biol.*, 26(19):7130–7144.

[Kobayashi and van den Elsen, 2012] Kobayashi, K. S. and van den Elsen, P. J. (2012). Nlrc5: a key regulator of mhc class i-dependent immune responses. *Nat Rev Immunol*, 12(12):813–820.

[König, 2002] König, R. (2002). Interactions between mhc molecules and co-receptors of the tcr. *Current opinion in immunology*, 14(1):75–83.

[Kortum et al., 2013] Kortum, R. L., Rouquette-Jazdanian, A. K., and Samelson, L. E. (2013). Ras and extracellular signal-regulated kinase signaling in thymocytes and t cells. *Trends in immunology*, 34(6):259–268.

[Kortum et al., 2011] Kortum, R. L., Sommers, C. L., Alexander, C. P., Pinski, J. M., Li, W., Grinberg, A., Lee, J., Love, P. E., and Samelson, L. E. (2011). Targeted Sos1 deletion reveals its critical role in early T-cell development. *Proc. Natl. Acad. Sci. U.S.A.*, 108(30):12407–12412.

[Kortum et al., 2012] Kortum, R. L., Sommers, C. L., Pinski, J. M., Alexander, C. P., Merrill, R. K., Li, W., Love, P. E., and Samelson, L. E. (2012). Deconstructing Ras signaling in the thymus. *Mol. Cell. Biol.*, 32(14):2748–2759.

[Krammer, 2000] Krammer, P. H. (2000). Cd95's deadly mission in the immune system. *Nature*, 407(6805):789–795.

[Krammer et al., 2007] Krammer, P. H., Arnold, R., and Lavrik, I. N. (2007). Life and death in peripheral t cells. *Nature reviews. Immunology*, 7(7):532–542.

[Krogsgaard and Davis, 2005] Krogsgaard, M. and Davis, M. M. (2005). How t cells 'see' antigen. *Nature immunology*, 6(3):239–245.

[Krogsgaard et al., 2003] Krogsgaard, M., Prado, N., Adams, E. J., He, X.-l., Chow, D.-C., Wilson, D. B., Garcia, K. C., and Davis, M. M. (2003). Evidence that structural rearrangements and/or flexibility during tcr binding can contribute to t cell activation. *Molecular cell*, 12(6):1367–1378.

[Krummel et al., 2000] Krummel, M. F., Sjaastad, M. D., Wülfing, C., and Davis, M. M. (2000). Differential clustering of cd4 and cd3zeta during t cell recognition. *Science (New York, N.Y.)*, 289(5483):1349–1352.

[Kuhns and Davis, 2012] Kuhns, M. S. and Davis, M. M. (2012). TCR Signaling Emerges from the Sum of Many Parts. *Front Immunol*, 3:159.

[Kuhns et al., 2006] Kuhns, M. S., Davis, M. M., and Garcia, K. C. (2006). Deconstructing the form and function of the tcr/cd3 complex. *Immunity*, 24(2):133–139.

[Labrecque et al., 2011] Labrecque, N., Baldwin, T., and Lesage, S. (2011). Molecular and genetic parameters defining t-cell clonal selection. *Immunology and cell biology*, 89(1):16–26.

[Labrecque et al., 2001] Labrecque, N., Whitfield, L. S., Obst, R., Waltzinger, C., Benoist, C., and Mathis, D. (2001). How much tcr does a t cell need? *Immunity*, 15(1):71–82.

[Lam Hui et al., 2012] Lam Hui, K., Wang, C., Grooman, B., Wayt, J., and Upadhyaya, A. (2012). Membrane dynamics correlate with formation of signaling clusters during cell spreading. *Biophysical journal*, 102(7):1524–1533.

[Lasserre et al., 2011] Lasserre, R., Cuche, C., Blecher-Gonen, R., Libman, E., Biquand, E., Danckaert, A., Yablonski, D., Alcover, A., and Di Bartolo, V. (2011). Release of serine/threonine-phosphorylated adaptors from signaling microclusters down-regulates t cell activation. *The Journal of cell biology*, 195(5):839–853.

[Lee et al., 2002] Lee, K. H., Holdorf, A. D., Dustin, M. L., Chan, A. C., Allen, P. M., and Shaw, A. S. (2002). T cell receptor signaling precedes immunological synapse formation. *Science*, 295(5559):1539–1542.

[Leishman et al., 2001] Leishman, A. J., Naidenko, O. V., Attinger, A., Koning, F., Lena, C. J., Xiong, Y., Chang, H. C., Reinherz, E., Kronenberg,

M., and Cheroutre, H. (2001). T cell responses modulated through interaction between cd8alphaalpha and the nonclassical mhc class i molecule, tl. *Science (New York, N.Y.)*, 294(5548):1936–1939.

[Lesourne et al., 2009] Lesourne, R., Uehara, S., Lee, J., Song, K.-D., Li, L., Pinkhasov, J., Zhang, Y., Weng, N.-P., Wildt, K. F., Wang, L., Bosselut, R., and Love, P. E. (2009). Themis, a t cell-specific protein important for late thymocyte development. *Nature immunology*, 10(8):840–847.

[Lesourne et al., 2012] Lesourne, R., Zvezdova, E., Song, K.-D., El-Khoury, D., Uehara, S., Barr, V. A., Samelson, L. E., and Love, P. E. (2012). Interchangeability of themis1 and themis2 in thymocyte development reveals two related proteins with conserved molecular function. *Journal of immunology (Baltimore, Md. : 1950)*, 189(3).

[Lewis, 2007] Lewis, R. S. (2007). The molecular choreography of a store-operated calcium channel. *Nature*, 446(7133):284–287.

[Li et al., 2013] Li, Y., Yin, Y., and Mariuzza, R. A. (2013). Structural and biophysical insights into the role of cd4 and cd8 in t cell activation. *Frontiers in immunology*, 4:206.

[Li-Weber and Krammer, 2003] Li-Weber, M. and Krammer, P. H. (2003). Function and regulation of the cd95 (apo-1/fas) ligand in the immune system. *Seminars in immunology*, 15(3):145–157.

[Lillemeier et al., 2010] Lillemeier, B. F., Mörtelmaier, M. A., Forstner, M. B., Huppa, J. B., Groves, J. T., and Davis, M. M. (2010). Tcr and lat are expressed on separate protein islands on t cell membranes and concatenate during activation. *Nature immunology*, 11(1):90–96.

[Liu et al., 2000] Liu, L. F., Desai, S. D., Li, T. K., Mao, Y., Sun, M., and Sim, S. P. (2000). Mechanism of action of camptothecin. *Annals of the New York Academy of Sciences*, 922:1–10.

[Liu et al., 1999] Liu, S. K., Fang, N., Koretzky, G. A., and McGlade, C. J. (1999). The hematopoietic-specific adaptor protein gads functions in T-cell signaling via interactions with the SLP-76 and LAT adaptors. *Curr. Biol.*, 9(2):67–75.

[Lo et al., 2012] Lo, W.-L., Donermeyer, D. L., and Allen, P. M. (2012). A voltage-gated sodium channel is essential for the positive selection of cd4(+) t cells. *Nature immunology*, 13(9):880–887.

[Lyons et al., 1996] Lyons, D. S., Lieberman, S. A., Hampl, J., Boniface, J. J., Chien, Y., Berg, L. J., and Davis, M. M. (1996). A TCR binds to antagonist ligands with lower affinities and faster dissociation rates than to agonists. *Immunity*, 5(1):53–61.

[Macian, 2005] Macian, F. (2005). NFAT proteins: key regulators of T-cell development and function. *Nat. Rev. Immunol.*, 5(6):472–484.

[MacLeod et al., 2010] MacLeod, M. K., Kappler, J. W., and Marrack, P. (2010). Memory CD4 T cells: generation, reactivation and re-assignment. *Immunology*, 130(1):10–15.

[Magombedze et al., 2013] Magombedze, G., Reddy, P. B. J., Eda, S., and Ganusov, V. V. (2013). Cellular and population plasticity of helper cd4(+) t cell responses. *Frontiers in physiology*, 4:206.

[Manolios et al., 1994] Manolios, N., Kemp, O., and Li, Z. G. (1994). The t cell antigen receptor alpha and beta chains interact via distinct regions with cd3 chains. *European journal of immunology*, 24(1):84–92.

[Marzio et al., 1999] Marzio, R., Mauël, J., and Betz-Corradin, S. (1999). Cd69 and regulation of the immune function. *Immunopharmacology and immunotoxicology*, 21(3):565–582.

[McKeithan, 1995] McKeithan, T. W. (1995). Kinetic proofreading in T-cell receptor signal transduction. *Proc. Natl. Acad. Sci. U.S.A.*, 92(11):5042–5046.

[McNeill et al., 2007] McNeill, L., Salmond, R. J., Cooper, J. C., Carret, C. K., Cassady-Cain, R. L., Roche-Molina, M., Tandon, P., Holmes, N., and Alexander, D. R. (2007). The differential regulation of lck kinase phosphorylation sites by cd45 is critical for t cell receptor signaling responses. *Immunity*, 27(3):425–437.

[Mempel et al., 2004] Mempel, T. R., Henrickson, S. E., and Von Andrian, U. H. (2004). T-cell priming by dendritic cells in lymph nodes occurs in three distinct phases. *Nature*, 427(6970):154–159.

[Meuer et al., 1983a] Meuer, S. C., Acuto, O., Hussey, R. E., Hodgdon, J. C., Fitzgerald, K. A., Schlossman, S. F., and Reinherz, E. L. (1983a). Evidence for the T3-associated 90K heterodimer as the T-cell antigen receptor. *Nature*, 303(5920):808–810.

[Meuer et al., 1983b] Meuer, S. C., Hodgdon, J. C., Hussey, R. E., Protentis, J. P., Schlossman, S. F., and Reinherz, E. L. (1983b). Antigen-like effects of monoclonal antibodies directed at receptors on human T cell clones. *J. Exp. Med.*, 158(3):988–993.

[Michel et al., 2001] Michel, F., Attal-Bonnefoy, G., Mangino, G., Mise-Omata, S., and Acuto, O. (2001). CD28 as a molecular amplifier extending TCR ligation and signaling capabilities. *Immunity*, 15(6):935–945.

[Miller et al., 2003] Miller, M. J., Wei, S. H., Cahalan, M. D., and Parker, I. (2003). Autonomous T cell trafficking examined in vivo with intravital two-photon microscopy. *Proc. Natl. Acad. Sci. U.S.A.*, 100(5):2604–2609.

[Miller et al., 2002] Miller, M. J., Wei, S. H., Parker, I., and Cahalan, M. D. (2002). Two-photon imaging of lymphocyte motility and antigen response in intact lymph node. *Science*, 296(5574):1869–1873.

[Monks et al., 1997] Monks, C. R., Kupfer, H., Tamir, I., Barlow, A., and Kupfer, A. (1997). Selective modulation of protein kinase C-theta during T-cell activation. *Nature*, 385(6611):83–86.

[Morris and Allen, 2012] Morris, G. P. and Allen, P. M. (2012). How the tcr balances sensitivity and specificity for the recognition of self and pathogens. *Nature immunology*, 13(2):121–128.

[Motto et al., 1996] Motto, D. G., Musci, M. A., Ross, S. E., and Koretzky, G. A. (1996). Tyrosine phosphorylation of Grb2-associated proteins correlates with phospholipase C gamma 1 activation in T cells. *Mol. Cell. Biol.*, 16(6):2823–2829.

[Mrass et al., 2006] Mrass, P., Takano, H., Ng, L. G., Daxini, S., Lasaro, M. O., Iparraguirre, A., Cavanagh, L. L., von Andrian, U. H., Ertl, H. C., Haydon, P. G., and Weninger, W. (2006). Random migration precedes stable target cell interactions of tumor-infiltrating T cells. *J. Exp. Med.*, 203(12):2749–2761.

[Murphy et al., 2008] Murphy, K., Travers, P., and Walport, M. (2008). *Janeway's Immunobiology*. Garland Science, New York and London.

[Muzio et al., 1998] Muzio, M., Stockwell, B. R., Stennicke, H. R., Salvesen, G. S., and Dixit, V. M. (1998). An induced proximity model for caspase-8 activation. *The Journal of biological chemistry*, 273(5):2926–2930.

[Neveu et al., 2006] Neveu, B., Echasserieau, K., Hill, T., Kuus-Reichel, K., Houssaint, E., Bonneville, M., and Saulquin, X. (2006). Impact of cd8-mhc class i interaction in detection and sorting efficiencies of antigen-specific t cells using mhc class i/peptide multimers: contribution of pmhc valency. *International immunology*, 18(7):1139–1145.

[Nika et al., 2010] Nika, K., Soldani, C., Salek, M., Paster, W., Gray, A., Etzensperger, R., Fugger, L., Polzella, P., Cerundolo, V., Dushek, O., Höfer, T., Viola, A., and Acuto, O. (2010). Constitutively active lck kinase in t cells drives antigen receptor signal transduction. *Immunity*, 32(6):766–777.

[Northrop and Shen, 2004] Northrop, J. K. and Shen, H. (2004). Cd8+ t-cell memory: only the good ones last. *Current opinion in immunology*, 16(4):451–455.

[Obar et al., 2008] Obar, J. J., Khanna, K. M., and Lefrancois, L. (2008). Endogenous naive CD8+ T cell precursor frequency regulates primary and memory responses to infection. *Immunity*, 28(6):859–869.

[Offringa, 2009] Offringa, R. (2009). Antigen choice in adoptive T-cell therapy of cancer. *Curr. Opin. Immunol.*, 21(2):190–199.

[Oh et al., 2011] Oh, H. M., Yu, C. R., Golestaneh, N., Amadi-Obi, A., Lee, Y. S., Eseonu, A., Mahdi, R. M., and Egwuagu, C. E. (2011). STAT3 protein promotes T-cell survival and inhibits interleukin-2 production through up-regulation of Class O Forkhead transcription factors. *J. Biol. Chem.*, 286(35):30888–30897.

[Oh-hora and Rao, 2008] Oh-hora, M. and Rao, A. (2008). Calcium signaling in lymphocytes. *Curr. Opin. Immunol.*, 20(3):250–258.

[Park et al., 2010] Park, J.-H., Adoro, S., Guinter, T., Erman, B., Alag, A. S., Catalfamo, M., Kimura, M. Y., Cui, Y., Lucas, P. J., Gress, R. E., Kubo, M., Hennighausen, L., Feigenbaum, L., and Singer, A. (2010). Signaling by intrathymic cytokines, not t cell antigen receptors, specifies cd8 lineage choice and promotes the differentiation of cytotoxic-lineage t cells. *Nature immunology*, 11(3):257–264.

[Paster et al., 2013] Paster, W., Brockmeyer, C., Fu, G., Simister, P. C., de Wet, B., Martinez-Riaño, A., Hoerter, J. A. H., Feller, S. M., Wülfing, C., Gascoigne, N. R. J., and Acuto, O. (2013). Grb2-mediated recruitment of themis to lat is essential for thymocyte development. *Journal of immunology (Baltimore, Md. : 1950)*, 190(7):3749–3756.

[Patrick et al., 2009] Patrick, M. S., Oda, H., Hayakawa, K., Sato, Y., Eshima, K., Kirikae, T., Iemura, S.-I., Shirai, M., Abe, T., Natsume, T., Sasazuki, T., and Suzuki, H. (2009). Gasp, a grb2-associating protein, is critical for positive selection of thymocytes. *Proceedings of the National Academy of Sciences of the United States of America*, 106(38):16345–16350.

[Pepper and Jenkins, 2011] Pepper, M. and Jenkins, M. K. (2011). Origins of CD4(+) effector and central memory T cells. *Nat. Immunol.*, 12(6):467–471.

[Purbhoo et al., 2001] Purbhoo, M. A., Boulter, J. M., Price, D. A., Vuidepot, A. L., Hourigan, C. S., Dunbar, P. R., Olson, K., Dawson, S. J., Phillips, R. E., Jakobsen, B. K., Bell, J. I., and Sewell, A. K. (2001). The human cd8 coreceptor effects cytotoxic t cell activation and antigen sensitivity primarily by mediating complete phosphorylation of the t cell receptor zeta chain. *The Journal of biological chemistry*, 276(35):32786–32792.

[Rebollo and Martinez-A, 1999] Rebollo, A. and Martinez-A, C. (1999). Ras proteins: recent advances and new functions. *Blood*, 94(9):2971–2980.

[Reinherz and Acuto, 2011] Reinherz, E. L. and Acuto, O. (2011). Molecular T cell biology – basic and translational challenges in the twenty-first century. *Front Immunol*, 2:3.

[Remakus and Sigal, 2013] Remakus, S. and Sigal, L. J. (2013). Memory cd8? t cell protection. *Advances in experimental medicine and biology*, 785:77–86.

[Restifo et al., 2012] Restifo, N. P., Dudley, M. E., and Rosenberg, S. A. (2012). Adoptive immunotherapy for cancer: harnessing the t cell response. *Nature reviews. Immunology*, 12(4):269–281.

[Rhee and Bae, 1997] Rhee, S. G. and Bae, Y. S. (1997). Regulation of phosphoinositide-specific phospholipase C isozymes. *J. Biol. Chem.*, 272(24):15045–15048.

[Risueño et al., 2008] Risueño, R. M., Schamel, W. W. A., and Alarcón, B. (2008). T cell receptor engagement triggers its cd3epsilon and cd3zeta subunits to adopt a compact, locked conformation. *PloS one*, 3(3):e1747.

[Rizzuto et al., 2009] Rizzuto, G. A., Merghoub, T., Hirschhorn-Cymerman, D., Liu, C., Lesokhin, A. M., Sahawneh, D., Zhong, H., Panageas, K. S.,

Perales, M. A., Altan-Bonnet, G., Wolchok, J. D., and Houghton, A. N. (2009). Self-antigen-specific CD8+ T cell precursor frequency determines the quality of the antitumor immune response. *J. Exp. Med.*, 206(4):849–866.

[Robbins et al., 2011] Robbins, P. F., Morgan, R. A., Feldman, S. A., Yang, J. C., Sherry, R. M., Dudley, M. E., Wunderlich, J. R., Nahvi, A. V., Helman, L. J., Mackall, C. L., Kammula, U. S., Hughes, M. S., Restifo, N. P., Raffeld, M., Lee, C.-C. R., Levy, C. L., Li, Y. F., El-Gamil, M., Schwarz, S. L., Laurencot, C., and Rosenberg, S. A. (2011). Tumor regression in patients with metastatic synovial cell sarcoma and melanoma using genetically engineered lymphocytes reactive with ny-eso-1. *Journal of clinical oncology : official journal of the American Society of Clinical Oncology*, 29(7):917–924.

[Rock et al., 2002] Rock, K. L., York, I. A., Saric, T., and Goldberg, A. L. (2002). Protein degradation and the generation of MHC class I-presented peptides. *Adv. Immunol.*, 80:1–70.

[Roose and Weiss, 2000] Roose, J. and Weiss, A. (2000). T cells: getting a GRP on Ras. *Nat. Immunol.*, 1(4):275–276.

[Roose et al., 2005] Roose, J. P., Mollenauer, M., Gupta, V. A., Stone, J., and Weiss, A. (2005). A diacylglycerol-protein kinase c-rasgrp1 pathway directs ras activation upon antigen receptor stimulation of t cells. *Molecular and cellular biology*, 25(11):4426–4441.

[Roose et al., 2007] Roose, J. P., Mollenauer, M., Ho, M., Kurosaki, T., and Weiss, A. (2007). Unusual interplay of two types of Ras activators, RasGRP and SOS, establishes sensitive and robust Ras activation in lymphocytes. *Mol. Cell. Biol.*, 27(7):2732–2745.

[Rosenberg et al., 1998] Rosenberg, S. A., Yang, J. C., Schwartzentruber, D. J., Hwu, P., Marincola, F. M., Topalian, S. L., Restifo, N. P., Dudley, M. E., Schwarz, S. L., Spiess, P. J., Wunderlich, J. R., Parkhurst, M. R., Kawakami, Y., Seipp, C. A., Einhorn, J. H., and White, D. E. (1998). Immunologic and therapeutic evaluation of a synthetic peptide vaccine for the treatment of patients with metastatic melanoma. *Nature medicine*, 4(3):321–327.

[Rosette et al., 2001] Rosette, C., Werlen, G., Daniels, M. A., Holman, P. O., Alam, S. M., Travers, P. J., Gascoigne, N. R., Palmer, E., and Jameson, S. C. (2001). The impact of duration versus extent of tcr occupancy on

t cell activation: a revision of the kinetic proofreading model. *Immunity*, 15(1):59–70.

[Rybakin et al., 2011] Rybakin, V., Clamme, J.-P., Ampudia, J., Yachi, P. P., and Gascoigne, N. R. J. (2011). Cd8$\alpha\alpha$ and -$\alpha\beta$ isotypes are equally recruited to the immunological synapse through their ability to bind to mhc class i. *EMBO reports*, 12(12):1251–1256.

[Rybakin and Gascoigne, 2012] Rybakin, V. and Gascoigne, N. R. J. (2012). Negative selection assay based on stimulation of t cell receptor transgenic thymocytes with peptide-mhc tetramers. *PloS one*, 7(8):e43191.

[Saini et al., 2010] Saini, M., Sinclair, C., Marshall, D., Tolaini, M., Sakaguchi, S., and Seddon, B. (2010). Regulation of zap70 expression during thymocyte development enables temporal separation of cd4 and cd8 repertoire selection at different signaling thresholds. *Science signaling*, 3(114):ra23.

[Sakaguchi, 2003] Sakaguchi, S. (2003). The origin of foxp3-expressing cd4+ regulatory t cells: thymus or periphery. *The Journal of clinical investigation*, 112(9):1310–1312.

[Samelson, 2002] Samelson, L. E. (2002). Signal transduction mediated by the T cell antigen receptor: the role of adapter proteins. *Annu. Rev. Immunol.*, 20:371–394.

[San Jose et al., 2000] San Jose, E., Borroto, A., Niedergang, F., Alcover, A., and Alarcon, B. (2000). Triggering the TCR complex causes the downregulation of nonengaged receptors by a signal transduction-dependent mechanism. *Immunity*, 12(2):161–170.

[Sanderson et al., 2012] Sanderson, N. S. R., Puntel, M., Kroeger, K. M., Bondale, N. S., Swerdlow, M., Iranmanesh, N., Yagita, H., Ibrahim, A., Castro, M. G., and Lowenstein, P. R. (2012). Cytotoxic immunological synapses do not restrict the action of interferon-γ to antigenic target cells. *Proceedings of the National Academy of Sciences of the United States of America*, 109(20):7835–7840.

[Schamel et al., 2005] Schamel, W. W., Arechaga, I., Risueno, R. M., van Santen, H. M., Cabezas, P., Risco, C., Valpuesta, J. M., and Alarcon, B. (2005). Coexistence of multivalent and monovalent TCRs explains high sensitivity and wide range of response. *J. Exp. Med.*, 202(4):493–503.

[Schatz and Ji, 2011] Schatz, D. G. and Ji, Y. (2011). Recombination centres and the orchestration of v(d)j recombination. *Nature reviews. Immunology*, 11(4):251–263.

[Schmid et al., 2010] Schmid, D. A., Irving, M. B., Posevitz, V., Hebeisen, M., Posevitz-Fejfar, A., Sarria, J.-C. F., Gomez-Eerland, R., Thome, M., Schumacher, T. N. M., Romero, P., Speiser, D. E., Zoete, V., Michielin, O., and Rufer, N. (2010). Evidence for a tcr affinity threshold delimiting maximal cd8 t cell function. *Journal of immunology (Baltimore, Md. : 1950)*, 184(9):4936–4946.

[Schneider et al., 1977] Schneider, U., Schwenk, H. U., and Bornkamm, G. (1977). Characterization of ebv-genome negative "null" and "t" cell lines derived from children with acute lymphoblastic leukemia and leukemic transformed non-hodgkin lymphoma. *International journal of cancer. Journal international du cancer*, 19(5):621–626.

[Schrum et al., 2011] Schrum, A. G., Gil, D., Turka, L. A., and Palmer, E. (2011). Physical and functional bivalency observed among TCR/CD3 complexes isolated from primary T cells. *J. Immunol.*, 187(2):870–878.

[Schumacher and Restifo, 2009] Schumacher, T. N. M. and Restifo, N. P. (2009). Adoptive t cell therapy of cancer. *Current opinion in immunology*, 21(2):187–189.

[Schwarz and Bhandoola, 2006] Schwarz, B. A. and Bhandoola, A. (2006). Trafficking from the bone marrow to the thymus: a prerequisite for thymopoiesis. *Immunological reviews*, 209:47–57.

[Shaw et al., 1990] Shaw, A. S., Chalupny, J., Whitney, J. A., Hammond, C., Amrein, K. E., Kavathas, P., Sefton, B. M., and Rose, J. K. (1990). Short related sequences in the cytoplasmic domains of cd4 and cd8 mediate binding to the amino-terminal domain of the p56lck tyrosine protein kinase. *Molecular and cellular biology*, 10(5):1853–1862.

[Shim et al., 2011] Shim, E. K., Jung, S. H., and Lee, J. R. (2011). Role of two adaptor molecules slp-76 and lat in the pi3k signaling pathway in activated t cells. *Journal of immunology (Baltimore, Md. : 1950)*, 186(5):2926–2935.

[Sigalov, 2010] Sigalov, A. B. (2010). Protein intrinsic disorder and oligomericity in cell signaling. *Mol. BioSyst.*, 6:451–461.

[Simon et al., 1993] Simon, M. A., Dodson, G. S., and Rubin, G. M. (1993). An SH3-SH2-SH3 protein is required for p21Ras1 activation and binds to sevenless and Sos proteins in vitro. *Cell*, 73(1):169–177.

[Smith-Garvin et al., 2009] Smith-Garvin, J. E., Koretzky, G. A., and Jordan, M. S. (2009). T cell activation. *Annu. Rev. Immunol.*, 27:591–619.

[Sommers et al., 2002] Sommers, C. L., Park, C. S., Lee, J., Feng, C., Fuller, C. L., Grinberg, A., Hildebrand, J. A., Lacana, E., Menon, R. K., Shores, E. W., Samelson, L. E., and Love, P. E. (2002). A LAT mutation that inhibits T cell development yet induces lymphoproliferation. *Science*, 296(5575):2040–2043.

[Sondermann et al., 2004] Sondermann, H., Soisson, S. M., Boykevisch, S., Yang, S. S., Bar-Sagi, D., and Kuriyan, J. (2004). Structural analysis of autoinhibition in the Ras activator Son of sevenless. *Cell*, 119(3):393–405.

[Spitaler and Cantrell, 2004] Spitaler, M. and Cantrell, D. A. (2004). Protein kinase C and beyond. *Nat. Immunol.*, 5(8):785–790.

[Starr et al., 2003] Starr, T. K., Jameson, S. C., and Hogquist, K. A. (2003). Positive and negative selection of T cells. *Annu. Rev. Immunol.*, 21:139–176.

[Stefanová et al., 2003] Stefanová, I., Hemmer, B., Vergelli, M., Martin, R., Biddison, W. E., and Germain, R. N. (2003). Tcr ligand discrimination is enforced by competing erk positive and shp-1 negative feedback pathways. *Nature immunology*, 4(3):248–254.

[Stone et al., 2011] Stone, J. D., Artyomov, M. N., Chervin, A. S., Chakraborty, A. K., Eisen, H. N., and Kranz, D. M. (2011). Interaction of streptavidin-based peptide-mhc oligomers (tetramers) with cell-surface tcrs. *Journal of immunology (Baltimore, Md. : 1950)*, 187(12):6281–6290.

[Stone et al., 2009] Stone, J. D., Chervin, A. S., and Kranz, D. M. (2009). T-cell receptor binding affinities and kinetics: impact on t-cell activity and specificity. *Immunology*, 126(2):165–176.

[Stritesky et al., 2012] Stritesky, G. L., Jameson, S. C., and Hogquist, K. A. (2012). Selection of self-reactive T cells in the thymus. *Annu. Rev. Immunol.*, 30:95–114.

[Sun and Kavathas, 1997] Sun, J. and Kavathas, P. B. (1997). Comparison of the roles of cd8 alpha alpha and cd8 alpha beta in interaction with mhc

class i. *Journal of immunology (Baltimore, Md. : 1950)*, 159(12):6077–6082.

[Takeuchi and Akira, 2010] Takeuchi, O. and Akira, S. (2010). Pattern recognition receptors and inflammation. *Cell*, 140(6):805–820.

[Tanchot et al., 1997] Tanchot, C., Lemonnier, F. A., Pérarnau, B., Freitas, A. A., and Rocha, B. (1997). Differential requirements for survival and proliferation of cd8 naïve or memory t cells. *Science (New York, N.Y.)*, 276(5321):2057–2062.

[Tang and Bluestone, 2008] Tang, Q. and Bluestone, J. A. (2008). The foxp3+ regulatory t cell: a jack of all trades, master of regulation. *Nature immunology*, 9(3):239–244.

[Tartaglia et al., 1993] Tartaglia, L. A., Ayres, T. M., Wong, G. H., and Goeddel, D. V. (1993). A novel domain within the 55 kd tnf receptor signals cell death. *Cell*, 74(5):845–853.

[Thomas and Brown, 1999] Thomas, M. L. and Brown, E. J. (1999). Positive and negative regulation of Src-family membrane kinases by CD45. *Immunol. Today*, 20(9):406–411.

[Thomas et al., 2011] Thomas, S., Xue, S.-A., Bangham, C. R. M., Jakobsen, B. K., Morris, E. C., and Stauss, H. J. (2011). Human t cells expressing affinity-matured tcr display accelerated responses but fail to recognize low density of mhc-peptide antigen. *Blood*, 118(2):319–329.

[Topp et al., 2003] Topp, M. S., Riddell, S. R., Akatsuka, Y., Jensen, M. C., Blattman, J. N., and Greenberg, P. D. (2003). Restoration of cd28 expression in cd28- cd8+ memory effector t cells reconstitutes antigen-induced il-2 production. *The Journal of experimental medicine*, 198(6):947–955.

[Turner et al., 1990] Turner, J. M., Brodsky, M. H., Irving, B. A., Levin, S. D., Perlmutter, R. M., and Littman, D. R. (1990). Interaction of the unique n-terminal region of tyrosine kinase p56lck with cytoplasmic domains of cd4 and cd8 is mediated by cysteine motifs. *Cell*, 60(5):755–765.

[Valitutti et al., 1995] Valitutti, S., Muller, S., Cella, M., Padovan, E., and Lanzavecchia, A. (1995). Serial triggering of many T-cell receptors by a few peptide-MHC complexes. *Nature*, 375(6527):148–151.

[van der Merwe, 2001] van der Merwe, P. A. (2001). The TCR triggering puzzle. *Immunity*, 14(6):665–668.

[Van Laethem et al., 2007] Van Laethem, F., Sarafova, S. D., Park, J.-H., Tai, X., Pobezinsky, L., Guinter, T. I., Adoro, S., Adams, A., Sharrow, S. O., Feigenbaum, L., and Singer, A. (2007). Deletion of cd4 and cd8 coreceptors permits generation of alphabetat cells that recognize antigens independently of the mhc. *Immunity*, 27(5):735–750.

[von Boehmer and Kisielow, 2006] von Boehmer, H. and Kisielow, P. (2006). Negative selection of the T-cell repertoire: where and when does it occur? *Immunol. Rev.*, 209:284–289.

[Walker et al., 2013] Walker, L. J., Marrinan, E., Muenchhoff, M., Ferguson, J., Kloverpris, H., Cheroutre, H., Barnes, E., Goulder, P., and Klenerman, P. (2013). Cd8$\alpha\alpha$ expression marks terminally differentiated human cd8+ t cells expanded in chronic viral infection. *Frontiers in immunology*, 4:223.

[Wang et al., 2012] Wang, D., Zheng, M., Lei, L., Ji, J., Yao, Y., Qiu, Y., Ma, L., Lou, J., Ouyang, C., Zhang, X., He, Y., Chi, J., Wang, L., Kuang, Y., Wang, J., Cao, X., and Lu, L. (2012). Tespa1 is involved in late thymocyte development through the regulation of tcr-mediated signaling. *Nature immunology*, 13(6):560–568.

[Wang et al., 2011] Wang, H., Zeng, X., Fan, Z., and Lim, B. (2011). Rhoh modulates pre-tcr and tcr signalling by regulating lck. *Cellular signalling*, 23(1):249–258.

[Ward and Cantrell, 2001] Ward, S. G. and Cantrell, D. A. (2001). Phosphoinositide 3-kinases in T lymphocyte activation. *Curr. Opin. Immunol.*, 13(3):332–338.

[Warnecke et al., 2012] Warnecke, N., Poltorak, M., Kowtharapu, B. S., Arndt, B., Stone, J. C., Schraven, B., and Simeoni, L. (2012). Tcr-mediated erk activation does not depend on sos and grb2 in peripheral human t cells. *EMBO reports*, 13(4):386–391.

[Weissman et al., 1988] Weissman, A. M., Baniyash, M., Hou, D., Samelson, L. E., Burgess, W. H., and Klausner, R. D. (1988). Molecular cloning of the zeta chain of the T cell antigen receptor. *Science*, 239(4843):1018–1021.

[Werlen et al., 2000] Werlen, G., Hausmann, B., and Palmer, E. (2000). A motif in the alphabeta t-cell receptor controls positive selection by modulating erk activity. *Nature*, 406(6794):422–426.

[Williams et al., 1998] Williams, B. L., Schreiber, K. L., Zhang, W., Wange, R. L., Samelson, L. E., Leibson, P. J., and Abraham, R. T. (1998). Genetic evidence for differential coupling of Syk family kinases to the T-cell receptor: reconstitution studies in a ZAP-70-deficient Jurkat T-cell line. *Mol. Cell. Biol.*, 18(3):1388–1399.

[Wu et al., 2002] Wu, L. C., Tuot, D. S., Lyons, D. S., Garcia, K. C., and Davis, M. M. (2002). Two-step binding mechanism for t-cell receptor recognition of peptide mhc. *Nature*, 418(6897):552–556.

[Wyer et al., 1999] Wyer, J. R., Willcox, B. E., Gao, G. F., Gerth, U. C., Davis, S. J., Bell, J. I., van der Merwe, P. A., and Jakobsen, B. K. (1999). T cell receptor and coreceptor cd8 alphaalpha bind peptide-mhc independently and with distinct kinetics. *Immunity*, 10(2):219–225.

[Xu et al., 2008] Xu, C., Gagnon, E., Call, M. E., Schnell, J. R., Schwieters, C. D., Carman, C. V., Chou, J. J., and Wucherpfennig, K. W. (2008). Regulation of t cell receptor activation by dynamic membrane binding of the cd3epsilon cytoplasmic tyrosine-based motif. *Cell*, 135(4):702–713.

[Yasutomo et al., 2000] Yasutomo, K., Doyle, C., Miele, L., Fuchs, C., and Germain, R. N. (2000). The duration of antigen receptor signalling determines cd4+ versus cd8+ t-cell lineage fate. *Nature*, 404(6777):506–510.

[Yewdell et al., 2003] Yewdell, J. W., Reits, E., and Neefjes, J. (2003). Making sense of mass destruction: quantitating MHC class I antigen presentation. *Nat. Rev. Immunol.*, 3(12):952–961.

[Zamoyska, 2007] Zamoyska, R. (2007). Why is there so much cd45 on t cells? *Immunity*, 27(3):421–423.

[Zarnitsyna and Zhu, 2012] Zarnitsyna, V. and Zhu, C. (2012). T cell triggering: insights from 2D kinetics analysis of molecular interactions. *Phys Biol*, 9(4):045005.

[Zhang et al., 2011] Zhang, H., Cordoba, S.-P., Dushek, O., and van der Merwe, P. A. (2011). Basic residues in the t-cell receptor ζ cytoplasmic domain mediate membrane association and modulate signaling. *Proceedings of the National Academy of Sciences of the United States of America*, 108(48):19323–19328.

[Zhang et al., 1999] Zhang, W., Sommers, C. L., Burshtyn, D. N., Stebbins, C. C., DeJarnette, J. B., Trible, R. P., Grinberg, A., Tsay, H. C., Jacobs,

H. M., Kessler, C. M., Long, E. O., Love, P. E., and Samelson, L. E. (1999). Essential role of LAT in T cell development. *Immunity*, 10(3):323–332.

[Zhang et al., 2000] Zhang, W., Trible, R. P., Zhu, M., Liu, S. K., McGlade, C. J., and Samelson, L. E. (2000). Association of Grb2, Gads, and phospholipase C-gamma 1 with phosphorylated LAT tyrosine residues. Effect of LAT tyrosine mutations on T cell angigen receptor-mediated signaling. *J. Biol. Chem.*, 275(30):23355–23361.